UNIVERSITÀ DEGLI STUDI DI CASSINO

E DEL LAZIO MERIDIONALE

DIPARTIMENTO DI INGEGNERIA

CIVILE E MECCANICA

Corso di Dottorato in

Metodi, modelli e tecnologie per l'ingegneria

Ciclo XXXV

Life Cycle Assessment of hydrogen for mobility options and energy systems based on carbon neutral fuels

Supervisor: Ph.D. Candidate:

Prof. Dr. Giuseppe Spazzafumo Daniele Candelaresi

Academic year 2022/2023

Acknowledgements

I am sincerely grateful to Prof. Giuseppe Spazzafumo for his constant guidance during this challenging and yet very inspiring journey. Thanks for all the teachings, advices, stimuli and exchange of ideas, but above all for helping me to dream of a better and more sustainable world.

I would like to express my deepest gratitude to Dr. Antonio Valente, who in addition to being an excellent mentor and teaching me so much professionally, was also an exceptional friend, a model to follow and a source of inspiration to me. This endeavour would not have been possible without him.

Special thanks also to Prof. Javier Dufour and Dr. Diego Iribarren, for supporting me before, during and after my research stay in Madrid, for believing in my potential and for their continuous and enriching collaboration.

Finally, I would like to thank my family, my friends and all my beloved ones for their presence and their support. It would be impossible to list them all, but their belief in me has kept my spirits and motivation high during this process.

Abstract

Hydrogen produced from renewable or low-carbon energy sources is set to play a crucial role in the decarbonisation of energy systems. The use of hydrogen as a clean fuel, especially for the transport sector, has been under study for decades. In recent years, there has been a renewed confidence in technologies based on the use of hydrogen produced from renewable energy sources. However, the launch of a hydrogen economy still presents significant barriers that need to be overcome. Beyond the need to start from scratch a massive production of renewable-based hydrogen, there is also the need to solve other traditional problems related to the transport, distribution, storage and final use of hydrogen. In this context, therefore, it is essential to find smart and effective strategies that could facilitate this transition to clean hydrogen energy systems. Within the framework of this doctoral thesis, various strategies are presented aimed at circumventing some barriers and at favouring and speed-up the advent of a hydrogen economy. One of these possibilities lies in the production of carbon-neutral and synthetic renewable fuels, by combining renewable hydrogen with a carbon source. Regarding hydrogen vehicles instead, a part from the well-known fuel cells, several other technologies are conceivable. Moreover, being hydrogen an energy carrier which does not involve particular environmental criticalities during its use, it is essential to carefully check the environmental suitability of hydrogen-based fuels and technologies under a full life-cycle perspective. Three research lines were mainly conducted: i) proposal of innovative short-term national strategies to allow a faster implementation of renewable hydrogen in road transport, through assessment of the environmental suitability of renewable hydrogen as a fuel for sustainable mobility. Different technical vehicle and fleet options were evaluated; (ii) evaluation of the technical and environmental potentialities of systems for the production of carbon-neutral fuels (such as renewable-based substitute natural gas) and possible co-production of electricity, starting from renewable energy sources and biomass; (iii) evaluation of the life-cycle environmental performance of renewable hydrogen production systems (mainly through electrolysis) and environmental footprint of the produced hydrogen. Overall, this doctoral thesis provided advances and developments on sustainable energy systems and alternative vehicles based on hydrogen and carbon-neutral fuels, both from an energy and an environmental life-cycle perspective, paving the way towards a faster implementation of hydrogen in the current energy sector.

Table of Contents

Acknowledgements .... ***iii***

Abstract .... ***iv***

Table of Contents .... ***v***

List of Publications .... ***ix***

List of published Book Chapters .... ***x***

List of Figures .... ***xi***

List of Tables .... ***xiv***

Summary .... ***xvii***

Chapter 1 Introduction ***1***

1.1. Foreword: energy, environment and hydrogen 1

1.2. The current energy sector 3

1.3. Hydrogen energy systems 10

1.3.1. Introduction to basic properties of hydrogen 10

1.3.2. Hydrogen production 12

1.3.3. Hydrogen transport and distribution 15

1.3.4. Hydrogen storage 19

1.3.5. Hydrogen use in vehicles 20

1.4. Power-to-fuel 23

1.4.1. Power-to-fuel role in renewable energy storage 24

1.4.2. Main synthetic fuels 26

1.4.2.1. Methane 28

1.4.2.2. Methanol 30

1.4.2.3. Dimethyl Ether 31

1.4.2.4. Ammonia 32

1.4.2.5. Urea 33

1.4.2.6. Formic acid 34

1.5. Hydrogen and synthetic carbon-neutral fuels possible uses 35

1.5.1. Industry 35

1.5.2. Transport 37

1.5.3. Buildings 44

1.5.4. Power generation 46

1.6. Assessment of hydrogen energy systems and carbon-neutral fuels under a life-cycle perspective 50

Chapter 2 Objectives and methodology........ 52

2.1. Objectives 52

2.2. Methodology........ 53

2.2.1. Methodological framework of life cycle assessment 53

2.2.1.1. Stage 1: Goal and scope definition 56

2.2.1.2. Stage 2: Life cycle inventory analysis 57

2.2.1.3. Stage 3: Life cycle impact assessment 60

2.2.1.4. Stage 4: Interpretation 62

2.2.2. Environmental analysis of vehicles: differences between Well-To-Wheels analysis and Life Cycle Assessment 62

2.2.3. Specific methodological aspects considered in LCA of vehicles and fleets 67

2.2.3.1. Fuel life-cycle 67

2.2.3.2. Vehicle life-cycle 73

Chapter 3 Hydrogen mobility options: Proposal for implementation of short-term national hydrogen strategies in (Italian) road transport 91

3.1. Need for decarbonisation of the transport sector 91

3.2. Comparative life cycle assessment of hydrogen-fuelled passenger cars 98

3.2.1. Motivation and background 98

3.2.2. Material and methods 100

3.2.3. Data acquisition 102

3.2.4. Results and discussion 107

3.2.5. Conclusions 113

3.3. Life cycle assessment of hydrogen passenger cars and sensitivity to technical parameters 114

3.3.1. Goal and scope 115

3.3.2. Key technical parameters in LCA of passenger vehicles 117

3.3.3. Sensitivity of the LCA results to the variation of key technical parameters 120

3.4. Novel short-term national strategies to promote the use of renewable hydrogen in road transport: a life cycle assessment of passenger car fleets partially fuelled with hydrogen 129

3.4.1. Motivation and novelty 129

3.4.2. Definition of the case studies 131

3.4.3. Energy analysis and national contextualisation 133
3.4.4. LCA framework and data acquisition 137
3.4.5. Energy analysis results 142
3.4.6. Environmental results 145
3.4.7. Perspectives and final remarks 149
3.4.8. Conclusions 151
Chapter 4 Modelling and environmental impact of renewable Substitute Natural Gas production pathways........ 152
4.1. Life cycle assessment of substitute natural gas production from biomass and electrolytic hydrogen 152
4.1.1. Case studies 152
4.1.2. Goal and scope 155
4.1.3. Life cycle inventory 156
4.1.4. Results and discussion 159
4.1.5. Energy output as the functional unit 162
4.1.6. Multifunctionality handling 163
4.1.7. Conclusions 165
4.2. Heat recovery from a PtSNG plant coupled with wind energy 166
4.2.1. Background and scope 167
4.2.2. PtSNG plant description 168
4.2.3. Heat recovery management 171
4.2.3.1. Thermal storage 172
4.2.3.2. Electrical storage 173
4.2.4. Heat recovery system sizing criteria 174
4.2.5. Performance parameters 175
4.2.6. Results and discussion 177
4.2.6.1. PtSNG mass and energy balance results 177
4.2.6.2. Thermal energy requirement 179
4.2.6.3. Thermal storage results 182
4.2.6.4. Electrical storage results 182
4.2.6.5. Annual performances results 184
4.2.7. Conclusions 186
4.3. Production of substitute natural gas integrated with Allam cycle for power generation 188

4.3.1. Background and motivation 189
4.3.2. Definition of the proposed system 190
4.3.3. Allam cycle 191
4.3.4. Description of the proposed cogeneration plant 194
4.3.5. Model 197
4.3.6. Results 201
4.3.7. Conclusions 206
References 208
Appendix A Life Cycle Inventories of considered vehicle options 231
Appendix B Results of sensitivity analysis on vehicle technical parameters 264

List of Publications

Publication 1

Candelaresi D, Valente A, Iribarren D, Dufour J, Spazzafumo G.
Comparative life cycle assessment of hydrogen-fuelled passenger cars*.*
International Journal of Hydrogen Energy, 2021, 46 (72), 35961-35973; Elsevier.
https://doi.org/10.1016/j.ijhydene.2021.01.034

Publication 2

Bargiacchi E, Candelaresi D, Valente A, Frigo S, Spazzafumo G.
Life Cycle Assessment of Substitute Natural Gas production from biomass and electrolytic hydrogen.
International Journal of Hydrogen Energy, 2021, 46 (72), 35974-35984; Elsevier.
https://doi.org/10.1016/j.ijhydene.2021.01.033

Publication 3

Candelaresi D, Moretti L, Perna A, Spazzafumo G.
Heat recovery from a PtSNG plant coupled with wind energy*.*
Energies, 2021, 14 (22), 7660; MDPI.
https://doi.org/10.3390/en14227660

Publication 4

Candelaresi D, Valente A, Iribarren D, Dufour J, Spazzafumo G.
Novel short-term national strategies to promote the use of renewable hydrogen in road transport: a life cycle assessment of passenger car fleets partially fuelled with hydrogen. *Science of the Total Environment, 2023, 859 (2), 160325; Elsevier.*
https://doi.org/10.1016/j.scitotenv.2022.160325

Publication 5

Candelaresi D and Spazzafumo G.
Production of substitute natural gas integrated with Allam cycle for power generation.
Energies, 2023, 16 (5), 2162; MDPI.
https://doi.org/10.3390/en16052162

Original works pending publication

1. Candelaresi D, Valente A, Bargiacchi E, Iribarren D, Dufour J, Spazzafumo G. *Life Cycle Assessment of hydrogen passenger cars and sensitivity to technical parameters*. ICH2P-2021.
2. Candelaresi D, Maddula SMKR, Iribarren D, Dufour J, Spazzafumo G. *Exploring the life-cycle environmental performance of hydrogen from current and future PEM electrolysis*. HYPOTHESIS XVII.
3. Candelaresi D, Di Cicco G, Spazzafumo G. *Life cycle assessment of renewable hydrogen production by means of alkaline water electrolysis*.

List of published Book Chapters

Publication 6

Candelaresi D, Spazzafumo G. ***Introduction: the power to fuel concept.***
Chapter 1 in book: "Power to fuel: how to speed up a hydrogen economy", pp. 1-15. Academic Press, 2021.
https://doi.org/10.1016/B978-0-12-822813-5.00005-9

Publication 7

Bargiacchi E, Candelaresi D, Spazzafumo G. ***Power to methane.***
Chapter 4 in book: "Power to fuel: how to speed up a hydrogen economy", pp. 75-101. Academic Press, 2021.
https://doi.org/10.1016/B978-0-12-822813-5.00001-1

Publication 8

Candelaresi D, Spazzafumo G. ***Power to methanol.***
Chapter 5 in book: "Power to fuel: how to speed up a hydrogen economy", pp. 103-122. Academic Press, 2021.
https://doi.org/10.1016/B978-0-12-822813-5.00002-3

Publication 9

Candelaresi D, Spazzafumo G. ***Power-to-fuel potential market.***
Chapter 10 in book: "Power to fuel: how to speed up a hydrogen economy", pp. 239-265. Academic Press, 2021.
https://doi.org/10.1016/B978-0-12-822813-5.00009-6

Publication 10

Candelaresi D, Valente A, Bargiacchi E, Spazzafumo G.
Life cycle assessment of hybrid passenger electric vehicle.
Chapter 16 in book: "Hybrid Technologies for Power Generation", pp. 475-495. Academic Press, 2022.
https://doi.org/10.1016/B978-0-12-823793-9.00017-6

List of Figures

Figure 1. World primary energy demand by fuel in 2021. Total: 14214.9 Mtoe. 4
Figure 2. World total primary energy supply in 2019. Total: 14485.8 Mtoe. 5
Figure 3. Some of the possible hydrogen production pathways 13
Figure 4. Comparison among different energy storage systems. 26
Figure 5. Standardised general methodological structure of LCA. 55
Figure 6. Example of a set of unit processes within a product system. 58
Figure 7. Scheme of a generic product system. 59
Figure 8. System boundaries of a generic LCA for passenger road transportation 63
Figure 9. Well-to-Tank and Tank-to-Wheels 65
Figure 10. Well-to-Wheels analysis and LCA 66
Figure 11. Breakdown by sector of the global GHG emission. 91
Figure 12. Final energy consumption in transport, broken down by type of fuel. 92
Figure 13. Projections on transportation sector world energy consumption 93
Figure 14. Greenhouse gas emissions broken down by source sector. 93
Figure 15. Projections on passenger transportation world energy consumption, by transport mode 94
Figure 16. Final energy consumption in Europe, by sector 95
Figure 17. Greenhouse gas emission in Europe, by sector 95
Figure 18. Emissions of greenhouse gases caused by the transport sector in the European Union, broken down by transport mode, data from 1990 to 2020. 96
Figure 19. Modal split of inland passenger transport in European Union, in 2017 96
Figure 20. Contribution of hydrogen fuel and vehicle infrastructure to the carbon and acidification footprint, in the life-cycle environmental profile of a fuel cell electric vehicle . 99
Figure 21. Vehicle concepts under comparison 100
Figure 22. System's boundaries and functional unit for each of the vehicles under comparison 102
Figure 23. GWP results, absolute values 108
Figure 24. CED results, absolute values 109
Figure 25. AP results, absolute values 109
Figure 26. Relative environmental impacts of the three pure-hydrogen vehicle systems and the two CNG systems 110
Figure 27. Hythane and H2-Gasoline life-cycle impacts relative to FCEV 112
Figure 28. System boundaries and functional unit considered in the study 115
Figure 29. Baseline results of hydrogen vehicles 116
Figure 30. Baseline results, impact breakdown for three selected vehicle options 116
Figure 31. Influence of vehicle technical parameters on GWP impact, Hythane vehicle 122
Figure 32. Influence of vehicle technical parameters on CED impact, Hythane vehicle 122
Figure 33. Influence of vehicle technical parameters on AP impact, Hythane vehicle 123
Figure 34. Influence of vehicle technical parameters on GWP impact, FCEV 124
Figure 35. Influence of vehicle technical parameters on GWP impact, H2-ICE 125

Figure 36. Influence of vehicle technical parameters on GWP impact, HEV H2-ICE 126
Figure 37. Influence of vehicle technical parameters on GWP impact, H2-Gasoline............127
Figure 38. Key findings on vehicle technical parameters and identification of priority intervention areas to reduce the environmental impact of vehicles......................................127
Figure 39. Graphical conceptualisation of the proposed scientific-assisted policy-making process leading to the implementation of national hydrogen strategies in road transport 129
Figure 40. Vehicle concepts involved in fleet composition 132
Figure 41. Calculation procedure for the target use of hydrogen in Italian passenger cars in 2025 135
Figure 42. Main assumptions for the energy analysis of fleets 136
Figure 43. System boundaries: (a) single vehicle, and (b) fleet 138
Figure 44. Breakdown of the carbon footprint of the proposed fleets per km travelled 146
Figure 45. Total carbon footprint of the different fleet strategies proposed, and total distance travelled 147
Figure 46. Breakdown of the energy and acidification footprints of the proposed fleets per km travelled 148
Figure 47. System diagram in case only SNG is produced (HG case) 153
Figure 48. System diagram in case SNG and electricity are co-produced 154
Figure 49. Impact breakdown for the GWP indicator for the six analysed layouts 160
Figure 50. Impact breakdown for the AP indicator for the six analysed layouts 160
Figure 51. Impact breakdown for the CEDnr indicator for the six analysed layouts 161
Figure 52. GWP, AP and CEDnr impacts for all investigated layouts.................................162
Figure 53. GWP, AP and CEDnr relative impacts for all investigated layouts, in the base-case scenario (avoided burdens approach) 163
Figure 54. GWP, AP and CEDnr relative impacts for all investigated layouts, in the second scenario (energy allocation approach)...164
Figure 55. Conceptual scheme of the proposed waste heat recovery system for a PtSNG plant coupled with wind energy...166
Figure 56. PtSNG plant layout 169
Figure 57. Conceptual schemes and energy flows of the two proposed waste heat recovery systems: (a) Thermal storage; (b) electrical storage 171
Figure 58. Schematic diagram of thermal storage system..172
Figure 59. Schematic diagram of electrical storage system 173
Figure 60. Functional scheme of the ORC 174
Figure 61. Results of the statistical analysis and distribution of the standby periods 181
Figure 62. Diathermic oil circuit for waste heat recovery from the methanation unit, sized for coupling with the ORC power unit...183
Figure 63. Results for the ORC power unit 184
Figure 64. Conceptual scheme of the proposed system. Electricity and SNG are cogenerated starting from water, renewable electricity surplus and biomass..188
Figure 65. Simplified scheme of the proposed system...191
Figure 66. Conventional Allam cycle fuelled by natural gas 192
Figure 67. Scheme of the proposed cogeneration plant..194

Figure 68. Model of the solid oxide electrolyser section 198
Figure 69. Model of the biomass gasifier section..199
Figure 70. Model of the Allam cycle power section 199
Figure 71. Model of the methanation section for SNG production 201
Figure 72. Detail of the syngas flows in the gasification section 202
Figure 73. Sequence of the obtained SNG composition...205
Figure 74. Toyota Mirai cutaway 249
Figure 75. Polarization curves for a cell with Gore-Select membrane..................................252
Figure 76. Impact breakdown of the FCEV (Baseline) 264
Figure 77. Influence of vehicle technical parameters on CED impact, FCEV.......................264
Figure 78. Influence of vehicle technical parameters on AP impact, FCEV..........................265
Figure 79. Impact breakdown of the H2-ICE vehicle (baseline)...265
Figure 80. Influence of vehicle technical parameters on CED impact, H2-ICE 266
Figure 81. Influence of vehicle technical parameters on AP impact, H2-ICE 266
Figure 82. Impact breakdown of the HEV H2-ICE (baseline) 267
Figure 83. Influence of vehicle technical parameters on CED impact, HEV H2-ICE 267
Figure 84. Influence of vehicle technical parameters on AP impact, HEV H2-ICE..............268
Figure 85. Impact breakdown of the Hyhtane vehicle (baseline)..268
Figure 86. Impact breakdown of the H2-Gasoline vehicle (baseline)...................................269
Figure 87. Influence of vehicle technical parameters on CED impact, H2-Gasoline vehicle 269
Figure 88. Influence of vehicle technical parameters on AP impact, H2-Gasoline vehicle...270

List of Tables

Table 1. Hydrogen main characteristics 11
Table 2. Main hydrogen production options 12
Table 3. Energy density of different fuels 27
Table 4. Main technical specifications of an average European passenger car 75
Table 5. Main technical characteristics of the hydrogen vehicles considered in the study 101
Table 6. Main inventory data for vehicle manufacture (values per one vehicle) 103
Table 7. Fuel economy and tailpipe emissions for the vehicles under study 106
Table 8. Main inventory data for vehicle operation and maintenance (values per total kilometres travelled) 107
Table 9.Life-cycle profile of each vehicle system (values per FU) 108
Table 10. Main technical parameters to consider in LCA of passenger cars 117
Table 11. Variation ranges and variation step of main technical parameters considered for sensitivity analysis 121
Table 12. Fuel economy and tailpipe emissions for the vehicles involved in fleets composition 136
Table 13. Main inventory data for vehicle production (values per one vehicle). 139
Table 14. Main inventory data for vehicle operation and maintenance (values per total kilometres travelled by one vehicle during its useful life). 141
Table 15. Fleets' energy performance expressed as annual km travelled and annual passenger-km (pkm). 144
Table 16. Number of vehicles, fleets composition and national fleet penetration. 144
Table 17. Consumption of fuels per km travelled by each fleet and distance travelled with each vehicle type. 145
Table 18. Inventory data for the SNG technologies considered in this study. (Amount per kg of SNG produced) 156
Table 19. Italian 2030 energy mix for electricity production (TWh) 158
Table 20. Allocation factors for the two co-products (SNG and electricity) in the energy allocation scenario 158
Table 21. Operational data of the PtSNG plant. 177
Table 22. Mass and energy balances under nominal conditions 178
Table 23. Thermal powers available from the methanation unit and SNG inlet and outlet temperatures in the heat exchangers 179
Table 24. Annual operation time of the 1 MW PtSNG plant. 179
Table 25. Thermal energy requirements of the methanation unit 180
Table 26. Results of the statistical analysis and distribution of the standby periods 181
Table 27. Operating conditions and performance of the ORC unit 183
Table 28. Annual mass and energy balance and annual performances 184
Table 29. Composition and calorific values of the selected biomass 195
Table 30. Characteristics of the main flows of the gasification section 202
Table 31. Characteristics of the main flows of the electrolysis section 203

Table 32. Main oxygen, exhaust gas and condensed water flows of the Allam section 203
Table 33. Main carbon dioxide flows of the Allam section 204
Table 34. Characteristics of the main flows of the methanation section 204
Table 35. Global energy balance of the proposed system 206

Appendix A – Life cycle inventories

Table A1. Body and Chassis, material composition, weight, kg 231
Table A2. Vehicle fluids, weight, kg 232
Table A3. Internal combustion engine for ICE vehicles 233
Table A4. Internal combustion engine for HEVs 234
Table A5. CNG fuel system 234
Table A6. Hydrogen fuel system 235
Table A7. Gasoline fuel system 235
Table A8. Gasoline tank 235
Table A9. CNG-II tank 236
Table A10. CNG-I Tank 236
Table A11. Hydrogen tank for FCEV, H2-ICE and HEV H2-ICE 236
Table A12. Hydrogen tank for H2-Gasoline 237
Table A13. Catalytic converter for CNG and HEV CNG 237
Table A14. Exhaust system for CNG and HEV CNG 238
Table A15. Catalytic converter for Hythane vehicle 238
Table A16. Exhaust system for Hythane vehicle 239
Table A17. Catalytic converter for H2-ICE and HEV H2-ICE vehicles 239
Table A18. Exhaust system for H2-ICE and HEV H2-ICE vehicles 239
Table A19. Catalytic converter for H2-Gasoline vehicle 240
Table A20. Exhaust system for H2-Gasoline 240
Table A21. Electric motor for FCEV 241
Table A22. Electric motor for HEVs 241
Table A23. Balance of plant for FCEV 242
Table A24. Gearbox 242
Table A25. Alternator 243
Table A26. Starter battery (lead acid) 243
Table A27. Starter motor 243
Table A28. Starting system for ICE 244
Table A29. Cooling system for ICE 244
Table A30. Electronics for control unit 244
Table A31. Inventory for the production of 1 tyre 245
Table A32. Vehicles kerb weight, kg 245
Table A33. Vehicle Components Composition, % by weight 246
Table A34. Material composition for each component, % by weight 246
Table A35. GWP results, absolute values 247

Table A36. CED results, absolute values 247
Table A37. AP results, absolute values 247
Table A38. Technical datasheet of the FCEV 248
Table A39. Nafion base material and Nafion solution 253
Table A40. PTFE, Polytetrafluoroethylene 253
Table A41. Expanded Polytetrafluoroethylene, ePTFE 254
Table A42. Reinforced membrane Nafion/ePTFE 254
Table A43. Catalyst ink, for PEMFC for automotive applications 255
Table A44. Catalysed reinforce membrane, roll calendering of catalyst ink and membrane. 256
Table A45. Polyacrylonitrile fibre 256
Table A46. Carbon fibre cloth 258
Table A47. Thermoforming 258
Table A48. MEA assembly 259
Table A49. Titanium zinc plate 260
Table A50. Bipolar plate 261
Table A51. Coolant gasket 261
Table A52. End plates and current collector 262
Table A53. Tie rods 262
Table A54. Cell assembly 262
Table A55. Stack assembly 263
Table A56. FC stack 263

Summary

Hydrogen produced from renewable or low-carbon energy sources is set to play a crucial role in the decarbonisation of energy systems. The use of hydrogen as a clean fuel, especially for the transport sector, has been under study for decades, with alternating waves of enthusiasm and periods of disillusionment. In recent years, however, there has been a renewed confidence in technologies based on the use of hydrogen, especially when produced from renewable energy sources. In this sense, the Covid-19 pandemic was a watershed and it was seen by many as an opportunity to start over again in a different way, entrusting the restart and return to normal life to clean, interconnected and resilient energy systems. In the last three years, there has been more and more talk of "green" and "blue" and "grey" hydrogen and of all the other colours that human imagination has managed to assign to hydrogen, with growing enthusiasm from the industrial world, the academic one and last but not least, the political one, perhaps as never seen before. Probably, one of the most significant events that confirmed this ferment around hydrogen was the presentation, in June 2020, of the European Hydrogen Strategy by the European Commission, followed by several hydrogen strategic plans of the different Member States. Since then, something has changed, the projects and the will to set up energy systems based on hydrogen have multiplied dramatically and the political objectives have become increasingly ambitious. However, the launch of a hydrogen economy still presents significant barriers that need to be overcome and this will be the challenge for the years to come. Beyond the need to start from scratch a massive production of renewable-based hydrogen, there is also the need to solve other traditional problems related to the transport, distribution, storage and final use of hydrogen. From an economic point of view, the required investments are enormous, both by those who will undertake the production and distribution of hydrogen and by those who want to use it. If the end-user faces high prices (e.g., to buy a car with fuel cells), there will be risks to limit the hydrogen demand and no one will undertake to produce an under-demanded good in large quantities, just as no one will spend money to create a distribution infrastructure that will be underused. Incentives may come from the governments of many countries, but they may not be sufficient.

In this context, therefore, it is essential to find smart and effective strategies that could facilitate this transition to clean hydrogen energy systems.

Within the framework of this doctoral thesis, various strategies are presented aimed at circumventing some barriers and at favouring and speed-up the advent of a hydrogen economy.

The various solutions presented generally focus on taking one step at a time. The first step can be that of production, since without production there can be neither distribution nor use. The key point might be to create a great hydrogen demand which, however, will not be used in pure form, at least in the first moment. The rationale behind is trying to make the most of existing (or slightly modified) infrastructure or end-use equipment while guaranteeing at the same time a gradual decarbonisation. In this way, investments will be concentrated first on the production plants, while at the same time research will keep developing to overcome technical obstacles and to reduce costs for the end-user. Of course, hydrogen should no longer be produced from fossil fuels as it is done currently. Indeed, it should replace commonly used fuels. Then only at a later stage, when production of renewable hydrogen will be ripe and plentiful enough, efforts could be concentrated elsewhere, such as on distribution and use of pure hydrogen.

Both the sustainable mobility options and the energy systems based on hydrogen or carbon-neutral fuels proposed in this doctoral thesis, follow the same rationale.

Regarding carbon-neutral fuels, these are environmentally sustainable fuels (at least from a climate change perspective), that can be synthesised using renewable resources, for instance by combining carbon (of biogenic origin or deriving from air or from industrial waste- and by-products) with renewable-based hydrogen. To be carbon-neutral, the synthetic fuel should produce no net-greenhouse gas emissions when used, and this concept is actually based on a closed carbon cycle and on the circularity of carbon emissions. In practice, this usually means that these fuels are made using carbon dioxide as a feedstock. Carbon-neutral fuels production rely on the concept of power-to-fuel: converting electricity produced from renewable sources into hydrogen, and, in case, combining hydrogen with carbon. Furthermore, at least for now, using hydrogen to produce synthetic fuels is capable of replacing traditional fuels without requiring major changes to the distribution infrastructure and end-use equipment. In addition, synthetic fuels could be used to gradually decarbonise hard-to-abate sectors. Such a strategy would allow a significant increase in the hydrogen demand and consequently a significant increase in the use of renewable energy sources. Therefore, power-to-fuel seems to be one of the most reasonable ways towards a fast decarbonisation of the energy system.

As far as concerns hydrogen-based sustainable mobility, the proposed strategies explore different options, both in terms of vehicle technology itself and in terms of hydrogen distribution and on-board storage. The aim is to investigate solutions that can alleviate the technical problems and make possible the use of existing infrastructures and mature technologies, with the least effort in terms of required modifications and enabling a widespread and within everyone's reach use of renewable hydrogen, starting from now. Again, this could favour hydrogen demand and production, thus fostering the start of a hydrogen economy.

In any case, beyond being technically and economically viable, it is essential to verify that the proposed alternative solutions are valid, or at least better than the conventional options, both from an energy and an environmental point of view.

Regarding environmental-related aspects, both hydrogen and synthetic carbon-neutral fuels are energy carriers, and they are often referred to as "zero emission fuels". This is because, in their use, they do not involve direct carbon emissions or net greenhouse gas emissions, respectively. However, one aspect needs to be clarified: in reality, there is no human activity that does not have an environmental impact, and these fuels are no exception. Since hydrogen and synthetic carbon-neutral fuels do not show particular environmental criticalities in their use phase, comprehensive analyses that can evaluate their environmental profile under a holistic life-cycle perspective are needed. In this regard the Life Cycle Assessment (LCA) methodology arises as a well-established tool.

Actually, (as it also happens for electricity) it may be that the environmental burdens of these fuels simply shifted to other stages of their life cycle, such as, for instance, at the stage of their production. In fact, being them energy carriers, their production stage generates an environmental impact that these fuels carry with them even before being used. In case the focus is on the impact related to climate change and greenhouse gas emissions, this concept is known as carbon footprint. To ensure a low carbon footprint, their production should rely on renewable or low-carbon energy sources. Under this perspective, although conceptually simpler and more intuitive, it probably does not make too much sense to talk about the vague concept of green hydrogen and all the other colours: life-cycle analyses can provide a precise and scientifically sound value of the environmental impact linked to hydrogen production, which can be seen as a certain shade of green.

The creation of an established market for hydrogen and other renewable fuels will not be based simply on colours, but will require the creation of reliable environmental labelling schemes based on the full life cycle of these fuels.

This is confirmed by the direction taken by the European Commission with the recent publication in February 2023 of the two Delegated Acts on renewable hydrogen, supplementing the Renewable Energy Directive 2018/2001 (RED-II). In addition to defining when hydrogen, hydrogen-based fuels or other energy carriers can be considered as a “renewable fuel of non-biological origin” (RFNBO), the Commission also set the methodology, to calculate greenhouse gas emissions and the associated savings from RFNBOs and recycled carbon fuels, taking into account the full life cycle of the fuels.

Another relevant point is that, in addition to the production impact of the fuel, more sophisticated (and impactful) technologies could also be required for the use of the fuel itself. For example, in the case these fuels are used in "zero emission" vehicles, some of the overall environmental impact may have simply shifted to the vehicle itself.

Clarified the general context and the background in which this doctoral thesis is framed, the main goals and results of the research activities carried out are presented below.

The main objectives of the research activity carried out were: (i) to assess the environmental suitability of renewable hydrogen as a fuel for sustainable mobility under different technical vehicle options and to propose innovative short-term national strategies to allow a faster implementation of renewable hydrogen in road transport. This objective was pursued by evaluating the energy and environmental potentialities of hydrogen produced from renewable energy sources as a clean fuel for vehicles (mainly passenger cars), used both in fuel cells and in internal combustion engines, pure or mixed with natural gas or gasoline; (ii) to evaluate the technical and environmental potentialities of systems for the production of a renewable-based substitute natural gas (SNG) and systems for the co-production of carbon-neutral synthetic fuels and electricity starting from renewable energy sources (biomass and electricity surplus produced by non-programmable renewable energy sources such as wind and solar); (iii) to evaluate the life-cycle environmental performance of renewable hydrogen production systems (mainly through electrolysis) and the environmental footprint of the produced hydrogen.

In addition to energy analysis, in most of the cases the LCA methodology was applied to the investigated systems, in order to evaluate the environmental impact associated with the individual life-cycle stages (and the overall life-cycle) of a product or system. Indeed, as previously mentioned, in the case of the investigated energy systems, the benefit of zeroed or reduced direct emissions in the use phase could be reduced or even counter-balanced by the upstream or downstream processes (i.e., the impact could be shifted from the fuel use phase to other life cycle stages). Therefore, thorough life cycle analyses are needed to verify the environmental suitability of hydrogen and carbon-neutral fuels. In this sense, the LCA methodology - standardized according to the ISO 14040 and ISO 14044 standards - is widely applied and represents a useful tool for identifying potential bottlenecks or hot-spots in the environmental life-cycle performance of product systems, on which intervention should be prioritised. By means of LCA it is also possible to compare systems that perform a same function, in order to identify the most environmentally sustainable solution, with the possibility of evaluating multiple environmental impact categories at the same time. LCA analyses were performed by using SimaPro software with ecoinvent database.

Regarding the activities related to the use of renewable hydrogen as a fuel for sustainable mobility, the research focused first on the LCA modelling of individual hydrogen vehicles and subsequently on the composition of those vehicles in fleets and on a contextualisation of the study at national (Italian and non-Italian) and European level. In second place, sensitivity analyses were conducted to ensure the robustness of the obtained results. In particular, the contextualisation for the different national strategy scenarios was carried out taking into account: i) the national situation of the vehicle fleet, the national energy balance, energy consumption in the Italian transport sector, short-term forecast scenarios; ii) main European directives (RED-II) and national directives on the promotion of the use of renewable energy sources (with a greater focus on the transport sector) and national plans on energy and climate goals (NECP/NRRP); iii) study of the various European and national hydrogen strategies, especially concerning the implementation of "green" hydrogen. Some of these national hydrogen strategies, including the Italian one, are still not complete or under definition. By means of LCA it is therefore possible to suggest targeted, effective and scientifically-based actions to support the definition of energy-environmental policies. The considered set of vehicles includes hydrogen fuel cell electric vehicles and internal combustion engine vehicles fuelled (alternatively) by hydrogen, gasoline, compressed natural gas, hydrogen-natural gas blends, hydrogen-gasoline blends, and also all the related hybrid electric versions (full-hybrid) of the same vehicles. The life cycle inventory modelling consisted in the identification and quantification of all the flows of materials, energy, waste and emissions associated with the manufacturing, maintenance and use stages of the analysed vehicles. Finally, the inventories were parameterised in order to make it possible to conduct sensitivity analyses in order to ensure the robustness of the results. The individual vehicles were then composed into fleets, partially fuelled with hydrogen and partially with natural gas or gasoline, given the limited amount of renewable hydrogen available on the national territory in the short-term. For the purpose of a fair comparison, all fleets have been placed under equal conditions, particularly in terms of energy input (e.g., available fuel). Finally, the fleets have been scaled up to the Italian national level, taking into account the amounts of renewable hydrogen that could be reasonably available in the short-term (2025) in accordance with the NECP and NRRP goals, limited by a relatively modest national hydrogen production. An energy analysis was then conducted in combination with an LCA analysis. In this way, it was possible to identify the most convenient fleet both in energy and environmental terms, i.e., the one that uses the amount of hydrogen at its disposal in the best way. A further analysis focused on the individual vehicles that compose the fleets, by carrying out sensitivity analyses with respect to the variation of the main vehicle technical parameters (useful service life, passenger occupancy rate, vehicle weight, fuel consumption, emission factors). This analysis ensured the robustness of the study and highlighted the main technical criticalities in the life-cycle of the different hydrogen vehicle options considered, i.e., the priority intervention areas on which to concentrate efforts were identified in order to improve the vehicles' environmental performance. Regarding the topic of sustainable hydrogen-based mobility, three studies were obtained: i) a life cycle comparison between vehicles fuelled by hydrogen (pure or blended with conventional fuels), and alternative vehicles fuelled by natural gas (*Publication 1*); ii) proposal of innovative national strategies to accelerate the implementation of renewable hydrogen in road transport in the short-term (*Publication 4*); iii) sensitivity analysis of the LCA results for hydrogen vehicles and identification of critical vehicle technical parameters (*Original work 1*). The results of the studies carried out show that: i) pure hydrogen vehicles (with hydrogen produced from renewable energy sources), all represent excellent decarbonisation solutions, more easily applicable in the medium-/long-term, while vehicles fuelled by hydrogen-natural gas and hydrogen-gasoline mixtures could represent good environmental solutions in the short-term as bridging options towards a hydrogen economy; ii) the fleets made up of vehicles fuelled by mixtures of renewable hydrogen and a conventional fuel, both in the case of simple combustion engine powertrain and in their hybrid electric powertrain version, represent excellent hydrogen implementation strategies in the short-term, both in terms of energy and environmental performance. The results were obtained for a set of different environmental impact categories (global warming potential, cumulative energy demand and acidification potential: GWP, CED and AP respectively). In particular, the fleets that use blended fuels obtained, simultaneously, better energy and environmental performance than the fleets that use the same amounts of hydrogen and fossil fuel separately in dedicated vehicles, thus allowing greater diffusion and penetration of hydrogen in the national vehicle fleet, with an overall lower environmental impact. In addition, the use of blends could favour a series of technical, economic and social aspects as the use of existing infrastructure or improved social acceptance; iii) the functional dependencies obtained from the sensitivity analysis showed how all the considered vehicle technical parameters have a significant influence on the LCA results, with a particular criticality found for fuel consumption and occupancy rate. Service life and occupancy rate showed a hyperbolic influence, while fuel consumption and vehicle weight showed a linear influence. Finally, fuel consumption and tailpipe emissions are critical especially for those hydrogen vehicles (pure or blended hydrogen) equipped with an internal combustion engine, highlighting how these vehicles show significant margins for technological improvement.

Regarding the research activities related to systems aimed at SNG production or co-production of electricity and carbon-neutral fuels, different types of systems have been analysed. All the investigated systems involve the use of hydrogen and/or electrolytic oxygen produced using renewable electricity, therefore they fall within the Power-to-gas technologies, useful for the storage of surplus renewable energy, both in the event that there is a lack of electricity demand and in the event that the poor quality of the electricity produced can cause grid instability problems. For the production of synthetic methane, carbon dioxide (captured from industrial sources or of biogenic origin) is hydrogenated via a thermochemical process (Sabatier reaction) with electrolytic hydrogen inside fixed bed methanation reactors. This research line led to the development of three different studies: i) LCA of six different co-production systems for SNG and electricity (*Publication 2*); ii) technical analysis on the recovery of waste heat from a SNG production plant with possible co-production of electricity (*Publication 3*); iii) technical analysis of a system for co-production of SNG and electricity using an Allam cycle as power unit (*Publication 5*).

The first study (*Publication 2*) concerns the LCA analysis of plant schemes previously analysed by the co-authors using Aspen Plus software. In particular, the LCA was used for the comparison in terms of environmental performance between six different systems that co-produce electricity and a carbon-neutral SNG starting from biomass and non-programmable renewable energy sources. Five of the six case-studies include biomass gasification using electrolytic oxygen as gasifying agent, a CO_2 separation system, a thermochemical methanation process and a power unit for co-generation of electricity (gas turbine, STIG turbine, internal combustion engine, solid oxide fuel cell at 6 bar and 30 bar). Another case study instead involves a biomass hydrogasification system and a methanator, for the sole production of SNG without the co-production of electricity. In all cases, the obtained SNG possess a high calorific value, being mainly composed of CH_4 and, to a lesser extent, of H_2. The efficiency of the different analysed layouts varies between 52.4% and 73.8%, with a chemical power (fuel) varying between 75% and 100% of the total output. A modelling of the life cycle inventories for the various systems was therefore carried out, together with some analyses in Aspen Plus for the determination of the plants operational parameters. Furthermore, a methodological discussion regarding different approaches to LCA of multifunctional systems was carried out. The different multifunctionality handling approaches include energy allocation and the so-called "avoided burdens" using an expected energy mix for Italy in 2030 (retrieved from the NECP). Results of the study show that: i) the hydrogasification-based layout showed the lowest impacts under all the considered cases, with a single exception given by the approach selected to deal with multifunctionality; ii) all the proposed layouts showed lower impacts than fossil natural gas production in terms of carbon footprint and non-renewable energy footprint, but higher acidification footprints; iii) impact breakdown shows that the largest environmental loads on GWP, AP and CED are attributable to SNG combustion, electrolyser infrastructure and wind power generation, respectively; iv) when applying the avoided burdens approach, the credits for the electricity fed into the grid are relevant, although linked to the chosen energy mix (Italian energy mix 2030). Finally, the approach selected by the LCA practitioner to deal with multifunctionality can influence the choice of the best result.

Regarding the second study (*Publication 3*) a simulation analysis was carried out using the Aspen Plus and Thermoflex software starting from plant schemes analysed within the context of the SinBio project, funded by the Lazio Region. The proposed study aims at exploiting the waste heat deriving from the SNG production plant in order to increase its efficiency and reduce its costs. In particular, the waste heat from the methanation unit was recovered, to be then made available to two different storage systems (thermal storage in one case and thermo-electric storage in the other case) which serve to ensure the self-sufficiency of the plant during the standby moments and to reduce the portion of plant energy demand satisfied by external sources. The waste heat was recovered from the methanation section, by means of heat exchangers located downstream the adiabatic methanators, using a heat transfer fluid (diathermic oil) and it was made available to a hot tank. In the first case, the diathermic oil was used to satisfy the plant thermal requirements (in particular that of the methanation reactors) during the non-production moments (hot standby), while in the second case, the oil was used for the heat supply to an Organic Rankine Cycle (ORC) using isobutane as the evolving fluid, enabling the subsequent electricity production. The electric energy produced is stored in a battery to satisfy the plant internal thermal energy demands and/or to fulfil the ancillary equipment energy demand. Results show that an SNG injectable into the natural gas network is obtained from the plant (> 95% methane content), favouring the storage of renewable energy through the gas network. Furthermore, the proposed heat recovery systems positively influence the plant annual efficiency with the advantage of being relatively simple to be implemented. However, the waste heat available from the methanation unit turned out to be much greater than the energy needed to cover the internal needs of the plant. Therefore, to further increase the overall plant efficiency, it is desirable to combine the plant itself with additional thermal or electrical utilities.

The third study (*Publication 5*) concerned the technical analysis of a system for the co-production of electricity, SNG and possibly excess hydrogen and/or oxygen, starting from water, biomass and electricity produced from variable/non-programmable renewable energy sources. The proposed system involves an electrolyser powered by renewable electricity for the production of hydrogen and oxygen, a biomass gasifier and a thermochemical methanator, in this case coupled to an innovative thermodynamic cycle for the production of electricity (Allam cycle), which uses CO_2 under supercritical conditions as the main evolving fluid. The main advantage deriving from the use of the Allam cycle lies in the oxy-combustion of the selected fuel (biomass syngas in this case), since the resulting exhaust gas is mainly composed of CO_2 and water (steam), thus greatly simplifying the CO_2 separation and capture, that can be simply obtained via water condensation. The captured carbon dioxide is then used for the subsequent methanation process together with renewable hydrogen coming from the electrolyser. The analysis carried out first validated a model of the Allam cycle in Aspen Plus against literature data and then dealt with the subsequent integration of this power unit into the proposed system, evaluating the optimal plant parameters through simulations. The results showed the co-production, with high efficiencies, of electricity and of a high-calorific-value SNG composed of 89.2% methane and 8.8% H_2, which would be injectable into the existing gas network in compliance with regulatory updates that should arrive soon. Simulations showed also that, by further optimisation of the methanation section, it is possible to obtain SNG composed of 97% methane and 2% H_2. The overall plant efficiency resulted as high as 67.6% on an LHV basis and 71.57% on an HHV basis. The validated and analysed system was then scaled down to a smaller size, such as to allow its implementation with the electrolysers currently available on the market. This system could be used to produce not only SNG but also other carbon-neutral fuels or chemicals such as green methanol, for instance, just by changing the methanation unit into an appropriate one.

The third line of research activities concerned the LCA of electrolysis-based hydrogen production systems, in order to evaluate the life-cycle environmental impact of the resulting hydrogen produced using different electrolysis technologies. In particular, proton exchange membrane (PEM) electrolysers (*Original work 2*) and alkaline electrolysers (*Original work 3*) have been evaluated. In particular, inventory data were collected both for the modelling of the electrolysers and for the various components of the balance of plant, with additional attention to the eco-design aspects of the electrolysis systems. By means of LCA, therefore, the environmental impact of hydrogen produced using electrolysis systems, corresponding both to the current state of the art and to future electrolysis technology (2030), was assessed. For the modelling of the prospective scenarios, the relevant European objectives in the expected evolution of the main key performance indicators (KPIs) of the electrolysers were taken into account. The electrolysers were then remodelled in order to take into account the design changes required in some components (e.g., in number of components and/or quantity and type of materials used) in order to obtain improved KPIs (e.g., improved current density). In this sense, sensitivity analyses were carried out (for example on the variation of membrane thickness, bipolar plate material, amount and type of catalysts, etc.) which led to the evaluation of eco-design aspects of electrolysis systems (PEM and alkaline). Moreover, for the prospective study in (*Original work 2)* some models that made it possible to consider the impact of electricity produced from wind energy in Spain or that of the Spanish electricity grid mix, both in 2020 and 2030, were considered as electricity input for the electrolysis process. In addition, electricity from photovoltaics was also considered for the study on alkaline electrolysers. The results show that hydrogen produced using wind power has very low carbon footprints ($0.7 \div 0.4$ kg CO_2 eq/kg H_2), while the use of electricity taken from the grid in future systems (2030) can effectively lead to consider the produced hydrogen as "low-carbon", particularly where the electricity mix is made up of significant amounts of energy sources with low carbon

emissions (renewables and/or nuclear). Finally, when electricity from renewable sources is used, the manufacturing impact of the electrolysis system itself (infrastructure) becomes non-negligible, therefore it becomes essential to consider also the electrolyser eco-design aspects.

Overall, this doctoral thesis provided advances and developments on sustainable energy systems and alternative vehicles based on hydrogen and carbon-neutral fuels, both from an energy and an environmental life-cycle perspective, paving the way towards a faster implementation of hydrogen in the current energy sector.

Chapter 1

Introduction

1.1. Foreword: energy, environment and hydrogen

In its broadest, not just physical meaning, energy is the *ability to produce changes*.

Energy, in its many forms, is the basis not only of all natural phenomena but also of human civilization itself. Indeed, going back over the millennia, from the dawn of civilization to the present day, it would be difficult not to recognize in every age and in every place the close and clear interdependence between the availability of energy and the economic, ethical and social development of peoples.

Although initially humankind was able to exploit relatively simple forms of energy to its advantage, such as the mechanical energy supplied by farmed livestock, or the wind or hydraulic energy available near a river, it soon learned to control increasingly complex energy forms [1].

A very rapid impetus to technological development was then given by switching from wood to the use of fossil fuels, mostly coal, during the Industrial Revolution. It was then that humanity ceased to be *carbon-neutral*, to draw on a huge source of energy compared to the one known until then, but above all comfortable and easy to transport and use. By switching then to oil and finally to natural gas new horizons have opened up, allowing, for example, a significant increase in mobility and connections between peoples and a better access to heat for domestic or industrial use. All of this gradually improved people's living standards, but, at the same time, enormously increased the fossil fuel consumption and the demand for energy.

Then through electricity, whose most disparate applications are under our eyes every day, it was even possible to delocalize these and other energy sources, transforming them into an *energy carrier*, that is, a form of secondary energy produced starting from the most varied primary energy sources, which lends itself to being transported more efficiently to the place of use. Usually, attention is not paid to this, but it is enough to reflect for a moment to see that, directly or indirectly, at the origin of all our possibilities today there is always the availability of energy.

Human beings have the need to dispose, what is more to a significant extent, essentially of three forms of energy: thermal energy, used for space heating and in numerous industrial processes, mechanical energy, required for example for the various means of transport, and electrical energy, often obtained through the transformation of mechanical energy. Electricity can then be transported and reconverted into useful forms, at the right time and place.

From the first Industrial Revolution up to the present day, most of this huge energy demand has been met almost entirely by fossil fuels, which, in addition to raising concerns about their exhaustibility, have begun to cause enormous problems to the environment, interfering with the natural carbon cycle and causing the well-known global warming and climate change.

Although energy is linked to the *development* of peoples, it has only been a few decades since *sustainable development* started to be considered.

Awareness of the relationship between energy and environment, between the consumption of fossil fuels and climate change and of the need not to exceed the natural limits of the planet have grown considerably in recent years, giving rise to mounting environmental concerns in the whole society.

For this reason, an energy transition towards clean and reliable energy systems is more and more being advocated by many sides, and recent years have seen a flourishing of several goals in this sense. Tackling climate change is one of the most significant challenges of our times. Following the Paris Agreement ratification, the number of plans and policy actions to reach ambitious climate targets set by governance is growing worldwide.

Renewable energy sources, which can be respectful of natural resources and which do not involve direct carbon emissions, are seen as one of the most promising solutions to address global warming. However, the typical unpredictability and non-programmability of some of these sources (such as wind and solar power) poses various obstacles to this energy transition.

In fact, almost all these sources are characterised by intermittent availability and generally do not have their own storage capacity. The solution to many problems of renewables lies in accumulation and the development of suitable energy storage systems is pivotal to increase the penetration of renewable sources in the energy mix. However, at least with current technologies, it could be very difficult to directly store electricity produced from renewable energy sources. Furthermore, not all the final energy uses can be easily electrified to draw on energy produced from renewable sources. As electricity, also hydrogen is an energy carrier, and it can be produced from a large variety of feedstocks and primary energy sources. From an environmental point of view the most interesting ones are probably water and electricity produced from renewable energy sources, respectively.

The possibility of accumulating renewable energy in the form of hydrogen makes it particularly interesting, as it would allow to make renewable energy production stable and to exploit the water cycle, rather than the carbon one. Water, very abundant in nature, could therefore represent both the starting point and the emission of using hydrogen.

In this sense, hydrogen could play a crucial role, capable of generating an epochal energy revolution, similar to the one that took place with electricity in the 19^{th} century.

Hydrogen could represent the ideal solution to energy and environmental problems both in the short and long term, but the current barriers to the start of a hydrogen economy need to be overcome.

1.2. The current energy sector

In 2021, the world primary energy demand, according to data published by British Petroleum (Figure 1), amounted to 595.15 exajoules (EJ) or 14,214.9 million tonnes of oil equivalent (Mtoe), 743.8 Mtoe more than in 2020, corresponding to a growth in primary energy demand by 5.8%. This annual growth was more intense than in previous years, also due to the decrease in energy demand in the year of the pandemic and the subsequent rebound and recovery of economic activity in 2021. Indeed, primary energy use in 2021 was only 1.3% above 2019 levels.

As regards energy sources, oil continues to dominate the world energy mix (31.0%), followed by coal (26.9%) and natural gas (24.4%), with the latter still showing a growing trend. The picture is completed by nuclear power (4.25%), hydroelectric power (6.8%) and other renewables (6.7%) [2].

The International Energy Agency (IEA) instead, in its reports, provides slightly different data, breakdown, aggregation and assumptions and with a different time delay, thus it is also interesting to report these data to highlight some differences, especially regarding the role played by renewable sources in the world energy scenario.

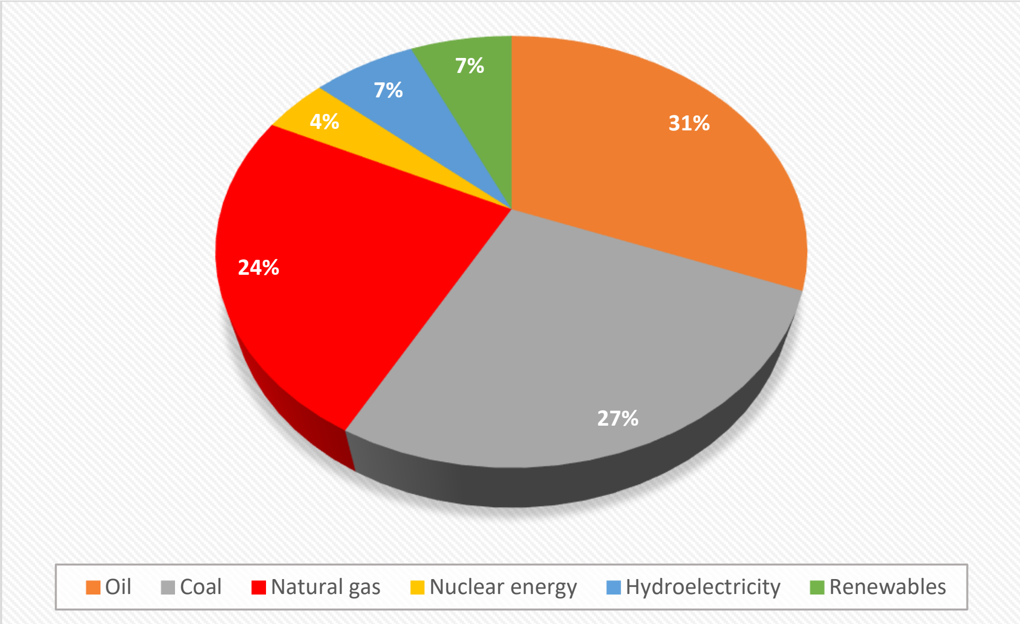

Figure 1. World primary energy demand by fuel in 2021. Total: 14214.9 Mtoe.
Source: BP Statistical Review of World Energy 2022 [2].

According to most recent IEA data currently available, in 2019 the world total primary energy supply amounted to 606 EJ, corresponding to 14,485.8 Mtoe [3]. Of these, 26.8% was derived from coal, 31.5% from oil and 23.2% from natural gas. The remaining part is supplied by nuclear (5.0%), hydroelectric (2.5%), biofuels and waste (9.4%) and other renewable sources such as geothermal, wind and solar and tide/wave/ocean (2.2%), as depicted in Figure 2. Overall, in both cases, around 81% of the world total energy demand is currently met by fossil fuels. On the other hand, even if the percentage satisfied by the various renewable sources is different between these two data sources, it is still a very small fraction of the overall energy demand.

It is expected that in the coming years the world energy situation will undergo significant changes compared to today, but, in any case, it will be necessary to deal with a sharp increase in energy demand.

The reported data are certainly worrying, since fossil fuels, which satisfy humans' energy needs to such a massive extent, are running out, without considering their role as the main culprits of environmental pollution and global warming.

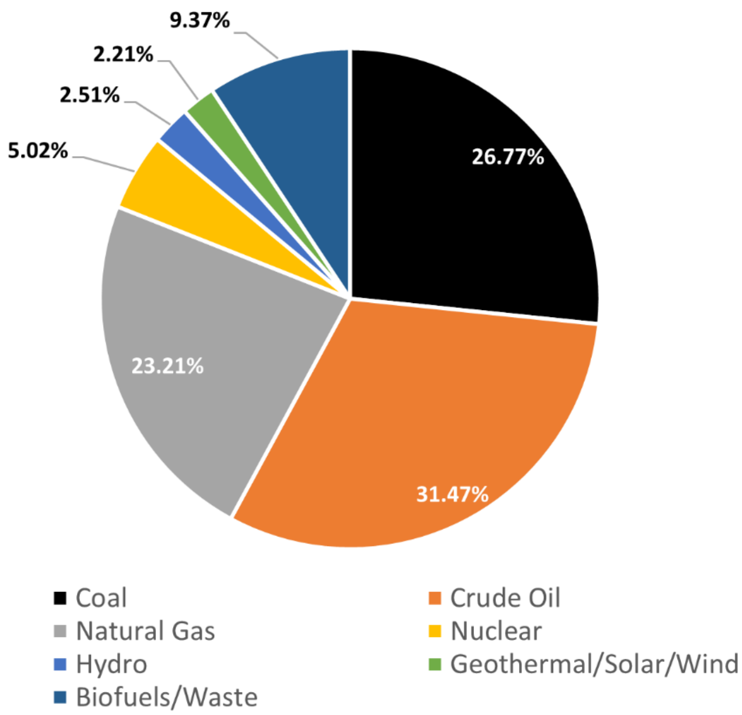

Figure 2. World total primary energy supply in 2019. Total: 14485.8 Mtoe.
Source: International Energy Agency (IEA), Key World Energy Statistics 2021 [3].

The processes of extraction and combustion of fossil fuels essentially release two types of substances into the atmosphere, causing a series of environmental issues:

- climate-altering gases, mainly carbon dioxide, an inevitable combustion product of carbon-containing compounds, and methane, deriving for example from leaks in the drilling of reservoirs, during exploration and extraction processes. These substances usually are not toxic, but cause and amplify the well-known greenhouse effect, with associated global warming and climate change;
- pollutants, on the other hand, come in various forms, all of which have in common the fact that they are directly or indirectly harmful to living beings. Among these, can be found: carbon monoxide, an asphyxiant with a high affinity for binding with haemoglobin, preventing tissue oxygenation; sulphur oxides, severe respiratory irritant and responsible for acid rains and acidification of natural environments, with toxic effects on vegetation or aquatic organisms; unburnt hydrocarbons compounds and nitrogen oxides. These last two pollutants can cause carcinogenic effects, photochemical smog, cardio-respiratory diseases and other secondary effects. Finally, the combustion of fossil fuels also generates particulate matter and fine dust, pollutants composed of small particles of a solid or liquid nature, consisting of a carbonaceous

nucleus with diameters in the order of microns, on which substances of various kinds are deposited, often harmful to human health. These particles can remain suspended in the air for a long time and they are capable of causing considerable problems to the respiratory system, especially those with a nanometric diameter or slightly larger. Particulate matter is currently the pollutant considered to have the greatest impact in urban areas and on human health.

Despite the variety of environmental issues related to human activity, most of the media attention is mainly paid to climate change, which in turn manifests as global warming and extreme weather events and which is perceived as one of the greatest issues of humanity, like a time bomb ticking towards extinction. It is therefore evident that a transition towards more sustainable energy consumption patterns is not only necessary, but also urgent.

Indeed, climate change is intimately related to energy issues. According to a large part of the scientific community, the main cause of these climatic changes lies in the sharp increase in CO_2 and other greenhouse-gas (GHG) concentrations in the atmosphere compared with pre-industrial times due to humans' massive use of fossil fuels for energy purposes [4,5]. Currently, annual GHG emissions amount to around 50 billion tonnes of equivalent carbon dioxide (CO_2eq), of which around three-quarters come from the energy sector [6,7]. According to the International Energy Agency, in the year 2021, the overall energy-related global GHG emissions reached a new record of 40.8 Gt of CO_2eq, where the 89% of this amount consisted exactly of CO_2 emissions from combustion for energy purposes and industrial processes [8].

In recent years, environmental concerns have grown at an increasingly considerable rate among the world's population. Awareness of responsibility for anthropogenic climate change has grown worldwide, and environmental issues are gaining centrality in the public debate. Policy and scientific actors worldwide recognise, with ever greater strength, the urgency for actions to avoid a climate catastrophe in the years to come. In December 2015, during the "Paris climate conference (COP 21)", near 200 countries negotiated and adopted the Paris agreement, the first universal and legally binding covenant on the global climate, aiming to limit global warming to well below +2 °C compared to the pre-industrial era [9], in view of the fact that limiting the temperature increase below +1.5 °C would significantly reduce the risks and impacts of climate change. Furthermore, some years later, the Intergovernmental Panel on Climate Change (IPCC) underlined the urgency to act drastically by 2030 to limit global warming below +1.5 °C, otherwise a point of no return will be reached and the penalty will be the drift and irreversibility of climatic conditions. The IPCC report, significantly entitled “Global Warming of 1.5 °C” [10] was clear: at that time, the goals set by politicians for 2030 were ambitious, but still not enough. Mitigating the worst effects of global warming is still possible, but to do so requires “rapid, far-reaching and unprecedented changes in all aspects of society”. Two main points underscore the urgency for action: we need to limit global warming to 1.5 °C rather than aiming for 2 °C, and we need to do it now, before the CO_2 budget at our disposal, expendable by 2030, is exhausted. The temperature difference appears to be small on paper, but it would entail large differences in environmental damage in reality. According to the report, for example, by 2100, global sea level rise would be 10 cm lower assuming 1.5 °C of warming, instead of 2 °C. The probability of having an Arctic Ocean completely free of ice during the summer would also significantly decrease and coral reefs would still have an opportunity for survival, where +2 °C would instead mean the complete disappearance of the aforementioned ecosystems. The IPCC has also drawn up a list of solutions to contain global warming, which calls for anthropogenic carbon dioxide emissions to decrease by about 45% by 2030, compared to 2010 levels, reaching “net zero” by 2050. This report has been the scientific basis for several environmental policy claims and targets set by governments, such as the European Green Deal.

In this context, Europe has set a carbon-neutrality target by 2050 with the adoption of the European Green Deal [11], setting more and more ambitious intermediate goals for 2030, in a process of constant upward revision. One of the most recent examples of this increasing ambition is also the adoption in 2021 of the “Fit for 55” package and of the European climate law regulation, by adopting which, the EU and its member states committed, with a legal obligation, to cutting net greenhouse gas emissions in the EU by at least 55% by 2030, compared to 1990 levels [12,13].
Also the recent 26th and 27th United Nations Climate Change conferences of Glasgow and Sharm El-Sheikh [14], basically confirmed the need to pursue efforts to maintain global warming below the 1.5 °C increase.

It is thus of paramount importance to undertake actions fostering the integration of affordable and clean technologies into the current energy landscape. The need to invest in renewable energy sources, such as solar and wind power, to replace fossil fuels and to start a huge green energy transition, is becoming increasingly important. Indeed, renewable energy sources (RESs) are widely indicated as the ideal candidate not only to mitigate climate change and environmental issues [15,16], but more in general to move towards a more sustainable and equal world. One of the virtues of RESs is their plenty and distribution on the planet: sun, wind, water, biomass, waste, and heat from the Earth are available in abundance all around us, in addition, they are constantly replenished by nature and emit little to no greenhouse gases or pollutants into the air. This widespread diffusion could reduce the energy and geopolitical dependency of many countries, which currently import fossil fuels. According to United Nations, about 80% of the global population lives in countries that are net-importers of fossil fuels, that is about 6 billion people who are dependent on fossil fuels from other countries, which makes them vulnerable to geopolitical shocks and crises [17].

In any case, with the current technologies, the most widespread renewable energy sources usually generate almost exclusively electricity, while the final uses of energy are mainly satisfied by electricity and fuels with an average ratio of 1:4. Regarding the electricity generation sector alone, its global CO_2 emissions amounted to 13 Gt in 2021, or over one-third of all CO_2 emissions related to the energy sector [18]. However, despite the recent increase in the demand for electricity, the rapid expansion of RESs such as solar photovoltaic and wind power is beginning to stem the growth in GHG emissions.

Nonetheless, some difficulties remain regarding the exploitation and reliability of these alternative sources which, in any case, would not be exactly equally distributed throughout the planet. The criticisms raised regard in particular the need for large spaces required for the energy harvest, the intermittent availability joint with unpredictability and randomness, both on a daily and a seasonal level. Precisely because of their characteristic discontinuity and non-programmability in production, it can often happen that in moments of greater supply of "green" electricity, when there is abundancy of wind or sun, there is actually no electricity demand and vice versa. Moreover, it is a hard task to accumulate electricity, which is why it is immediately fed into the grid for consumption. The connection of an increasing number of variable RESs plants to the grid has recently been causing quite a few problems in the dispatching and distribution of electricity, as the grid itself is not able to perfectly handle the instability and the intermittence deriving from the input of power from renewables [19–21].

One could then think of somehow accumulating the electricity produced to remove the intermittence constraint. Under this perspective, energy storage systems are key to alleviate some of the problems of RESs and increase their penetration in the energy mix, both not to jeopardise the stability of the electricity grid and to decouple the production of energy from its demand and manage the surplus energy avoiding energy curtailment [22–24].

To date, batteries are not yet a fully mature technology, they can store energy for relatively short times, are still very expensive for large-scale plants and, moreover, they would require a significant exploitation of rare earths and critical raw materials for their production, such as lithium and cobalt. The hydroelectric storage basins, on the contrary, are by now fully mature and capable of longer-lasting storage duration. Anyway, in the very near future, with the increase in renewables penetration in the market, existing pumped storage hydropower systems alone will no longer be sufficient to absorb the energy fluctuations of the network, while the construction of new artificial basins, where technically feasible, would involve evident modifications of natural environments.

Hydrogen stands as an ideal energy storage system and is among the most promising options. Green hydrogen produced starting from RES power could represent an effective and reliable strategy for accumulating renewable energy on a large scale and for a long time.

Being an energy carrier, hydrogen is not present in nature in its free molecular state, except in space, needing (similarly to electricity) to consume primary energy to be produced. By splitting the water molecule, for instance through electrolysis driven by RES power, hydrogen would be a clean energy vector that could be more easily accumulated for long times than electric current.

Furthermore, hydrogen is gaining importance in a wide range of areas in the path towards a clean energy sector. However, there are strengths and weaknesses that have to be considered for this energy carrier. For instance, on the one hand, hydrogen can be produced through a large number of technological pathways, energy sources and feedstocks. This flexibility allows hydrogen to be potentially produced worldwide as a global solution, establishing the so-called "*Hydrogen economy*". On the other hand, it has to be taken into account that techno-economic barriers linked to stages beyond hydrogen production (such as the lack of investments for a well-developed infrastructure for its distribution) have to be still overcome. In light of this, this thesis focuses on the development of innovative strategies that can circumvent the obstacles currently present and can favour a more rapid development of an economy based on renewable-based hydrogen as a clean and sustainable energy vector.

1.3. Hydrogen energy systems

1.3.1. Introduction to basic properties of hydrogen

Hydrogen is the lightest chemical element. The hydrogen atom consists of a single proton and a single electron, which has a mass about 1800 times lower than that of the proton. The atomic weight is 1.00794 amu. The radius of the orbit of the electron is about 100,000 times higher than the radius of the proton and, therefore, the space occupied by the atom is practically empty. Elemental hydrogen is very abundant in nature, but on our planet it can only be found bonded to other atoms, mainly in water molecules, organic molecules and hydrocarbons. On the other hand, pure hydrogen in the free molecular state, i.e. H_2, is not present. For this reason, on Earth, hydrogen is not a primary energy source (as instead occurs in the Sun), but rather an energy carrier, or a form of secondary energy, which needs to consume primary energy in order to be produced.

At atmospheric pressure and ambient temperature, diatomic hydrogen (H_2) is a colourless, odourless and tasteless gas, non-toxic, insoluble in water and highly flammable, forming explosive mixtures with air with flammability limits between 4% and 75%. It has a high specific volume (i.e., low density), resulting 14 times lighter than air, therefore it disperses by buoyancy and leaves the atmosphere rapidly. For this reason, it is not directly available in pure form on the Earth. Hydrogen shows a remarkable high energy density per unit mass (120 MJ/kg on a LHV basis), but a low energy density per unit volume (11 MJ/Nm^3). However, by increasing the pressure it is possible to increase the volumetric energy density. In the liquid state, the calorific value per unit volume is even higher, but this state needs to be maintained at very low temperatures, since the boiling point is equal to 20.3 K (-252.88 °C). Hydrogen higher heating value on a mass basis (141.8 MJ/kg) is the highest among fuels. The main physicochemical properties and characteristics of hydrogen are summarised in Table 1.

Hydrogen gas was first artificially produced and observed (unknowingly) in the early 16th century by Phillippus von Hohenheim (known as Paracelsus) by the reaction of strong acids on metals. He only noticed that the gas was a by-product, but was unaware that the flammable gas produced by this chemical reaction was a new chemical element. In 1671, Robert Boyle rediscovered the reaction between iron lings and dilute acids, which results in the production of hydrogen gas. He noted that these fumes were highly flammable and that the flame gave a lot of heat but not much light. In 1766, Henry Cavendish was the first to recognize hydrogen gas as a discrete substance, by identifying the gas from a metal-acid reaction "flammable air" and further finding in 1781 that the gas produces water when burned. This characteristic of producing water when burned gave hydrogen its name. It was Antoine Lavoisier, in 1783, that gave the element the name of “hydrogen”, from the ancient Greek meaning “water-generator”, from ὕδωρ (hydor, “water”) and γείνομαι (ghéinomai, “that generates”) [25].

Table 1. Hydrogen main characteristics [24,26]

Critical temperature	33.25 K
Critical pressure	13.2 bar
Density (@0 °C, 1 atm)	0.0898 kg/Nm^3
Density (@0 °C, 200 atm)	15.42 kg/m^3
Density (@0 °C, 700 atm)	40.6 kg/m^3
Density (liquid)	70.8 kg/m^3
Fusion point	14 K
Boiling point	20.3 K
Molar volume	$11.42 \cdot 10^{-3}$ m^3/mol
Gas constant	4.12 kJ/kg K
Specific heat at p=cost	14.89 kJ/kg K
Speed of sound	1270 m/s at 298.15 K
Lower heating value (LHV)	119.93 MJ/kg
Higher heating value (HHV)	141.86 MJ/kg
Energy density (gas, @0 °C, 1 atm)	10.78 MJ/Nm^3
Energy density (gas, @0 °C, 200 atm)	1850 MJ/m^3
Energy density (gas, @0 °C, 700 atm)	4869 MJ/m^3
Energy density (liquid)	8491 MJ/m^3
CAS number	1333-74-0
Colour of the cylinder ogive	Red

Hydrogen is one of the most abundant chemical substances in in the universe, constituting roughly 75% of all normal matter by mass and more than 90% by number of atoms. In the universe, hydrogen can be found in gaseous nebulae, playing an important role in star formation, in stars and in gas giant planets. Stars such as the Sun are mainly composed of hydrogen in the plasma state.

The H_2 molecule is composed of two atoms that are covalently bonded and the molecular weight is 2.016 amu. The hydrogen molecule can exist as two different spin isomers, i.e., compounds that differ only in the spin states of their nuclei: the proton spins can be parallel (ortho-hydrogen) or antiparallel (para-hydrogen). The ratio ortho-hydrogen/para-hydrogen depends on the temperature, and it confers important characteristics to hydrogen when considering its accumulation in liquid form. In standard conditions, hydrogen gas refers to normal-hydrogen (i.e., a blend of 75% ortho-hydrogen and 25% para-hydrogen). When decreasing the temperature, ortho-hydrogen is spontaneously converted to para-hydrogen through a slow and exothermic process. Since this conversion produces enough heat to favour hydrogen evaporation, leading to its leakage, it represents a technical inconvenient when considering the liquefaction process and liquid hydrogen storage [27].

1.3.2. Hydrogen production

One of the main advantages of hydrogen is that it can be produced from a wide variety of energy sources, both fossil and renewable, and through numerous direct or indirect processes, technological pathways and feedstocks (Table 2 and Figure 3).

Table 2. Main hydrogen production options [24]

<table>
<tr><th>Process</th><th>Energy source</th><th>Hydrogen donor</th></tr>
<tr><td>Coal gasification</td><td>Coal</td><td>Water/Coal</td></tr>
<tr><td>Hydrocarbons partial oxidation</td><td rowspan="2">Hydrocarbons</td><td rowspan="2">Water/Hydrocarbons</td></tr>
<tr><td>Hydrocarbons reforming</td></tr>
<tr><td>Kvaerner Process</td><td rowspan="2">Fossil/Nuclear/Renewable</td><td>Methane</td></tr>
<tr><td>Electrolysis</td><td rowspan="3">Water</td></tr>
<tr><td>Thermolysis</td><td>Nuclear/Renewable</td></tr>
<tr><td>Photoelectrolysis</td><td rowspan="4">Sun</td></tr>
<tr><td>Photosynthesis</td><td rowspan="3">Water/Biomass</td></tr>
<tr><td>Biomass gasification</td></tr>
<tr><td>Biomass anaerobic digestion</td></tr>
<tr><td>Reaction water/hydride</td><td>Chemical hydride</td><td>Water/Hydride</td></tr>
</table>

Among the main processes that involve the use of fossil fuels, there are the gasification of coal and the steam reforming of methane, through which a synthesis gas, called syngas, is first obtained and subsequently purified to obtain hydrogen.

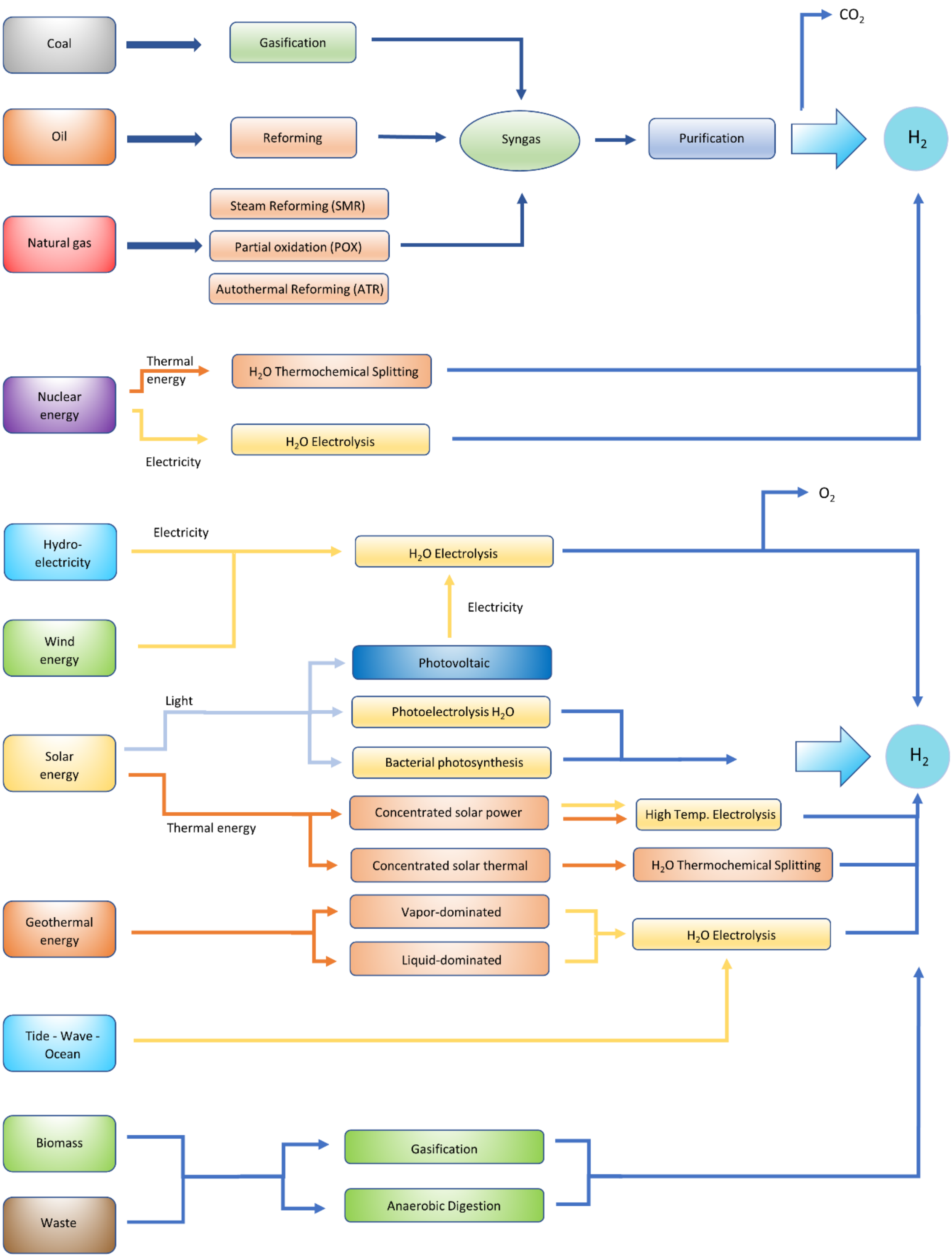

Figure 3. Some of the possible hydrogen production pathways

Due to the incompleteness of the purification processes, hydrogen produced starting from fossil sources can contain traces of carbon monoxide, which is particularly harmful for proton exchange membrane fuel cells, since it is able to quickly poison the catalysts. Most of the hydrogen produced in the world nowadays derives from the steam reforming of natural gas and coal gasification, or, as a by-product, from refineries and chemical industries, in which it is often also consumed, for example in hydrotreatment process, to remove sulphur and other impurities from oil products, or in the synthesis of methanol and ammonia [28].

As far as production from renewable energy sources is concerned, the hydrogen donor can be water, in most cases, or biomass. Biomass-derived hydrogen can be produced both through gasification and via biological fermentation processes.

On the other hand, considering the traditional technologies used for renewable energy production, i.e. hydroelectric, photovoltaic and wind power, the electricity produced with these methods is used as an intermediate to power a water electrolysis process.

By means of electrolysis it is possible to split the water molecule into gaseous hydrogen and oxygen, obtaining them as two separate products. Furthermore, the hydrogen produced from water electrolysis is of extremely high purity, making it suitable also for use in fuel cells.

Among all the examined hydrogen production pathways, in the present thesis work the attention is focused mainly only on hydrogen produced by electrolysis driven by renewable energy sources. Wind power electrolysis was considered in most of the case studies, while photovoltaic power and electricity taken from the grid in future scenarios were also explored as alternatives in some cases. Syngas deriving from gasification of lignocellulosic biomass was also addressed in some cases as an intermediate product and a carbon-donor for the production of carbon-neutral fuels.

Currently, the global demand of hydrogen in its pure form is estimated to be around 70 million tonnes (Mt) per year, mostly employed as a chemical for industrial processes such as oil refining and ammonia manufacture for fertilisers. A further 45 Mt H_2 per year is used in industry without prior separation from other gases (i.e. as a synthesis gas) for industrial processes such as methanol production or steel production via direct reduction of iron ore [28]. Its production almost entirely relies on thermochemical pathways involving the use of fossil feedstock, 76% from natural gas and almost all the rest, 23%, from coal. A certain amount of hydrogen is also produced from refineries as a by-product. Only around 2% of hydrogen is produced through electrolysis, mainly as a by-product in chlor-alkali industry, while less than 0.1% of dedicated hydrogen production globally comes from water electrolysis today, and the hydrogen produced by this means is mostly used in markets where high-purity hydrogen is necessary. Around 275

Mtoe of energy are used for the production of hydrogen today (2% of global total primary energy demand) [28].

1.3.3. Hydrogen transport and distribution

Regarding hydrogen transport and distribution, a small distribution network already exists in some places for the current industrial uses of hydrogen, consisting of short gas pipelines, with diameters of 25-30 cm and average pressures of 10-20 bar, or in limited road transports where hydrogen is stored in gas cylinders and loaded onto lorries. However, for an extensive deployment of hydrogen in end-uses of energy it is necessary to imagine at least an adequate network of gas pipelines for areas with high demand and road connections for areas with low demand, such as rural areas.

As far as hydrogen pipelines are concerned, these would require different materials from those with which natural gas pipelines are usually built. In fact, in some materials, hydrogen can cause a phenomenon known as “hydrogen embrittlement”, in particular in steels with a body-centred cubic crystal structure, especially when hydrogen is at high temperatures and/or pressures.

This phenomenon is generally not found with austenitic stainless steels, copper and aluminium and with their respective alloys, which therefore result as suitable materials for the construction of hydrogen pipelines and tanks. Some plastic materials such as polyethylene are also suitable for distribution pipelines at low pressure [29].

Currently, hydrogen is mainly distributed in the gaseous state by means of:

- cylinder packs, consisting of 16-20 cylinders and transported by lorry;
- (CGH2) tube trailers, i.e. semi-trailers equipped with a protective frame, containing a series of long cylinders stacked together, which can store compressed hydrogen, usually at around 200 bar; the material generally used is Chrome-Molybdenum steel to avoid hydrogen embrittlement. Steel tube trailers are most commonly employed and carry approximately 380 kg of H_2 onboard, anyway their carrying capacity is limited by the weight of the steel tubes. Recently, also composite storage vessels have been developed, allowing higher storage pressure (e.g., 500 bar), and these can reach capacities of 560-900 kg of hydrogen per trailer depending on the selected pressure and the tank volume. Such composite tube trailers are currently being used to deliver compressed natural gas in other countries [30,31]. The largest tank volumes for gaseous hydrogen

transport are currently 26 cubic meters, that at pressure of 500 bar results in a load of around 1100 kg hydrogen per lorry [32].

A smaller amount of hydrogen is distributed in liquid form, in large insulated cryogenic tanks kept at -252 °C, by sea transport, by rail, or by road with cryogenic liquid tanker lorries. In comparison to pressure gas vessels, more hydrogen can be carried with an LH2 trailer, as the density of liquid hydrogen is higher than that of gaseous hydrogen. At a density of 70.8 kg/m^3, around 3500 kg of liquid hydrogen or almost 40,000 Nm^3 can be carried at a loading volume of 50 m^3 [32]. Liquid hydrogen transport is usually more cost-effective over longer distances and LH2 trailers can reach a driving range of approximately 4000 km.

In a developed market, the transmission of gaseous hydrogen over long distances and its distribution would have similar characteristics to those of natural gas. In fact, this is not a new technology: a hydrogen pipeline over 200 km long was already built in Germany in 1939. The availability of a hydrogen pipeline would eliminate the risks of road transport and ensure a constant supply. However, the current global extension of hydrogen pipelines is limited to a few thousand km due to the high costs of the system (in turn due to the greater care required for gas tightness problems), the higher quality of the materials used to avoid the risk of embrittlement, the need for leak detectors and suitable safety devices. These high initial investments would be justifiable only in presence of large size end-users, that would therefore demand high volumes. Nevertheless, one possibility for developing pipeline networks for hydrogen distribution is local or regional networks, known as micro-networks or hydrogen valleys. These could subsequently be combined into transregional networks. Of the 4500 km of hydrogen pipelines totally already available worldwide the longest pipelines are operated in the USA, in the states of Louisiana and Texas, followed by Belgium and Germany [32]. In very recent times major projects have been announced for the construction of hydrogen pipelines in Europe, both for long-distance transmission and for shorter-distance distribution. Among these, some examples stand out such as the Mediterranean hydrogen pipeline "H2Med", which should be operational from 2030 and which will bring green hydrogen from the Iberian Peninsula to the rest of Europe. Portugal, Spain, France and Germany participate jointly in the project. The pipeline under the Mediterranean Sea will carry green hydrogen, made from water via electrolysis using renewable energy and it should supply about 10% of the European Union's hydrogen demand in 2030 or something like two million tonnes of hydrogen annually [33]. Another relevant project is the European Hydrogen Backbone initiative, consisting of a group of thirty-two energy infrastructure operators from 28 countries, aiming at the gradual creation of a large-scale and pan-European dedicated hydrogen network, starting from main corridors and based on new hydrogen pipelines to be built or existing natural gas pipelines to be repurposed [34]. In UK, under the framework of the “H21 programme” lead by the company “Northern Gas Networks”, multiple projects such as the “H21 North of England” and “Leeds City Gate” are demonstrating the feasibility of converting existing natural gas distribution pipelines (made of polyethylene) to hydrogen, especially for domestic use [29,35]. In any case, the possibility of reconverting existing pipes highly depends on the material they are made of and many existing traditional natural gas pipelines are not suitable for the transport of 100% hydrogen; however, there is also the need to replace pumping stations.

Finally, another possible solution for the distribution of hydrogen that is under study by several years is the blending of hydrogen with natural gas into existing natural gas pipelines [28,36]. This simple idea would allow to use hydrogen immediately, avoiding major storage and distribution problems. Blending can be performed with no or minor associated technical issues up to certain volumetric percentages. Many projects, first of all NaturalHy, have shown that usually, up to 20% by volume of hydrogen, there are no particular criticalities, but higher concentrations could be also feasible. Several papers connected to the EU project NaturalHy, completed in 2009, are downloadable from the project website [37]. In the case of blending even less valuable materials for pipes or tanks can be used, since hydrogen embrittlement is related to pressure, and at low concentrations the partial pressure of hydrogen in the mixture is low enough to greatly alleviate the embrittlement problems [38]. The end user could burn the mix of natural gas and hydrogen or could separate hydrogen for specific application (e.g., low temperature fuel cells). However, separating hydrogen from natural gas immediately before the end-use does not appear to be the most cost-effective route. On the contrary, the convenience of the mixtures lies in the fact that they could and should be used as they are. When burning the blend, it is necessary to take into account that some properties change depending on the hydrogen content. Recently SNAM, a leading Italian energy infrastructure operator, tested the distribution of natural gas added with $5\%_{vol}$ and $10\%_{vol}$ of hydrogen to a pasta factory and both distribution and utilisation were successful [39]. Together with Baker Hughes, SNAM also tested a gas turbine fuelled by natural gas blended with 10% of hydrogen [40] and demonstration projects continue to grow.

Thanks to the possibility of injecting hydrogen into existing natural gas distribution infrastructure, it would be possible to delay the significant investment in a dedicated hydrogen distribution network later in time, focusing first on increasing the production of hydrogen from RESs. It is also possible to vary the mixing percentages and this would ensure a gradual energy transition as well as a progressive reduction in CO_2 emissions. At the same time, this possibility has some disadvantages. First of all, an obstacle to be overcome consists in the harmonisation of the regulations regarding the percentage of hydrogen admissible within the gas network, not only at national level but also at the border level [28]. Secondly, a hydrogen injection could lead to an increase in the cost of natural gas for consumers, which must be carefully evaluated.

Another problem is linked to the lower calorific value of hydrogen per unit of volume compared to that of natural gas, which is reflected in the energy density of the mixture depending on the hydrogen content. The main concerns would be a reduction in the ability to transport energy by pipelines, the need for consumers to use larger volumes to meet an energy requirement, the adjustment of energy metering by gas meters and the purity of the gas supply for some industries. Finally, there are technical limitations on the percentage of hydrogen admissible in a mixture with natural gas. The upper limit of this amount is mainly dictated by the various users or equipment connected to the network, in particular by those with a lower tolerance level.

Some existing components already have a high hydrogen tolerance without any need for upgrades, for instance many European gas heating and cooking appliances can tolerate up to 23% hydrogen. The Ameland project, in Netherland, tested successfully some equipment for heat provision in buildings such as boilers, gas hobs and cooking appliances [41] with hydrogen mixtures with natural gas until 20%. In some cases, no problems were found until 30%. Other elements of the network such as gas meters and distribution and transmission networks also appear to have high levels of tolerance to hydrogen. Generally speaking, the most problematic elements from this point of view are compressors (10%), engines (5%), turbines (2-5%) and some type of compressed natural gas (CNG) tanks (2%) depending on the materials of which they are made, but in many cases it is possible to overcome these limitations with minor modifications which allow to increase their tolerance, for example by changing seals and nozzles in gas turbines [28,42]. These limit values often derive from legislative and/or technical limitations designed for generic cases, but there are components designed specifically for individual specific applications that can easily exceed them (e.g., some stationary internal combustion engines). Natural gas-hydrogen mixtures will also be addressed in other chapters of this thesis.

1.3.4. Hydrogen storage

Whichever the selected distribution model, the hydrogen storage issue will also need to be addressed, both on a large and small scale. In vehicular applications it is essential to have little weight on board and occupy the least possible volume.

For instance, in vehicle tanks, where accumulation density is very relevant, gaseous hydrogen can be stored at high pressure (350-700 bar) in cylinders made of composite or semi-composite material, and this seems to be, at the least for the moment, the most effective method.

The safety features are usually very high, thanks to the robustness of the tanks and the introduction of anti-explosion fuses and valves which intervene in the event of fire and circuit cut-off valves that act in the event of a collision.

More advanced solutions are also being studied, such as glass microspheres, metal hydrides, chemical hydrides and adsorption on activated carbon.

However, none of these technologies seems, for now, to meet the storage criteria desired by producers and users:

- gaseous phase storage is a mature technology, but, although the most used, still inadequate in terms of weight, volume and costs, therefore not particularly suitable for use on vehicles. In this sense, research aims to increase the ratio between the mass of stored hydrogen and the weight of the cylinder. The storage capacity in weight percentage of hydrogen (with respect to the cylinder weight) is currently around 5-6% for tanks in composite material, pressurised at 700 bar;
- liquid phase storage has better volumetric efficiency, which would make it more suitable for on-board vehicle use, but the complexity of handling liquid hydrogen, boil-off losses during storage and the energy required for liquefaction (about 1/3 of the energy content of hydrogen itself) make difficult its commercial outlet;
- metal hydrides, however very safe, allow storage at low temperatures and with reasonable volumetric efficiency, but they are heavy and managing their heating on board the vehicle poses many problems;

- chemical hydrides present issues related to cost, recycling, energy efficiency and infrastructure;
- adsorption on activated carbon is an emerging technology, but the knowledge of the process and that of the development of materials is still in the deepening stage; very contradictory results have been obtained with carbon nanotubes and carbon nanofibers and, at the moment, scepticism about this approach seems to prevail.

For innovative solutions, the durability of materials and the speed of hydrogen release must also be tested for thousands of load/unload cycles; fundamentally, since we are moving on an unexplored territory, the future is still uncertain.

1.3.5. Hydrogen use in vehicles

Another of hydrogen's strengths is that in addition to being a fuel it is also a very versatile chemical substance and therefore it lends itself very well to a wide variety of end uses, whether energy uses or not. Some of the possible uses of hydrogen will be addressed in other specific sections of this thesis (Section 1.5) and a more extensive and detailed description on the different possible uses of hydrogen is provided in *Publication 9*.

Given the relevance that hydrogen as a clean fuel for transportation and sustainable mobility applications has in this thesis, a brief overview of some aspects related to hydrogen use in vehicles is provided in this section.

The great hydrogen’s prerogative of high versatility of use, is also reflected in the field of mobility, where it can be used both for vehicles propelled by internal combustion engine and for those equipped with fuel cells. Internal combustion engines can accept and tolerate also hydrogen of lower purity.

Although in recent years there has been a rapid technological evolution to allow the electrification of some segments of the transport sector, fuels still remain a reliable option for the majority of transport modes. Potentially, all types of means of transport could be run on hydrogen or synthetic renewable fuels thus enabling emission reduction. In particular, hydrogen has been a subject of interest for many years as a potential clean transport fuel, since it can be produced from water and it could emit only water as its main waste product, especially if is used in a fuel cell. One of the main advantages of hydrogen in fact, is that it does not emit carbon in its direct use. Strictly speaking, when hydrogen is burned with air in internal combustion engines, it also produces low amounts of nitrogen oxides as a secondary relevant emission with respect to water [43].

In the past, vehicles with internal combustion engines fuelled only with hydrogen have already been tested, and currently some car models with proton exchange membrane fuel cells are already in the commercial stage. However, current automotive technologies for the use of pure hydrogen still present some problems, for example the lack of lubricating action by hydrogen in internal combustion engines.

Fuel cells, although they have made significant progress in the last decade, still present problems of relatively low durability and degradation of their electrochemical performance with prolonged use, at levels still considered problematic for the automotive industry or at least not yet competitive with traditional internal combustion engines, according to the U.S. DOE [44–46].

A further difficulty in using pure hydrogen, both for vehicles with internal combustion engines and for those with fuel cells, lies in the storage system and on-board fuel distribution system and on the lack of an extensive and widespread refuelling infrastructure.

For all applications in transport, hydrogen presents a main technical difficulty linked to the volume occupied: considering the energy content on a mass basis, hydrogen contains 120 MJ/kg (around three times more energy per kg than gasoline or diesel), but its energy content on a volume basis is very low, around 10.7 MJ/m^3 at standard conditions. Typically, the storage pressures used for transport applications are 350 bar and 700 bar (energy density of about 4700-4900 MJ/m^3, but still around seven times lower than that of conventional fuels). To further increase the energy density, hydrogen can be stored in liquid form, but this requires large amounts of energy for liquefaction. Furthermore, many other technologies for efficient, safe and compact hydrogen storage are under study. To date, very small amounts of hydrogen are used for automotive purposes, mostly in demonstration projects or, to a limited extent, in niche market present in some world regions such as California, Japan and Germany. In 2018, approximately 11,200 hydrogen cars were on the road, with a growth of 56% compared to 2017, equal to 4000 new cars sold [28]. Although they have been growing rapidly in recent years, these numbers are still very small when compared to the stock of battery electric cars in the same year (5.1 million) and to that of global cars (more than 1 billion).

From a hydrogen supply chain perspective, in addition to all the distribution and storage barriers already mentioned, the considerable shortage of refuelling stations for motor vehicles has to be considered, with a few refuelling stations present only in those countries that have begun to use small quantities of hydrogen even in road transport.

As already mentioned, in the automotive sector, hydrogen can be used in fuel cell electric vehicles (FCEVs) or in internal combustion engines (ICEs).

In internal combustion engines, the low level of exhaust emissions achievable at the vehicle tailpipe make hydrogen very interesting, as it would mainly emit water vapor according to the reaction:

$$H_2 + \frac{1}{2}O_2 \rightarrow H_2O \tag{1.1}$$

and, as a side effect of combustion, nitrogen oxides (NO_x) due to the high flame temperatures reached and the use of air as a comburent rather than pure oxygen, according to the Zeldovich mechanism:

I. $$O + N_2 \rightarrow NO + N \tag{1.2}$$

II. $$N + O_2 \rightarrow NO + O \tag{1.3}$$

III. $$N + OH \rightarrow NO + H \tag{1.4}$$

However, the energy contained in hydrogen can equally be released electrochemically, therefore in the absence of combustion, by means of a fuel cell, resulting only in emissions of water.

1.4. Power-to-fuel

In sections 1.2. and 1.3. the role of hydrogen as a potential clean energy carrier has been analysed. Hydrogen energy systems could revolutionise the current energy landscape and hydrogen, especially if produced from renewable energy sources, stands as an ideal energy storage system. However, barriers to the widespread adoption of hydrogen energy systems still remain, as highlighted in section 1.3, being distribution and storage the main bottlenecks in the supply chain. A possible solution to temporarily bypass the existing barriers could be to use hydrogen produced from renewable sources as an intermediate to produce carbon-neutral synthetic fuels or other hydrogen carriers and chemical substances. These fuels are usually based on the concept of combining renewable-based hydrogen with carbon-based substances (usually carbon dioxide) to produce hydrocarbons, or with nitrogen, as in the case of ammonia and urea. For a fuel to be carbon-neutral and environmentally sustainable (at least from a climate change perspective), in addition to hydrogen, it is essential to carefully evaluate the carbon source in order to obtain a closed carbon cycle, i.e. a circularity of emissions that leads to a neutral carbon balance. Basically, to be carbon-neutral, the synthetic fuel should produce no net-greenhouse gas emissions under its use for energy purposes. In this regard, possible suitable carbon sources to obtain a cleaner fuel could be biomass, waste, or carbon dioxide contained in air. Anyway, even industrial waste- and by-products such as fossil-based carbon dioxide deriving from combustion could be captured and used.

The advantage of using these renewable synthetic fuels, rather than pure hydrogen, often lies in the fact that they can leverage already existing infrastructure for distribution and storage, but also for the final use. In addition, they can be used to decarbonise the so-called "hard-to-abate sectors", where electrification is not possible or is not economically viable and fuels remain a more convenient choice.

Renewable synthetic fuels can be produced with various techniques. One of the best known is the so-called Power-to-gas. Power-to-Gas is a concept which aims to accumulate excess electricity deriving from renewable energy sources, in the form of chemical energy contained in a synthetic fuel, with the possibility of producing hydrogen and/or methane. Hydrogen produced by electrolysis is always the first step in accumulating renewable energy, but starting from hydrogen a wide range of other fuels or chemicals can be produced. In a broader sense, these production techniques are referred to as Power-to-fuel, since not all the producible fuels are gases, or Power-to-X when the end use is included.

1.4.1. Power-to-fuel role in renewable energy storage

This section highlights the strengths of Power-to-fuel as a solution for RESs energy storage on a large scale and for long periods of time. The content of this section is largely based on *Publication 6* and on the book "Power to fuel: how to speed-up a hydrogen economy", where further details can be found.

The renewable energy sources with the highest potential are solar and wind and luckily the cost of energy generated from these RESs is constantly decreasing. However, they mainly produce electric power which covers only around 20%-30% of the final energy demand, with the remaining part covered by fuels. Historically, the direction of energy conversion processes has always been from fuels to electricity, but today the reversal of this direction, that is from electricity to fuel, is carefully considered. The reason lies on the one hand in the need to replace fossil fuels with renewable and carbon-neutral fuels and on the other hand with the difficulty of storing the electricity obtainable from most RESs.

Unlike fossil resources, RESs are well spread on the planet and this is undoubtedly a great advantage. Unfortunately, the time distribution slows down the spread of exploitation. Almost all RESs are in fact characterised by a random availability accompanied by the lack of intrinsic storage capacity. Actually, apart from large hydropower, only geothermal energy offers constant availability, whereas tidal energy is variable, but its variability is foreseeable. Biomass can be stored, however, the sources whose exploitation shows the most favourable diffusion trend are solar and wind power, which generates electricity and are characterised by intermittency, with consequent mismatch between production and demand. Moreover, a local surplus of electric power could not be completely transferred to another region due to probable grid instability problems. This will force to find an energy storage solution to allow the continuous replacing of fossil fuels with renewable and non-climate-changing fuels.

Therefore, electricity from solar and wind can be fed into the grid only if there is an effective demand and if the quality of the energy produced is such as not to jeopardize the stability of the grid itself. Otherwise, it is necessary to accumulate the surplus electricity.

In the event that the problem lies in the lack of electricity demand, it is still possible to transfer the surplus to centralised storage systems, such as for example pumping stations. If, on the other hand, the inability to transfer electricity to the grid is linked to the poor quality of the energy produced, then it is necessary to increase in some way its quality or to store energy on-site.

Electricity can be easily stored in rather small amount and for short periods, whereas the most promising system for storing large quantities of energy over long periods seems to be the conversion of the surplus of electricity into hydrogen by means of the electrolysis process. Hydrogen would be a key element to significantly increase the exploitation of RESs and their penetration in the market well beyond the absorption capacity of the electricity grid. Furthermore, hydrogen could play an important role to achieve a greater energy system integration, creating new links between different sectors, energy carriers and infrastructures, which today are separate from each other. This would result in a more interconnected, flexible, efficient and cleaner energy system. Finally, electrolytic hydrogen produced from RESs power can also be used as a basis to obtain a variety of chemicals and synthetic carbon neutral fuels, such as those that will be presented in the following paragraphs.

Actually, it is not easy to go directly from electricity to a synthetic fuel and therefore the first step of a power-to-fuel process is always the power-to-hydrogen carried out through the electrolysis process. The production of renewable synthetic fuels can be decisive in accelerating the transition towards a system based mainly on electricity and hydrogen. In fact, among the synthetic fuels that can be produced, there are some that lend themselves very well to replace traditional liquid and gaseous fossil fuels, with the advantage of not requiring substantial changes to the existing distribution system. Another great advantage of synthetic fuels is the possibility of accumulating energy on a large scale and for a long time (from days to seasons).

An example above all, able to combine these advantages, is the synthetic renewable methane. Injecting synthetic methane into existing natural gas pipelines is probably the closest solution to obtain a vast decarbonisation of the energy system. As shown in Figure 4, this solution is suitable to store large quantities of energy and for a long time (hourly to seasonal storage), allowing therefore to solve some of the main obstacles to a greater diffusion of systems based on renewable sources.

Furthermore, power-to-methane systems can act as a bridge that connects the electricity grid and the gas grid increasing their flexibility and interconnection. By accepting storable chemicals produced starting from excess electricity from RESs, the gas grid can act as a huge energy storage pool, helping to achieve electricity grid balancing and the match between electricity demand and production.

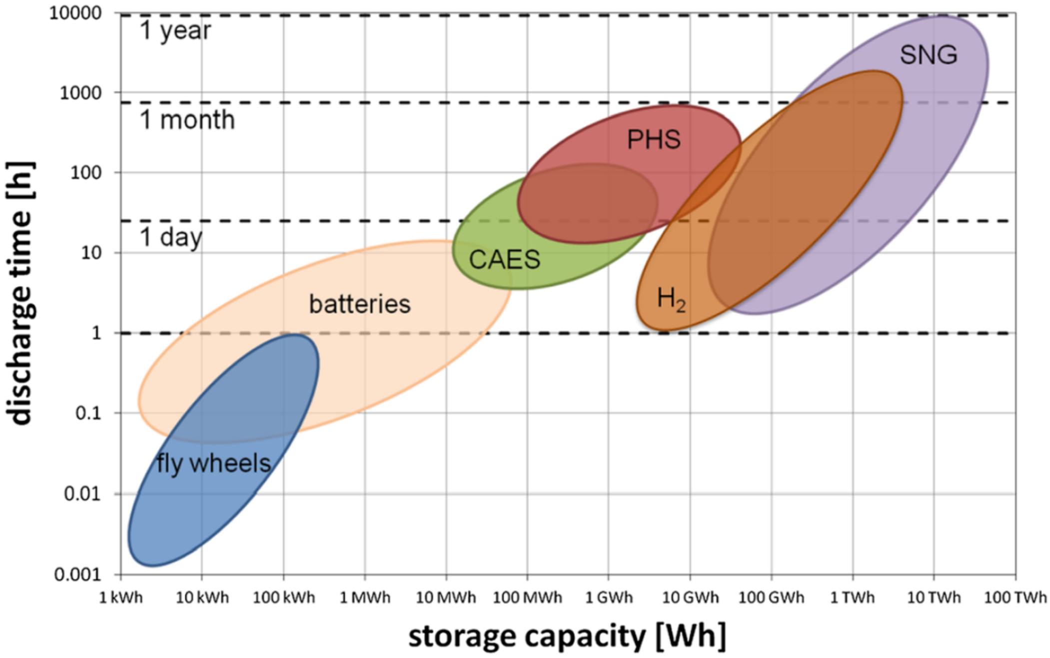

Figure 4. Comparison among different energy storage systems.
CAES, compressed air energy storage; PHS, pumped hydro storage; SNG, substitute natural gas [47]

In this way, it will be possible to increase the level of replacement of fossil fuels with carbon-neutral fuels and this will require an investment concentrated above all on a greater exploitation of renewable sources and on a greater production of hydrogen, leaving the investment in the pure hydrogen distribution infrastructure at a later date, when hopefully hydrogen storage and distribution systems technically better and less expensive than the current ones will be available.

The main synthetic fuels such as methane, methanol, dimethyl ether, ammonia, urea and formic acid which can be obtained by applying the concept of power-to-fuel are briefly described in the next section.

1.4.2. Main synthetic fuels

The most interesting synthetic fuels which can be produced starting from hydrogen and a carbon source are methane, methanol, dimethyl ether (DME), urea and formic acid. In addition, also ammonia, which does not contain carbon, can be considered, since it can be produced starting from electrolytic hydrogen and a source of nitrogen. Next sections report a brief summary of their characteristics. Table 3 shows a comparison in terms of energy content between various synthetic and traditional fuels.

Table 3. Energy density of different fuels [24]

Fuel	LHV [MJ/m^3]	Status[a]	HHV [MJ/kg]	LHV [MJ/kg]
Hydrogen	10.78	gas	141.86	119.93
	8491	liquid		
Methane	32.56	gas	55.53	50.02
	20920	liquid		
Propane	86.67	gas	50.36	45.60
	23489	liquid		
Gasoline	31150	liquid	47.50	44.50
Diesel fuel	31436	liquid	44.80	42.50
Methanol	15800	liquid	22.88	19.96
Dimethyl Ether	59.3	gas	31.68	28.70
	19230	liquid		
Ammonia	14.34	gas	22.50	18.65
	12700	liquid		
Urea	12103	solid	10.40	9.10
Formic Acid	5606.18	liquid	5.53	4.59

[a] For volumetric energy density, gas density is considered at STP conditions, liquid density at boiling point temperature and ambient pressure

The main potential carbon sources are fossil fuels, biomass and carbon dioxide. Obviously "green carbon" can be obtained only from biomass or directly captured from the air. Taking into consideration the low CO_2 concentration into the atmosphere, a very large volume of air should be treated to obtain even a single cubic metre of CO_2, with a great energy consumption associated. However researchers are working on carbon dioxide direct capture from air and new technologies are continuously developed [48].

During the transition to a carbon-free energy system we will continue to use fossil fuels, albeit in smaller and smaller quantities. So, there will be availability of carbon dioxide in great concentration at the smokestack of power plants and industrial plants that will make use of fossil fuels. These could be the main short- and medium-term carbon source. Oil industries are also working in this direction [49]. Obviously, a separation and purification process will be necessary.

The most used technology for carbon dioxide capture is chemical absorption with amines, either monoethanolamine or diethanolamine. Amines are liquid sorbents capable to separate carbon dioxide from a gas stream and regenerable by heating, generally using steam available inside the plant or generated by heat recovery. Other capture technologies are based on solid materials capable to adsorb carbon dioxide on their surface and releasing it by pressure or temperature changes. Porous or semi-porous membranes can also be used and in this case the driving force is given by the difference in pressure between the two sides of the membrane.

As already stated, also biomass can be a source of carbon. When biomass is burned or converted into a syngas or when biofuel is burned in a stationary plant, carbon dioxide can be captured with the same technologies above mentioned. An interesting alternative is the direct treatment with hydrogen of biomass (hydrogasification) or biogas (methanation).

Finally, it is interesting to consider the by-product of electrolysis: oxygen. Often electrolytic oxygen is released into the atmosphere if there is no possibility to sell it. The use of oxygen for oxycombustion of fossil fuels, biomass or biofuels allow to obtain exhaust gases with a higher carbon dioxide concentration and consequent easier capture process.

1.4.2.1. Methane

Methane is the lightest hydrocarbon composed by a carbon atom and four hydrogen atoms located at the top of a regular tetrahedron, in the centre of which the carbon atom is located. It was discovered and isolated by the Italian scientist Alessandro Volta in the second half of XVIII century.

At room temperature and standard pressure, methane is a colourless and odourless gas. It is non-toxic, but it is an asphyxiant since its presence in the air reduces the oxygen concentration. It is extremely flammable and may form explosive mixtures with air when in volume concentration between 5 and 15%.

It is by far the main constituent of natural gas, representing it for at least 85-90% by volume in most cases, and pure methane can be used for all applications in place of natural gas, including direct use in high temperature fuel cells. Moreover, large methane reservoirs in the form of clathrates ($4\ CH_4 \cdot 23\ H_2O$) are located on the ocean floor and in the arctic permafrost. These clathrates are not only a significant amount of fuel, but constitute also a potential risk for global warming, since the global warming potential of methane is 28-36 times and 84-87 times that of carbon dioxide over a period of 100 years and 20 years respectively [5,50].

Most of the world's methane emissions are anthropogenic and derive mainly from waste landfills, coal mines, oil industry, agriculture and livestock and for this reason its concentration in the atmosphere has more than doubled in the last 250 years, from the pre-industrial level of 722±25 ppb to 1803±2 ppb in the year 2011 [5].

Methane can also be produced starting from biomass and from the humid fraction of waste materials and, in this case, it is called bio-methane. The common process is anaerobic digestion, that allows to obtain a raw gas which main components are methane and carbon dioxide. A subsequent purification step proceeds to remove carbon dioxide to upgrade biogas to biomethane. In addition to being a renewable fuel, bio-methane contributes to reducing the emissions of climate-changing gases that would be emitted into the atmosphere due to the natural activity of microorganisms on the biomass left outdoors and on the wet waste sent to landfills.

Methane can also be obtained from methanation reactions, i.e. hydrogenation of carbon oxides with hydrogen:

$$CO + 3\,H_2 \rightarrow CH_4 + H_2O \tag{1.5}$$

$$CO_2 + 4\,H_2 \rightarrow CH_4 + 2\,H_2O \tag{1.6}$$

and this can be a renewable fuel when hydrogen is produced from a renewable energy source and carbon comes from biomass or from captured CO_2.

Reactions (1.5) and (1.6) are exothermic reactions favoured at low temperature. The reverse reactions, endothermic and occurring at high temperature, constitute the steam methane reforming process and together with the water shift reaction allow to generate hydrogen from methane. Therefore, methane can be considered also a hydrogen carrier.

The production of renewable synthetic methane from electrolytic hydrogen and CO_2 captured from a carbon source (e.g., from biomass) usually occurs thermochemically via the Sabatier reaction (1.6) inside adiabatic and fixed-bed catalytic reactors. However, several reactor types and different methanation pathways such as biological methanation exist. Further details and an extensive dissertation on power-to-methane are provided in *Publication 7.*

Since the major constituent of natural gas is methane, the gas produced via methanation is also often referred to as substitute natural gas (SNG). SNG will be also addressed in other chapters of this thesis.

1.4.2.2. Methanol

Methanol is the simplest alcohol and is composed by a methyl group and a hydroxyl group (CH_3-OH). It is a volatile, colourless, flammable liquid (flammability limits 6.7-36%), toxic with an odour similar to that of ethanol. Methanol is miscible with water and biodegradable, therefore unlike gasoline cannot accumulate in water, air or soil. It is used also as a polar solvent.

Methanol is industrially produced by hydrogenation of carbon monoxide:

$$CO + 2\,H_2 \rightarrow CH_4O \tag{1.7}$$

usually starting from a syngas obtained from partial oxidation of fossil fuels. A similar process can be accomplished also using lignocellulosic biomass as a feedstock and the final product is renewable and called bio-methanol. Obviously, the hydrogen required as a feedstock could also come from electrolysis using power from RES: this option can be known as Power-to-Methanol.

The production of "green methanol" via power-to-methanol is very attractive as it would allow for the decarbonisation of several sectors. In addition to being a fuel, methanol is also a very important basic chemical substance in the chemical industry (see also section 1.5.1.) and it could even be used to produce substitutes for gasoline, diesel or plastics. A number of other chemicals are derived from methanol. Regarding its use as a fuel, methanol can also be burned or used directly in low temperature fuel cells (Direct Methanol Fuel Cells).

Hydrogen can be obtained from steam reforming of methanol:

$$CH_4O + H_2O \rightarrow 3\,H_2 + CO_2 \tag{1.8}$$

therefore, combining reaction (1.7) and (1.8) methanol can be also considered as a hydrogen carrier. The main advantage of synthetic methanol versus hydrogen and methane as a hydrogen carrier lies in its liquid form at ambient conditions, which makes it easier to store and transport it, as it already happens with oil derivatives.

As in the case of methane, also methanol can be produced using a wide range of different reactor structures and different technological routes. Further details and an extensive dissertation on power-to-methanol are provided in *Publication 8*.

1.4.2.3. Dimethyl Ether

Dimethyl ether (DME) is the simplest ether (CH_3OCH_3) and is a colourless, non-toxic, non-carcinogenic, non-teratogenic, non-mutagenic and highly flammable gas in the range 3.4-27% by volume when mixed with air [51]. It can be produced by dehydration of methanol:

$$2\,CH_3OH \rightarrow (CH_3)_2O + H_2O \tag{1.9}$$

but even directly from syngas or biogas. Syngas can be produced from conventional feedstock such as coal, oil or natural gas but also from renewable sources including biomass, biogas or residues from agriculture or paper industry [52,53]. Furthermore, methanol can be synthesised from CO_2 and H_2. By using green methanol produced from power-to-methanol as a building block for the DME synthesis the production of carbon-neutral DME is possible.

Power-to-DME allow to produce a liquid DME product with a broad spectrum of applications as a green fuel, as a compound for the chemical industry and as a chemical building block for the production of value-added chemicals [54]. DME is a volatile compound, however liquefaction can be achieved by cooling to -24.9 °C at atmospheric pressure or by pressurizing to an absolute pressure of 0.6 MPa at 25 °C [53,55]. The vapour pressure is comparable to propane and butane, making DME a suitable substitute or blending component for liquefied petroleum gas (LPG). Furthermore, DME can be used as a green solvent, refrigerant and propellant. In addition to its application as final product, DME plays a key role as an intermediate in many subsequent synthesis routes for fuels and chemicals. Particular focus is directed towards the use of DME as an alternative fuel and energy carrier.

Besides the mentioned potential as LPG substitute DME is very interesting as an alternative fuel for diesel engines since it requires minor modifications of a diesel engine, is sulphur free and has a cetane number of 55-60, slightly higher than that of oil derived diesel fuel (51-54). DME is discussed intensively as a green fuel. A major benefit of DME compared to conventional fuels is the absence of carbon-to-carbon bonds, leading to a practically soot-free combustion [56]. This additionally entails the advantage that DME engines can be operated with higher exhaust gas recirculation rates in order to reduce NO_x emissions, regardless of the NO_x-soot-trade-off present at conventionally fuelled engines [57].

DME direct fuel cells have been also developed and tested [58]. Furthermore, hydrogen can be produced from DME, so that also DME can be considered a hydrogen carrier. Further details on power-to-DME can be found in [54].

1.4.2.4. Ammonia

Ammonia is the simplest nitrogen hydride, composed by a nitrogen atom and three hydrogen atoms (NH_3). It is a colourless gas, lighter than air, with a characteristic pungent smell. It was first isolated by the Scottish chemist Joseph Black. Its boiling point is -33.3 °C, whereas the freezing point is -77.7 °C. Ammonia can act both as a base, forming salts containing ammonium ion (NH_4^+), and as an acid, forming compounds containing amide ion (NH_2^-). The ammonia molecule is polar and highly miscible with water.

The Haber–Bosch process, developed by Fritz Haber and Carl Bosch in the first decade of XX century, is the main process for ammonia production. Hydrogen and nitrogen react together at high temperature (300-550 °C) and under high pressure (15-30 MPa). A mixture of iron, potassium oxide and aluminium oxide is used as a catalyst. The produced ammonia is then liquefied at -33.3 °C and separated from the residual gaseous mixture of hydrogen and nitrogen. The hydrogen used as a feedstock for the current industrial ammonia production process is produced starting from fossil fuels, typically via steam methane reforming, but it would be possible to use hydrogen generated starting from RESs to obtain “green ammonia” [59]. Nitrogen, on the other hand, is usually obtained by fractional distillation from air at cryogenic temperatures.

Although it is caustic and hazardous in its concentrated form, ammonia is widely used, especially at industrial level. It is a common nitrogenous waste, particularly among aquatic organisms, and it contributes significantly to the nutritional needs of terrestrial organisms by serving as a precursor to food and fertilisers. Ammonia is also used for the synthesis of many pharmaceutical products and for many commercial cleaning products.

In addition to being a chemical, ammonia is also a fuel, although it burns with difficulty in air and only when mixed at a concentration of 15-27%:

$$4\,NH_3 + 3\,O_2 \rightarrow 2\,N_2 + 6\,H_2O_{(g)} \tag{1.10}$$

However, it could also be used as a fuel in Direct Ammonia Fuel Cells.

Finally, ammonia can be decomposed in hydrogen and nitrogen when heated at high temperature (850-950 ºC) in the presence of a suitable catalyst (e.g., nickel). Therefore, ammonia can be considered also a hydrogen carrier, and actually it is one of the substances that has aroused the most interest, especially in the transport of hydrogen over long distances. With a relative molecular mass of 17.031 g/mol, the hydrogen mass content of one kilogram of ammonia is around 17.6%. Therefore, one litre saturated liquid ammonia contains more hydrogen (120 kg H_2/m^3) then one litre liquefied hydrogen at -265 °C (71 kg H_2/m^3). This fact offers to ammonia the potential to become the main carrier of renewable hydrogen.

Its high hydrogen content, the possibility to easily obtain its liquid form, its established infrastructure for both storage and distribution and the already established industrial know-how on how to handle it, make ammonia a prominent candidate for storing fluctuating renewable energy. Green ammonia produced from renewable sources is very interesting to achieve the decarbonisation of several sectors: it is in fact one of the most important substances in the chemical industry (see also section 1.5.1) and can be also used as fuel, raising particular interest especially for naval applications. Further details on green ammonia can be found in [60].

1.4.2.5. Urea

Urea was characterised in XVIII century by the Dutch chemist Herman Boerhaave and is an amide with formula $CO(NH_2)_2$, that is composed by two $-NH_2$ groups and a carbonyl functional group CO=. It is a colourless, odourless solid, highly soluble in water, and can irritate skin, eyes, and the respiratory tract.

The German chemist Friedrich Wöhler produced urea artificially in 1828, but the industrial process (Bosch–Meiser) was developed only one century later, in 1922. This process is based on the reaction between ammonia and carbon dioxide:

$$2\ NH_3 + CO_2 \leftrightarrow NH_4[H_2NCO_2] \tag{1.11}$$

The ammonium carbamate is then decomposed in urea and water by supplying heat:

$$NH_4[H_2NCO_2] \leftrightarrow CO(NH_2)_2 + H_2O \tag{1.12}$$

Urea is widely used in fertilisers because it has a higher nitrogen content than that of other solid fertilisers and because many bacteria can produce ammonia from urea.

Urea can be used as a hydrogen carrier: electrolysis of urea aqueous solutions requires a voltage of 0.37 V [61] that is much lower than the voltage required for water electrolysis. Moreover urea (and urine) can be directly used in alkaline fuel cells to produce electric power [62].

1.4.2.6. Formic acid

Formic (or methanoic) acid is the simplest carboxylic acid (HCOOH) and at room temperature is a colourless liquid having a penetrating odour, with flammability limits 12-38%. It is slightly toxic, but it is urticant: in nature it is found in some plants (e.g., nettle) and animals (especially ants), and actually its name comes from “formica”, the Latin word for ant. It was first isolated by the English naturalist John Ray and was first synthesised by the French chemist Joseph Gay-Lussac.

It is miscible in water, methanol, glycerol, and ethyl acetate. It is a strong reducing agent.

Formic acid can be obtained from several chemical processes, for example by hydrolysis of methyl formate in presence of a large water excess:

$$HCO_2CH_3 + H_2O \rightarrow HCOOH + CH_3OH \tag{1.13}$$

in a two steps process which produces the methyl formate from methanol and carbon monoxide:

$$CH_3OH + CO \rightarrow HCO_2CH_3 \tag{1.14}$$

resulting in the global reaction:

$$CO + H_2O \rightarrow HCOOH \tag{1.15}$$

Power-to-formic acid enables the production of a renewable chemical starting from hydrogen produced from RESs (e.g., via electrolysis) and captured CO_2. The interesting thing in this pathway is that, in presence of suitable catalysts, the global reaction has no by-products and all the hydrogen and carbon dioxide provided as reactants can be fully converted (see reaction (1.16) from right to left) [63].

Thermal decomposition of formic acid can produce carbon monoxide and water which in turn can be converted in carbon dioxide and hydrogen with the water gas shift reaction:

$$HCOOH \rightarrow CO + H_2O \leftrightarrow CO_2 + H_2 \tag{1.16}$$

Direct decomposition to hydrogen and carbon dioxide can be also obtained in presence of catalysts like platinum and ruthenium. Therefore, also formic acid can be considered a hydrogen carrier. The hydrogen content of formic acid is 53 g/l at room temperature and atmospheric pressure. Formic acid fuel cells have also been developed and tested.

1.5. Hydrogen and synthetic carbon-neutral fuels possible uses

This section provides an overview of the possible uses of hydrogen and carbon-neutral synthetic fuels, highlighting the opportunities for decarbonisation in various sectors. This section is largely based on *Publication 9* where more details are provided.

1.5.1. Industry

Hydrogen use today is dominated by industrial applications. In both pure and mixed forms, hydrogen is primarily used for oil refining (33%), ammonia production (27%), methanol production (11%) and steel production via direct reduction of iron ore (3%) [28]. Another future potential industrial use of hydrogen, currently still unexplored, would consist in generation of high-temperature heat.

Refineries

In refineries hydrogen is used as a feedstock, reagent or energy source, accounting for about 38 Mt H_2/year. This hydrogen demand is met for about one-third by on-site refineries by-products (e.g., from catalytic naphtha reforming), while about two-thirds are met by dedicated on-site production or merchant supply. Hydrogen in refineries is mainly used to remove impurities from crude oil, such as sulphur, and to upgrade heavier crude, through two processes: hydrotreatment and hydrocracking [28]. Hydrotreatment is the process by which sulphur is removed, together with other impurities, by crude oil to obtain low-sulphur diesel fuel for instance, and to meet regulation standards regarding a variety of fuels. This process is often simply referred to as “desulphurisation” and it is largely hydrogen consuming. Due to growing concern about air quality, increasing regulatory pressure is expected to further reduce the sulphur content of fuels, thereby increasing the demand for hydrogen by refineries. Hydrocracking is a process used to upgrade heavy residual oils into other oil products or lighter fractions, as they present a higher market value. In addition, hydrogen is used by refineries for a variety of other minor processes such as upgrade of oil sands and hydrotreating of biofuels. Under current trends, overall hydrogen demand in refineries is expected to grow by 7%, up to 41 Mt H_2/year in 2030 [28].

Chemical sector

The vast majority of hydrogen required by the chemical sector is produced from fossil fuels. The chemical sector output consists in a large variety of chemicals such as plastics, fertilisers, explosives and solvents. Anyway, seven primary chemicals can be considered: ammonia and methanol mostly, followed to a lesser extent by other “elementary bricks” used to obtain higher value chemicals, namely ethylene, propylene, benzene, toluene and xylene. These seven chemicals account roughly for around two-thirds of the chemical sector’s energy consumption and feedstocks. In particular, ammonia production (175 Mt/year), which requires 31 Mt H_2/year, and methanol production (97 Mt/year), requiring 12 Mt H_2/year, represent the second and third hydrogen consuming sectors. A large part of ammonia (around 80%) is used for production of fertilisers such as urea and ammonium nitrate, while the remaining part is used for the manufacturing of explosives, synthetic fibres, pharmaceuticals and other chemicals for industrial applications [64,65]. On the other hand, methanol is used as a basis for the production of several other chemicals like dimethyl ether (DME), formic acid, formaldehyde, methyl methacrylate and various solvents [66]. In some regions, methanol also find application in the methanol-to-gasoline process. Two other processes, still in the demonstration phase, namely methanol-to-olefins and methanol-to-aromatics could increase the demand for methanol, for the production of plastics and other high added value chemicals [67,68]. Demand for hydrogen for ammonia and methanol production is set to increase from today’s 44 Mt H_2/year to 57 Mt H_2/year by 2030 and to 65 Mt H_2/year by 2050, only accounting use in chemical industry, thus without taking into account the possibility of their use as hydrogen carriers or as synthetic renewable fuels [28].

Iron and steel production

Direct reduction of iron-electric arc furnace (DRI-EAF) is a method for producing steel from iron ore, using a mixture of hydrogen and carbon monoxide as a reducing agent [69,70]. This process today accounts for a hydrogen demand of 4 Mt H_2/year, corresponding to a 7% of the global primary steel production (1809 Mt of steel in 2018). Around 75% of this dedicated hydrogen production comes from natural gas, while the remaining 25% derives from coal. Like other sectors, also the iron and steel sector produce hydrogen as a by-product, often in mixed form with other gases (e.g., coke oven gas). A portion of this by-product hydrogen (9 Mt H_2/year) is internally consumed within the sector or burned inside blast furnace-basic oxygen furnace (BF-BOF) process and another part (5 Mt H_2/year) is distributed for use in other sectors [28]. Hydrogen produced via electrolysis could be therefore an interesting opportunity of decarbonisation for the existing steel production processes. Furthermore, in order to reduce steel production emissions, many efforts are being made to promote the development of novel "green steel" production processes, still in the demonstration phase, consisting in a particular DRI-EAF that use only hydrogen as the key reducing agent. First commercial scale plants are expected for 2030 [71]. On a current trend basis, the global steel demand is set to increase by around 6% by 2030. Hydrogen demand from the iron and steel sector would increase from 4 to 8 Mt H_2/year by 2030, accordingly with the growth of the DRI-EAF process, from 7% to 14% of primary steel production. In the hypothesis of a 100% steel production by means of DRI-EAF process by 2050, hydrogen demand could theoretically reach 62 Mt H_2/year [28]. Of course, even renewable methane could be used to provide heat or to replace the currently used fossil natural gas.

High temperature heat generation

High temperature heat production for use in industrial applications could become another important source of hydrogen demand in the coming years, although there are currently no applications in this regard. In the industrial sector, heat is a utility required for a wide range of different processes, such as chemical reactions, gasification, drying, melting etc. Heat can be used directly, as in a furnace or an oven, or indirectly by means of a hot fluid such as steam, air, pressurised-water and so on. The classification of heat for industrial uses is given on the basis of temperature ranges: low temperature (<100 °C), medium temperature (100–400 °C) and high temperature (>400 °C). The current demand for high-temperature heat in industry is about 1280 Mtoe/year, of which only 370 Mtoe/year (29%) are not consumed for chemical and iron/steel sectors. Roughly half of this high-temperature heat (185 Mtoe) is consumed inside cement production plants. To date, almost all industrial high-temperature heat derives from fossil fuels (around 65% from coal, 20% natural gas and 10% from oil). A small part of high-temperature heat is also produced by using biomass or waste. Electricity is widely used in industries to produce high-temperature heat, such as in the production of carbon fibre or in the electric arc furnaces, however electricity is often produced using fossil fuels. The level of demand for high-temperature heat is expected to grow, from 370 to about 400 Mtoe/year by 2030, which could potentially be provided by 130–140 Mt H_2/year [28] or 335 Mt of renewable synthetic methane.

1.5.2. Transport

Different aspects related to the use of hydrogen in vehicular applications have already been addressed in section 1.3.5. highlighting also the technical barriers to its widespread application, especially regarding distribution and storage for passenger cars. In this section instead, an overview of possible uses of hydrogen and other carbon-neutral fuels in cars, trucks and buses, ships and airplanes is provided. In the meantime, waiting for the main problems related to hydrogen to be resolved, the use of other renewable fuels produced through power-to-fuel could allow to circumvent these obstacles, using already consolidated technologies while reducing emissions at the same time. All synthetic fuels presented in section 1.4. have a certain range of potential applications in transport, in particular methane, methanol and dimethyl ether (DME) have direct uses also in internal combustion engines, while ammonia, urea and formic acid could primarily play a role as hydrogen carriers. Some of these fuels could also be used directly in specific fuel cells.

Cars

FCEVs have the advantage of having no tailpipe emissions (like battery electric vehicles) with exception for water, therefore they would reduce local air pollution and also global carbon dioxide emissions if "green hydrogen" is used. Furthermore, fuel cells have an efficiency of about 55–60%, more than double that the average efficiency of a conventional oil-fuelled ICE, drastically reducing fuel consumption. Due to their characteristics, proton exchange membrane fuel cells (PEMFC) type is mainly used in the automotive sector. When hydrogen is used in ICEs instead, tailpipe emissions mainly consist of water, variable amounts of nitrogen oxides (depending on the operating point of the engine) and very small amounts of carbon monoxide and particulate matter, resulting from the partial combustion of the lubricant oil. Even in this case a reduction in local air pollution would be obtained, if compared to that deriving from traditional gasoline or diesel vehicles. Furthermore, thanks to improved and faster combustion, the use of hydrogen increases the efficiency of the engine compared to a traditional vehicle, although not to the levels of efficiency obtainable with a fuel cell.

Another possibility, explored in the field of research, consists in the use of hydrogen mixtures with a traditional fuel (diesel, gasoline or natural gas) to feed an ICE. In this case, the advantage lies in reducing emissions and increasing efficiency, as hydrogen improves combustion characteristics. It also makes possible to use modest amounts of hydrogen, thus representing a possible temporary solution, while waiting for a greater diffusion of fuel cells. This solution is extensively explored in Chapter 3 of this thesis, in *Publication 1* and *Publication 4*.

One of the main obstacles to the spread of hydrogen as a fuel for transport lies in the scarce diffusion of refuelling points. On the contrary, natural gas can count on an already very extensive distribution network, especially in some countries (Argentina, India, Italy, for example). Renewable synthetic methane could replace the natural gas used today to power ICEs, referred to as compressed natural gas (CNG) vehicles. Similarly, renewable methanol and DME could also be used to feed ICEs, with characteristics similar to those of gasoline and diesel. In particular, DME is very suitable as a possible substitute for diesel fuel. Unfortunately, the calorific value of these two fuels is lower than that of traditional fuels: methanol has an energy content per kg equal to about 40% of that of gasoline, while DME has a lower heating value of 28.7 MJ/kg, equal to approximately 65% of that of diesel fuel. Finally, ammonia could also be used in ICEs, but due to the low flame propagation speed (5-13 cm/s), it is not optimal for use in automotive engines, however it may burn more rapidly if used in mixture with other fuels such as hydrogen [72]. Ammonia, urea and formic acid could instead be used as hydrogen carriers, even stored on board, releasing the hydrogen that they contain to be used for example in a hydrogen-powered fuel cell or in direct fuel cells.

Trucks and Buses

Regarding medium-duty and heavy-duty road transport, the same technologies already discussed for cars can be adopted. In this case, however, the power required by the propulsion system is greater, while there are less stringent limitations regarding the volume that can be occupied by the storage system. In this sense, fuel cell electric buses and trucks can take advantage of large hydrogen tanks and use lower storage pressures, usually 350 bar. Compared to battery electric buses and trucks, fuel cell ones have faster refuelling times (a few minutes versus a few hours), greater autonomy (km that can be travelled between a refuelling and another) and less weight of the energy storage system. Even in this case one of the obstacles to the diffusion of these systems, lies in the lack of a capillary supply infrastructure. Despite this, buses and trucks are seen as possible forerunners for the use of hydrogen, thanks to their mission characteristics: buses can refuel in their depot, run their public transport service for a certain time and then return back to the depot to refuel again. Therefore, by operating in hub-and-spoke missions, they can circumvent the problem of lack of refuelling points on the road. Trucks, on the other hand, are intended for long-distance journeys, especially long-haul trucks. They can therefore easily be used to reach two refuelling points even very far from each other without the need for intermediate refuelling, spending most of the time on highways, which could be more easily equipped with hydrogen fuelling stations.

As for cars, these vehicles can also use different technologies and alternative fuels. In some countries, CNG buses are quite common, and could easily run on renewable synthetic methane. The same applies to CNG trucks for logistical use, although less diffused. Higher-class trucks for heavier transports need monofuel CNG engines specially designed to meet the required power characteristics. IVECO and other companies are developing engines of this type and are carrying out research in the field of methane-hydrogen and diesel-hydrogen mixtures [73,74]. Also in this case, renewable DME lends itself well, due to its characteristics, to replace diesel fuel [75]. Ammonia and urea are already commonly transported on-board on diesel trucks, albeit in small amounts, to ensure the proper functioning of the exhaust gas after-treatment systems, known as selective catalytic reduction (SCR). On a technological level, therefore, it would be quite simple to transport ammonia or urea as hydrogen carriers, to then use the latter inside hydrogen fuel cells. The demand for energy from buses is equal to approximately 5.3% of the energy dedicated to road transport, or around 107.2 Mtoe, of which 104.9 Mtoe of oil and 2.3 Mtoe of natural gas [76,77]. Energy demand by trucks corresponds to 31.7% of the energy dedicated to road transport, or approximately 636 Mtoe (622 oil + 14 natural gas) [76,77]. Detailed analysis on the possible demand for synthetic renewable fuels are provided in *Publication 9.*

Trains

Rail transport is already widely electrified in many countries. Anyway, hydrogen could be used to meet decarbonisation targets in non-electrified railways. Today, non-electrified lines are mostly served by diesel-powered trains. Some of these lines could easily be electrified, at low cost and with minor technical complications, while for other lines the electrification costs are very high or construction feasibility is technically challenging. In these situations, hydrogen fuel cell trains could take over, replacing diesel-powered trains. Some Alstom demonstration projects have already been launched in Germany, with Coradia iLint train, while some countries have already planned to purchase tens of hydrogen trains for the next few years, like UK, France, and recently also Italy with an agreement between Snam and Alstom [78,79]. Hydrogen fuel cell trains could be competitive especially for long distance movement of large trains combined with a low-frequency network utilisation. These two conditions are quite common for rail freight. The energy demand from non-electrified trains, therefore fuelled with diesel or petroleum-derived fuels, is equal to 28.84 Mtoe/year [76,77]; detailed analysis on the possible demand for synthetic renewable fuels is provided in *Publication 9.*

Ships

Ships are typically powered by large and slow two-stroke diesel engines. In the naval sector, growing environmental concerns are slowly translating into regulatory pressures, in particular on the acceptable sulphur content in the diesel fuel burned and on emissions of nitrogen oxides and sulphur oxides. Nevertheless, the International Maritime Organization (IMO) has set the goal to reduce the total annual greenhouse gas emission by at least 50% by 2050 compared to 2008 and, eventually, fully eliminate harmful emissions [80]. Limitations on CO_2 emissions instead have been set via the energy efficiency design index adopted by IMO. To achieve these goals, the global maritime industry has begun to consider carbon-free and sulphur-free fuels such as hydrogen and ammonia, or carbo-neutral synthetic fuels such as renewable methane or renewable methanol. The application of hydrogen fuel cells or electric batteries has been demonstrated on small ships used for shorter routes like ferries, but it still appears to be temporally distant for trans-oceangoing vessels [81]. Over the years, Man Energy Solutions has tested and developed various marine engines capable of using alternative fuels, including natural gas and liquefied natural gas (LNG), liquefied petroleum gas (LPG) propane and butane, ethane, ethanol, methanol, and finally ammonia. Hydrogen in gaseous or liquid form would also be a suitable fuel for marine ICEs. Compressed gaseous hydrogen entails major problems regarding the volume occupied by storage tanks, with consequent loss of cargo, while liquid hydrogen (at -253 °C) has a higher volumetric energy density but requires the use of cryogenic tanks. Liquid hydrogen ships could also be used for hydrogen imports and exports, consuming a small part of it for the propulsion of the ship itself. As already happens for LNG, liquid hydrogen would then need to be brought back in gaseous form once on land. For some boats and ships, the metal hydrides option is very interesting. They are very compact and very safe, but for mobile applications they have the drawback of being very heavy. However, this is not a drawback for boats and ships which have a fixed ballast to provide stability since metal hydride tanks can replace such a ballast. Ammonia is also a very promising fuel for ships: it constitutes a quite good energy storage solution since it has a higher volumetric energy density than liquid hydrogen, but it is less expensive and complex to transport and store. Used as a fuel inside an ICE, it does not emit carbon or sulphur. In the case of marine engines, which are much slower than automotive ones, the ammonia flame propagation speed is sufficiently high [82]. Moreover, ammonia can count on well-established production, management and storage methods, therefore has the potential to enter the market relatively quickly. If “green ammonia” were used, it would also possible to strongly reduce the carbon footprint. Finally, ammonia transported by ship could act not only as a fuel but also as an efficient liquid hydrogen carrier for hydrogen imports/exports. Another important characteristic of ammonia is related to safety on board, because ammonia is much less explosive than hydrogen. Australia has recently launched a strategy that plans to export large amounts of green ammonia by ship to Japan and China, where it would then be converted into hydrogen [83,84]. Currently, the worldwide energy demand from ships amount to 271.3 Mtoe [76] and detailed analysis on the possible demand for synthetic renewable fuels is provided in *Publication 9*.

Aviation

Decarbonisation is a major challenge for aviation. The aviation sector is responsible for the emission of about 900 Mt CO_2/year. Despite the fact that the efficiency improvement targets are set by the International Civil Aviation Organization (ICAO) at a growth of 2% per year [85], emissions are expected to more than double by 2050. The Air Transport Action Group (ATAG) has set a goal of a 50% reduction in CO_2 emissions by 2050 compared to 2005 levels, while the European Union has set a more ambitious target of carbo-neutrality by the same year. In addition to carbon dioxide, aircraft also emit carbon monoxide, unburned hydrocarbons, nitrogen oxides, soot, and water vapour, which create contrails and cirrus clouds [86]. Given these targets, it is urgent to start implementing decarbonisation measures, even in the short-term. To date, aircraft mostly use jet-fuel or jet-propellant, a fuel derived from kerosene, within aircraft turbines or piston-based engines. In some cases, this can also be derived from – or mixed with – gasoline or naphtha, depending on the type of aircraft or engine. Although revolutionary electrically-propelled aircraft have been proposed, such as those powered by photovoltaic cells, fuel cells, or ultracapacitors, gas turbines will remain the most reliable and economically competitive option for many years. This is also because gas turbines have an excellent ratio between power output and weight, combined with the high energy density of liquid fuels, which allows aircraft to travel long distances. In this sense, large commercial aircraft, especially those used for longer journeys, seem to have few alternatives to liquid fuel, at least for the short and medium term. Moreover, there are rigorous safety procedures, which imposes stringent quality standards on the characteristics of the propellant fuel used. Considering that aircraft are often refuelled in different countries, and that some countries could have different jet fuel quality, it is required that these technical fuel specifications are harmonised [85]. To face environmental problems even in the near term, the aviation industry is developing alternative Sustainable Aviation Fuels (SAFs). These can be of the "drop-in" type, that is kerosene-like fuels, which can be distributed with the same infrastructure and can be burned in the same aviation turbines already in use without any adaptation, while allowing emissions to be reduced. Drop-in SAFs therefore, represent a quick substitute for conventional jet fuel, completely interchangeable or mixable with it, and can be used “as is” on currently flying aircraft. On the contrary, any “non-drop-in” SAF would involve safety concerns and major adaptations. To meet these characteristics, a certain number of drop-in SAF have been under developing in recent years. Among these, biofuels are very promising, such Hydroprocessed Esters and Fatty Acids (HEFA) that can be produced from biomass or waste, and other advanced biofuels producible from crops, algae, non-food biomass, municipal wastes, cooking oil and agricultural residues. Another important option is given by the so-called “synfuels” or “electrofuels” that use power combined with Fischer-Tropsch process to produce a liquid drop-in SAF similar to kerosene. By combining electrolytic H_2 produced from RES and CO_2 captured from a non-fossil source, a carbon-neutral drop-in fuel can therefore be obtained.

The global energy demand from aircrafts amounts to 323.4 Mtoe [76]. Through power-to-fuel technologies proposed in this thesis, aircrafts could be powered alternatively by hydrogen in fuel cell, hydrogen in turbine (better if liquid but also in gaseous form), or renewable methane, methanol, DME or ammonia in turbine. All these fuels are potentially exploitable to power aircraft, but not being “drop-in” type fuels, they are among the new propulsion technologies. The combustion of hydrogen inside aeronautical turbines (with low-NO_x emission) is feasible, but requires the development of dedicated turbines still under study and the resolution of storage systems and refuelling problems. Assuming these technical developments, H_2 propulsion would be initially best suited for commuter, regional, short-range, and medium-range aircraft. Even long-range aircrafts could be powered by hydrogen, but they would be subject to major design changes and to the evaluation of economic convenience to 2050. Already in the early 2000s Airbus together with other airlines, universities and research centres explored the use of liquid hydrogen in aircrafts as part of the Cryoplane European project, while in recent years other projects involving hydrogen aircrafts financed by large private investors have begun to flourish [87,88]. Finally, for all new propulsion technologies, the year of entry-into-service must be taken into consideration. Conventional aircraft development cycles occur about every 15–20 years until a new aircraft platform is introduced, while older fleets retire. For short-range aircraft, which make up the bulk of emissions, the next window of opportunity is expected to be around 2030–2035 [86].

1.5.3. Buildings

The global buildings sector alone accounts for 2848 Mtoe, corresponding to about 30% of total final consumption of energy. Of this energy demand (electricity included), 72.4% comes from the residential sector and 27.5% from commercial and public services. About 2200 Mtoe of this energy is dedicated to heat provision, such as space heating, hot water production and cooking. Roughly, half of this is produced directly from fossil fuels: natural gas accounts for 630 Mtoe, oil products for 299 Mtoe and coal for 109 Mtoe [28,76]. Most of the remaining heat production in buildings is met by electrical equipment as electric resistance radiators and induction cook-stoves, heat pumps but also by district heating. To date, this energy is also produced mostly (85%) from fossil fuels, even if indirectly. Besides, solid biomass for heating purposes is still very significant in developing countries. Overall, the buildings sector is responsible for a 28% of global CO_2 emissions related to energy uses. With respect to heat provision, it is very likely that various technologies will coexist in the future, taking into account also as geothermal and solar thermal energy and heat pumps. In this scenario, power-to-fuel offers many possibilities for decarbonisation, both in the near and in the long term. The first that can come to mind is the partial or total replacement of natural gas with renewable synthetic methane. This would make it possible to continue to use the already existing distribution infrastructure as well as existing devices such as natural gas boilers. Even hydrogen arises as a suitable decarbonisation solution both in the near term, through injections in small amounts in the natural gas pipelines, and in the long term in a dedicated 100% hydrogen infrastructure.

Renewable methane

To date, the global methane distribution network can count on a large extension of approximately 3 million km of pipelines, to which are added an enormous underground storage capacity and international trade of LNG transported by ship. The global demand for natural gas today is approximately 3900 billion of m^3, corresponding to 3106.8 Mtoe [76]. Replacing all this natural gas with biomethane would be impossible due to concerns about land use change and competition of energy with food crops. Even considering replacing with biomethane only the 630 Mtoe of NG used for heating buildings, it would mean facing a 90-fold increase in biomethane production in the European Union and a 20-fold increase with respect to current world production [28]. Power-to-methane could overcome these limitations by producing renewable synthetic methane. Compared to hydrogen, the disadvantage consists in a lower production efficiency and a higher cost, associated with the additional methanation process.

This could probably lead to an increase in gas prices for final consumers, if compared to fossil natural gas. Regarding the production of heat in buildings alone, power-to-methane could replace the 630 Mtoe of natural gas used today with 527 Mt CH_4 of synthetic renewable methane, while the replacement of all fossil fuels used for direct heat provision in buildings (1038 Mtoe) would need 868 Mt CH_4.

Pure hydrogen

Currently, hydrogen is not used in the buildings sector, except for some demonstration projects, which are trying to explore different possible future uses of the fuel. Some of these projects are experimenting hydrogen blending in the natural gas pipelines, other projects instead involve supply of pure hydrogen to various devices such as hydrogen boilers, fuel cells or burners. The current largest project regarding 100% hydrogen supply via dedicated hydrogen pipeline to buildings is the H21 North of England [29]. This project also demonstrated the feasibility of reusing the existing (polyethylene) pipeline network and it is testing hydrogen boilers. In addition, the largest demonstration projects concerning stationary fuel cells for residential and commercial buildings and cogeneration for residential use are ene.field in Europe and ENE-FARM in Japan [89,90]. In the Japanese project, natural gas or LPG are reformed locally to produce hydrogen to feed fuel cells, thus bypassing the problem of hydrogen distribution up to the building. In addition to generating electricity, hot water is also produced for domestic use, achieving a total declared energy efficiency of 97% [91].

Coming to a future perspective, a complete electrification of consumption by means of electric heat pumps is not adequate for some type of buildings: unless major improvements are made in building energy efficiency at the same time, these could lead to large seasonal imbalances in the demand for electricity. Anyway, there are many opportunities for hydrogen use in buildings, which can be classified into two main categories: hydrogen blending in existing natural gas network and direct use of pure hydrogen for heat (and/or electricity) production in buildings. A third option regards indirect use of hydrogen to heat or cool buildings by using centralised systems in neighbourhoods.

From a longer-term perspective, if a dedicated 100% hydrogen distribution network were developed, it would be possible to meet the energy demand of buildings in different ways. Hydrogen boilers could provide the thermal energy necessary for space heating of buildings and for the production of hot water, without any CO_2 emissions. Another option is the cogeneration of heat and electricity using stationary fuel cells, as already seen for the ene.field and ENE-FARM projects. Finally, heating, cooling and electricity demand of buildings could be met by sending hydrogen to local district power plants for the cogeneration of electricity and heat and distribution of hot or cold flows through district energy networks. Potentially if hydrogen became cost competitive, it could replace all the natural gas dedicated to the production of heat for buildings with 220–362 Mt H_2.

Another possible solution, particularly interesting in the short-term, is blending hydrogen with natural gas, that was already addressed in section 1.3.3.

1.5.4. Power generation

In 2017, 25,606 TWh of electricity were generated globally: 21,605 TWh came from electricity plants and 4001 TWh from CHP plants. Fossil sources together account to a total of 64.78% of electricity generation, using an amount of primary energy of 2351 Mtoe of coal, 215 Mtoe of oil and 1200 Mtoe of natural gas. It could be thought of directly replacing electricity generated from fossil sources with electricity generated from RESs, however the non-programmability of RESs constitutes an obstacle to their greater exploitation. To increase the possibilities of RESs exploitation, an energy storage system is needed to decouple production from demand. One of the possibilities is to produce a synthetic fuel, easier to store, and then reconvert it in electricity when needed. This technique is also known as Power-to-Power. Although this double conversion involves significant efficiency losses, to date it represents one of the few viable and reliable alternatives to store energy on a large scale and for long periods (e.g., seasonal storage).

All the synthetic fuels presented in section 1.4. offer various opportunities for decarbonising the electricity generation sector. In general, the greater the number of conversion steps, the greater the energy losses and the reduction in efficiency. From this point of view, hydrogen would be the most advantageous solution; however, the possibility of using existing distribution infrastructures and more or less consolidated technologies, also increases the interest in more complex fuels such as synthetic methane and ammonia. Taking methane as an example, which is already one of the most widespread energy sources, it could be possible to replace natural gas burned today in power generation plants, with around 1004 Mt of renewable synthetic methane, without making any change to the existing plants. If electricity generation from coal and oil were also totally replaced by synthetic methane, 1968 Mt CH_4 and 180 Mt CH_4 would be needed respectively, for a total of 3152 Mt CH_4 to obtain a complete defossilisation of this sector using already proven technologies.

To date, hydrogen is not used for the generation of electricity, except in very few industrial sites where it is recovered as a waste product from nearby petrochemical or steel industries and then burned in a gas turbine or an internal combustion engine to produce electricity, or in a few small-scale demonstration plants such as power plants with stationary fuel cells. Several examples of power generation from hydrogen (pure or mixed with other substances) in demonstration projects or real applications that have existed for decades, at both small and medium scales, are provided in *Publication 9*. In addition to traditional power plants and distributed generation with stationary fuel cells, other possible interesting applications for the generation of electricity, using fuel cells, consist in the supply of electricity in those situations where one cannot rely on the grid, namely portable generators, uninterruptible power suppliers and off-grid power solutions. Renewable synthetic methane could be used also (directly or after local reforming) to feed solid oxide fuel cells. Ammonia is another promising synthetic fuel for power generation, as it can be used either as a hydrogen carrier or as an actual fuel, alone or in combination with other fuels, in a boiler, a turbine, an internal combustion engine or even in a fuel cell.

Renewable synthetic fuels in power generation

Many fossil fuel plants currently already in operation will remain so for many years to come. In this sense, it is essential to find a way to reduce as much as possible their emissions. Most of the synthetic fuels already presented can be used alone or in combination with traditional fuels in existing power plants with only minor plant changes.

For instance, hydrogen could be co-fired together with coal, oil or natural gas in a traditional boiler for steam generation, or blended with natural gas in different concentrations and burned in a gas turbine. This technique is known as dual fuel combustion. The reduction of emissions in this case would be greater than the simple reduction due to the replacement of a part of fossil fuel, as the addition of hydrogen also improves the characteristics and completeness of combustion. Similarly, hydrogen can also be mixed with oil or gas in internal combustion engines for stationary generation, as already discussed for engines for transport applications. Another option consists in the so-called attached-cycles: in this case hydrogen is not co-fired with the fossil fuel, but is burned with oxygen in a mixing superheater, to superheat the evolving fluid from within the fluid itself [92]. The oxycombustion of hydrogen in fact generates only water vapour and heat. Taking a traditional coal-fired steam plant as an example, it is possible to replace the traditional superheater with a mixing superheater of this type. On the one hand, this simplifies the plant layout, avoiding the necessity to return to the boiler to re-heat the steam, on the other hand it makes possible to reach much higher superheating temperatures, thus improving plant efficiency and performance with respect to a traditional steam plant. Given its high hydrogen content, ammonia can also play similar roles to hydrogen and can be used as an energy storage and then decomposed to obtain hydrogen, or directly as ammonia in combination with fossil fuels. In this sense, the co-combustion of ammonia with coal seems very promising, since ammonia is currently cheaper and easier to store and manage than hydrogen. Some examples of demonstrative projects on the megawatt-scale that require only minor changes to traditional plants are provided in *Publication 9*.

Regarding electricity generation based 100% on renewable synthetic fuels, there are still some technical challenges that make this option more likely for a medium-long term time horizon. Most of the gas turbines used today are already able to accept hydrogen levels from 3 to 5%, some can accept up to 30%, while in other cases percentages close to 100% can be reached depending on the design of the turbine [93,94]. Standard turbines capable of being fuelled entirely with hydrogen are expected by 2030 [95,96]. Ammonia direct combustion in gas turbines has been already demonstrated in some micro gas turbines (powers lower than 300 kW) [97], while larger gas turbines (>2 MW power) present some technical hurdles that researchers are trying to solve, such as flame stability and speed or containment of nitrogen oxide emissions [72]. Furthermore, for hydrogen the possibility exists of carrying out advanced thermodynamic cycles which reckon on direct steam generation, by means of oxycombustion of hydrogen in special burners/mixture superheaters, which mix the steam already present with that generated by hydrogen combustion. The steam thus obtained is made to expand in a steam turbine, but the thermodynamic efficiency of the cycle is higher with respect to a traditional Hirn cycle because it is possible to exceed the temperature limits, normally dictated by the boiler [92]. To make the most of these cycles would require turbines and materials capable of withstanding high temperatures, which could be developed in years to come. Synthetic fuels obtained through power to fuel, in particular hydrogen, synthetic methane, methanol, DME and ammonia, can also be used in internal combustion engines for stationary generation, such as those for cogeneration plants. Fuel cells stacks can also be used to obtain a decarbonised and flexible electric energy system at the same time. These have several advantages, in fact they have a high efficiency (today around 50–55%) and show little or no emissions, moreover they are modular and without moving mechanical parts, which makes construction and management very simple both for a centralised generation plant or a distributed generation system. To date, however, stationary fuel cells still have to face some weaknesses, such as high costs, a shorter lifespan and lower power than turbines. At the moment, therefore, fuel cells seem more suitable for distributed generation, but in the future a normal building could house several modular fuel cell stacks for a zero-emission power plant. Furthermore, fuel cells, depending on the type of cell, can be fuelled not only with hydrogen, but also with methane, methanol, ammonia, urea and formic acid.

Bakcup and off-grid power

Some applications require an uninterrupted supply of electricity even in the event of a blackout. In this case the constant supply of electricity can be guaranteed through uninterruptible power suppliers that are activated only when needed. Moreover, isolated or mobile applications exist. In this case power generators are required. Nowadays, most generators for back-up electricity supply or for off-grid applications are internal combustion engines, often fuelled by diesel. Even hybrid systems with diesel generator and batteries or photovoltaic panels and batteries are used, while fuel cells, still not very widespread today, could represent in the near future the optimal solution to reduce emissions in this sector. The most promising fuel cells for this type of applications are currently those fuelled by hydrogen, methanol or ammonia, directly or after reforming. These systems are used for example for data centres, telecommunication towers, hospitals or rural villages and small islands. Many telecom towers, especially in developing countries, are powered by diesel generators, as they are located in hardly accessible places where the electricity network is absent. Some telecom base stations in South Africa and Kenya are already powered by fuel cells today in the context of experimental projects [98–100]. Hospitals and clinics, as well as data centres and some banks need protection from blackouts. In this case, dedicated generators or uninterruptible power supplies with fuel cells could be used. In South Africa, a clinic that needs a continuous supply of electricity to refrigerate vaccines and medicines has relied on an uninterruptible power supply with stationary fuel cells since 2015 [101,102]. Even in case of emergencies where it is not possible to rely on the electricity grid, such as field hospitals or relief in the event of hurricanes or earthquakes, mobile generators with fuel cells could be used, but also in outdoor events or concerts. Another case of stationary generation demand may come from non-electrified rural villages. Some trial project in South Africa have provided electricity to small rural villages using methanol fuel cells with appropriate methanol tanks and batteries [103,104].

Long term and large-scale energy storage

Energy storage on a seasonal scale can make possible to balance seasonal variations both in terms of electricity demand and supply. Especially in an energy system strongly or totally based on RESs, it will be necessary to store huge amounts of energy. Some criticalities of batteries and hydro pumping storage systems have already been highlighted in section 1.2. Although there are various other alternatives for energy storage, such as flow batteries or solid-state batteries, flywheels and accumulation of compressed air, the best viable solution seems to be the power-to-fuel technology which does not suffer from losses of stored energy along the time.

As anticipated in section 1.4.1., one of the advantages of the power-to-methane technology is the possibility of energy exchange between the electricity grid and the natural gas network which can be seen as a huge storage basin for renewable sources. As is already the case with the natural gas infrastructure, synthetic green gases can also be stored for entire seasons in underground caves or salt caverns. Salt caverns, thanks to their characteristics of good tightness and low gas contamination, appear very promising in particular for the storage of hydrogen. In addition, other underground storage systems are currently being studied, such as depleted oil or natural gas fields and pore storage. Ammonia is another suitable synthetic fuel for long-term and large-scale energy storage, since large steel refrigerated tanks are already commonly used in the fertiliser industry for storing liquid ammonia.

1.6. Assessment of hydrogen energy systems and carbon-neutral fuels under a life-cycle perspective

The previous sections highlighted the role of renewable hydrogen as a possible key factor for the decarbonisation of many sectors and the main challenges to a widespread adoption of hydrogen energy systems. In this sense, *Chapter 1* has already highlighted some possible technical solution, such as the production of carbon-neutral fuels. The alternative solutions proposed in this thesis, which will be addressed in detail in *Chapters 3* and *4*, generally focus on trying to circumvent the main existing bottlenecks to the development of a hydrogen energy system. This is valid both in the case of hydrogen use in sustainable mobility (*Chapter 3*), and in the case of carbon-neutral fuels (*Chapter 4*).

In any case, beyond being technically and economically viable, it is essential to verify that the proposed alternative solutions are valid, or at least better than the conventional options, both from an energy and an environmental point of view.

Regarding environmental-related aspects, both hydrogen and synthetic carbon-neutral fuels are energy carriers, and they are often referred to as “zero emission fuels”. This is because, in their use, they do not involve direct carbon emissions or net greenhouse gas emissions, respectively. However, one aspect needs to be clarified: in reality, there is no human activity that does not have an environmental impact, and these fuels are no exception. Since hydrogen and synthetic carbon-neutral fuels do not show particular environmental criticalities in their use phase, comprehensive analyses that can evaluate their environmental profile under a holistic life-cycle perspective are needed. In this regard the Life Cycle Assessment (LCA) methodology arises as a well-established tool and details on methodological aspects are provided in *Chapter 2*.

Actually, (as it also happens for electricity) it may be that the environmental burdens of hydrogen and carbon-neutral fuels simply shifted to other stages of their life cycle, such as, for instance, at the stage of their production. In fact, being them energy carriers, their production stage generates an environmental impact that these fuels carry with them even before being used. For instance, in case one is focused on the impact related to climate change and greenhouse gas emissions, this concept is known as carbon footprint. To ensure a low carbon footprint, their production should rely on renewable or low-carbon energy sources. Under this perspective, although conceptually simpler and more intuitive, it is probably not sufficient to talk only about “green hydrogen”: life-cycle analyses can provide an accurate and scientifically sound value of the environmental impact linked to hydrogen production, which can be seen as a certain shade of green. The creation of an established market for hydrogen and other renewable fuels will not be based simply on colours, but will require the creation of reliable environmental labelling schemes based on the full life cycle of these fuels.

Another relevant point is that – as in the case of vehicular applications – in addition to the production impact of the fuel, more sophisticated (and impactful) technologies could also be required for the use of the fuel itself. For example, in the case these fuels are used in “zero emission” vehicles, some of the overall environmental impact may have simply shifted to the vehicle itself (e.g., to vehicle production or final disposal).

Clarified the general context and the background in which this doctoral thesis is framed, the main goals, methodological aspects and results of the research activities carried out are presented below.

Chapter 2

Objectives and methodology

2.1. Objectives

The general aim of this doctoral thesis is to propose innovative and effective strategies that could facilitate the transition towards environmentally sustainable hydrogen energy systems, even in the short-term, and to carefully evaluate the environmental suitability of the proposed alternative solutions under a life-cycle perspective.

The various proposed solutions are aimed at circumventing some barriers and at favouring and speed-up the advent of a hydrogen economy.

Both the sustainable mobility options and the energy systems based on hydrogen or carbon-neutral fuels proposed in this doctoral thesis, follow this rationale.

As far as concerns hydrogen-based sustainable mobility, the proposed strategies explore different alternatives, both in terms of vehicle technology itself and in terms of hydrogen distribution and on-board storage. The aim is to investigate solutions that could alleviate the technical criticalities and make possible the use of existing infrastructures or more less consolidated technologies, requiring in some cases minimum changes and modifications. The scope is to rapidly enable a widespread use of renewable hydrogen, starting from now. This could favour hydrogen demand and production, thus fostering the start of a hydrogen economy. A further goal in this sense is to investigate on which strategy could be the most energetically convenient and environmentally sustainable in order to suggest environmental policies that could also take into account a careful use of the few renewable hydrogen currently available.

Regarding carbon-neutral fuels these could be used to replace conventional fossil fuels without requiring major changes to the distribution infrastructure and end-use equipment. Furthermore, hard-to-abate sectors could also be gradually decarbonised by means of synthetic renewable fuels. Such a strategy would allow a significant increase in the hydrogen demand and consequently a significant increase in the use of renewable energy sources.

Finally, another objective of this thesis regards the evaluation of the environmental footprint of hydrogen produced via electrolysis driven by variable renewable energy sources and the assessment of eco-design aspects of electrolysers under a life-cycle perspective. This could be relevant both for the future creation of environmental label schemes on hydrogen and for identifying possible environmental hot-spots and improvement opportunities. Finally, advances in the life-cycle modelling of such systems and results on hydrogen environmental profile could also be useful to other researchers for the analysis of other hydrogen systems.

The main objectives of the research activity carried out in this doctoral thesis were: (i) to assess the environmental suitability of renewable hydrogen as a fuel for sustainable mobility under different technical vehicle options and to propose innovative national short-term strategies to allow a faster implementation of renewable hydrogen in road transport. This objective was pursued by evaluating the environmental potentialities of hydrogen produced from renewable energy sources as a clean fuel for vehicles (mainly passenger cars), used both in fuel cells and in internal combustion engines, pure or mixed with natural gas or gasoline; (ii) to evaluate the technical and environmental potentialities of systems for the production of a renewable-based substitute natural gas (SNG) and systems for the co-production of carbon-neutral synthetic fuels and electricity starting from renewable energy sources (biomass and electricity surplus produced by non-programmable renewable energy sources such as wind and solar); (iii) to evaluate the life-cycle environmental performance of renewable hydrogen production systems (mainly through electrolysis) and the environmental footprint of the produced hydrogen.

2.2. Methodology

In addition to energy analysis, the Life Cycle Assessment (LCA) methodology was applied to the investigated systems, in order to evaluate the environmental impact associated with the individual life-cycle stages (and the overall life-cycle) of a product or system. Indeed, in the case of the investigated energy systems, the benefit of zeroed or reduced direct emissions in the use phase could be reduced or even counter-balanced by the upstream or downstream processes, i.e. the impact could be shifted from the fuel use phase to other life cycle stages. Therefore, comprehensive life cycle analyses are needed to verify the environmental suitability of hydrogen and carbon-neutral fuels.

2.2.1. Methodological framework of life cycle assessment

Life cycle assessment is a standardised and scientifically sound methodology that represents an objective analytical tool useful to thoroughly evaluate the environmental aspects and impacts of product systems. By means of LCA, it is possible to take into account the entire life cycle of a product or a service, from the extraction and acquisition of raw materials to the production of goods or services, including the end-of-life treatment and final disposal (cradle-to-grave approach). This systemic approach allows identifying potential environmental loads both of individual processes and life cycle stages, so that a possible shifting of a potential environmental burden between life cycle stages or individual processes can be identified and possibly avoided. Life-cycle economic and social implications and impacts are out of the scope of an environmental LCA, but could be taken into account by considering other tools that can be seen as expansion of the LCA methodology, namely Life Cycle Costing (LCC) and Social Life Cycle Assessment (SLCA). The union of these three methodologies, known as Life Cycle Sustainability Assessment (LCSA) can lead to holistic and three-dimensional evaluations of aspects related to sustainability. In this thesis only LCA is considered, while LCC and SLCA are out of the scope.

The usefulness of LCA is not limited to the assessment of the environmental profile of a single product. For instance, LCA is particularly suitable for carrying out comparative studies, between products that perform a same function, estimating the potential environmental impact connected to their life cycle, through the consumption of resources and the polluting emissions released in the various environmental compartments (water, air, soil). The aim of comparative studies is to identify, among the possible alternatives, the most appropriate solutions for a reduction of environmental loads.

In addition, LCA can also be used to:

- identify environmental bottlenecks and opportunities to improve the environmental performance of products in the various stages of their life cycle, revealing which are the most critical stages or processes on which priority intervention is needed;
- provide information to policy-makers in governmental organizations, or to decision-makers in industry or non-governmental organizations (e.g., strategic planning, public policy-making, prioritisation choices, product or process design or re-engineering);
- choose relevant environmental performance indicators with related measurement techniques;
- set up marketing (e.g., for the implementation of eco-labelling schemes, to make environmental claims or to produce an environmental product declaration).

The main general guidelines, structure and requirements of LCA are defined in the standards ISO 14040 (Environmental management - Life cycle assessment - Principles and framework) and ISO 14044 (Environmental management - Life cycle assessment - Requirements and guidelines) [105,106]. Standardization is particularly important in order to provide the characteristics of completeness, reliability and reproducibility of the analysis.

As defined in the standards, the LCA methodology involves four main interrelated stages (Figure 5). Performing a LCA is divided into several phases. Most of these are performed sequentially, but there are also iterative parts, where previous phases have to be reconsidered. In particular, the four standardised stages are:

- Definition of goals and scopes
- Life Cycle Inventory analysis (LCI)
- Life Cycle Impact Assessment (LCIA)
- Interpretation

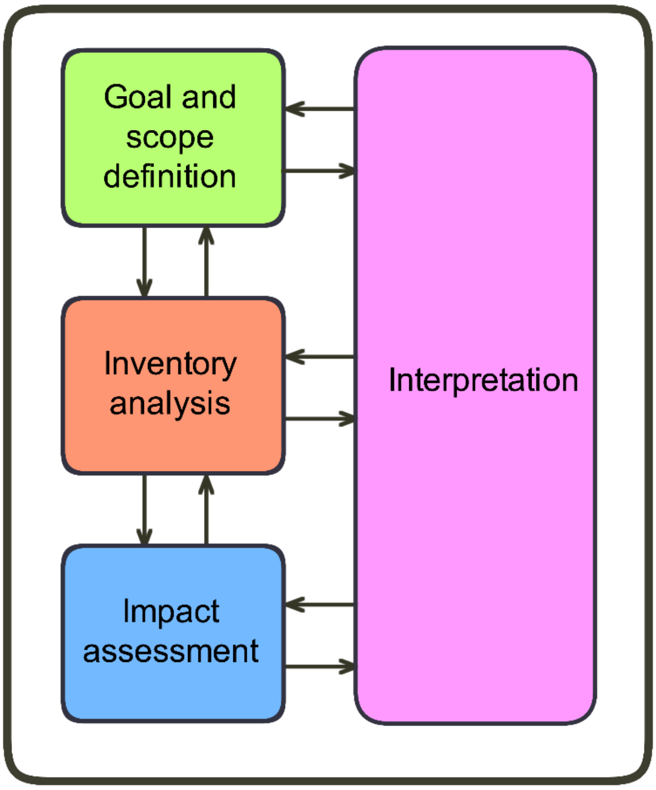

Figure 5. Standardised general methodological structure of LCA. Based on [105,106].

Figure 5 also shows the iterative nature of the LCA, in fact once the goal of the work has been defined, the initial scope settings are derived, which define the requirements for the subsequent work. However, as more information becomes available during the life cycle inventory and data collection phase, and during the subsequent impact assessment and interpretation, the initial settings of the scopes will generally need to be refined and redefined. In this sense, the interpretation interacts with all phases of the LCA.

2.2.1.1. Stage 1: Goal and scope definition

In the first stage –goal and scope definition– key aspects such as the objectives of the study, its restrictions and assumptions, the functional unit (FU), the environmental impact categories, and system boundaries are addressed.

During the goal definition, several aspects have to be defined such as the intended application, the method used, the main assumptions and limitations, the geographical and time scope of the study, the reasons for carrying out the study and the decision-contexts. The target audience to which the study is addressed is also defined, together with a possible declaration on whether the results are intended to be used in comparative studies that will be made public, who commissioned the study and so on [107–109].

In the definition of the scopes, on the other hand, the actual methodological aspects of the LCA that will be performed are defined, such as the definition of the function, the functional unit and the reference flow, how the LCI will be modelled (especially if there is a need to apply criteria to deal with multi-functionality), the definition of the system boundaries, the cut-off criteria, the impact assessment methods and the impact categories that will be used in the LCIA stage. Additionally, other methodological aspects such as the type, quality and sources of required data and information, the Data Quality Requirements (DQR) and the representativeness of data, how to ensure comparability between systems, the identification of critical review needs and the intended reporting are defined during the scope definition stage.

One of the most relevant aspects of a LCA is the choice of the functional unit. The FU is the quantified performance of a product system, to be used as a reference unit. The functional unit qualitatively and quantitatively describes the function(s) and duration of the product in scope. The choice of the FU can strongly affect the conclusions of the study (especially in comparative studies) and must be defined in accordance with the goal and scope of the study. The reference flow is the amount of product needed to provide the defined function. All other input and output flows in the analysis quantitatively relate to it. The reference flow may be expressed in direct relation to the functional unit or in a more product-oriented way.

Another very relevant aspect is the definition of the system boundary. The system boundary is defined as the set of criteria specifying which unit processes are part of a product system. In system boundaries definition, it is crucial to identify the life-cycle stages that will be included in the study, as well as all the relevant parts, subsystems, components or processes, that are to be considered included in the product system (and for which, therefore, a modelling effort will be required). Processes excluded from system boundaries or those for which secondary data may be used (background processes) should also be clearly identified. The system boundary shall be defined following a general supply-chain logic, including all stages from raw material acquisition and pre-processing, production of the main product, product distribution and storage, use stage and end-of-life treatment of the product (if appropriate). The co-products, by-products and waste streams of at least the foreground system shall be clearly identified.

According to the General Guide for Life Cycle Assessment [110], the modelling approach (attributional or consequential) has to be specified in this step. In this respect, the International Reference Life Cycle Data system [110] defines the attributional approach as a life cycle inventory (LCI) modelling frame that inventories the input and output flows of all processes of a system as they occur. In contrast, consequential approach is defined as an LCI modelling principle that identifies and models all processes in the background system (i.e., the part of the system beyond the influence of the central decision-maker) in consequence of decisions made in the foreground system (i.e., the part of the systems under the influence of the central decision-maker).

2.2.1.2. Stage 2: Life cycle inventory analysis

Life cycle inventory (LCI) analysis is the second stage of the LCA methodology. The LCI constitutes the input to the life cycle assessment associated with the provision of the functional unit. In this stage, all input and output flows of materials, energy, waste and emissions (into air, water and soil) referred to the FU are quantified for the system under study along the product supply chain and compiled in an inventory used as a basis for the modelling.

A flow is an input or output from a process or product system. There are several types of flows, but they can be mainly classified as:

- Elementary flows, are defined in ISO 14040 as "*material or energy entering the system being studied that has been drawn from the environment without previous human transformation, or material or energy leaving the system being studied that is released into the environment without subsequent human transformation*." [105]. Elementary flows are, for example, resources extracted from nature or emissions into air, water, soil that are directly linked to the characterisation factors of the impact categories. This means that an elementary flow can be, for example, crude oil or a mineral resource as an input, or a CO_2 emission released to air as a non-further treated output;

- Non-elementary (or complex) flows, which are all the remaining inputs (e.g. electricity, human-processed materials, transport processes) and outputs (e.g. waste, by-products) in a system that require further modelling efforts to be transformed into elementary flows [111]. These can include for instance product flows, material flows or energy flows, waste flows, intermediate flows or intermediate products. Product flows, are defined in ISO 14040 as "*products entering from or leaving to another product system*". For instance, hydrogen produced by electrolysis would be an output product flow, while electricity consumed by the electrolysis would be an input product flow entering the system, coming from another product system (electricity production). Waste flows instead represent interaction between a system or a process and an end-of-life treatment process (e.g., a waste output from the system can be an input for a recycling process).

Flows are connected together by means of (unit) processes (Figure 6). According to the standards, a process is defined as "*a set of interrelated or interacting activities that transforms inputs into outputs*". A unit process is defined as "*the smallest element considered in the LCI for which input and output data are quantified*" [105].

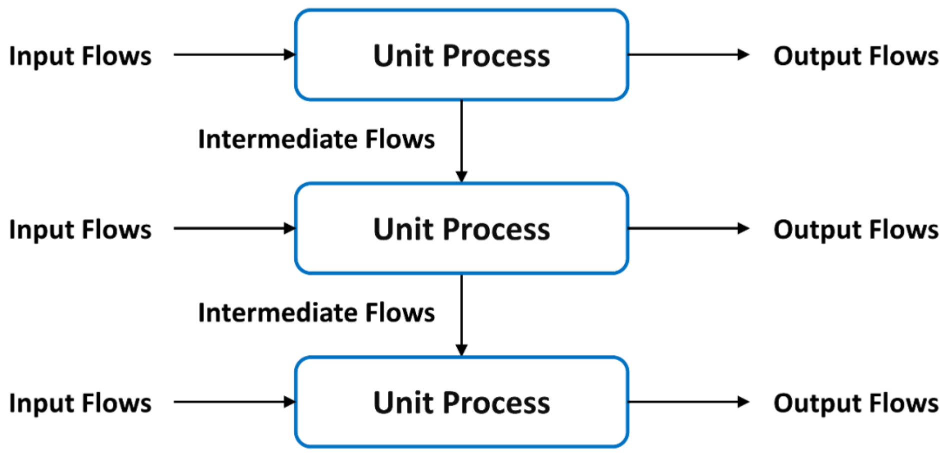

Figure 6. Example of a set of unit processes within a product system. Based on [105,106].

A set of unit processes constitutes a product system. Unit processes are linked to one another by flows of intermediate products and/or waste for treatment, to other product systems by product flows, and to the environment by elementary flows.

Thus, a product system is defined as a "*collection of unit processes with elementary and product flows, performing one or more defined functions, and which models the life cycle of a product*". Dividing a product system into its component unit processes facilitates identification of the inputs and outputs of the product system.

Figure 7 shows a diagram of a generic product system. A model of the product system is conceived, to represent the interaction of the product system itself with the environment. There is therefore a "physical" boundary of the system with respect to the environment. A product system can be connected with other product systems through product flows, and it is connected with the environment through elementary flows.

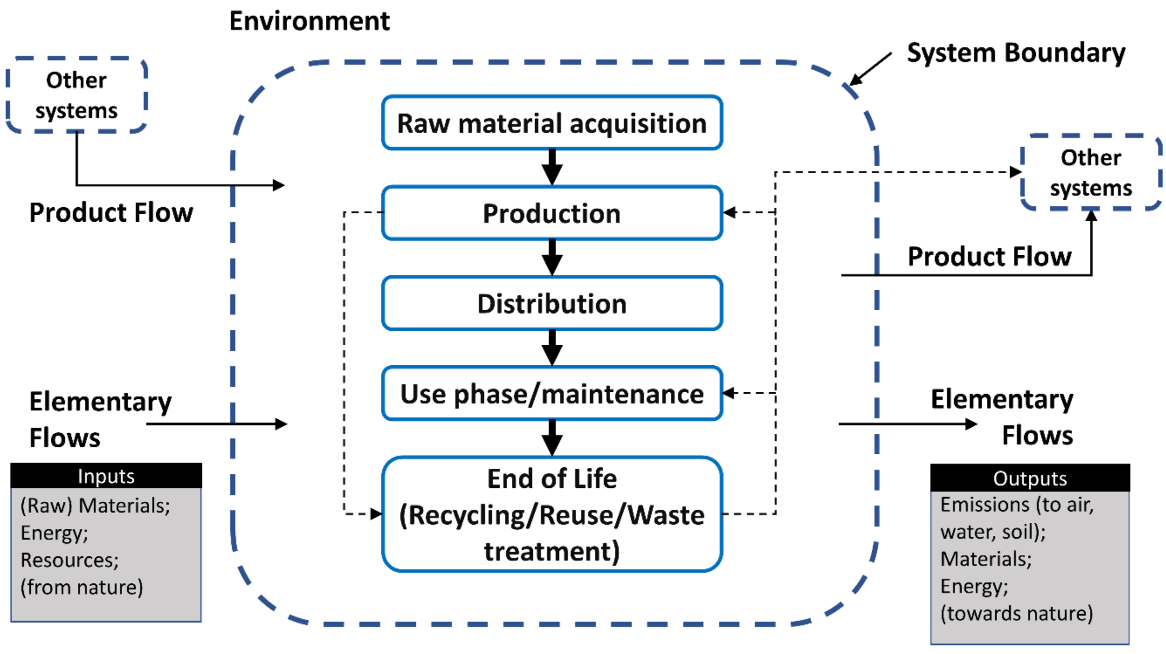

Figure 7. Scheme of a generic product system. Based on [105,106].

The modelling of the Life Cycle Inventory and the data collection stage is probably the most complex and delicate part of the whole study. After collecting the necessary data, the model is normally fed into dedicated LCA software, covering each life cycle stage defined in goal and scopes (e.g., from raw material extraction to end-of-life of the product), in a series of interconnected steps (i.e., unit processes). Inventory analysis involves data collection and calculation procedures to quantify relevant inputs and outputs of a product system. All calculation applied in the study to determine the elementary flows must be explicitly documented and reported in the study. Data must be properly validated, for instance, by checking mass and energy balance law of conservation. Interaction with the environment is represented by elementary flows that cross the system boundary, for example resources taken from nature, or emissions deriving from combustion, physical, thermal or chemical processes and which are discharged from the system into the environment. Product flows usually represent interactions with the "technosphere" and they can be translated in elementary flows during the LCI result calculation stage. The compilation of all the elementary flows and of all the processes therefore represents the LCI stage.

Furthermore, for those systems performing more than one function (e.g., multi-product systems), the approach followed to address multifunctionality has to be detailed. In particular, the possible approaches to deal with multifunctionality can be subdivision, system expansion, or allocation. System subdivision consists in dividing the unit process into two or more sub-processes and collecting the input and output data related to these sub-processes. System expansion considers the additional functions as substitutes for the conventional ones, whose environmental burdens are avoided. The use of allocation approaches involves the distribution of inventory data between functions according to physical or other relationships (e.g., mass, energy or economic allocation). In this regard, LCA standards prioritise process subdivision and system expansion over the use of allocation approaches.

In the first two stages, the focus has been more on the product system, in the next step, however, the focus will be shifted to the environment.

2.2.1.3. Stage 3: Life cycle impact assessment

The third phase called Life Cycle Impact Assessment (LCIA), deals with assessing the potential environmental impact deriving from the elementary flows that cross the system boundaries. In the LCIA, the large number of elementary inputs and outputs (resources taken from nature and emissions flows) that make up the LCI results are translated into a handful of environmental impact categories and indicators (selected in goal and scope definition).

Three mandatory phases are involved in the LCIA: (i) selection of impact categories, category indicators and characterisation models; (ii) classification to associate inventory data (elementary flows of the LCI results) with impact categories; and (iii) characterisation to provide the values of the category indicators. The selection of impact categories shall cover relevant environmental issues related to the product system analysed under the goal and the scope of the study. The exclusion of relevant impact indicators shall also be clearly justified. Regarding the LCIA methods, impact assessment methods at the endpoint level and methods at the midpoint level are distinguished. Impact categories at the midpoint level are calculated at the place where a common impacting mechanism occurs. For example, global warming, which begins with the release of greenhouse gases, ends with potential impacts on different areas such as humans and ecosystems (endpoint level). However, from the emission of the greenhouse gases to the endpoint effects, there is an intermediate stage in which the greenhouse gases emissions have an effect on the radiative forcing, this represents the indicator at the midpoint level for the impact category of global warming [112]. While endpoint impact categories are commonly associated with three main “areas of protection” (human health, natural environment, natural resources), at the midpoint level a higher number of impact categories are differentiated. It should be highlighted that results at the midpoint level are considered to be more accurate than those at the endpoint level [110]. During classification, each LCI elementary flow is attributed to one or more impact categories. In the following characterisation step, within each category, the flows are aggregated using equivalence factors called "characterisation factors". Indeed, the characterisation phase consists in the calculation of the impact category results by multiplying the elementary flows for a characterisation factor that represents the specific impact of the substance emission (or consumption) in the specific impact category. These factors are based on the physical and chemical properties of the impacting substances, as well as on the fate of the flows once they leave the product system and head towards the environment (specific compartments). The aggregated value is called "potential impact", and it could be expressed, for instance, in kg equivalents of a certain reference substance for the respective category. For example, the unit for the impact category "Global Warming Potential" (GWP) is "kg of equivalent carbon dioxide" (kg CO_2 eq.). Fossil methane, according to the IPCC 2021 method [113], has an impact on global warming about 29.8 times higher than that of carbon dioxide, in a time horizon of 100 years. As regards the impacts of greenhouse gases, therefore, when these are aggregated according to the GWP category, the impact generated by an elementary flow containing one kg of fossil methane emitted in the atmosphere will be equal to 29.8 kg CO_2 eq. [114,115]. LCA only addresses potential environmental impacts and does not predict absolute or precise environmental impacts due to:

- the relative expression of potential environmental impacts to a reference unit;
- the integration of environmental data over space and time;
- the inherent uncertainty in modelling of environmental impacts;
- the fact that some possible environmental impacts are clearly future impacts.

Optionally, normalisation, grouping and weighting can be applied for an evaluation of the results from a different perspective. Regarding normalisation, it quantifies the magnitude of category indicator results with respect to a reference value to provide a measure of the relative magnitude of a result. Weighting refers to the possibility of aggregating indicators across impact categories using numerical factors based on value-choices and it may include the aggregation of the weighted results. Basically, it assigns to each impact category a weight factor allowing the aggregation of different impact categories in a single score index. In this respect, when weighting is included, supporting data and information to justify the weighting factors shall also be provided.

2.2.1.4. Stage 4: Interpretation

Eventually, the fourth stage of LCA – interpretation of the results – focuses on summarising and discussing the results in accordance with the goal and scope of the study. During the iterative procedure, the step of interpretation is aimed to guide potential improvements of the LCI modelling. Once the final LCI and the corresponding results are achieved, the interpretation has the main objective of deriving robust conclusions and recommendations relating to the previously defined goals and scopes. The results of all the other stages are considered collectively and analysed in terms of accuracy obtained, representativeness and completeness of the data used and of the hypotheses made, eventually reiterating the whole process if necessary. Issues found to be relevant to the results (e.g., technical parameters, processes, materials, units, etc.) have to be identified and evaluated. Through these evaluations, conclusions and additional considerations should be finally formulated according to the goal and the scope of the results. Overall, in LCA studies, the stages of goal and scope definition and interpretation frame the LCA, while the phases of LCI and LCIA produce the core information on the product system under analysis.

2.2.2. Environmental analysis of vehicles: differences between Well-To-Wheels analysis and Life Cycle Assessment

As mentioned in section 2.2.1.1., the definition of system boundaries is a crucial methodological aspect of an LCA. However, in the automotive field also another type of analysis is very popular, the so-called Well-to-Wheels (WTW) analysis, most frequently conducted with respect to LCA [116–118]. The main difference between a WTW and a LCA lies in the system boundaries. This section aims to highlight the methodological differences between a WTW and a vehicle LCA.

In the specific case of LCAs of vehicle, the life cycle is typically divided into two distinct sub-life-cycles, namely the vehicle life cycle and the fuel life cycle [119–122]. Figure 8 shows the system boundaries applied to a generic LCA of a vehicle together with the main life cycle stages.

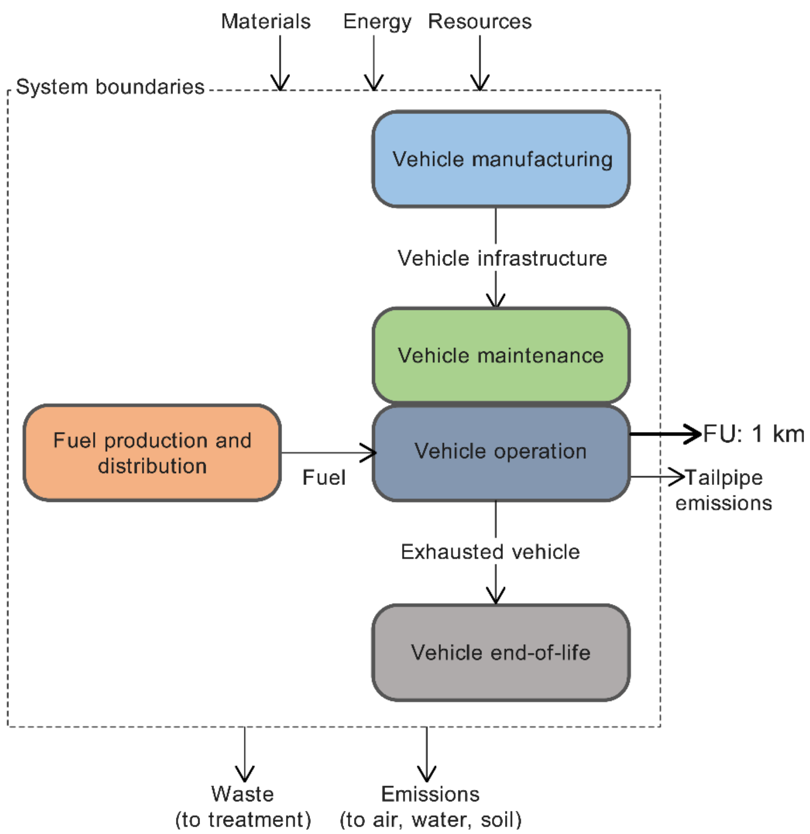

Figure 8. System boundaries of a generic LCA for passenger road transportation. Based on [119,120].

From top to bottom Figure 8 depicts the vehicle life cycle while from left to right the fuel life cycle, which have in common the stage of vehicle operation, i.e., when the vehicle tank is filled with the fuel. More in detail, the vehicle life cycle typically includes the stages of [119–123]:

- Vehicle manufacturing, from the extraction of raw materials through the various transformations that lead to the final product (passenger car or vehicle infrastructure);
- Vehicle operation, which refers to the period when the vehicle is performing its main function (passenger or load transportation). This phase involves the use of fuel(s);
- Vehicle maintenance, which occurs when there is a need to replace consumable components and materials such as tires or lubricating oil to ensure the vehicle functionality during its operation over the useful life;

- Vehicle end of life, which refers to the phase in which the vehicle is transferred to the final disposal at the end of its useful life. It can include different disposal strategies such as recycling, reuse and landfill disposal depending on several factors such as the considered materials, the recycling technologies as well as regulatory aspects in matter of waste management specific of the region of the study.

The fuel life cycle includes the following phases [119–122]:

- Fuel production;
- Fuel transport (e.g., by ship or oil pipeline);
- Conditioning and treatment (desulphurisation, refining, etc.);
- Distribution (e.g., by road in tanker trucks, up to the refuelling point for cars);
- Refuelling station infrastructure and operation;
- Fuel use, i.e., combustion in the vehicle engine when it is transformed into tailpipe emissions.

The various stages of the fuel life cycle, however, may differ depending on the fuel or the energy carrier considered.

Instead, WTW analyses consider the system boundaries from the *well* (for fuel extraction) to the *wheel* (of the running vehicle). Obviously the well refers to the traditional oil extraction well, but the meaning is to be understood also extended to other types of fuels or energy carriers, such as "production stage" of the fuel. The wheel instead refers to the vehicle operational stage, when the fuel is used, the wheels spins and the vehicle is in motion. Therefore, WTW analyses cover the overall fuel life cycle, including the fuel use phase. From a vehicle perspective, only the vehicle operational phase is taken into account, i.e., excluding vehicle production and end of life. Optionally, the vehicle maintenance can be included in a WTW, merged with the vehicle operational stage [119,124].

Moreover, WTW analyses include different subsets, that are related to different life-cycle stages of the fuel [116,124,125]:

- Well-to-Tank (WTT) or Well-to-Pump (WTP), depending on where the chain of processes related to the fuel is truncated in the analysis. This first subset generically refers to the fuel supply, i.e. fuel production and distribution stages. In WTT the stages of fuel production, distribution and refuelling are considered, up to when the fuel reaches the vehicle tank. Indeed, vehicles need to consume energy in order to be able to fulfil their task, and they typically accumulate energy in a tank (or in a battery in the case of electric cars). It is precisely inside the tank that the vehicle life-cycle meets that of the fuel. However, stopping at the tank, WTT do not include the fuel use phase necessary for the vehicle traction. The other option, WTP, is similar to WTT. The only difference in WTP is that the system boundaries range from fuel extraction up to the transportation to the service station (the pump); however, in this case the fuel does not reach the vehicle tank as the refuelling stage is excluded.

- Tank-To-Wheels (TTW) or Pump-to-Wheels (PTW) is the second subset, and is referred to the vehicle operational stage. In the TTW stage, the chemical energy contained in the fuel stored in the tank is released and converted into mechanical power useful for traction. Depending on the technology considered, this also entails tailpipe emissions. This use phase is shared by both the vehicle and the fuel. The TTW also takes into account specific technological aspects of the vehicle such as its energy conversion efficiency, its energy consumption and emission characteristics. In the PTW, the phases from the refuelling to the vehicle operational stage are considered.

The combination of the WTT and the TTW is defined as a Well-To-Wheel (WTW) analysis, and the latter is capable of providing a synthetic judgment on the environmental performance of the combination vehicle plus fuel.

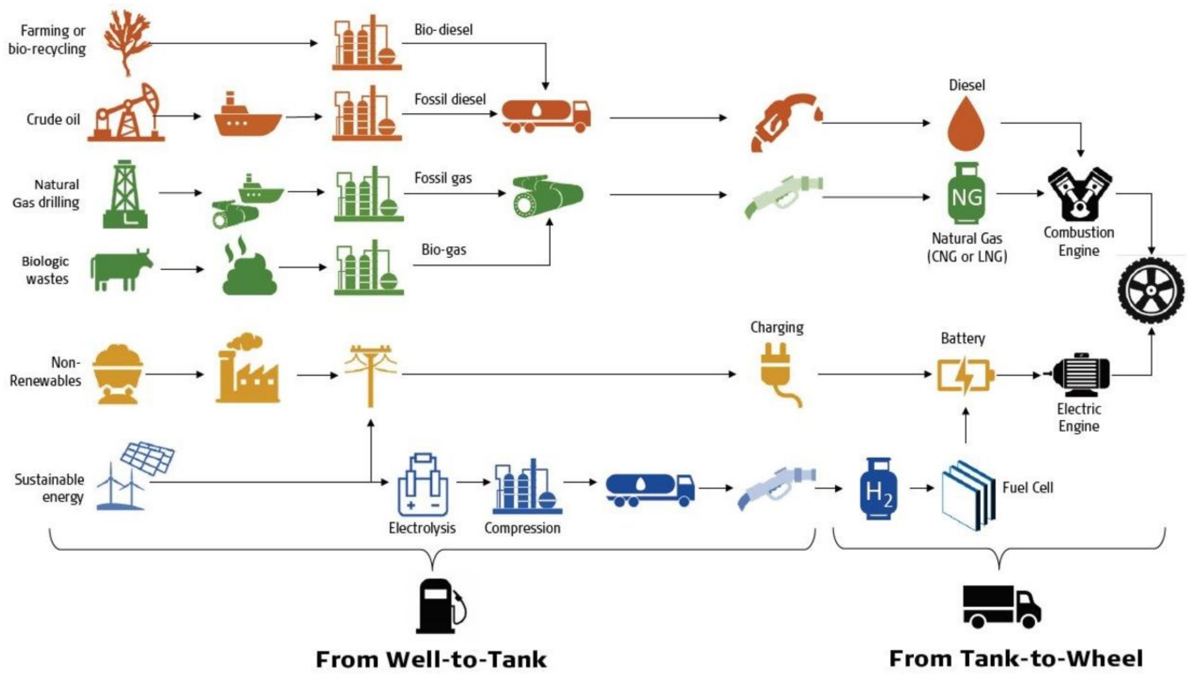

Figure 9. Well-to-Tank and Tank-to-Wheels [126]

Thus, the main difference between a WTW and an LCA lies in the definition of the system boundaries. In particular, in addition to the fuel life cycle, LCAs include other vehicle life cycle stages such as vehicle manufacturing and vehicle end of life (Figure 10). Overall, a vehicle LCA can include both the vehicle life-cycle, "from cradle to grave", and the whole fuel life-cycle within the system boundaries.

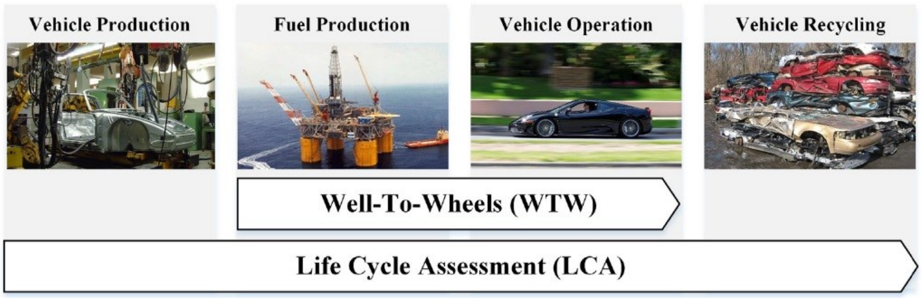

Figure 10. Well-to-Wheels analysis and LCA [116]

If for conventional vehicles (e.g., diesel engines) the WTW analysis, or even the TTW alone, could have been sufficient in many cases, in the case of "zero emission" vehicles such as electric vehicles or those powered by hydrogen or carbon-neutral fuels, the TTW it is not sufficient and it is necessary to at least conduct a WTW, or even better, an LCA which allows to look at the complete picture.

Let it consider, for instance, an electric car: in its operational stage, the vehicle will consume electricity previously stored in a battery (similarly to what happens with a car that consumes fuel contained in a tank), and will fulfil its function of mean of transport with zero exhaust emissions associated. Neglecting particulate emissions from wear of tires and from braking, the electric car will boast zero Tank-To-Wheel impact, as no tailpipe emissions are released. However, this does not change the fact that the electricity used could has been produced, for example, in a thermoelectric coal power plant, and then it has been distributed through the network. This electricity will therefore be associated with an evident impact of production and distribution, which takes the name of Well-To-Tank. Overall, therefore, an electric car has a Well-To-Wheel impact other than zero, as the emissions have simply been delocalised upstream, from the vehicle to the power plant. Moreover, the manufacturing and the end-of-life stages of both the battery and the whole car could have a significant environmental impact that is not considered in the Well-To-Wheels. Therefore, LCA arises as a suitable tool to comprehensively evaluate the environmental suitability of vehicles fuelled with hydrogen or synthetic carbon-neutral fuels.

2.2.3. Specific methodological aspects considered in LCA of vehicles and fleets

As regards the present thesis and the solutions presented in *Chapter 3* (*Publication 1* and *Publication 4*) some methodological choices and technological aspects of the case studies involved in the execution of the LCA are presented below. The first step concerns the definition of the product system and of the system boundaries; in this section the fuels used and the vehicles under comparison are defined from a perspective of fuel life-cycle and vehicle life-cycle.

2.2.3.1. Fuel life-cycle

The fuel life-cycle has a great relevance in the overall impact generated by a vehicle, not only during the vehicle operational life-stage by means of exhaust gases emissions. By means of LCA indeed, all those flows of raw materials, energy, waste and emissions that are involved in the various life-cycle stages of the fuel itself (i.e., production, distribution, storage and use) are also taken into account.

This chain of processes associated with the fuel life-cycle, and having an environmental impact of its own, that depends on the intrinsic characteristics of the fuel, can take various forms depending on the number and type of phases considered [119].

The hydrogen fuel life-cycle has already been addressed in *Chapter 1*. However, renewable-based hydrogen produced by wind power electrolysis has been considered for the various vehicle case studies. The pure hydrogen was then distributed in gaseous form by lorry and compressed up to the vehicle tank pressure (e.g., 700 bar for FCEVs). Specific details on hydrogen fuel life-cycle will be provided in *Chapter 3*. In this section, however, the life cycles of conventional fuels (gasoline and natural gas) and that of mixtures of hydrogen and natural gas, namely "hythane", will be addressed.

Conventional fossil fuels

The production cycle of fossil fuels, oil and natural gas, and their derivatives, is well-known and consolidated, as it has been a long time since it reached full technological maturity. It goes through different production stages, traditionally grouped into three sets of processes [127–129]:

- **Upstream**: includes the set of procedures to be carried out in order to extract crude oil and natural gas from the subsoil; the main upstream procedures are: the search for the reservoir or fields (Exploration), the preparation of wells for lifting (Drilling) and the process of lifting from the subsoil (Extraction) [130,131];

- **Midstream**: includes the procedures relating to transport from the production site to the transformation site, and those relating to storage [132,133];
- **Downstream**: includes the transformation processes of crude oil (Refining) and natural gas (Regasification, Odorization, etc.) for the purpose of obtaining derivative products intended for trade, and their distribution and sale [133,134].

The midstream and downstream processes are diversified according to whether they refer to crude oil or natural gas. Upstream processes, on the other hand, are often common to both, indeed frequently, both crude oil and the so-called "associated" natural gas are extracted simultaneously from the same reservoir and then separated. In other cases, natural gas is extracted from separate deposits, in which gas is almost exclusively present, and in jargon this is called "non-associated" gas [135,136].

In order to be able to model these production cycles in the LCA, their differences are highlighted below, up to the final products, gasoline and natural gas, which will be destined to the automotive sector.

Gasoline [127,135,137]

- **Upstream**: after exploration, drilling of the field and extraction of oil from the subsoil, a pre-treatment of crude oil is often carried out on site, in order to separate it from the so-called production waters and injection waters. The production waters, which often contain toxic organic and inorganic compounds, are then further treated in order to be disposed.
- **Midstream**: includes the transport of crude via oil pipelines, oil tankers (ships) or special railway wagons, from the extraction site to the refinery site, and the storage of the oil itself. There are also some operations preliminary to transport. As soon as it is extracted, crude oil is made up of a mixture of hydrocarbons to which water, dissolved gases, salts, sulphur and inert substances such as sand and heavy metals are added. Before being introduced into the pipelines, therefore, the extracted oil must undergo a series of treatments, such as degassing, dehydration, desalination and desulphurisation (stripping). After undergoing the various treatments, the crude oil is normally stored in cylindrical steel tanks waiting to be transported to the refineries by pipeline or oil tanker.

- **Downstream**: once it reaches its destination, the oil is processed in a refinery to obtain the derivative products. Refining consists of a fractional distillation process which allows the lightest parts of the crude to be separated from the heaviest ones, according to the different boiling temperature. A large variety of petroleum products is obtained, including diesel, kerosene, naphtha, gasoline and LPG. Finally, the cut that constitutes the gasoline will have to undergo several processes, as the topping gasoline has a low octane number and therefore the processes of isomerization and reforming are used. In many cases additives are also added to the gasoline in order to enhance its quality, improve the octane rating or to act as corrosion inhibitors or lubricants. Finally, due to regulatory aspects fossil gasoline may be also mixed with biofuels (e.g., bioethanol) in different amounts depending on the regions. The final product for automotive application is then transported on road, via oil tanker truck, to the refuelling station where is deposited waiting to be fed to a vehicle tank.

Natural gas [136,138,139]

Natural gas is mostly composed of methane, but it also typically contains heavier hydrocarbons in smaller amounts, such as ethane, propane, butane, and pentane.

In addition, modest percentages of gaseous substances other than hydrocarbons are also always present, such as carbon dioxide, nitrogen, oxygen (in traces), hydrogen sulphide (H_2S) and, in some cases, helium, radon and krypton. Mixtures that mainly contain methane are called "dry", while when hydrocarbons such as propane and butane are also present, they are called "wet".

Before being sent to use, natural gas is treated to eliminate carbon dioxide and nitrogen, which make it less flammable, hydrogen sulphide which is a toxic and corrosive gas, and mercury which is a harmful contaminant.

- **Upstream**: after extraction, if the gas leaving the reservoir is particularly humid, it undergoes a preliminary treatment to separate the methane from the other gaseous hydrocarbons such as propane, butane and ethane. The separation is facilitated by the fact that methane has a much lower critical temperature. Natural gas then undergoes a desulphurisation process which allows the elimination of sulphur compounds, mainly H_2S.
- **Midstream**: natural gas is transported in the gaseous state by means of long gas transmission pipelines, or with methane tankers, i.e. ships onto which it is loaded in the

liquid state (LNG or Liquefied Natural Gas). As far as gas pipelines are concerned, compression stations are installed every 100–200 kilometres, which serve to restore sufficient pressure to move the gas at the right speeds. The pipeline networks also include storage stations, in which part of the gas is kept available for any emergency situations. Depleted reservoirs located near the areas of greatest consumption are preferably used as deposits. Their geological characteristics guarantee good safety against possible leaks. The storage of natural gas is in any case carried out through an integrated set of infrastructures: depleted fields, gas treatment plants, compression plants and operational dispatching systems. In the case of LNG, on the other hand, the gas is liquefied at -161 °C and loaded onto an LNG tanker ship, equipped with thermally insulated tanks and sophisticated safety systems.

- **Downstream**: once it has reached its destination, the LNG undergoes a "regasification" process, i.e. it is heated, brought back to its gaseous state and introduced, after having reached an adequate level of pressure, into the methane pipeline network. As regards gas transmission pipelines, these are instead connected to the national network for subsequent distribution and sale. From the large-diameter pipes of the national transport network, thousands of kilometres of smaller pipes branch off, called connections, which transport natural gas directly to industries and homes. In the city networks, managed by the distribution companies, the gas pressure is kept at lower levels than in the large transport networks, for technical and safety reasons. Before being introduced into the distribution network, the gas is odorised, i.e. mixed with very strong-smelling substances called "mercaptans". In this way, the user immediately notices even the slightest loss. Through the city distribution network, the gas finally reaches the vehicle refuelling station, where it is recompressed up to 200–250 bar, to then be stored in the cylinders on board the vehicle.

The environmental impacts that may occur during the transport and distribution phases are mainly linked to gas emissions into the atmosphere due to uncontrolled leaks. To avoid gas leaks, the pipelines are subjected to continuous monitoring and pressure checks along the entire distribution line so that any leaks can be reported. It is estimated that over a distance of 4000 km, less than 1% of the transported gas is lost. Typically, losses are higher in low-pressure distribution networks, such as city distribution networks, which carry gas to populated centres, as these are often old pipes. Replacing old distribution networks and using innovative materials is the best solution to drastically reduce losses.

Hythane

As mentioned above, the gaseous hydrogen produced via electrolysis could be conveniently transported by gas pipelines, similarly to what happens today for natural gas. Unfortunately, except in some special cases, the current natural gas network could not be repurposed and used to transport pure hydrogen, as the pipes requires to be made of materials not subject to embrittlement phenomena. The need to build a capillary network from scratch specifically designed for the distribution of hydrogen is one of the major obstacles to the take-off of the so-called hydrogen economy. Section 1.3.3. already addressed the blending of hydrogen with natural gas in the current natural gas network as a possibility to partially and temporarily circumvent this obstacle. It emerged that generally for volume fractions of hydrogen up to 20% no particular complications arise and only modest technical and safety additional precautions are required. The injection of modest quantities of hydrogen into the natural gas network would therefore represent a bridging solution capable of giving a boost to a hydrogen-based economy, allowing the investment in a distribution infrastructure to be delayed over time, and to initially concentrate economic efforts on the production of hydrogen from renewable sources. Furthermore, biomethane could also be jointly injected into the network, further reducing fossil CO_2 emissions.

Hydrogen-natural gas blends have also attracted some interest as an automotive fuel for internal combustion engines. Actually, several experiments have already been carried out since 2010: the Italian companies Fiat and Iveco have already experimented with the use of H_2-natural gas mixtures in ICEs, demonstrating the possibility of using mixtures with $20\%_{vol}$ or even up to $30\%_{vol}$ of H_2 [74,140–142] under the requirement of minimum engine modifications. Moreover, there are several studies in the scientific literature dealing with H_2-natural gas or even other kind of mixtures such as H_2-gasoline and H_2-diesel mixtures, at different proportions, to fuel ICEs [38,73,143–145]. Generally, the results show that –after optimising the engine parameters– the addition of hydrogen improves the combustion characteristics, increasing engine efficiency and reducing fuel consumption and emissions [146]. However, in the case of use as a vehicle fuel, the mixing of hydrogen and natural gas could also take place locally at the refuelling station, after having transported the hydrogen by road. Further details are provided in *Chapter 3*. In any case, H_2-natural gas blends for automotive use are often indicated with the acronym HCNG (followed by a number that refers to the volumetric percentage of hydrogen), or with the name of "hythane". Actually, the name Hythane® is a commercial name that always refers to a specific gaseous mixture of 20%$_{vol}$ H_2 and 80%$_{vol}$ natural gas.

The use of hythane in an ICE would make it possible to avoid many of the issues regarding the use of pure hydrogen in vehicles, pending future developments in hydrogen storage systems and a decrease in fuel cells costs and platinum loading.

In particular, the advantages deriving from the use of hythane in spark-ignited ICE, compared to the use of pure hydrogen are [38,43,143,147–152]:

- Possibility of using hydrogen-natural gas mixtures, up to 30%$_{vol}$ H_2, in current ICEs with few minor changes linked to the presence of hydrogen (gaskets, injectors, valve seats etc.). In some cases, this could also avoid the need to buy a new vehicle by retrofitting existing CNG vehicles;
- Injection of modest volumes of hydrogen into the engine cylinders for each operating cycle, with consequent improvement in volumetric efficiency when compared to hydrogen-fuelled ICE;
- Possibility of using a single and more compact tank, not very different from those used today for CNG cars;
- Accumulation at lower pressures that benefits to safety, weight and costs of the tank;
- Less formation of nitrogen oxides when compared to hydrogen-fuelled ICE.

The advantages compared to the use of pure natural gas in ICEs are instead [38,143,147–152]:

- Increase in combustion speed, with consequent approach to the ideal thermodynamic process of isochoric heat adduction. This increases the engine efficiency and consequently reduce the fuel consumption;
- Increase in engine detonation (knock) resistance, which makes it possible to use higher compression ratios, with a consequent further increase in engine efficiency and in the mechanical power it delivers;
- Extension of the flammability range of the engine fresh charge, consequently enabling the possibility of using very lean air-fuel mixtures, without sacrificing the engine stability. This further reduces fuel consumption as more air and less fuel are used;
- Better completeness of combustion, with consequent greater heat release and reduction in emissions of unburnt products (carbon monoxide and hydrocarbons) which in turn are associated with an increase in engine efficiency and in a reduction in the noble

metals load required by the aftertreatment system. Thus, the use of hydrogen mixtures, compared to conventional fossil-fuelled engines, would result in a reduction in harmful emissions greater than the simple effect due to replacement of the conventional fuel with hydrogen, thanks to the benefits of improved combustion;

- Reduction in flame's wall-quenching distance, which results in less unburnt hydrocarbons (HC) formation;
- Reduction in CO_2 emissions due to the replacement of a part of natural gas with hydrogen, only mildly countered by the increase in the conversion of CO into CO_2;
- Reduction in particulate matter emissions (PM) both thanks to the partial replacement of natural gas with hydrogen, and to the simultaneous presence of high compression ratios, high flame temperatures and very lean mixtures, which favour PM destruction;
- Increased tolerance to exhaust gas recirculation (EGR), thus allowing NO_x emissions to be kept under control;
- Possibility of achieving ultra-lean combustion, capable of drastically reducing NO_x formation.

2.2.3.2. Vehicle life-cycle

The vehicle life-cycle takes into account the environmental burdens generated during all the various stages of a vehicle's existence; therefore, it mainly consists of four phases: vehicle manufacturing, maintenance, operational phase and end-of-life (EoL) [119–123].

In the vehicle manufacturing stage, all the processes that take place starting from the raw materials extraction (or recycling and use of secondary materials), passing through the semi-finished products, the different assemblies, the transport of various components from one plant to another, up to the finished product, i.e. the brand-new car, are considered. In this stage, therefore, all the flows of materials, energy, waste and emissions involved in the production of a vehicle must be considered, a truly difficult task if it is considered that, as order of magnitude, approximately 20,000 components are involved in the manufacturing of a car [123].

The maintenance phase includes the need for spare parts, replacement of tyres and batteries, and consumable materials such as lubricating oil or antifreeze fluid, but also car washing, etc.

The operational phase is the one in which the vehicle performs its function as a means of transport, travelling several kilometres and carrying passengers on-board. During this stage, which coincides with the Tank-To-Wheel, TTW, are considered all the necessary refuelling, the direct emissions deriving from the use of the car and the amount of fuel consumed to travel for a certain distance and carry a certain number of passengers. In this stage, therefore, the functional unit of the car is expressed [119–123].

Finally, in the EoL stage, the exhausted vehicle is sent to a collection centre, where still useful components are recovered for reuse. The vehicle is secured by removing the battery, airbags, fuels, oils and all operating fluids. The car is subsequently dismantled and demolished and some components in good conditions can be put back on the market as used spare parts or used as the basis for refurbished parts. All other components are recycled, if economically possible. Hazardous materials are collected and sent to specialised centres for recovery or safe disposal. The secured and demolished carcasses are sent to a shredding process, where end-of-life vehicles are divided into parts and then shredded into smaller parts that are sorted for further recycling or recovery. After sorting, ferrous materials, non-ferrous materials and other residues are obtained. All the different materials therefore follow different paths, which can be summarised in reuse, recycling, and disposal (e.g., in landfills). All the metal fractions are recycled and used in the metal industry, while the other fractions are mostly incinerated or landfilled [120,153–156]. Through a recycling-oriented design, it is possible to facilitate at least a partial vehicle circular economy, which allows the use of high percentages of recycled material to obtain a new car, thus closing the cycle [157,158].

In this thesis, particular attention has been paid to the modelling of the vehicle manufacturing stage, and to the operation and maintenance stage. However, it was not possible to model the vehicle end-of-life due to the acknowledged need for robust inventory data on this stage [159,160]. In addition, the different vehicles and powertrain under comparison would have very different level of maturity regarding the end-of-life and waste treatment processes and also different data availability, especially for some components (e.g., recycling of a fuel cell vs recycling of an ICE). A well-known problem is that especially for less technologically mature components and processes it may be difficult to imagine how the end-of-life process will look like in 10 or 20 years from now. However, end-of-life modelling could be the subject of further studies.

Reference vehicle

Since different vehicles with different powertrain technologies are being considered in the analysis, the need arises to develop the life-cycle models according to a reference vehicle, in order to ensure a fair comparison. This reference vehicle is intended as an ideal product to be taken into account during data collection, in order to put all the different vehicles under examination as much as possible in similar and comparable conditions.

In order to subsequently model the fleets as presented in *Chapter 3* and *Publication 4*, it is first necessary to model the LCIs of all the single vehicles, having this reference vehicle in mind. An average European gasoline car, sedan, 5-door, belonging to car market segment C (small family cars/compact cars/medium cars) [124,161,162] was considered as reference, with an overall rated vehicle power of 80 kW [163]. The main technical specifications of the considered average vehicle are listed in Table 4.

Table 4. Main technical specifications of an average European passenger car [164]

Parameter	**Value**
Vehicle rated power	80 kW
Kerb weight	1200 – 1350 kg
Lifespan	250,000 – 300,000 km (20 years)
Average European driving performance	12,000 – 15,000 km·year^{-1}

The general modelling approach for all the vehicles consisted in conducting a first break down into car glider and powertrain, to then further subdivide the inventory into main subsystems and components (ICE, air intake system, fuel system, exhaust gas system, control unit, etc.). Each subsystem was then subdivided into several components (e.g. for the exhaust gas system the main components were catalytic converter, exhaust gas manifold, muffler, piping, gaskets, lambda sensors, etc.) [123,165]. In general, all the vehicles were modelled taking into account common components such as the glider (body, chassis, glass surfaces etc.) as well as all major differences between powertrains. In fact, for the other vehicles modelled in this thesis, vehicle weights and lifespans differ from the reference vehicle, mainly due to differences in powertrains. Regarding ICEs, in addition to rated power, several engine technical parameters were also taken into account during data collection, in order to ensure comparability between different engines and different technologies. The comparability should be granted for both engine constructive characteristics and operational parameters such as fuel consumption and tailpipe emissions. An example of these technical parameters could be the engine displacement, that for an 80 kW vehicle was considered suitable when between 0.9 and 1.5 litres, depending if the engine was turbocharged or naturally aspirated, with port-fuel injection or with direct injection etc. In fact, a larger engine displacement, even with the same nominal power developed by the engine, would lead to an increase in fuel consumption and emissions, which would not make it comparable with the reference vehicle. In this way the technological representativeness of the collected data was ensured.

Regarding the general data quality requirements, the following hierarchy has been defined for the collection of inventory data:

1. Producer and manufacturer data, manufacturer declarations, technical data-sheets;
2. Data retrieved from scientific literature, both experimental data, generic data or life-cycle inventories derived from available and transparent literature studies;
3. Software simulations;
4. Estimated data.

As far as concern geographical and time representativeness, the selected data were considered of good quality when belonging as much as possible to the European context and to the most recent years. A distinction was also made between background data (for which less effort is required in the modelling, using data from literature or already contained in the dedicated life-cycle databases and software) and foreground data (for which a high level of precision in the modelling and higher effort in collecting activity data is required). In the present study the background data mainly concerned fuels, electricity, and most of the materials, while vehicle modelling has been considered as the system foreground.

The following paragraphs analyse the main technical features of the vehicles under comparison, in particular from a point of view of powertrain constructive characteristics and vehicle operating principle. Details on the operating parameters are instead provided in *Chapter 3, Publication 1* and *Publication 4*.

Internal combustion engine (ICE) vehicles

The vehicles equipped with a spark-ignition internal combustion engine modelled in this thesis work are essentially:

- Vehicle equipped with ICE fuelled with gasoline (Gasoline vehicle);
- Vehicle equipped with ICE fuelled with compressed natural gas (CNG vehicle);
- Vehicle equipped with ICE fuelled with hythane (Hythane vehicle);
- Vehicle equipped with ICE fuelled with a mixture of gasoline and gaseous hydrogen (H2-Gasoline vehicle);
- Vehicle equipped with ICE fuelled by pure hydrogen (H2-ICE vehicle).

Compression ignition engines, such as diesel engines, were not considered in this thesis.

Regarding the modelling approach, for the sake of greater generality, the various subsystems that make up the propulsion system of an ICE vehicle were first considered, in order to then be able to better evaluate the differences between one vehicle and another.

In general, it is possible to schematise the powertrain of a car equipped with an ICE, as composed of the following subsystems [123,152,166]:

- Internal combustion engine;
- Air intake system;
- Fuel supply system;
- Exhaust gas system;
- Lubrication system;
- Cooling system;
- Mechanical power transmission system;
- Ignition system (spark plugs, distributor, etc.);
- Electrical system (battery, alternator, starting system, etc.);
- Electronic control unit and control system.

Other subsystems belonging to the vehicle but not to the powertrain/propulsion system are also present. These subsystems belong to the vehicle glider. For the sake of the comparison between different vehicles they are considered almost identical for the majority of the vehicles considered in the set. In some cases, slight differences were taken into account. In any case, background data from the GREET model [167] were used to model the glider. Namely, the subsystems belonging to the glider are [123,152,166]:

- Braking system
- Suspensions
- Steering system
- Wheels and tyres
- Chassis, body and glass surfaces
- Vehicle interior
- Air conditioning system
- Safety equipment

- On-board instrumentation

The different technologies involved in the powertrain and the different components that make up the various subsystems were carefully modelled and taken into account (foreground), paying particular attention to the modelling of those components that may contain critical materials.

Going beyond the particular constructive solutions adopted by each car manufacturer, it is possible to catalogue more in detail the components generally belonging to the various subsystems, being based on the operating principle of an ICE vehicle.

In this way it is possible to state, for instance, that an exhaust system consists of [123,152,166]:

- An exhaust gas manifold;
- A flexible sleeve;
- Piping;
- Gaskets;
- Muffler;
- A trivalent catalytic converter (three-way catalyst);
- One or two lambda probes;
- A possible exhaust gas recirculation (EGR) system;
- A possible gasoline particulate filter (GPF, present only in gasoline direct injection or GDI engines).

The subdivision into subsystems and the breakdown into components was carried out for all vehicles and subsystems considered. Regarding the conventional gasoline vehicle taken as a reference, it is not addressed in detail here listing all its possible components as it is a well-known technology and it is under our eyes every day. It is only highlighted the constructive simplicity of the fuel supply system, normally consisting of a plastic tank with a capacity of about 50 litres, a feed pump which, after the passage through a filter, sends the pressurised fuel to a group of injectors, a doser, an accumulator, a pressure regulation system and so on.

This simplicity is lost in vehicles fuelled with a gaseous fuel. Regarding CNG cars, it was considered a “monofuel” vehicle, specifically designed to run on natural gas only. However, it should be emphasised that to date, even some vehicles that could run alternatively on CNG or gasoline (“bifuel” vehicle) are classified as monofuel vehicles in case some specifications are met. Namely, also those CNG vehicles that, in addition to the CNG tank, are also equipped with a small gasoline tank with a capacity of less than 15 litres, are considered as monofuel [168]. This gasoline tank may be maintained as a reserve fuel tank for reasons of emergency driving range and vehicle autonomy, given the still poor penetration of methane refuelling stations in some regions. In this case, the methane fuel supply system on-board is simply added to the common supply circuit dedicated to gasoline. It is evident that an engine that is designed to run alternatively on natural gas or gasoline it is not well optimised for neither of the two fuels, and being the gasoline the most problematic fuel (as detonation should be avoided) the engine must give up some of the advantages that would derive from an optimisation to run on natural gas only, first of all a higher compression ratio [152].

The fuel supply system in a CNG vehicle consists of: a gas filler neck, a system of non-return valves, pipes made of higher quality materials (often copper) than in gasoline cars, a group with several valves mounted on the high-pressure CNG tank and other components [152,166,169–171]. These include, for example, a solenoid valve which regulates the fuel flow from the tank to the engine, a valve dedicated to refuelling, overpressure valves, safety valves which intervene in the event of a collision or fire and so on. The gas tank, typically with a capacity of around 100 litres for the vehicle segment considered, is one of the most characteristic elements of this vehicle. Tanks of several construction types can be found (CNG-I, II, III, IV) depending on the amount of steel or other metals and composite material involved. Overall, the gas tank can be divided into one or more cylinders. One possibility is to have a high-pressure tank in which the gas is stored at about 200 bar, making its expansion more gradual through so-called low-pressure cylinders, which act as a rapid-use accumulation for the engine. From these cylinders the gas is then sent to a pressure reducer, which reduces the gas pressure on average down to 8 bar. The pressure reducer is placed near the engine, and it is crossed by a flow of water at 80-90 °C coming from the engine cooling circuit, since the strong expansion undergone by the compressed methane gas would cause the freezing of the various components. From the pressure reducer, the methane is then sent to a system composed of filter, doser and accumulator (rail), until it arrives in a dedicated injection group, different from the one used for gasoline [172]. In almost all cases, an indirect injection of methane into the intake manifold (port fuel injection or PFI), multipoint, sequential and timed, is preferred; in very rare cases, still under study and improvement, a direct injection (DI) of methane into the engine cylinders is used in place of PFI. An ICE fuelled with compressed natural gas does not present any particular constructive difference compared to a common gasoline engine, except for some minor features, such as the presence of reinforced valve seats (e.g., made of tungsten carbide), and other small changes generally linked to the lower lubricating capacity of the gas compared to gasoline or diesel. Finally, the three-way catalytic converter presents different amounts of catalysts and noble metals, since in CNG engines it is particularly important to prevent unburned CH_4 from ending up in the atmosphere. This implies an enhancement of the emissions abatement and of the exhaust gas after-treatment system, which in this case translates into an increase in the load of oxidizing catalysts (usually platinum and palladium).

In summary, a CNG vehicle differs from a gasoline vehicle mainly in the addition of: a CNG storage and on-board distribution system, minor engine modifications, amounts of catalysts in the three-way catalytic converter (TWC).

As regards the vehicle fuelled with hythane, it can be considered almost identical to a CNG vehicle. In fact, there are only slight differences compared to a methane-fuelled car, mostly linked to the presence of hydrogen. There is a single cylinder in which the already premixed hythane is stored, at pressures similar to those of natural gas, making it possible to also use tanks of the type CNG-I or CNG-II. Indeed, up to 200 bar, even pure hydrogen can be transported in steel cylinders without the occurrence of hydrogen embrittlement, which can however be solved with suitable internal lining materials. The use of more resistant cylinders (type II, III or IV) could be considered in order to increase the storage pressure, possibly up to 350 bar, so as to recover the volume subtracted by the addition of hydrogen and increase the driving range (distance that can be driven between one refuelling and another). More effective gaskets to avoid hydrogen leaks, and a safety system to avoid possible flashbacks due to the increased flammability range are also present. The engine does not show any noteworthy change compared to what has been describe for CNG, except for the injectors. Hydrogen embrittlement does not seem to be a problem for the engine combustion chamber, as commonly used materials already offer good resistance to this phenomenon. For example, aluminium with its various alloys is often used for pistons, mainly AlSi alloys with different concentrations of silicon (generally from 12 to 21%), AlCu alloys, or pistons in ceramic materials.

Finally, in case it is preferred to maintain a more conservative attitude, the hythane-fuelled vehicle presents a load of noble metals within the TWC similar to that of the CNG vehicle. If, on the other hand, the advantages obtained in combustion deriving from the addition of hydrogen are considered (reduction in HC and unburnt CH_4 emissions, ultra-lean combustion, greater tolerance to EGR that leads to lower NO_x emissions, etc.), the hythane vehicle could boast a reduced noble metals load with respect to the CNG vehicle.

Furthermore, the vehicle fuelled by a blend of hydrogen and gasoline in ICE (H2-Gasoline) deserves a separate mention. This does not differ much from a common gasoline vehicle, to which only a fuel supply and storage system dedicated to pure hydrogen is added. Since gasoline and hydrogen cannot be mixed in the tank (but only in the engine cylinders during combustion), two separate fuel systems are required on-board: the conventional gasoline one is retained, while a new fuel system related to hydrogen is added. The latter consists of:

- A small storage system for pure hydrogen in gaseous phase, at low pressure (e.g., 200 bar in a steel cylinder) or at high pressure (e.g., in a type IV composite material cylinder at 700 bar), or in the "solid" phase (in a metal hydride cylinder);
- A hydrogen supply system (filler neck, valves, special pipes, systems to prevent backfire, pressure reducer, injectors, etc.);
- Minor engine modifications (gaskets, valve seats, etc.);
- Simplified after-treatment system and TWC containing a lower or equal load of platinum group metals (PGM) than a conventional gasoline vehicle, thanks to improvements in combustion given by the hydrogen addition.

In this case, the addition of hydrogen in the engine cylinders consists of small injections, that can be direct (DI) or indirect (PFI), at each engine operating cycle, which simply add up to those of gasoline. An ICE with these characteristics is in fact defined as "dual-fuel", whereby the engine will always burn mixtures of air-gasoline-hydrogen, but (almost) never only hydrogen or only gasoline. This system offers considerable advantages compared to a traditional gasoline-fuelled spark-ignition engine, as:

- Only small quantities of hydrogen are needed for each cycle: on the one hand this does not penalise too much the engine cylinder volumetric filling nor the power delivered by the engine, on the other hand it makes it possible to use less bulky and/or less heavy hydrogen storage systems, since few hydrogen has to be stored on-board;
- It allows to replace a part of fossil fuel with a clean fuel, depending on the energy input provided by hydrogen and the injected quantities;
- Significantly improves the combustion characteristics, speeding up combustion (thanks to the high flame speed of hydrogen). This reduces the risk of detonation, increases engine efficiency and reduces fuel consumption;

- Makes it possible to use more lean blends without compromising the engine stability, by extending the charge flammability limits, and this reduce the overall fuel consumption;
- Reduces the formation of HC and CO thanks to the greater completeness of combustion;
- Improves combustion in cold starts, when the emission of pollutants is higher;
- Increases tolerance to EGR, through which it is possible to contain the increase in NO_x caused by the higher temperatures reached in the combustion chamber if stoichiometric mixtures for the charge are used in the presence of hydrogen

A disadvantage lies in the more complicated management of NO_x emissions, in any case a little higher than those of a common gasoline vehicle, but significantly lower than those which would be obtained with an ICE fuelled only with hydrogen, considering mixtures close to the stoichiometric value [43,173]. In any case, this problem can be easily solved with some engine techniques, the use of lean mixtures, or with exhaust gas post-treatment systems.

Regarding the H2-ICE vehicle, this vehicle has a powertrain based on a hydrogen internal combustion engine, i.e. pure hydrogen and air are burned within a spark-ignition ICE. Thanks to the combustion characteristics, this vehicle can count on very high efficiency and low polluting emissions, also allowing the use of ultra-lean (air-fuel) mixtures for the charge. The latter can dramatically reduce both fuel consumption and NO_x emissions [43,174]. Structurally, its ICE is almost identical to a CNG one [175–177], with the main engine modifications (with respect to a conventional engine) related to the use of a gaseous fuel. Of course, some engine operational and technical parameters should be optimised for operation with hydrogen. From a vehicle powertrain perspective, there are minor differences between the CNG and the H2-ICE vehicles, mainly related to the storage of hydrogen on board. Indeed in the H2-ICE vehicle, the main structural modifications –with respect to the CNG vehicle– for the use of hydrogen are the presence of a more sophisticated hydrogen tank, a different fuel distribution system, and possible modifications to the catalytic converter in the exhaust system. As already mentioned above, it should be noted that hydrogen embrittlement does not represent a limitation for the use of hydrogen in the engine combustion chamber since the commonly used materials already offer good resistance to this phenomenon [43,177–179]. Similarly to FCEVs, in the case of H2-ICE more hydrogen has to be stored on-board with respect to the vehicles that use hydrogen blends, as hydrogen is the only fuel providing energy. Moreover, the H2-ICE vehicle consumes higher amount of fuel compared to a FCEV, thus further increasing the need to store significant amount of hydrogen, such as to obtain an acceptable driving range. If a pure gaseous hydrogen storage is considered, higher tank storage pressure is also needed, to compensate the low hydrogen density without increasing the tank volume excessively. Therefore, the H2-ICE vehicle could be equipped with the same tank in composite material (type IV) that would be used with a FCEV. This option was considered for the modelling of the H2-ICE in *Publication 1*. Alternatively, it could also be appropriate to use a liquid hydrogen storage or a metal hydrides cylinder, for instance. The fuel system show many similarities with that of the CNG vehicle [180,181] including pipes, fittings, gaskets, valves, pressure reducer, safety system etc, needing to take into account hydrogen specific characteristics (e.g. pipes resistant to hydrogen embrittlement, tighter gaskets to avoid hydrogen leaks etc.). In many cases the components could be exactly the same, such as the copper pipes used for CNG. The exhaust system could also be similar to that of a conventional vehicle, showing no particular criticalities as water vapour is the main exhaust emission. Even in this case, the noble metals loads in the TWC could be reduced considering the lower engine emissions [182–187]. In fact it should be noted that in a hydrogen engine the fuel is carbon-free, and the only carbon source is the lubricating oil, which can partially burn in small quantities, forming very small amounts of CO, HC and PM [175,176,188]. This problem can be partially solved using lubricating oils specifically designed for hydrogen engines, and research is already active on this field. Regarding NO_x emissions, this is a common concern related to hydrogen internal combustion engines. However, high NO_x emissions are obtained only in case a near stoichiometric mixture is used for the engine charge. Several strategies could heavily reduce NO_x emissions, first of all the use of ultra-lean mixtures (e.g., λ = air-fuel equivalence ratio = 2) or the use of EGR. Using these strategies would allow to obtain NO_x emission much lower than conventional fossil fuel-based engines, in turn allowing to reduce the reducing catalysts (e.g., rhodium) in the TWC. Starting from very low engine emission and through a carefully designed after-treatment and emission abatement system, the H2-ICE could achieve almost zero-emissions. Further technical details on the vehicles under comparison are provided in *Publication 1* and *Publication 4*.

Fuel cell electric vehicles (FCEV)

Electric vehicles get their name from the fact that they are powered by an electric motor. Among these can be considered pure electric cars, which accumulate energy in a battery pack through an electric recharge, or vehicles with fuel cells, called fuel cell electric vehicles (FCEV). Cars equipped with fuel cells store the energy in chemical form by means of a fuel, typically hydrogen, inside a tank. This energy is then converted directly into electricity via an electrochemical process, therefore in the absence of combustion, inside a fuel cell. The electrical energy thus generated on-board is then used to put in rotation an electric motor, which supplies the mechanical power necessary to move the vehicle. It is therefore important to specify that the fuel cell, unlike a battery, does not accumulate energy inside it in any way, rather acting as an electricity generator, as long as fuel is supplied to its ends. Pure electric vehicles with large battery packs on board are never treated in this thesis, but only FCEVs. Anyway, FCEVs are often also equipped with a rather small battery to improve their performance thanks to hybridisation of the powertrain that enables some useful features such as regenerative braking.

Similarly to what has been described for ICE vehicles, some subsystems that make up the powertrain of a FCEV can be considered [189–192]:

- Fuel cells stack;
- Hydrogen tank;
- Battery;
- Power control unit (PCU);
- Electric motor;
- Balance of Plant (BoP):
- Mechanical power transmission system;

The fuel cell stack, by analogy with an internal combustion engine, represents the on-board electric power generator. The stack is supplied with hydrogen, stored in a special tank, and atmospheric air sucked in by means of a compressor. The electric motor is usually an alternating current (AC) synchronous motor with permanent magnets. Since the electrical energy produced by the fuel cell is in direct current (DC), a power control unit is interposed between the fuel cell stack and the electric motor, made up of various electrical/electronic devices, including an inverter (DC/AC), a rectifier (AC/DC) and an electronic converter (DC/DC). In fact, the task of the PCU is to manage in a smart way the electric power flows, for instance by sending alternating current to the electric motor, or direct current at a different voltage to the battery, when needed. The PCU also manages the power flows related to regenerative braking or to boost for strong accelerations. The battery, can be usually of the nickel metal hydride (Ni-MH) or lithium ion (Li-Ion) type, in this case is very small in size (rated energy capacity, mass and volume), i.e. not comparable to a battery pack in a pure electric car, and stores a small amount of electrical energy due to limited capacity. The energy stored in the battery is then released, converted by the inverter and sent to the synchronous motor, in particular moments when it is required, for example in cold starts or accelerations and transients that require more power. The mechanical transmission system, on the other hand, often uses a particular epicyclic mechanism which allows energy to be recovered during braking. The mechanical energy during braking is therefore partially recovered and reconverted into electrical energy, following a backward path from the wheels to the battery. Finally, the balance of plant includes all the auxiliary equipment, i.e. compressor and air pipes, hydrogen distribution pipes, gaskets, filters, fuel cell cooling circuit, exhaust system, etc. Only water is emitted at the tailpipe of a FCEV.

Hybrid electric vehicles (HEV)

A hybrid electric vehicle (HEV), more properly a vehicle with a hybrid propulsion system (or hybrid powertrain), is a vehicle mainly equipped with two components used for traction purposes, an internal combustion engine and an electric motor, which work in synergy with each other. The presence of the electric powertrain is intended to achieve either better fuel economy than a conventional vehicle or better performance [193–195].

The two engines are suitable for coexisting as they have complementary characteristics. The internal combustion engine transforms the chemical energy of the fuel (which has a considerable energy density and it is easy and rapid to supply) with an acceptable efficiency, especially in certain operating points. The electric motor is able to convert energy that is available on board in smaller quantities (for example in the battery) with greater efficiency and versatility, also being able to operate both as a motor and as a generator. This characteristic of the electric motor makes it suitable for recovering kinetic energy during braking, by means of electric energy generation, which can be stored in the battery and subsequently reused. Another complementary feature between the two engine types lies in their characteristic curves. Usually, an attempt is made to couple a thermal engine, which delivers a high torque when it is operated at a relatively high number of revolutions per minute, with an electric motor, which by its nature delivers a high driving torque at a low number of revolutions. In this way it is possible to obtain optimal performance over a wide range of vehicle operation by switching from an engine to the other one. Furthermore, in HEVs, one of the defects of the internal combustion engine is overridden, i.e. the inertia the ICE has in starting from a standstill, by starting the vehicle with an electric motor, which instead is much less affected by this problem. Another advantage lies in the possibility of using both engines to obtain greater thrust during particularly heavy accelerations [193–195].

The powertrain of a hybrid electric vehicle can therefore be broken down into the following two main subsystems:

- Thermal system
- Electric system

The thermal system is basically the same already described for ICEs. The only differences lie in the different maximum or rated power that can be delivered by the internal combustion engine (that in this case is downsized and could use slightly different thermodynamic cycles or control strategies), and in the use of a particular epicyclic gear in the mechanical power transmission system, such as to allow and facilitate the energy recovery during braking. A HEV usually produces lower tailpipe emissions than a comparably sized ICE gasoline car, since the HEV's gasoline ICE is usually smaller than that of a conventional gasoline-powered vehicle.

The electrical system, on the other hand, characterises the degree of hybridisation (or the degree of electrification) and is mainly composed of:

- Electric motor-generator
- Electricity storage system
- Power control unit

Depending on the degree of electrification, the electricity storage can be performed with batteries (with a wide range of possible rated energy capacity), supercapacitors or electrically operated flywheels. In any case, only batteries will be considered in the vehicles under examination, which are usually of the Ni-MH or Li-Ion type.

Depending on how the thermal and the electrical systems interact and how they are integrated with each other, some powertrain construction schemes (called powertrain architectures) can be defined. Indeed, the integration of the thermal engine with an electric motor, can be achieved with different management strategies of the energy flows: series hybrid, parallel hybrid and series/parallel architectures. The latter is a combination of the series and the parallel architectures and it is also known as mixed hybrid or power-split.

In the series hybrid, the internal combustion engine is smaller and mechanically decoupled from the wheels, and is instead mechanically coupled (in series) to an electric generator. The internal combustion engine can therefore work at a fixed working point, usually at its point of maximum efficiency, supplying –through the alternator– electrical energy to the electric motor, which in turn will provide traction to the vehicle. Thus, the series hybrid is always moved by an electric motor, but also the ICE often remains in operation. Excess electricity is used to recharge the batteries, which in this architecture are usually larger. When more power is required, this is drawn from both the internal combustion engine and the batteries. This technology is also referred to as a "range extender", since it can be considered similar to a pure electric vehicle, whose autonomy is extended by a small internal combustion engine. The major disadvantage of series hybrids lies in the reduction of efficiency in driving conditions of high and constant speed (e.g., highways), due to the energy conversion in several steps. Instead, they have a great advantage in urban traffic with respect to conventional vehicles, since they can use the electric motor (powered by the battery or by the ICE) avoiding the severe ICE partialization and throttling which usually causes high efficiency losses.

In the parallel hybrid, on the other hand, there is a mechanical power coupling node in the mechanical transmission system, to which both the ICE and the electric motor are connected (in parallel). For this reason, both motors can work simultaneously, supplying torque to the wheels. The thermal engine can also be used to recharge the batteries in case of need, being also coupled to an alternator, but parallel hybrids rely more on regenerative braking. In most cases, the internal combustion engine is the dominant engine while the electric motor has the simple function of assisting the ICE by providing more power when needed (mainly when starting off, accelerating, and at maximum cruising speed). The presence of the electric motor therefore allows to reduce the ICE displacement. Usually, parallel hybrids use an almost full-size ICE, with a small (<20 kW) electric motor and a small battery pack, as the electric motor is designed to assist the main ICE and not to provide pure electric traction. Nonetheless, some recent parallel hybrids are equipped with more powerful electric motors (e.g., 50 kW) which enables some electric driving at moderate acceleration. Parallel hybrids are more efficient than comparable non-hybrid vehicles especially during urban stop-and-go conditions with frequent braking and accelerations, where the electric motor is permitted to contribute, softening the ICE’s transients. During highway operation they can also rely on both the engines to provide traction. In some cases, the advantage of starting in electric also makes it possible to eliminate the lowest gears, i.e. those that consume the most fuel.

Finally, series/parallel hybrids have both a mechanical node and an electrical node for the power coupling, allowing the power control unit to determine the most suitable energy management strategy depending on the conditions. In this architecture the motive power can be provided by the ICE, by the electric motor, or by a combination of both as it combines the advantages of series hybrid and parallel hybrid. This is one of the most common hybrid powertrain schemes for full-hybrids, and it is the architecture that was actually considered to model hybrid vehicles analysed in this thesis.

Depending on the degree of hybridisation (i.e., the ratio between the rated power of the electric motor and the total vehicle rated power) and the ability of the hybrid powertrain to store electrical energy on-board, some main categories of hybridisation are defined [193–197]:

- Micro-hybrid
- Mild-hybrid
- Full-hybrid
- Plug-in hybrid

Micro hybrids are almost conventional vehicles as they are only equipped with a very limited rated power electrical motor, that is actually an electrical starter that allows them to use a start-stop function. Nowadays, this has practically become a standard for most conventional vehicles, in order to reduce energy consumption and emissions when in traffic. A part from micro hybrids, also all the other HEVs are capable to use this start-stop system which reduce idle emissions by shutting down the ICE at idle and restarting it when needed. Anyway, micro hybrids are not capable of regenerative braking nor of other more sophisticated functions.

The mild-hybrid HEV is equipped with a slightly more powerful electric motor but still in the order of magnitude of few kilowatt. Also the battery has a very limited rated energy capacity (typically between 0.1 and 0.8 kWh). The electrical system can be usually sized for a rated voltage of 12 V or 48 V, depending on the battery installed and on the degree of electrification. For these reasons, mild hybrids are unable to drive in pure electric mode (only some recent models can do it, but just for few tens of metres or during parking maneuvers). Mild-hybrids are more similar to an ICE vehicle with a light degree of hybridisation that allows to reduce the fuel consumption and emissions. This is possible as, through the electric motor-generator, they are capable of energy recovery under braking and of more efficient accelerations and transients, since the electric motor can assist the ICE. In fact, since the electric motor intervenes providing a boost during strong accelerations, the ICE can work under less severe transients and in better efficiency conditions. Mild-hybrids have often a parallel powertrain architecture.

A HEV is defined as full-hybrid when it is capable to run for few kilometres in pure electric mode (usually around 10 km, having a typical battery capacity around 1 kWh and a battery high voltage). The hybrid powertrain architecture in this case is often of the serial/parallel type. The full-hybrid HEV could be capable of carrying out a single standardised driving cycle or a portion of it in all-electric driving mode (for example NEDC or WLTC cycle used for vehicle type-approval). The pure electric range obviously depends on the battery rated energy capacity installed on-board. These vehicles (together with the mild-hybrids) are also defined as “non-plug-in hybrids” since, not having a charging socket, it is not possible to recharge the battery from an external source. Full-hybrids usually start their operation in electric mode, especially during urban driving. Once the so-called "break-off criterion" is reached (e.g., when urban driving speed is exceeded, i.e., >50 km/h) or when the battery is empty, the ICE is turned on and a switch is made from the electric motor to the internal combustion engine, or both are used together. In these vehicles, therefore, the battery can only be recharged via the electrical energy generated on board, either by the electric motor-generator via regenerative braking, or by the internal combustion engine, by converting a part of the mechanical energy it delivers into electricity by means of an electric generator.

Mild-hybrids, together with full-hybrids are both non-plug-in hybrid vehicles and these are also defined as “not off-vehicle charging hybrid electric vehicles” (NOVC-HEVs).

The plug-in hybrid is similar to a full-hybrid system but presents a higher degree of electrification. The hybrid powertrain architecture is often of the serial/parallel type even in this case. Plug-in HEVs owe their name to the fact that they are equipped with a charging socket (plug), which makes possible to recharge the battery also from an external source, as it happens for pure electric vehicles. In addition, as for the full-hybrids, they can recharge the battery with electricity generated on-board by the ICE or by regenerative braking. These characteristics make the plug-in HEVs the only type of hybrid vehicle capable of exploit a dual mode for the energy procurement, via fuel refuelling or via electric recharge by means of a charging column. Plug-in HEVs usually have a more powerful electric motor than full-hybrids, but above all a larger battery pack, which allows them to achieve a wider all-electric driving range. Typical battery energy capacity installed in plug-in HEVs are around 10 kWh, allowing to drive around

50 kilometres in pure electric mode. These vehicles are also defined as “off-vehicle charging hybrid electric vehicles” (OVC-HEVs).

In the present thesis only full-hybrid HEVs were modelled, disregarding plug-in hybrids and mild-hybrids.

Regarding particular components to be considered in the modelling, in full-hybrids the electric motor is usually of the synchronous type, in alternating current (AC), with permanent magnets. The power control unit, exactly as for the FCEV, intelligently manages the electric power flows (from the battery to the electric motor and vice versa) by means of an electronic control unit with particular power flows management strategies. It also consists of a DC/AC inverter, AC/DC rectifier and a DC/DC converter. In the case of parallel hybrid or series/parallel hybrid powertrain architectures, the PCU also handle the delivery of mechanical power by the internal combustion engine or by the electric motor (or both together), deciding each time and case by case, the most valid hybridisation strategy.

In particular, 5 hybrid vehicles have been modelled in this thesis work:

- Hybrid electric vehicle with gasoline-powered internal combustion engine (HEV Gasoline);
- Hybrid electric vehicle whose ICE is fuelled with natural gas (HEV CNG);
- Hybrid electric vehicle whose ICE is fuelled with hythane (HEV Hythane);
- Hybrid electric vehicle equipped with a dual-fuel ICE powered by a mixture of hydrogen and gasoline (HEV H2-Gasoline);
- Hybrid electric vehicle whose ICE is fuelled with pure hydrogen (HEV H2-ICE).

These vehicles are all based on a full-hybrid system with series/parallel architecture, for a B/C car segment (similar to the Toyota Yaris hybrid), for an overall rated power of the hybrid propulsion system of 80 kW. The type of hybridisation therefore determines the ratio between the rated power of the internal combustion engine (58.4 kW) and that of the electric motor (48.6 kW).

Chapter 3

Hydrogen mobility options: Proposal for implementation of short-term national hydrogen strategies in (Italian) road transport

3.1. Need for decarbonisation of the transport sector

Chapter 1 presented the current world energy scenario, highlighting how the energy sector still heavily depends on fossil fuels and how the need to decarbonise it in order to tackle climate change is increasingly relevant. Currently, the annual global GHG emissions are estimated to be around 50 billion tonnes of CO_2eq [6,7]. In turn, the overall energy sector can be divided into various sub-sectors that accounts for different final uses of energy and are responsible for the emission of different amount of greenhouse gases. Figure 11 shows the breakdown of the main contributions by economic sector.

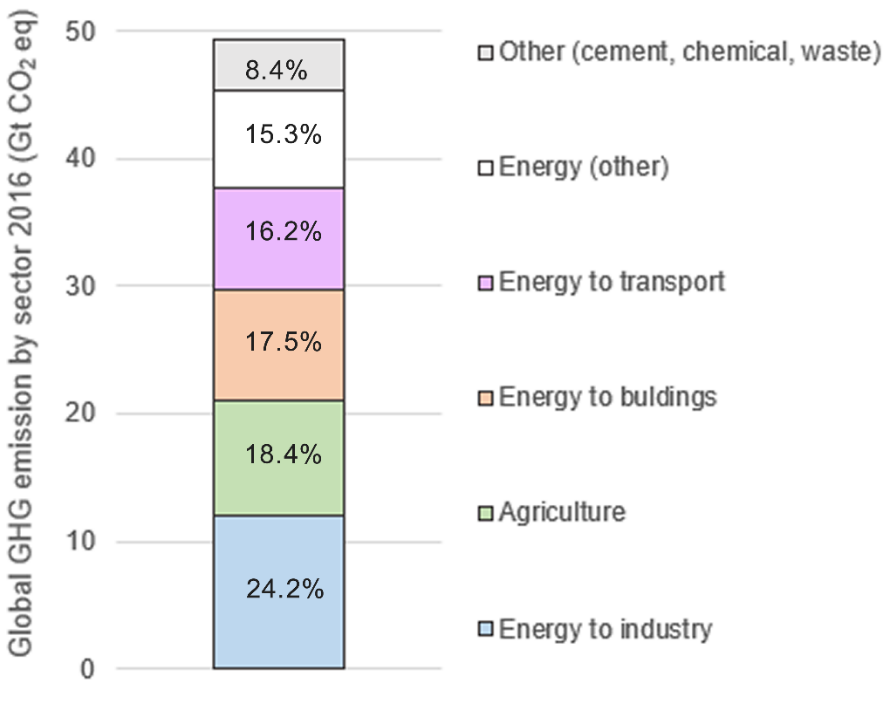

Figure 11. Breakdown by sector of the global GHG emission. Based on [6]

The overall energy sector accounts for more than 73% of the total amount of GHG emissions, with the share for production of electricity, heat and fuels for industry (iron and steel, chemicals, etc.) and buildings (residential and commercial purposes) around 42%. Of the remaining 31% of the emissions allocated to energy, the transport sector accounts for around 16%. Other activities associated to the energy sector (fugitive emissions from energy productions, unallocated fuel combustion, energy to agriculture and fishing) contribute for approximately 15%. The greenhouse gas emissions in turn are strictly related to the energy demand satisfied by fossil fuels. Focusing on the transport sector, this is particularly energy demanding and still relies almost entirely on fossil fuels, thus releasing a considerable amount of greenhouse gas emissions.

According to IEA data, in 2018 the world primary energy demand amounted to 14,282 Mtoe, of which around 81% was met by fossil fuels. In particular, the transport sector alone accounted for 2891 Mtoe, equal to 20% of the global total primary energy supply and to around 29% of the total final energy consumption. To date, this demand is met almost entirely by fossil fuels (96%) and dominated by petroleum-derived products (92%) [198], mainly oil and its derivatives (gasoline, naphtha, diesel, etc.), followed by natural gas, electricity and other forms of energy in smaller amounts. Figure 12 shows some statistics from British Petroleum regarding the energy consumption in transport by fuel type [199].

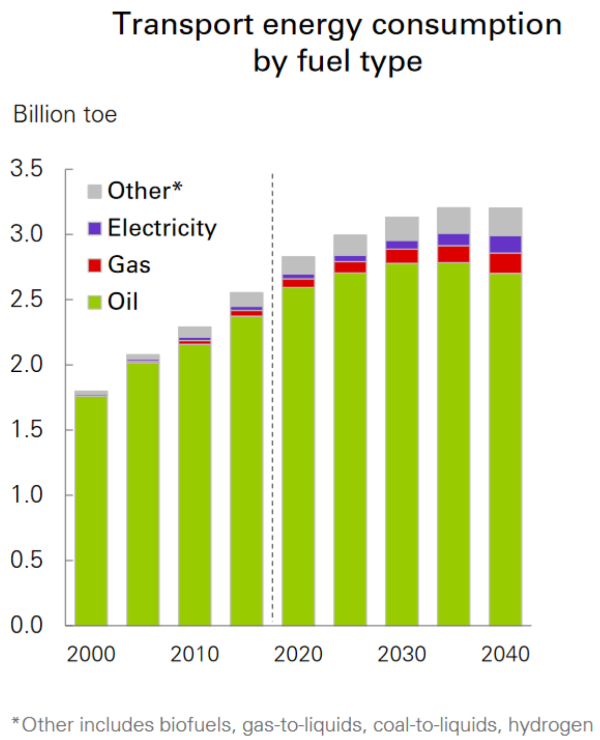

Figure 12. Final energy consumption in transport, broken down by type of fuel.
Data are expressed in billion tons of oil equivalent (Gtoe). Source: BP Energy Outlook 2018 [199]

Therefore, this huge amount of fossil fuels consumption largely contributes on the one hand to global warming, and on the other hand to the emission of pollutants that directly contaminate our cities, continuously exposing people to substances harmful to human health.

Moreover, there is a continuous growth in fuel consumption for transport and an increase in the number of vehicles, especially in non-OECD countries (Figure 13), that further stress the urgency of finding sustainable transport options [77].

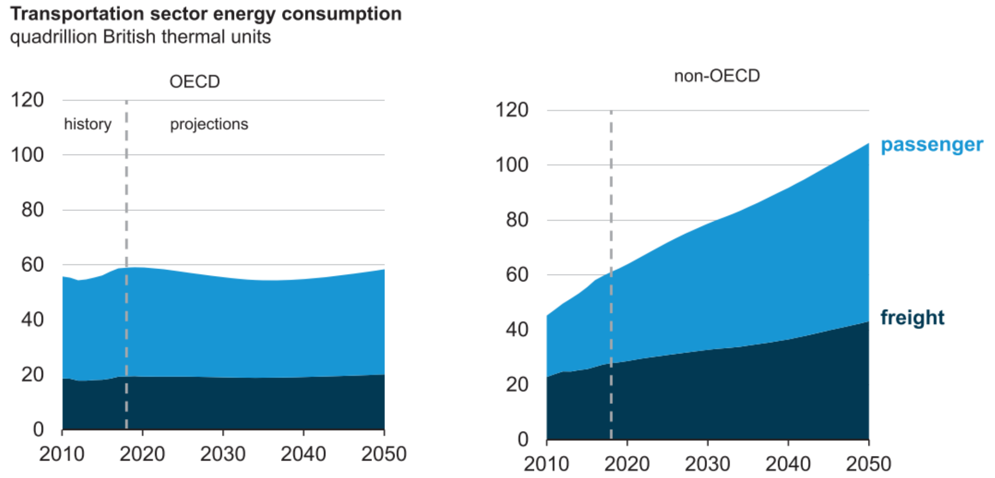

Figure 13. Projections on transportation sector world energy consumption [77]

For these reasons, the transport sector represents a hard core of the energy transition, being the only sector to have shown in recent years an increase, rather than a reduction, in greenhouse gas emissions (Figure 14) [200].

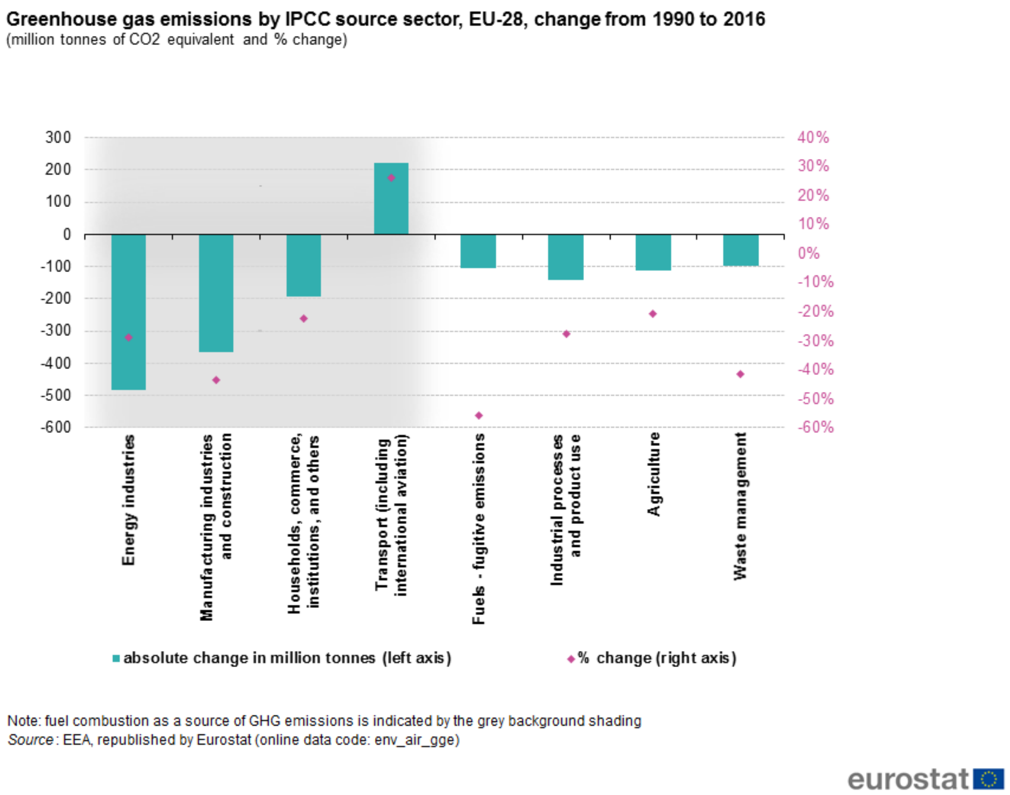

Figure 14. Greenhouse gas emissions broken down by source sector.
The data refer to the European Union countries and to the absolute and percentage variation between 1990 and 2016 [200].

In particular, road transport, dominated by light-duty vehicles and passenger cars represent a large part (46%) of the global energy demand from transport, namely 1323 Mtoe in 2018 (Figure 15) [77].

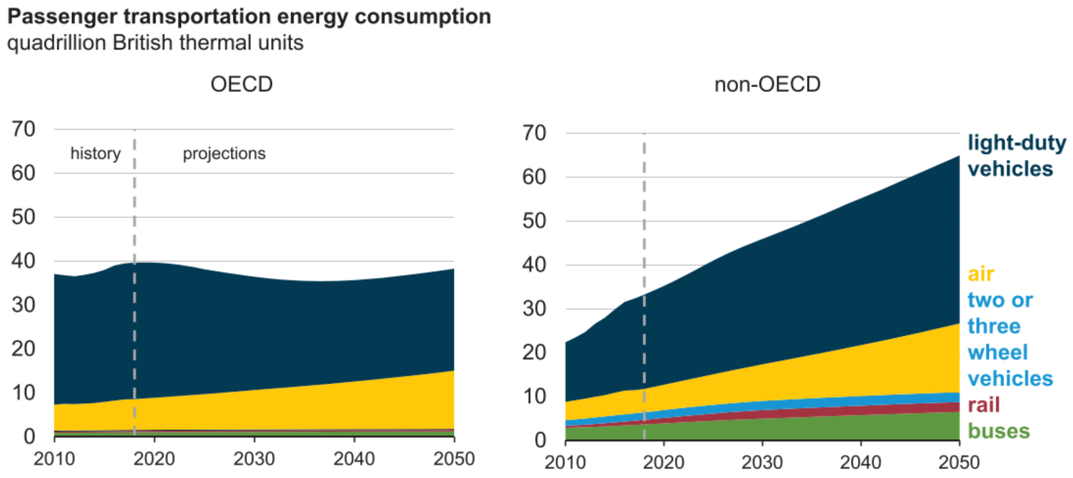

Figure 15. Projections on passenger transportation world energy consumption, by transport mode [77]

As far as concern the European situation, it reflects the world average scenario.
In Europe, the transport sector represents above 30% of energy consumption in final uses (287 Mtoe in 2018) [201] and is annually responsible for more than 1 Gt CO_2eq [202], corresponding to around 25% of the total European GHG emissions (Figure 17) [200]. This makes the transport sector the second largest greenhouse gas emitter in the European Union and its growing emissions can significantly undermine efforts made by other sectors to tackle climate change.

Road transport, for both freight and passengers, is by far the dominant transport mode in Europe (Figure 18), constituting more than 70% of the sectoral energy consumption and emissions [200–203]. Between freight and passenger transport, the greatest energy consumption is associated with passenger transport, in which the predominant vehicle category is constituted by light-duty vehicles and passenger cars, which in Europe make up 83% of inland passenger transport (Figure 19) [201]. Hence, the implementation of decarbonisation solutions for passenger cars is pivotal. In this sense, hydrogen produced from renewable energy sources arises as one of the most promising solutions as a clean fuel for transportation. Furthermore, hydrogen does not involve direct carbon emissions in its use. However, comprehensive analyses following a life-cycle perspective are required to check the environmental suitability of hydrogen and vehicle systems.

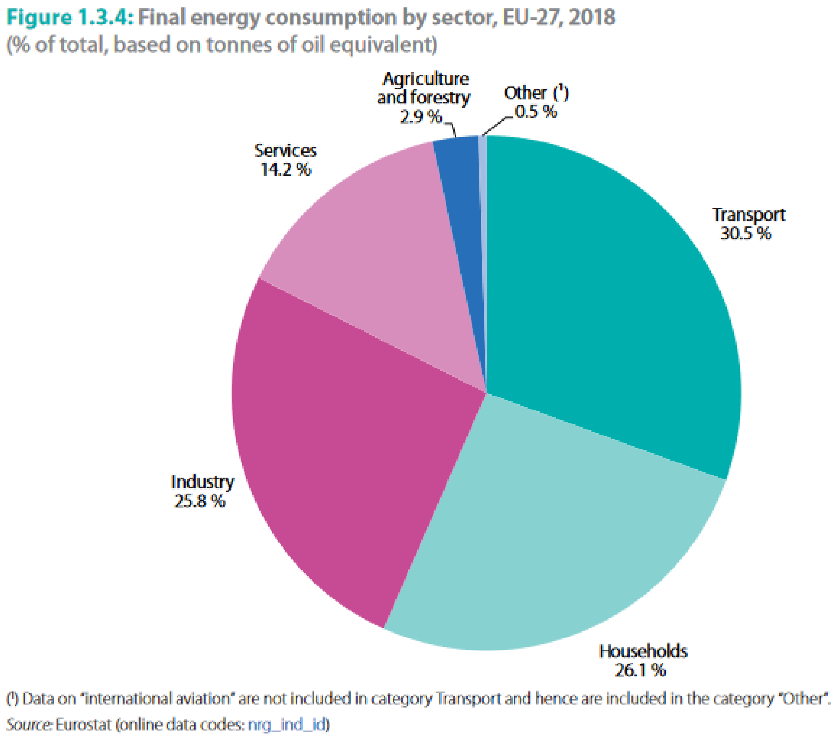

Figure 16. Final energy consumption in Europe, by sector [201]

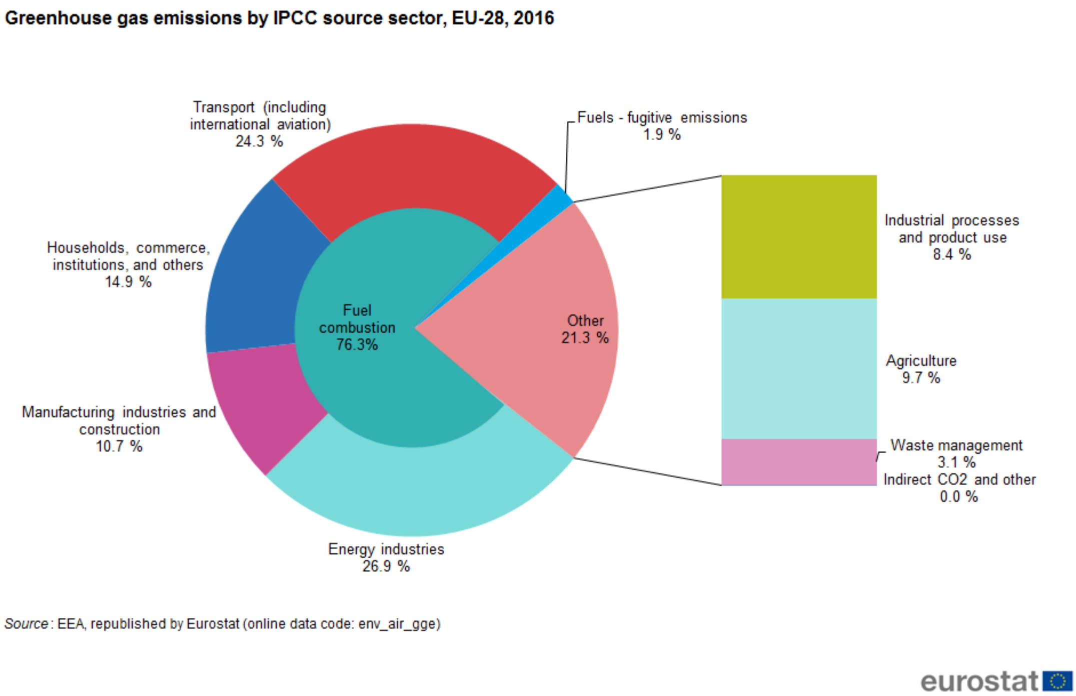

Figure 17. Greenhouse gas emission in Europe, by sector [200]

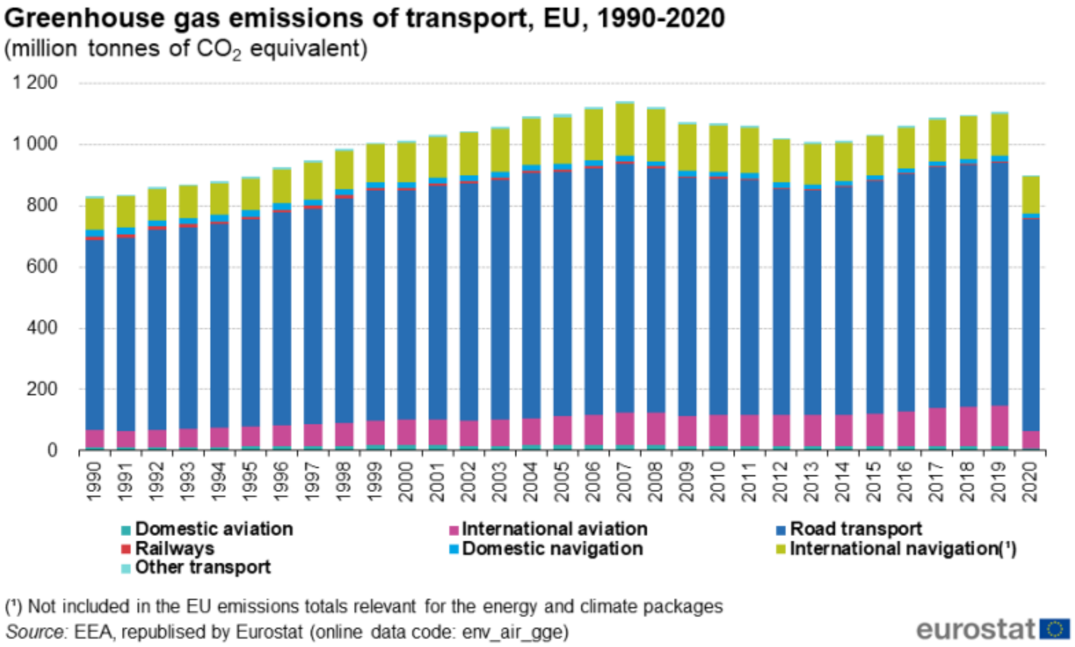

Figure 18. Emissions of greenhouse gases caused by the transport sector in the European Union, broken down by transport mode, data from 1990 to 2020 [200].

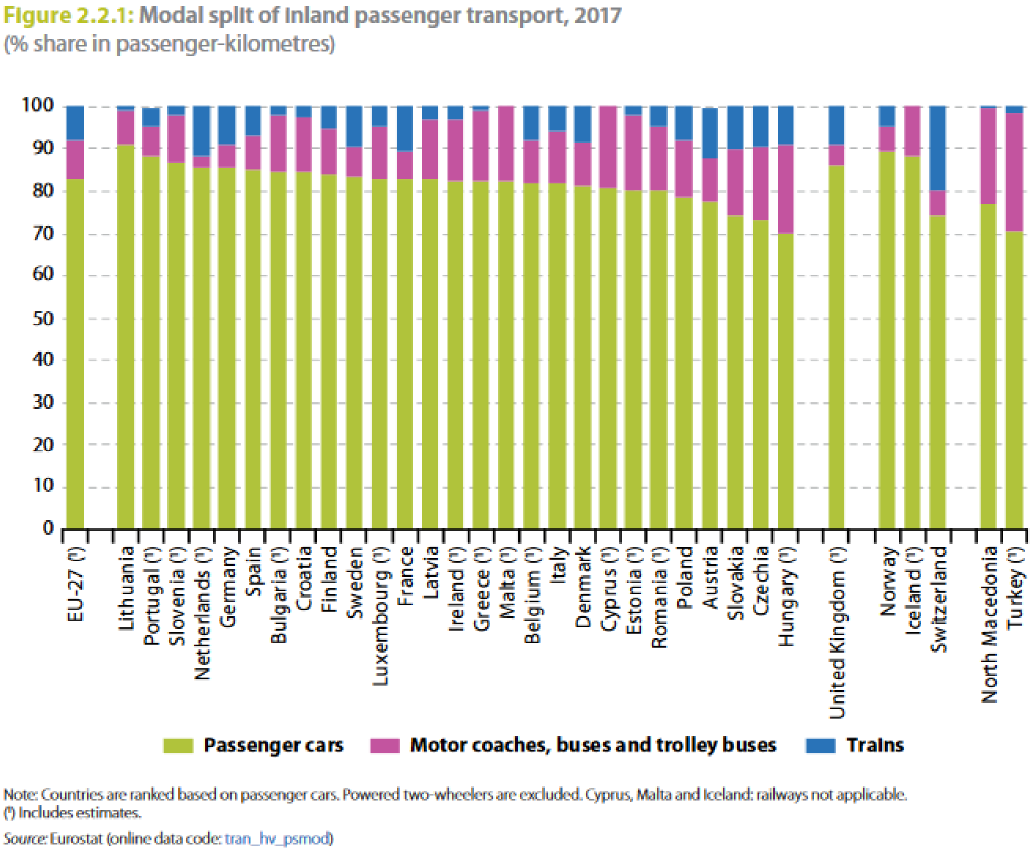

Figure 19. Modal split of inland passenger transport in European Union, in 2017 [201]

In this regard, the policy and decision-making in finding alternatives should not overlook the potential impacts of different points of the supply chain. In other words, environmental analyses should encompass the environmental burdens comprehensively, not limited to the sole fuel use phase or production phase but including all related upstream processes (i.e., the procurement and distribution of raw materials) and downstream stages (i.e., the dismantling and the end of life). Furthermore, environmental assessments should identify burdens shifting, from an impact category to another, from a point of the value chain to another and from a from a sustainability dimension to another (e.g., from the environmental to the economic dimension). When evaluating different options, sustainability criteria are an essential part of governments and companies' strategies, and, since each stage of a product value chain interacts with the society, the environment and the economy, it is crucial to follow a life-cycle perspective. In this context, focusing on the environmental dimension, the standardised LCA methodology represents a central tool to evaluate the potential impacts of human activities from a life-cycle perspective. LCA studies provide crucial scientific support to include a wide range of potential environmental impacts (not limited to carbon footprint) into policy-making processes.

In recent years, the European Union has paved the way to the energy transition with several policy actions aiming at greater sustainability: (i) with the new renewable energy directive 2018/2001 (RED-II) [204], (ii) by requiring that member states draw up national energy and climate plans (NECPs) to meet EU targets by 2030 [205], and (iii) by assigning a strategic role to hydrogen produced from renewables. The latter is evinced by the European strategy for hydrogen [206] and the development of various hydrogen national strategies [207–209], some of which are still under definition.

The RED-II and NECPs define, for the different countries, the target trajectories and the share of renewable energy to be achieved in the various energy uses, including transport. Many European countries such as Italy plan to fill a relatively small part of this renewable quota through the introduction of renewable hydrogen in transport, mainly by introducing fuel cell electric vehicles (FCEV) in their fleets [208–210]. Although this represents a starting point for the development of a hydrogen economy relevant to the transport sector, a large-scale deployment of FCEVs seems to be still a long way off. Core barriers involve (i) the need to start massive production of renewable hydrogen from scratch and, therefore, a limited green hydrogen availability in the short term; (ii) the lack of a hydrogen distribution grid/infrastructure and, in particular, refuelling points; and (iii) current limitations of a technical, economic or social nature at the vehicle level. Taking all these factors into consideration, the choice of the best technology for the use of hydrogen is not as obvious as it might seem and it will probably be a technologically neutral approach and a mix of different technologies that will guarantee the best results. Therefore, innovative strategies that circumvent these barriers while favouring the use of hydrogen in the short term should be explored.

3.2. Comparative life cycle assessment of hydrogen-fuelled passenger cars

In order to achieve gradual but timely decarbonisation of the transport sector, it is essential to evaluate which types of vehicles provide a suitable environmental performance while allowing the use of hydrogen as a fuel. The work presented in *Publication 1* compared the environmental life-cycle performance of three different passenger cars fuelled by hydrogen: a fuel cell electric vehicle, an internal combustion engine car, and a hybrid electric vehicle. Besides, two vehicles that use hydrogen in a mixture with natural gas or gasoline were considered. In all cases, hydrogen produced by wind power electrolysis was assumed. The resultant life-cycle profiles were benchmarked against those of a compressed natural gas car and a hybrid electric vehicle fed with natural gas. Vehicle infrastructure was identified as the main source of environmental burdens. Nevertheless, the three pure hydrogen vehicles were all found to be excellent decarbonisation solutions, whereas vehicles that use hydrogen mixed with natural gas or gasoline represent good opportunities to encourage the use of hydrogen in the short term while reducing emissions compared to ordinary vehicles.

3.2.1. Motivation and background

In a previous study, Valente, Candelaresi et al. [211] explored the role played by hydrogen as the fuel in the life-cycle environmental performance of a fuel cell passenger car, addressing three different hydrogen production technologies, namely steam methane reforming (SMR), biomass gasification (BMG) and wind power electrolysis (WPE). They showed that the choice of the hydrogen production technology significantly affects the whole life-cycle performance of vehicles. Renewable-based hydrogen, especially when produced through WPE, was identified as the preferred fuel option. When using hydrogen from WPE, the ratio of hydrogen impact to the total impact of the whole system dropped to values around 20% or less for the evaluated impact indicators, shifting the main contribution from the fuel to the vehicle infrastructure (Figure 20).

Considering this finding as the background, *Publication 1* aimed to identify the environmentally-preferred hydrogen-fuelled vehicle among different alternatives. In particular, alternative vehicle technological solutions were compared in order to ensure a low vehicle infrastructure impact, and thus an overall contained environmental burden when using renewable hydrogen. For instance, the high platinum load in FCEVs could pose problems both in terms of raw material procurement and environmental footprint [46,212]. Other technologies such as ICEs present greater technological maturity and require less critical raw materials, but on the other hand are less efficient than FCEVs. However, platinum is not the only possible environmental hot-spot, and comprehensive analyses taking into account the entire vehicle infrastructure and their operational parameters are required.

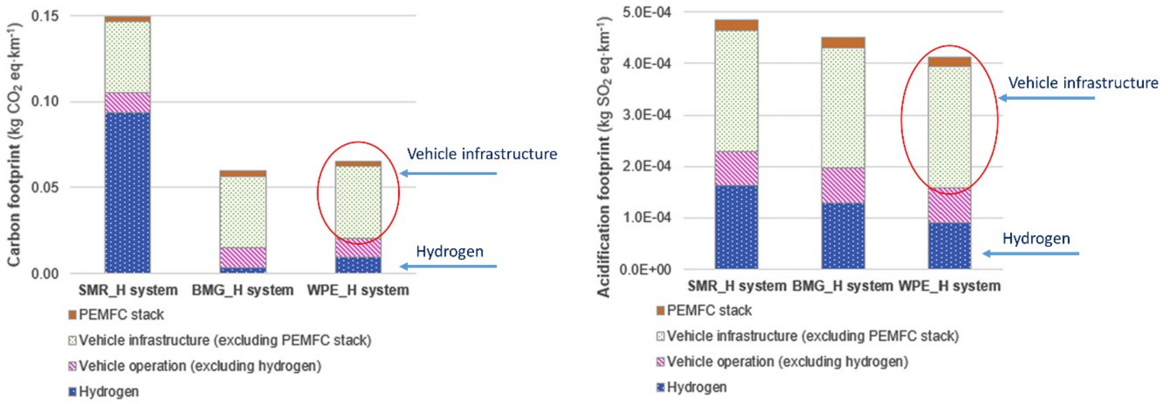

Figure 20. Contribution of hydrogen fuel and vehicle infrastructure to the carbon and acidification footprint, in the life-cycle environmental profile of a fuel cell electric vehicle [211]

LCA studies on hydrogen vehicles retrieved in literature usually consider only FCEVs. On the other hand, the few WTW analyses on hydrogen vehicles equipped with an ICE do not extend the boundaries of the system to the vehicle itself. Hence, this study aimed to compare different hydrogen powertrain technologies by means of a thorough LCA. Technologies for the use of both pure hydrogen and hydrogen mixed with fossil-based fuels were considered since the latter could represent a short-term solution to reduce vehicle emissions until hydrogen production is not large enough to fuel many vehicles. The main novelties of the study lie thus in: (i) comparing the environmental performance between different hydrogen-powered vehicles (FCEV, hydrogen vehicles equipped with internal combustion engines and hydrogen hybrid electric vehicles), (ii) providing detailed life-cycle inventories and the LCA of vehicles equipped with internal combustion engines fed with mixtures of hydrogen and a conventional fuel (namely natural gas or gasoline).

3.2.2. Material and methods

The goal of this comparative LCA study is to identify, according to the current technology level, which type of vehicle provides a suitable environmental performance when using hydrogen produced from renewable energy sources. In particular, all vehicles were assumed to be powered by hydrogen produced by WPE [211]. Three car options fuelled only by hydrogen were considered: (i) a fuel cell electric vehicle (FCEV), (ii) a hydrogen car equipped with an internal combustion engine (H2-ICE), and (iii) a hybrid electric passenger car fuelled with hydrogen (HEV H2-ICE).

The benchmarking of their environmental life-cycle performance against a compressed natural gas (CNG) vehicle and its hybrid version (HEV CNG) was pursued. Another objective addressed further comparison with two passenger vehicles fuelled by hydrogen-fossil fuel blends: a hythane vehicle equipped with an internal combustion engine fed with a gaseous mixture of 20%$_{vol.}$ H_2 and 80%$_{vol.}$ natural gas (Hythane), and a dual-fuel hydrogen-gasoline vehicle equipped with an internal combustion engine (H2-Gasoline) considering an energy ratio of the mixture equal to that of hythane (i.e., H_2 provides 7.3% of the mixture energy). Figure 21 shows a simplified diagram of the various vehicle concepts considered.

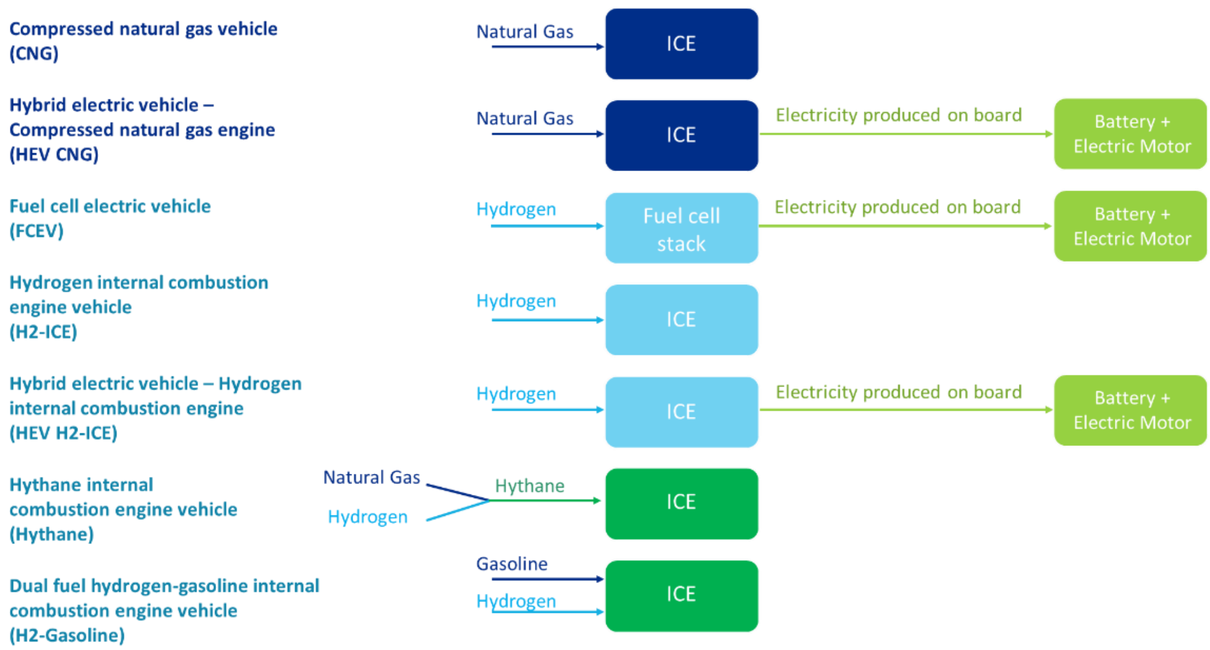

Figure 21. Vehicle concepts under comparison

Regarding the modelling approach, the reference vehicle and the specific methodological aspects presented in *Chapter 2* were considered. Further details can be retrieved in *Publication* **1**.

Table 5 reports some of the main technical characteristics of the three pure hydrogen vehicles considered in the study.

Table 5. Main technical characteristics of the hydrogen vehicles considered in the study

Parameter (unit)	FCEV	H2-ICE	HEV H2-ICE
H_2 consumption (kg/100 km)	0.76	1.68	1.27
Weight (kg)	1800	1380	1550
Lifespan (km travelled)	190,000[a]	300,000[b]	300,000[b]
Thermal engine power (kW)	-	80	58.4
Electric motor power (kW)	80	-	48.6
Driving range (km)	600	300	400
Storage pressure (bar)	700	700	700
Tank volume (l)	120	120	120
Hydrogen (kg)	5	5	5

[a] Based on [213]

[b] Based on [121,122]

The lifespan of the FCEV was assumed to be that of the fuel cell stack, limited by the durability of the membranes. However, research efforts are currently focused on improving the durability of fuel cell membranes in order to reach a life target of 250,000 km travelled [213,214]. For the other vehicles, the lifespan was considered to be that of the ICE [121,122]. In the three cases, the same type of tank was assumed, with gaseous hydrogen storage at 700 bar in a type IV tank (composite material). A full 120-litre tank at 700 bar can store about 5 kg H_2. Technical features of the different vehicles under comparison were provided in *Chapter 2* and additional details can be found in *Publication 1*.

Regarding specifical LCA methodological aspects, the general LCA framework and the specific requirements on LCA of vehicles presented in *Chapter 2* were followed. During the goal and scope stage, the system's boundaries, the functional unit, the impact categories and other relevant methodological aspects were carefully selected. Figure 22 shows the boundaries considered for each vehicle system, which involve both the fuel life-cycle and the vehicle life-cycle [119,121]. The former includes the stages of production, distribution and use of the fuel as a WTW-type analysis [117]. The latter involves the vehicle life-cycle stages of manufacturing, operation, and maintenance. However, it should be noted that vehicle end-of-life was not included in this study due to the acknowledged need for robust inventory data on this stage [159,160]. As shown in Figure 22, the FU of the study was defined as 1 km travelled by each vehicle. The life-cycle environmental performance of each vehicle system was characterised in terms of global warming impact potential (GWP), acidification impact potential (AP) and cumulative non-renewable energy demand (CED) using IPCC [5], CML [215] and VDI [216] methods, respectively. The selection of these categories was based on their relevance in the specific field of hydrogen energy systems, as reported in the extended literature review of Valente et al. [109].

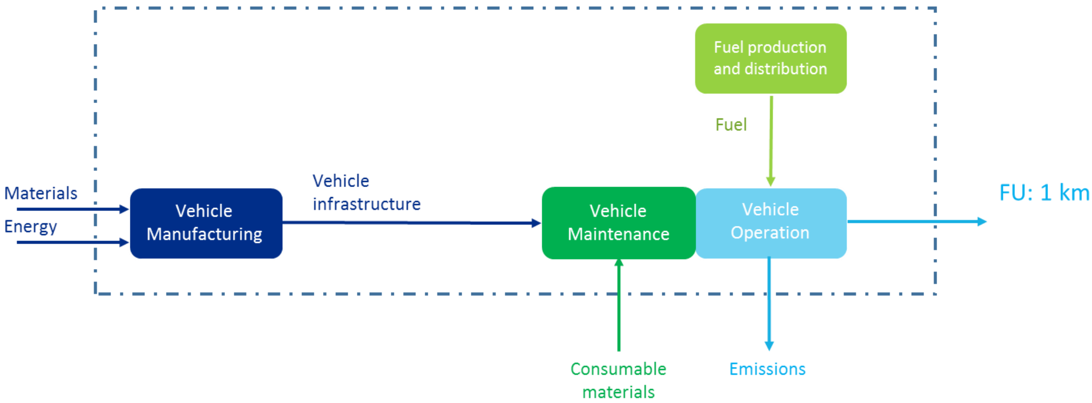

Figure 22. System's boundaries and functional unit for each of the vehicles under comparison

3.2.3. Data acquisition

In this section, a summary of the life-cycle inventories used is provided for each vehicle being compared. Detailed life cycle inventories are also provided in Supplementary Information of *Publication 1* and in *Appendix A* of this thesis for the sake of transparency and reproducibility of the study. Transparency in the assumptions made and in the inventory data used is an important aspect in a LCA study in order to also ensure comparability with other studies.

Concerning fuels, harmonised carbon [217], acidification [218] and non-renewable energy [219] footprints were used for the production of hydrogen via WPE, thus including capital goods, but adapting the system to the hydrogen pressure of 700 bar [211]. Hydrogen distribution was considered via road transport (100 km) [220]. Regarding fossil fuels, background data from the ecoinvent database [181] were used. In the case of hythane, hydrogen was assumed to be distributed (100 km) together with natural gas via pipeline up to the refuelling point [220].

The main inventory data for vehicle manufacturing are presented in Table 6. The main data sources for vehicle manufacturing, operation and maintenance were well-established life cycle databases (ecoinvent [181] and GREET model [167]), industry specifications, manufacturer's statements, reports and scientific literature (as further specified in each inventory table). For commercially available vehicles, data were retrieved from technical datasheets released by manufacturers. On the other hand, for non-commercially available vehicles, data collection was based on specific literature.

Table 6. Main inventory data for vehicle manufacture (values per one vehicle)

Item	Unit	FCEV	H2-ICE	HEV H2-ICE	CNG	HEV CNG	Hythane	H2-Gasoline	Ref. for inventory
Body and chassis	p	1	1	1	1	1	1	1	Table A1
Fluids	p	1	1	1	1	1	1	1	Table A2
ICE	kW	-	80	58.4	80	58.4	80	80	Tables A3-4
└Steel, low-alloyed	kg	-	50.41	36.80	50.41	36.80	50.41	51.86	
└Aluminium	kg	-	41.40	30.22	41.40	30.22	41.40	42.85	
└Polyphenylene sulphide	kg	-	24.68	18.02	24.68	18.02	24.68	27.59	
└Lubricating oil	kg	-	8.73	6.37	8.73	6.37	8.73	8.73	
Fuel system	p		1	1	1	1	1	1	Tables A5-7
└Copper	kg	-	3.94	3.94	1.97	1.97	3.94	3.94	
└Polyvinylchloride	kg	-	0.92	0.92	0.46	0.46	0.92	0.92	
└Reinforcing steel	kg	-	-	-	-	-	-	1.45	
Gasoline tank	p	-	-	-	-	-	-	1	Table A8
└Polyethylene, HDPE	kg	-	-	-	-	-	-	17.5	
└Injection moulding	kg	-	-	-	-	-	-	17.5	
Tank CNG-II	kg	-	-	-	80	80	80	-	Tables A9-10
└Steel, low-alloyed	kg	-	-	-	70	70	70	-	
└Epoxy resin, liquid	kg	-	-	-	6	6	6	-	
└Glass fibre	kg	-	-	-	4	4	4	-	
Hydrogen tank (CNG-IV)	kg	93	93	93	-	-	-	18.6	Tables A11-12
Exhaust system	p	-	1	1	1	1	1	1	Tables A13-20
└Reinforcing steel	kg	-	34.9	34.9	34.9	34.9	34.9	34.9	
└Synthetic rubber	kg	-	1.45	1.45	1.45	1.45	1.45	1.45	
└Talc	kg	-	1.4	1.4	1.4	1.4	1.4	1.4	
└Steel, low-alloyed	kg	-	25.2	25.2	25.2	25.2	25.2	25.2	
└Platinum	g	-	1.4	1.4	2	2	1.4	1.12	[182–187]
└Palladium	g	-	0.7	0.7	1	1	0.7	0.42	[182–187]
└Rhodium	g	-	0.64	0.64	0.4	0.4	0.64	0.48	[182–187]
└Cerium concentrate, 60% cerium oxide	kg	-	0.04	0.04	0.04	0.04	0.04	0.04	
└Zirconium oxide	kg	-	0.14	0.14	0.14	0.14	0.14	0.14	
└Aluminium oxide	kg	-	0.02	0.02	0.02	0.02	0.02	0.02	
└Polyphenylene sulphide	kg	-	0.1	0.1	0.1	0.1	0.1	0.1	
Fuel cell stack	kW	80	-	-	-	-	-	-	Tables A38-56
Li-ion battery	kWh	1.8	-	1.8	-	1.8	-	-	[221,222]
Electric motor	kW	80	-	48.6	-	48.6	-	-	Tables A21-22
Power control unit	kg	33.3	-	33.3	-	33.3	-	-	[189,190,221,223]
Balance of plant	kg	55	-	-	-	-	-	-	Table A23
Gearbox	kg	80	80	80	80	80	80	80	Table A24
Starting system	p	-	1	1	1	1	1	1	Tables A25-28
Cooling system ICE	kg	-	29.1	29.1	29.1	29.1	29.1	29.1	Table A29
Electronics for control units	kg	1.3	1.3	1.3	1.3	1.3	1.3	1.3	Table A30
Tyres	p	4	4	4	4	4	4	4	Table A31
Natural gas	MJ	1933	1933	1933	1933	1933	1933	1933	[181,224]
Electricity	kWh	691	691	691	691	691	691	691	[181,224]

The body and the chassis of ICE and HEV vehicles were modelled based on GREET [167], in proportion to a kerb weight of the reference vehicle of 1250 kg (Table A1 in *Appendix A* for further details). HEV and ICE vehicles were considered to involve the same glider; therefore, weight differences in vehicles are due to differences in powertrain configurations (additional components such as tanks and batteries). Details on inventory data for FCEV body, chassis and fluids are provided in *Appendix A* (Table A1-A2). The FCEV was modelled in detail in [211] and full life-cycle inventories for the fuel cell stack are provided in Table A38-A56).

Regarding the H2-ICE vehicle, the main structural modifications –with respect to the CNG vehicle– for the use of hydrogen were taken into account (e.g., hydrogen tank, fuel distribution system, and modifications to the catalytic converter in the exhaust system). It should be noted that embrittlement does not represent a limitation for the use of hydrogen in the combustion chamber since the commonly used materials already offer good resistance to this phenomenon [43,177–179]. The inventory for the manufacturing of an ICE car was mainly based on Notter [224] and ecoinvent (Golf A4) passenger car [225–227]. Tyres are based on [228]. The hydrogen tank was considered to be the same as that of the FCEV. The fuel system (adapted from that of the CNG vehicle [180,181]) includes pipes, fittings, gaskets, valves, pressure reducer, safety system, etc. The exhaust system was based on [180,224,229] and noble metals loads in the three-way catalytic converter (TWC) were adjusted with respect to engine emissions [182–187].

Concerning the inventory of HEV H2-ICE, the ICE and the electric engine were based on [230] and other sources [223,224,231], but adapted to the nominal vehicle power (80 kW). The ICE was considered as in the H2-ICE vehicle, but with lower nominal power (58.4 kW). The fuel system and the exhaust system were assumed the same as in H2-ICE. The electric motor inventory was based on [223,224] and assumed the same as the FCEV electric motor, but sized for lower nominal power (48.6 kW). The Li-ion battery [221,222] and the hydrogen tank [190,229,232] inventories were considered the same as in the FCEV. Hybrid vehicles involve the use of a planetary mechanism for the gearbox, which allows energy recovery during braking, and the presence of a PCU (DC/AC inverter, DC/DC converter, battery charger and management system, and power distribution unit) [223] as in the FCEV.

Regarding the CNG vehicle, the main blocks are the ICE, the CNG tank, the fuel system, and the exhaust system. A 100-litre CNG-II tank type was considered, with 200 bar as storage pressure [180,233]. Platinum group metals (PGM) in the TWC were modelled by taking into account the emission characteristics of a CNG engine [182–187]. In the CNG HEV, the same components of a CNG vehicle were considered, with the addition of the electrical system typical of hybrid vehicles. The thermal and electrical systems were sized as for HEV H2-ICE.

The inventory of the hythane vehicle slightly differs from that of the CNG car. There is a single cylinder in which the hythane is stored at pressures similar to those of natural gas, enabling the use of CNG-I (all metal cylinders) or CNG-II (metal liner hoop-wrapped with glass fibre and epoxy resin) type tanks which can store gases up to 200 bar and 250 bar, respectively [233]. The use of more resistant cylinders (type III or IV) could be considered in order to increase the pressure so as to recover the space taken away by the addition of hydrogen and increase driving range. Additional seals and safety systems to avoid possible backfires due to the increased flammability range are also present. The engine has no significant changes compared to previous cases, except for small changes in the gas injectors. The load of noble metals inside the TWC is similar to that of the CNG vehicle. However, considering combustion improvements from the addition of hydrogen, it is possible to reduce the PGM load in the TWC. Hydrogen addition involves a reduction in unburnt total hydrocarbons (HC) and CH_4, greater CO conversion to CO_2, and greater tolerance to exhaust gas recirculation (EGR) and ultra-lean combustion (decreasing NO_x emissions). In the present study, the inventory of the hythane vehicle includes a CNG-II tank (200 bar) with the modifications needed to use hydrogen.

Concerning the inventory of the H2-Gasoline vehicle, the main difference compared to a gasoline vehicle lies in the presence of a composite material cylinder at 700 bar (type-IV tank) and of small volume (1 kg H_2, 25-litre tank) for pure hydrogen storage. This greatly simplifies the hydrogen storage issues because of the small amount of hydrogen required. Other differences with respect to conventional gasoline vehicles refer to minor engine modifications (gaskets, reinforced valve seats, etc.), TWC with lower load of noble metals (linked to combustion improvements), and a hydrogen supply system (filler neck, valves, special pipes, systems to prevent backfire, pressure reducer, injectors, gaskets, etc.). In addition to the dedicated hydrogen fuel distribution system, the H2-Gasoline vehicle also presents a gasoline fuel system consisting of a plastic gasoline tank, fuel pump, tubes, and gasoline injectors.

Regarding the operational parameters of the vehicles, fuel economy (i.e., the reciprocal of consumption) and emission data were collected. Table 7 presents the fuel economy and tailpipe emission values for each of the seven vehicles under analysis. Information about direct emissions was retrieved from commercial vehicles similar to the chosen reference vehicle, using data declared by the manufacturers, technical datasheets and the Ecoscore database [220,234,235]. For non-commercial hydrogen vehicles (H2-ICE and HEV H2-ICE) and mixed concepts (Hythane and H2-Gasoline), data were collected from the GREET model or based on specific literature, following the principle of similarity to the reference vehicle. Values for fuel consumption refer to NEDC (New European Driving Cycle) under a combined cycle (urban/extra-urban route).

Regarding H2-ICE and HEV H2-ICE, data about fuel consumption and emissions were taken from GREET [167]. It should be noted that these values correspond with a conservative approach, especially those of CO emissions. In fact, in a hydrogen engine, the fuel is carbon-free, and the only carbon source is the lubricating oil, which can partially burn in small quantities [175,176,188]. While –in H2-ICE and HEV H2-ICE vehicles– CO, HC and particulate matter emissions are associated with the partial combustion of lubricating oil, in the remaining vehicles using CNG or gasoline these emissions are associated with both lubricating oil and fuel combustion.

Table 7. Fuel economy and tailpipe emissions for the vehicles under study

Vehicle	**Fuel economy** [km/kg]	**CO_2** [g/km]	**CO** [g/km]	**HC** [g/km]	**NO_x** [g/km]
FCEV[a]	131.58	-	-	-	-
H2-ICE[b]	59.239	-	0.05851	0.0082	0.0205
HEV H2-ICE[b]	78.985	-	0.05851	0.0082	0.0172
CNG	28.571[c]	94[c]	0.04825[c]	0.0294[d]	0.0168[d]
HEV CNG[e]	43.290	66.888	0.03233	0.0201	0.0049
Hythane[f]	34.382	75.670	0.02779	0.0194	0.0269
H2-Gasoline[g]	31.352	87.146	0.10227	0.0258	0.0337

[a] Based on [192]
[b] Based on [167]
[c] Based on [234]
[d] Based on [236,237]
[e] Calculated from CNG according to hybridisation factor, and contrasted with [167]
[f] Own calculation with amounts based on [238,239]
[g] Own calculation based on [145,240–243]

Concerning the CNG vehicle, fuel consumption, CO_2 and CO emissions were collected from commercial vehicles. HC and NO_x values for CNG refer to both commercial vehicles and real driving emissions (RDE) tests [236,237]. Emissions and consumption for CNG HEV were calculated proportionally to CNG by assuming the same proportion as between a gasoline vehicle and a gasoline HEV.

Fuel consumption and emissions values for Hythane and H2-Gasoline vehicles were based on literature about experimental tests and measures [145,240–243], according to the hydrogen percentage under examination. The values considered for these two vehicles correspond to a conservative approach and therefore present room for improvement through engine optimisation.

Finally, Table 8 shows the main inventory data for vehicle operation and maintenance. Tailpipe emissions and fuel consumption were derived from the values in Table 7. The particulate emissions generated by the abrasion of tyres, road and brakes were calculated in proportion to the weight of each vehicle. Regarding maintenance, one battery change and three tyres' replacements were considered over the vehicle useful life. Periodic lubricating oil and antifreeze replacements were also considered. All vehicles equipped with ICE require a larger amount of lubricating oil for their routine maintenance than FCEV. These amounts were retrieved from GREET.

Table 8. Main inventory data for vehicle operation and maintenance (values per total kilometres travelled)

Item	Unit	FCEV	H2-ICE	HEV H2-ICE	CNG	HEV CNG	Hythane	H2-Gasoline	Ref. for inventory
Operational inputs									
Vehicle infrastructure	p	1	1	1	1	1	1	1	Table 6
Hydrogen fuel	t	1.44	5.06	3.80	-	-	0.284	0.267	[211]
Natural gas	GJ	-	-	-	534	353	430	-	[181]
Gasoline (unleaded)	t	-	-	-	-	-	-	9.30	[181]
Maintenance inputs									
Lubricating oil	kg	3.56	34.6	34.6	34.6	34.6	34.6	34.6	[167,181]
Ethylene glycol	kg	12.9	12.9	12.9	12.9	12.9	12.9	12.9	[167,181]
Decarbonised water	kg	8.58	8.58	8.58	8.58	8.58	8.58	8.58	[167,181]
Tyres	p	12	12	12	12	12	12	12	[167,228]
Li-ion battery	kWh	1.8	-	1.8	-	1.8	-	-	[221,222]
Emissions									
Carbon dioxide	t	-	-		30.1	21.4	24.2	26.1	Table 7
Carbon monoxide	kg	-	17.6	17.6	15.4	10.3	8.89	30.7	Table 7
Hydrocarbons, unspecified	kg	-	2.47	2.47	9.41	6.43	6.21	7.73	Table 7
Nitrogen oxides	kg	-	6.15	5.17	5.38	1.57	8.6	10.1	Table 7
Brake wear emissions	g	304	368	414	379	422	393	356	[181]
Road wear emissions	kg	3.35	4.05	4.55	4.17	4.64	4.32	3.92	[181]
Tyre wear emissions	kg	19.6	23.7	26.6	24.4	27.1	25.3	22.9	[181]
Kilometres travelled	km	190,000	300,000	300,000	320,000	320,000	320,000	300,000	-

The life-cycle models presented in Table 3 and Table 5 were implemented in SimaPro using ecoinvent as the data source for background processes. The environmental characterisation was carried out by taking into account the selected life-cycle indicators and impact assessment methods.

3.2.4. Results and discussion

The inventories previously presented can be considered a key outcome of *Publication 1*. These inventories (see additional information in *Appendix A*) were all implemented in the LCA computation; in this regard, Table 9 presents the life-cycle profile calculated for each vehicle system (carbon, non-renewable energy and acidification footprints per one kilometre travelled). Under GWP and CED criteria, the most favourable environmental performance was found for HEV H2-ICE, H2-ICE, and FCEV. Hythane and H2-Gasoline show an intermediate performance between CNG and HEV CNG. Under the AP indicator, Hythane arose as the best option, followed by CNG and HEV CNG, whereas H2-Gasoline and FCEV show the highest values. HEV H2-ICE and H2-ICE rank in an intermediate performance. These findings indicate that the identification of the best vehicle option, from an environmental point of view, ultimately depends on the impact categories to be prioritised.

For a better and simple understanding, a graphical visualization of the results in Table 9 and of the rankings obtained for the various technologies – expressed as absolute impact values – is provided in Figure 23–25. These figures also show the impact breakdown, i.e. the different contributions to the overall value and the main sources of potential impact. In this regard, tank-to-wheels (TTW) and well-to-tank (WTT) contributions refer to vehicle operation (tailpipe emissions) and fuel production and distribution, respectively. Infrastructure contribution refers to vehicle manufacturing, while use and maintenance contribution includes the consumption of lubricating oil, spare parts and other consumables as well as wear emissions.

Table 9.Life-cycle profile of each vehicle system (values per FU)

	GWP [kg CO_2 eq·km^{-1}]	**CED** [MJ·km^{-1}]	**AP** [kg SO_2 eq·km^{-1}]
FCEV	$5.601 \cdot 10^{-2}$	$9.913 \cdot 10^{-1}$	$5.332 \cdot 10^{-4}$
H2-ICE	$4.343 \cdot 10^{-2}$	$7.450 \cdot 10^{-1}$	$3.618 \cdot 10^{-4}$
HEV H2-ICE	$4.103 \cdot 10^{-2}$	$7.227 \cdot 10^{-1}$	$3.500 \cdot 10^{-4}$
CNG	$1.317 \cdot 10^{-1}$	2.367	$2.161 \cdot 10^{-4}$
HEV CNG	$1.004 \cdot 10^{-1}$	1.734	$2.229 \cdot 10^{-4}$
Hythane	$1.106 \cdot 10^{-1}$	1.996	$2.113 \cdot 10^{-4}$
H2-Gasoline	$1.301 \cdot 10^{-1}$	2.211	$4.019 \cdot 10^{-4}$

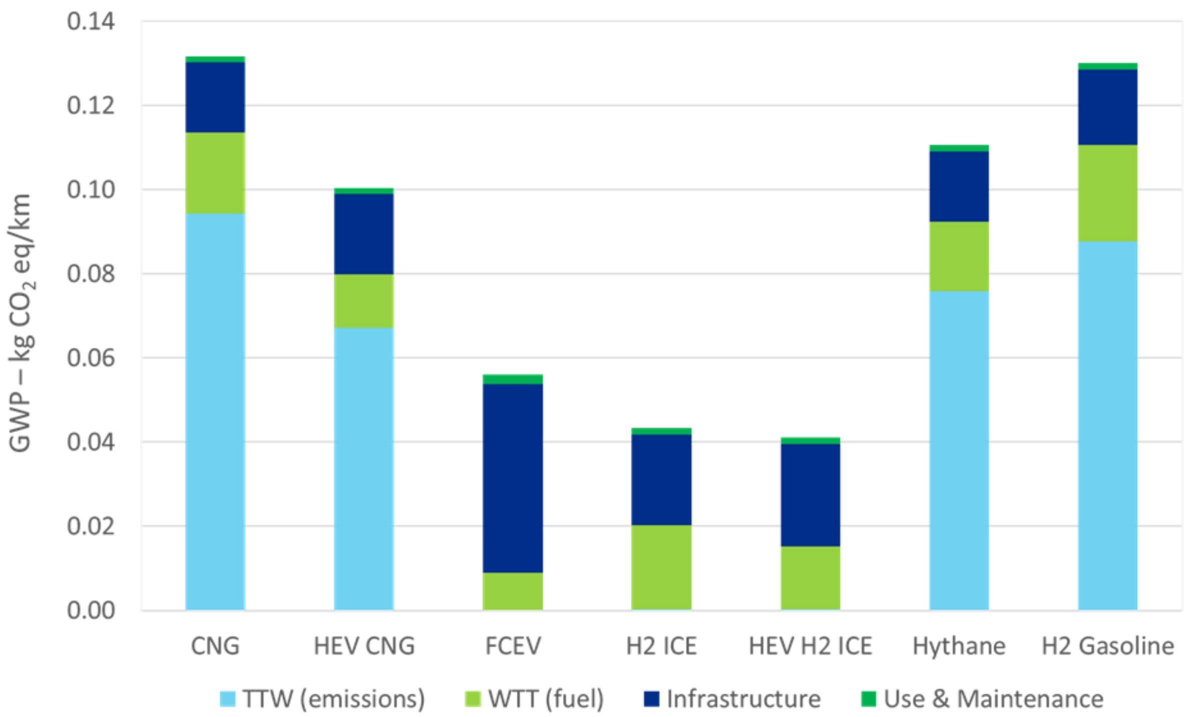

Figure 23. GWP results, absolute values

From Figure 23 it can be easily noted how the three pure hydrogen vehicles all represent excellent decarbonisation solutions. Nevertheless, the infrastructure impact of the FCEV was found to be significantly higher than the corresponding vehicle infrastructure impact of H2-ICE and HEV H2-ICE. More than the result in absolute value, the relationship between the different options under comparison should be underlined. For this reason, Figure 26 and 27 show the results expressed in relative terms with respect to a reference vehicle (benchmark).

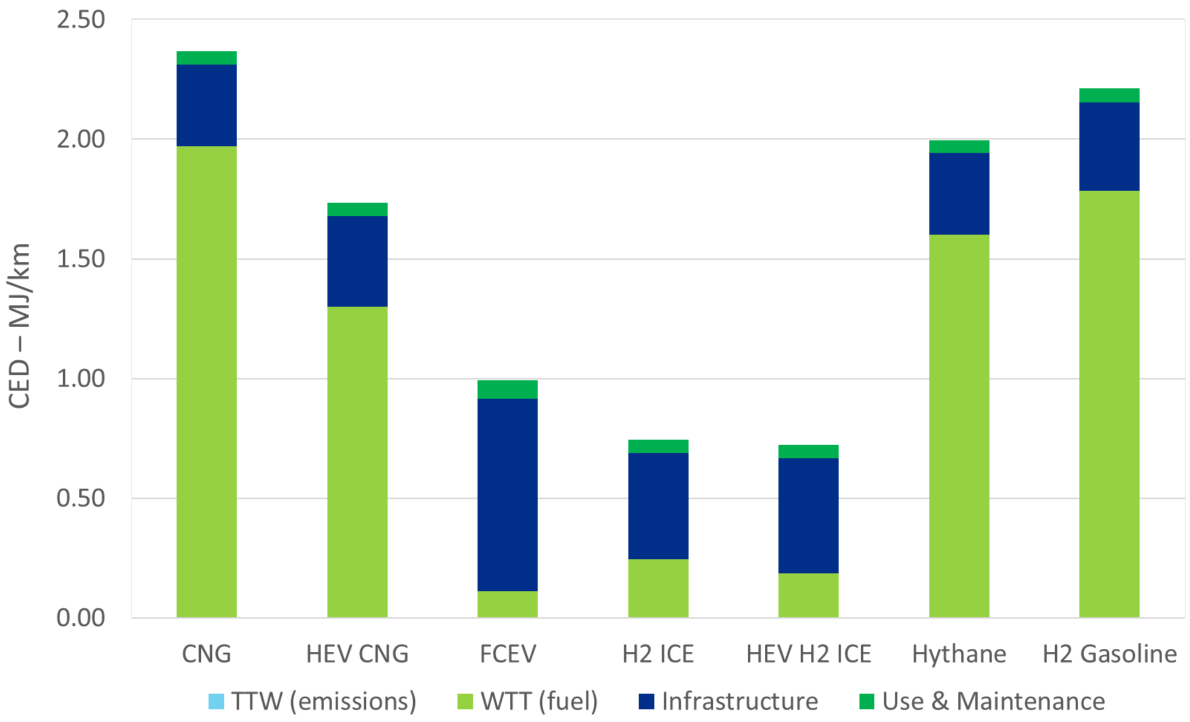

Figure 24. CED results, absolute values

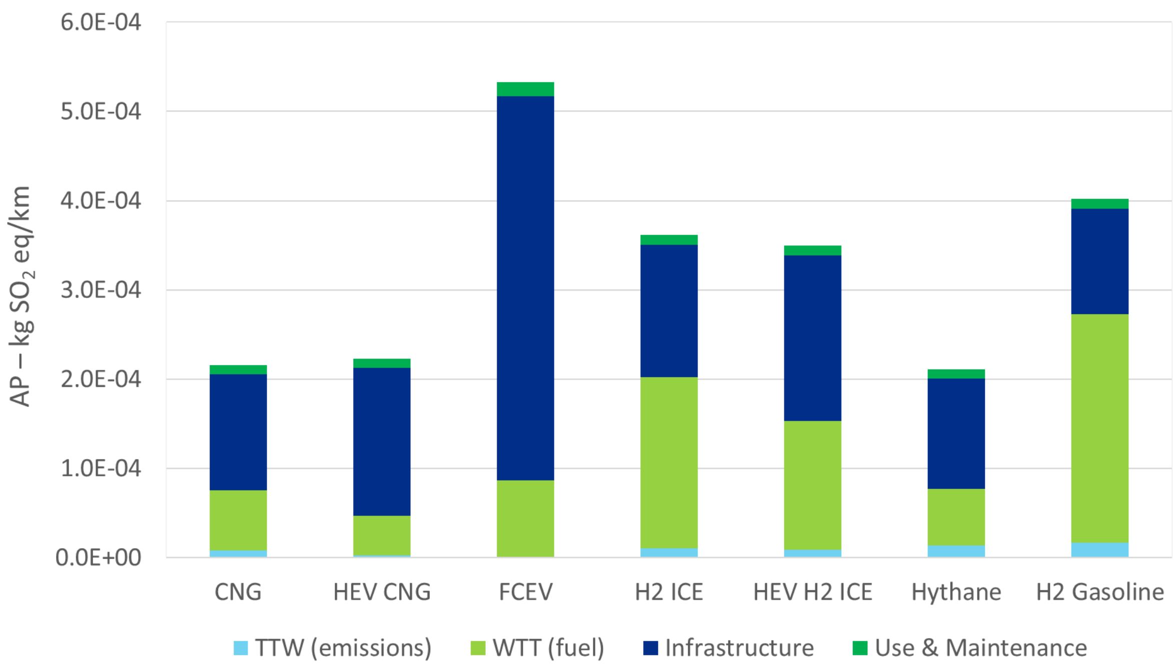

Figure 25. AP results, absolute values

Figure 26 shows the comparison of the pure-hydrogen alternatives with CNG and HEV CNG, using CNG as the benchmark.

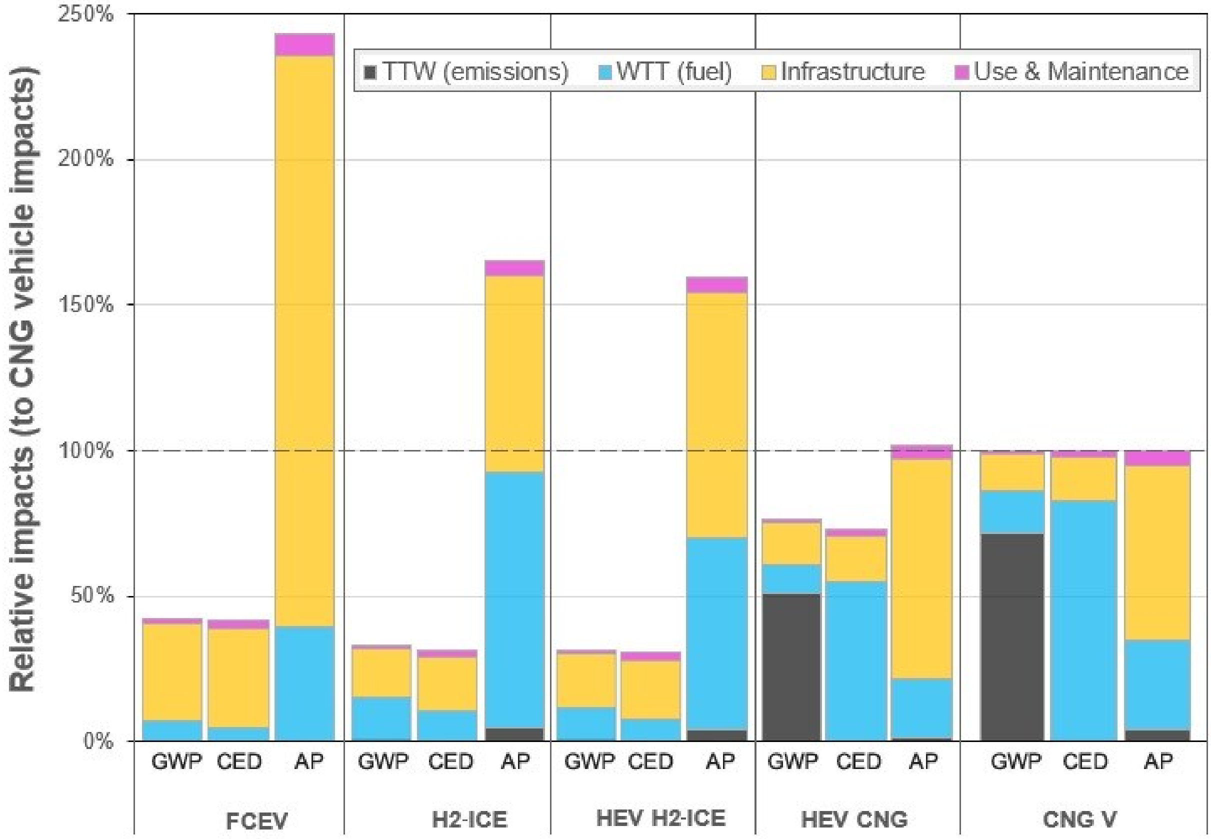

Figure 26. Relative environmental impacts of the three pure-hydrogen vehicle systems and the two CNG systems

Regarding GWP and CED, all vehicles fuelled only with hydrogen show the best performance, while an unfavourable performance was identified for the CNG car. HEV CNG shows an intermediate performance between CNG and hydrogen vehicles. The situation was found to be different in terms of AP, for which the fuel cell vehicle arose as the worst option due to vehicle infrastructure. The major contributors were found to be the steel-based car frame (vehicle body and chassis), carbon fibre for the hydrogen tank, battery and components of the vehicle's electrical system and, to a lesser extent, platinum group metals and other components of the stack.

Concerning vehicle infrastructure, the fuel cell vehicle is outperformed in all impact categories (especially AP) by vehicles with an internal combustion engine, which is closely linked to the lower construction complexity of the latter. In any case, the platinum group metals present in the catalytic converters of ICE vehicles, together with steel for vehicle body and engine and the electrical system for HEVs, provide a significant contribution to AP.

Regarding WTT impacts, the FCEV arose as the best option under GWP and CED indicators. This is closely related to the excellent fuel economy of this vehicle as well as to the choice of hydrogen produced through WPE. Under AP, the best value was found for HEV CNG.

As regards TTW impacts, hydrogen vehicles were found to be the best option under GWP. No tailpipe greenhouse gas emissions are associated with FCEV, while H2-ICE and HEV H2-ICE involve negligible values (related to non-CO_2 emissions). In the HEV CNG and CNG vehicles, the use of a fossil fuel (natural gas) has a great influence on TTW impacts due to CO_2 emissions. Under AP, the best TTW option is the FCEV (with no impact), followed by HEV CNG, CNG, HEV H2-ICE and H2-ICE. Nevertheless, it should be noted that –in all vehicles– the TTW-related AP (closely related to NO_x emissions) is very low.

Concerning use and maintenance contribution, in all cases, it has a minor influence on the results. Under all categories, the best option is given by the CNG vehicle, followed by HEV CNG, HEV H2-ICE and H2-ICE, while the FCEV shows a relatively unfavourable performance. This is mainly related to differences in the lifespan of the vehicles under study.

In order to closely explore the environmental performance of vehicles that involve the use of hydrogen (pure or blended), Figure 27 additionally shows the relative impacts of the Hythane and H2-Gasoline vehicle systems with respect to the FCEV values. Under the set of environmental indicators assessed, due to the use of natural gas instead of gasoline, the hythane vehicle shows a better performance than the H2-Gasoline vehicle. However, hydrogen-mixture vehicles were found to perform significantly worse than FCEV under GWP and CED (due to the involvement of a fossil fuel), unlike under AP (due to the lower construction complexity).

Hythane and H2-Gasoline show high TTW-related impacts in terms of GWP, which is linked to fossil-based CO_2 emissions. In fact, concerning TTW performance, the FCEV advantage of having no harmful emissions was noticeable only under the GWP category, in contrast to a minor effect on AP.

Regarding WTT impacts, FCEV is a better option than Hythane and H2-Gasoline under GWP and CED, which is linked to its low fuel consumption and the consideration of renewable hydrogen (produced through WPE). Under AP, the hythane vehicle shows a better WTT performance than FCEV, while H2-Gasoline involves the worst performance of all vehicles. This is linked to the acidification footprints of the three fuels. Hydrogen from WPE has a relatively high AP value, and it is consumed in reduced quantities in mixture vehicles but in high quantities in the FCEV. Gasoline has an intermediate AP value and natural gas has the lowest value. On the other hand, vehicle fuel consumption must be considered. The balance between these two terms determines the WTT impact. In this sense, in the comparison between hythane and FCEV, the reduced fuel consumption of the latter fails to counterbalance the reduced fuel-related AP value of the former. The situation is opposite for the H2-Gasoline vehicle.

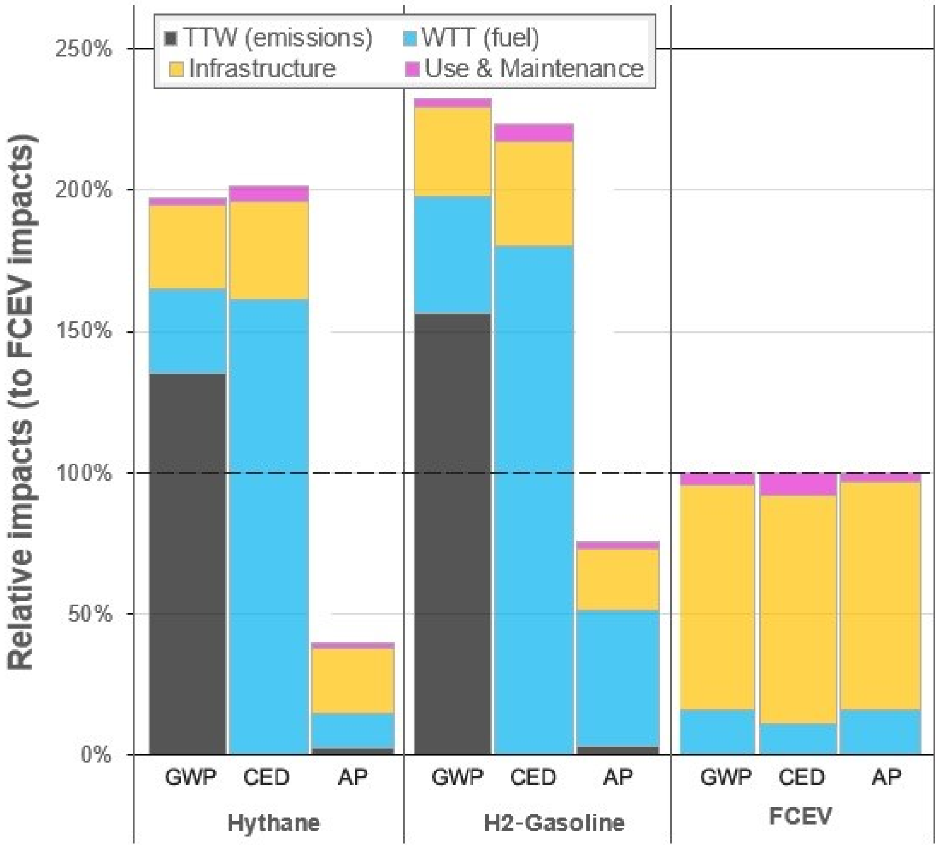

Figure 27. Hythane and H2-Gasoline life-cycle impacts relative to FCEV

Regarding use and maintenance, Hythane outperforms H2-Gasoline under all the categories. It should be noted that, due to the reduction in the formation of carbon particle deposits in the combustion chamber, natural gas vehicles have a greater lifespan than gasoline vehicles. The same could be applied to vehicles with hydrogen engines; however, a conservative approach was preferred due to lower technological maturity.

Overall, the outcomes of the present work expand the knowledge in the field of hydrogen vehicles by filling the literature gap in LCA of hythane, hydrogen-gasoline and hydrogen hybrid electric vehicles. Concerning the life-cycle performance of the other vehicles addressed in this work, the findings are in agreement with the recent literature. Notably, the LCA of the FCEV option finds agreement with the study of Evangelisti et al. [190] regarding the main contributions to carbon, acidification and energy footprint indicators, as well as with Benitez et al. [244] and Miotti et al. [245] under carbon footprint indicator. Finally, regarding the remaining vehicles, a contextualisation of the results with other authors' findings is possible only under the carbon footprint indicator. In particular, despite case-study-specific differences in scopes and life-cycle stages covered, the life-cycle impacts of CNG, HEV CNG, and H2-ICE vehicles are found to be broadly in line with the studies of Dai et al. [180], Bauer et al. [246], and Desantes et al. [247].

3.2.5. Conclusions

This comparative LCA study on vehicle systems showed that hydrogen vehicles are excellent decarbonisation solutions when fuelled using renewable hydrogen. In particular, albeit hybrid hydrogen cars with an internal combustion engine (HEV H2-ICE) require a larger amount of hydrogen with respect to fuel cell electric vehicles (FCEV), they were found to involve a better life-cycle environmental performance under the three indicators considered (carbon, energy and acidification footprints). A favourable environmental profile was also found for the option using hydrogen as the sole fuel in an internal combustion engine (H2-ICE), but the higher hydrogen consumption than its hybrid version makes its life-cycle performance slightly worse. This situation is due to the lower lifespan of the FCEV compared to other vehicles. Nevertheless, technological advances in fuel cell (membrane) durability could overturn this situation. Furthermore, in order to attain a reduction in the infrastructure impact of the FCEV, actions are needed on technical factors such as reduction in vehicle weight, use of steel (for the vehicle body) produced with new environmentally-friendly techniques, alternative storage system solutions (in particular regarding the carbon fibre of the tank) and alternative battery options.

Although HEV H2-ICE and H2-ICE vehicles were concluded to involve relatively low environmental impacts, from a technical point of view they suffer from a low driving range, which is a limitation for their application in the short term. There is thus a need to increase their driving range through engine optimisation and improvement of on-board hydrogen storage systems. For their deployment, a high penetration of refuelling points is required. Alternatively, they might be used in applications that do not have refuelling problems (e.g., hub-and-spoke missions).

Concerning vehicles that use hydrogen mixed with fossil fuels (gasoline and natural gas), they could be seen as a suitable short-term solution to give initial impetus to the hydrogen economy by temporarily circumventing major hydrogen storage and distribution issues. For instance, the

H2-Gasoline vehicle, despite an uninspiring life-cycle environmental performance, could count on a driving range of about 1000 km, reducing the problems related to the low diffusion of refuelling points in an early phase of the hydrogen economy. Nevertheless, in the medium term, pure-hydrogen vehicles remain a preferable decarbonisation solution.

3.3. Life cycle assessment of hydrogen passenger cars and sensitivity to technical parameters

In order to obtain robust outcomes from the comparative LCA study addressing several vehicle options, besides methodological consistency, it was found to be important to explore the influence of key vehicle technical parameters affected by uncertainty or variability. In this sense, *Publication 10* investigated the sensitivity of the LCA results to the variation of key vehicle technical parameters in the life cycle of the sole HEV Gasoline vehicle. In *Publication 1*, different types of passenger cars fuelled with renewable hydrogen (totally or partially) were compared by means of LCA: fuel cell electric vehicles as well as internal combustion engine and hybrid electric vehicles, fuelled with pure hydrogen or with mixtures of hydrogen and a conventional fuel. However, it is necessary to take into account that different assumptions regarding some technical parameters of the vehicles could lead to a different ranking in the comparative study. Furthermore, there is a need to understand which parameters critically affect the environmental performance of vehicles over their life cycle, especially for those vehicles that are not yet consolidated in the market. Thus, the purpose of this work (*Original work 1*) was to investigate the sensitivity of the results of *Publication* 1 (on the LCA study of different types of hydrogen-fuelled vehicles) to certain technical parameters of particular importance. The considered vehicles include a FCEV, a hydrogen-fuelled internal combustion engine (H_2-ICE), and its electric hybrid version (HEV-H_2ICE). Furthermore, the analysis is extended to the Hythane and H2-Gasoline vehicles using hydrogen-fossil fuel mixtures in an ICE, as already defined in the previous section. The sensitivity to the following technical parameters was assessed: i) useful life of the vehicle (lifespan), ii) fuel(s) consumption, iii) vehicle kerb weight, iv) average number of passengers on board (occupancy rate), and v) emission factor for tailpipe emissions. The functional unit selected for the study was 1 passenger·km, while the life-cycle indicators evaluated were the carbon, energy and acidification footprints. The results showed that all the vehicle technical parameters considered in this work have a significant influence on the LCA results, with a particular criticality found for fuel consumption and occupancy rate. Lifespan and occupancy rate showed a hyperbolic influence, while fuel consumption and vehicle weight a linear one. Finally, fuel consumption and tailpipe emissions are of paramount importance especially for those non-conventional hydrogen vehicles equipped with an ICE, since they show important room for technological improvement.

3.3.1. Goal and scope

In this study the sensitivity of the LCA results to the variation of key technical vehicle parameters was addressed. The sensitivity analysis was conducted for each of the five hydrogen-fuelled vehicles considered in *Publication 1*. The five case studies under investigation are namely the FCEV, the H2-ICE, HEV H2-ICE, Hythane and H2-Gasoline vehicles. Figure 28 depicts the system boundaries selected for each of the five vehicle systems. Global warming potential (GWP), cumulative non-renewable energy demand (CED) and acidification potential (AP) were the impact categories chosen to conduct the analysis.

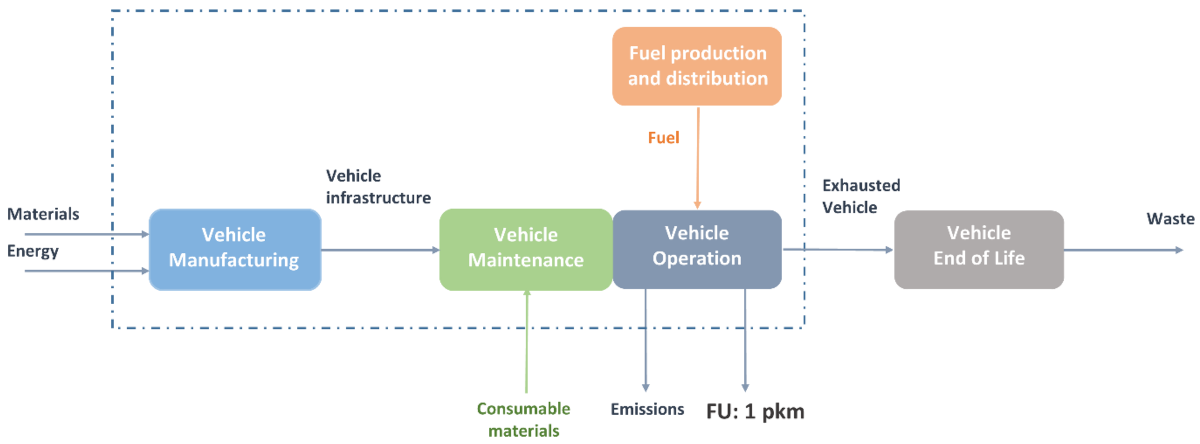

Figure 28. System boundaries and functional unit considered in the study

Functional unit deserves a more extensive discussion. The choice of the functional unit is crucial to ensure comparability among different LCA studies. Typical functional units for comparative studies in the field of transport can be referred to a distance travelled (e.g., 1 km travelled), typically applied when the vehicles under comparisons have the same characteristics in occupation rate or load capacity. When the comparisons are carried out between vehicles which function is to transport people (i.e., passenger cars, trains, buses, flights, etc.) with different occupation rates, the functional unit typically refers to the numbers of passengers that are transported over a unit distance (e.g., passenger·kilometre, pkm). Similarly, when the study goal is to compare vehicles respect to their freight load capacity (trucks, trains, flights, etc.), the functional unit should refer to a unit of weight transported over a unit of distance (e.g., tonne·kilometre, tkm). The functional unit selected for this study was 1 passenger·km (i.e., the main function of the vehicle is considered the transport of one passenger for one kilometre). Although in *Publication 1* the functional unit was 1 km and not 1 pkm, this does not affect the comparability of the results between the two studies. Indeed, the new baseline results are provided in Figure 29, being the old results simply scaled by a factor representing the vehicle occupancy rate with passengers, which in the baseline was selected equal to 1.6 for all the vehicles under investigation. The main reason for the selection of a different functional unit in the present study was the need to explore also the sensitivity of the results to the variation of the occupancy rate, which was deemed not possible using a functional unit of 1 km. From Figure 29 it is also possible to note clearly the main results obtained from the previous study: the three vehicles fuelled with pure hydrogen (FCEV, H2-ICE and HEV H2-ICE) all represent excellent decarbonisation solution (a part for the internal ranking between the three options), but the acidification potential was found to be higher for FCEV. As shown in Figure 30, which depicts the impact breakdown for the FCEV, H2-ICE and Hythane options, this situation is due mainly to FCEV vehicle infrastructure impact.

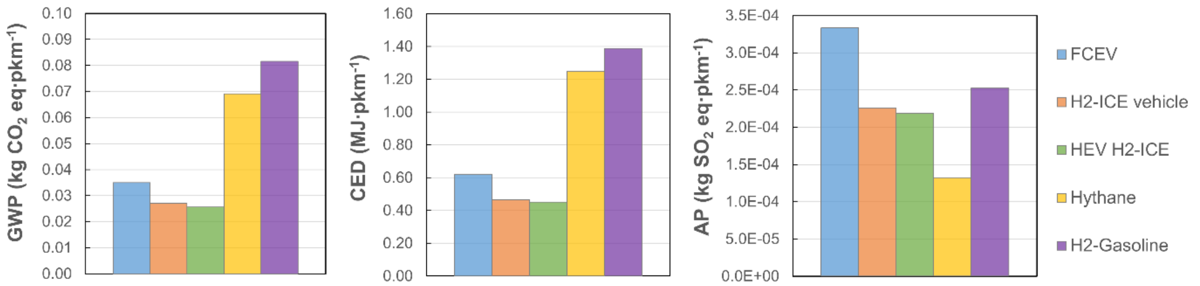

Figure 29. Baseline results of hydrogen vehicles

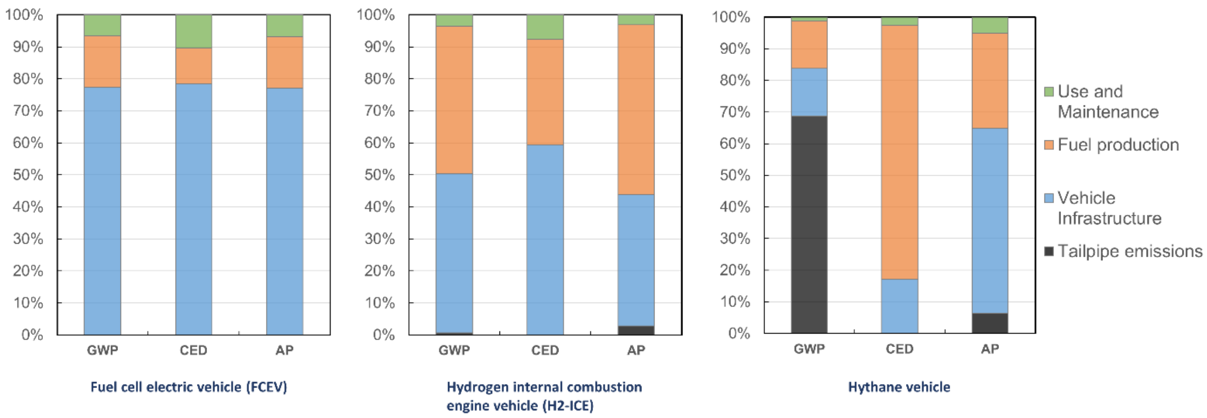

Figure 30. Baseline results, impact breakdown for three selected vehicle options

The situation was found to be different for the H2-ICE, in which the vehicle infrastructure and the fuel production stages assume a more balanced contribution, and for the Hythane vehicle, in which the main contribution to the life-cycle impact was related to tailpipe emissions.

Assuming these results as the background the main technical parameters were changed to observe the influence of their variation on the final results.

3.3.2. Key technical parameters in LCA of passenger vehicles

Table 10 summarises the key technical parameters that were taken into account for the LCA presented in this section. The values that are applied to the baseline case were already presented in section 3.2., a part from the occupancy rate, which here was selected equal to 1.6 for all the vehicles in the baseline case study.

Table 10. Main technical parameters to consider in LCA of passenger cars

Parameter	Unit	Description
Lifespan	km	Total kilometres travelled during the useful life of the vehicle
Occupancy rate	Passengers	Average number of passengers occupying one vehicle
Fuel consumption	kg/km	kg of fuel consumed per kilometre travelled by the vehicle
Weight	kg	Vehicle kerb weight (does not include passengers and cargo)
Emission factor	-	Scaling factor for all the tailpipe emissions (which in turn are expressed in g/km)

Concerning the lifespan parameter, in the specific case of passenger cars, it can be expressed in years of useful life, hours of operation or, in an equivalent way, in total distance travelled by the vehicle during its life (e.g., in km or mi). The conversion from operation hours to km can be easily obtained taking into account an average travel speed over the entire vehicle life expressed in km/h, while the conversion from years to km can be obtained taking into account the average annual distance travelled by the vehicle (e.g., km/year). A typical lifespan range for a conventional gasoline passenger car can be 15–20 years, 250,000–300,000 km (considering an average driving range of 15,000 km/year for an average European passenger car) or 5000-6000 h (considering an average speed of 50 km/h) [248]. Usually, the lifespan affects the product environmental impact, especially with respect to the manufacturing stage, in fact, the total product manufacturing impact is "spread" on the lifespan, so that with the same impact linked to production, a longer useful life usually brings beneficial effects in terms of impact per FU.

The average number of passengers occupying the vehicle during its life should also be taken into account when addressing comparative LCA studies of passenger vehicles. This parameter (occupancy rate) is measured in the average number of passengers (p) carried by the vehicle. For a 5-seater car, an average occupancy rate for a generic European car is 1.6 p [249]. The higher the number of people occupying the vehicle for a single journey, the greater the environmental benefit since (neglecting increases in fuel consumption linked to the greater weight onboard) the impact linked to the travelled distance will always be the same, but the system will have better fulfilled its passenger transportation function. The product between lifespan in distance (km) and occupancy rate in p gives the number of functional units provided by the vehicle (pkm) over its useful life.

Another parameter of acknowledged importance is the fuel consumption. According to common automotive practice, fuel consumption can be expressed in volume of fuel consumed per distance travelled (e.g., l/km) for liquid fuels such as gasoline or diesel, or in mass (e.g., kg/km) for gaseous fuels. Some authors express the fuel consumption in energy expenses per km (e.g., MJ/km) by multiplying the amount of fuel consumed per kilometre with its calorific value. In some cases, however, it is more convenient to consider the inverse of fuel consumption, namely the fuel economy, which represents the distance travelled by the vehicle per unit of mass, volume or energy of fuel consumed (e.g., km/kg, km/l or km/MJ). The fuel consumption of a vehicle is a highly uncertain parameter, as it depends on a considerable number of factors such as engine efficiency, the efficiency of the mechanical transmission from the engine to the wheels, vehicle kerb weight, additional weight due to the presence on-board of passengers and goods, vehicle speed, driving style, route, traffic, vehicle aerodynamic drag coefficient, wind, tires and road condition and many more [250]. The fuel consumption is provided by manufacturers in vehicle technical datasheets, measured according to standard test-driving cycles defined by regulations, necessary for the vehicle type approval and admission on the market. The data used in the present study refer to the New European Driving Cycle (NEDC) which provides three distinct consumption values based on the route: urban cycle, extra-urban cycle, and mixed or combined cycle (urban + extra-urban). In particular, for this LCA, only the consumption values in the mixed driving cycle were considered for greater adherence to a real possible situation (some km travelled in urban mode and some km travelled in extra-urban roads or highways). In Europe, the NEDC has recently been replaced by the new Worldwide harmonised Light-duty vehicles Test Cycle (WLTC) which provides four different classifications of consumption values based on cruising speed (low speed, medium speed, high speed, extra-high speed). In any case, at the time of data collection, given the transition phase from one test cycle to the other, it was still possible to find the consumption values expressed according to the NEDC. Future updates and actualization of the study should consider WLTC values. However, WLTC consumption values are deemed almost comparable with the NEDC ones, being the first more conservative and slightly higher than the second due to greater adherence to real-life driving situation. When compared to a conventional ICE vehicle, a HEV usually shows a great advantage in terms of fuel consumption especially in urban routes since the electric motor is used instead of the internal combustion engine that would be throttled by traffic. The advantage of a reduced fuel consumption gradually decreases with the increase of cruising speed: in high-speed extra-urban routes such as highways, the HEV advantage linked to regenerative braking is no longer valid, while its consumption values become comparable to those of a gasoline vehicle. Nowadays, for an average European B- or C-segment car, a fairly efficient gasoline-powered 80 kW car can show an NEDC fuel consumption in mixed cycles of around 20 km/l, while a gasoline-fuelled HEV (full-hybrid) shows a fuel consumption of 30-35 km/l in the mixed cycle and as much as 37-44 km/l in the urban cycle [251].

The vehicle kerb weight is another crucial parameter to be considered because it affects not only the fuel consumption but also the particulate emissions that are not related to combustion, i.e., those due to wear of tires, brakes and road.

Finally, the emission factor was here also defined to take into account a variation in vehicle tailpipe emissions. As for the fuel consumption, tailpipe emissions can be greatly affected by a significant number of factors, including for instance (in addition to those listed for the fuel consumption) the considered engine operating point, the engine control strategy and the design of the aftertreatment system. Tailpipe emissions are also declared by the car manufacturers and publicly disclosed in technical vehicle datasheets, since their determination is pursued during vehicle type approval tests (under NEDC or WLTP) and their declaration is subject to some European regulations such as Euro 6 or RDE (Real Driving Emissions). Typically, tailpipe emissions are collected, analysed to distinguish between the different chemical species and their amount is cumulated during the execution of a standard driving cycle. This cumulated amount for each substance is then divided by the distance travelled during the standardised driving cycle to obtain a value of emission expressed in grams per kilometre (g/km). Typically measured and reported emissions are CO_2 (strictly related to fuel consumption), CO, total unburnt hydrocarbons (HC) and nitrogen oxides (NO_x). In addition, the particulate matter (PM), the number of particles (PN) and their diameter distribution are also measured. To simplify the analysis, the emission factor parameter defined in this study is used to increase or decrease all emissions simultaneously by a certain percentage, therefore the existing proportion between the various chemical substances emitted at the vehicle tailpipe is kept unchanged with respect to the base case. More in-depth studies could consider a variation, and therefore a different emission factor, for each chemical substance individually.

3.3.3. Sensitivity of the LCA results to the variation of key technical parameters

Table 11 shows the variation range and variation step assumed for the key technical parameters selected, in order to perform the sensitivity analysis of the total impact results, for the five hydrogen-fuelled vehicles under investigation, as the technical parameters change. The sensitivity of the results was assessed for the total impact under the three considered impact indicators. It is highlighted that the parameters range were chosen taking into account possible realistic variations based on technical and technological characteristics of the vehicles. It should be also noted that, in addition to the fuel consumption, the fuel economy is also provided in Table 11. Manufacturers usually express fuel consumption in terms of fuel economy rather than its inverse (fuel consumption). Indeed, in several cases, the fuel economy is a more practical parameter: for this reason, the parameter's range and variation step were defined in terms of fuel economy for most of the vehicles, and then the fuel consumption was derived by calculating the inverse of fuel economy. Another parameter typically used for practical reasons is the fuel consumption expressed in kg/100km, which can be obtained simply by multiplying the fuel consumption expressed in kg/km by 100. Figure 31, 32 and 33 show the results of the sensitivity analysis for the GWP, CED and AP, respectively, for the Hythane vehicle, taken here as an example. Additional results for all the five vehicles under consideration are provided in *Appendix B*. In the above-mentioned figures, the x axis shows the percentage variation of the technical parameter with respect to the baseline case, while the y axis shows the relative variation of the total impact with respect to the base case for each impact category. It is possible to observe that for all the three impact indicators, the total impact follows a hyperbolic trend as the lifespan and occupancy rate parameters vary, while it follows a linear trend as fuel consumption, weight and emission factor vary. In particular, lifespan and occupancy rate generate descending hyperboles, so as these parameters increase, the total impact decreases, while fuel consumption, emission factor and vehicle kerb weight generate ascending lines, resulting in an increase in the total impact as their parametric value increases.

Table 11. Variation ranges and variation step of main technical parameters considered for sensitivity analysis

		FCEV		**H2-ICE**		**HEV H2-ICE**	
Parameter	**Unit**	**Range**	**Variation step**	**Range**	**Variation step**	**Range**	**Variation step**
Lifespan	km	150,000-300,000	25,000	250,000-350,000	25,000	250,000-350,000	25,000
Occupancy rate	Passenger	1.2-2	0.1	1.2-2	0.1	1.2-2	0.1
Fuel economy	km/kg	83.33-166.66	variable	40-80	5	60-100	5
Fuel consumption	kg/km	0.006-0.012	0.001	0.0125-0.025	variable	0.01-0.01667	variable
Weight	kg	1500-2100	300	1080-1680	300	1250-1850	300
Emission factor	-	-	-	0.8-1.2	0.1	0.8-1.2	0.1

		Hythane		**H2-Gasoline**	
Parameter	**Unit**	**Range**	**Variation step**	**Range**	**Variation step**
Lifespan	km	250,000-350,000	25,000	250,000-350,000	25,000
Occupancy rate	Passenger	1.2-2	0.1	1.2-2	0.1
Fuel economy	km/kg	25-50	5	25-50	5
Fuel consumption	kg/km	0.02-0.04	variable	0.02-0.04	variable
Weight	kg	1080-1680	300	975-1575	300
Emission factor	-	0.8-1.2	0.1	0.8-1.2	0.1

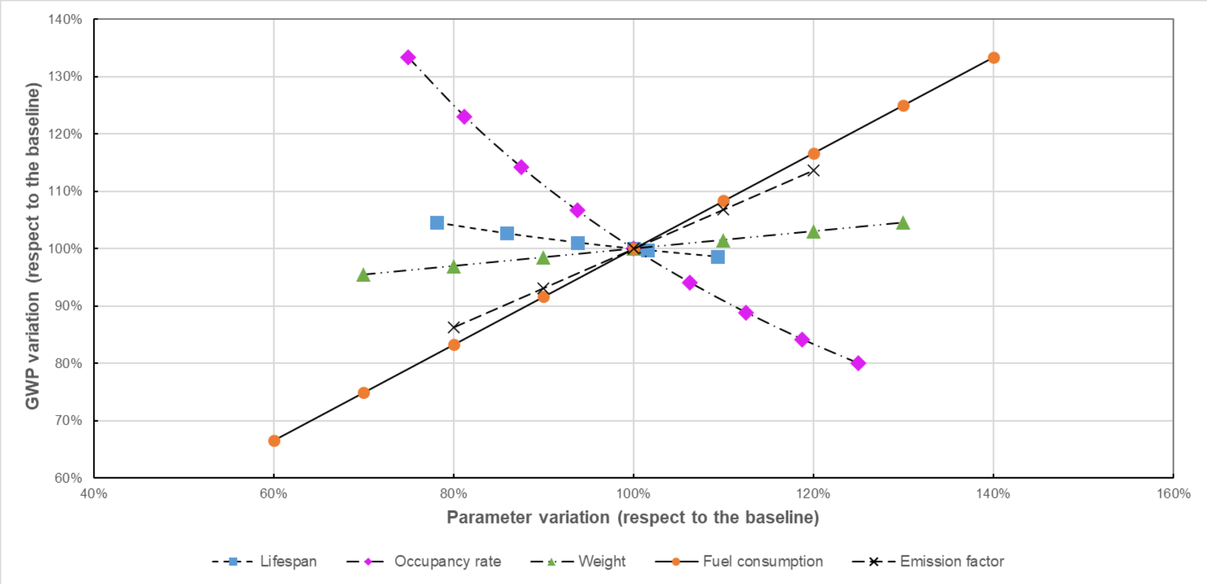

Figure 31. Influence of vehicle technical parameters on GWP impact, Hythane vehicle

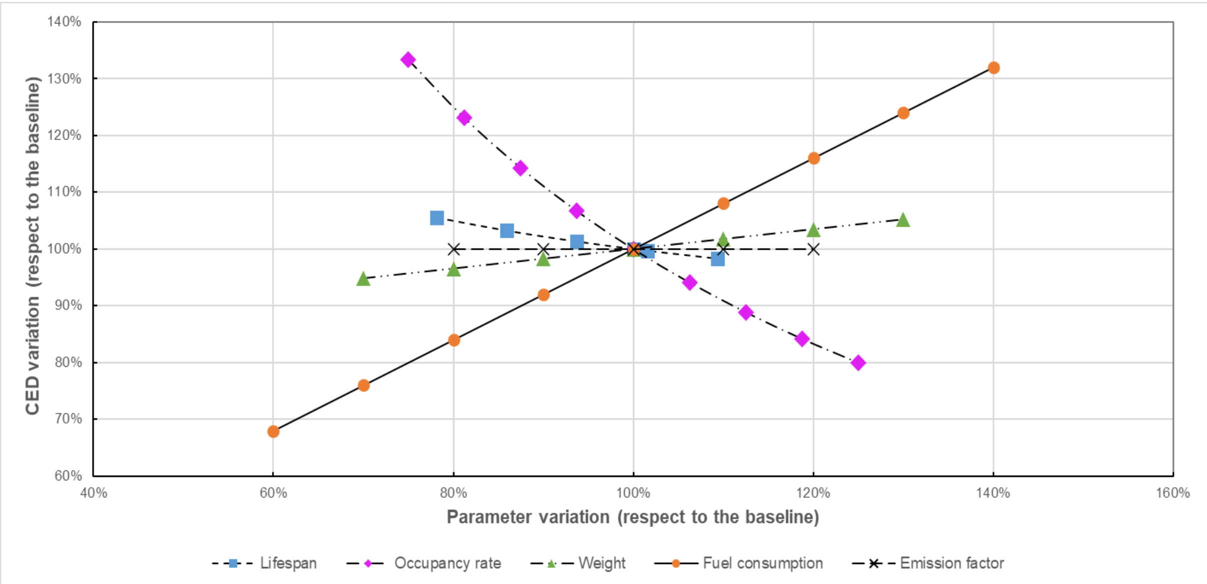

Figure 32. Influence of vehicle technical parameters on CED impact, Hythane vehicle

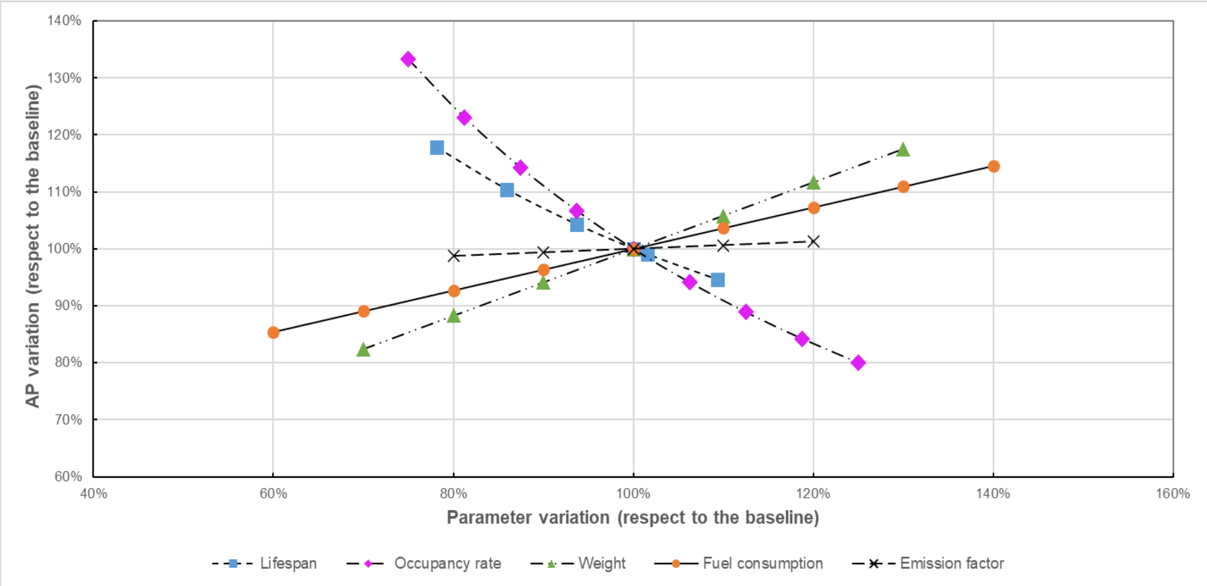

Figure 33. Influence of vehicle technical parameters on AP impact, Hythane vehicle

It can also be observed that the hyperbola linked to the occupancy rate is always more pending than the hyperbola of the lifespan, just as the fuel consumption line is always more pending than that of emissions and often also more pending than that of the weight. A small variation in the occupancy rate or fuel consumption parameters can therefore induce a large variation in the total impact value of a vehicle LCA.

By comparing the slopes of the curves related to the same parameter across the three different impact categories, it can be noted that in general the same parameter has a curve with a different slope under a different impact category. In many cases, the slope was found to be related to some contribution to the total impact that are visible from the impact breakdown in the baseline results (Figure 30). For instance, in the specific case of the Hythane vehicle, tailpipe emissions are very important in the case of GWP (both in the impact breakdown in Figure 30 and having a high slope in Figure 31), but assume a lower importance in the case of AP (again comparing the tailpipe emissions contribution in the AP impact breakdown in Figure 30 and the emission factor slope in Figure 33). Similarly, the slope of the fuel consumption line is related to the fuel production and distribution stage in the impact breakdown, while the lifespan (among other things) is always related with the vehicle infrastructure impact, since a higher vehicle lifespan decreases the vehicle manufacturing impact per FU.

Furthermore, by comparing the different slopes between the various figures, it can be concluded that the hyperbola linked to the occupancy rate always shows the same slope under the three impact categories, so this parameter has the same incidence for all the impact categories analysed. This result is valid for all the vehicles under consideration, even if the occupancy rate slope is different from a vehicle to another one. In the specific case of Hythane vehicle the lifespan has a much more marked incidence on AP, intermediate on CED and lower on GWP, since its slope varies between the three figures and is greater in AP. For the same reason regarding the slope of the curve between the various figures, fuel consumption shows a greater influence on GWP, intermediate on CED and lower on AP, while vehicle weight shows a greater influence on AP and lower on GWP. This greater influence of the vehicle weight on the AP was found to be related to the non-exhaust emissions of particulate matter due to wear of tyres, brakes and road.

Few selected results are shown in the following figures to provide an overview of the obtained results for different vehicles. Additional results for all the vehicles considered in this study can be found in *Appendix B*. Figure 34 shows the results of the sensitivity analysis for the FCEV under the GWP impact indicator. It can be noted that the lifespan is a crucial technical parameter for a FCEV, considering the hyperbola slope, and a small variation in the value assumed for the lifespan parameter in the LCA of a FCEV could greatly influence the final impact result. This confirms again the relationship existing between the vehicle infrastructure impact (which is the main driver for environmental burdens in a FCEV) and the lifespan. The last point on the bottom-right corner corresponds to a lifespan of 300,000 km, that is a well-known technical target on the durability of a FCEV (in particular of a fuel cell stack and of its membranes) pursued by many research entities such as the U.S. DOE [213].

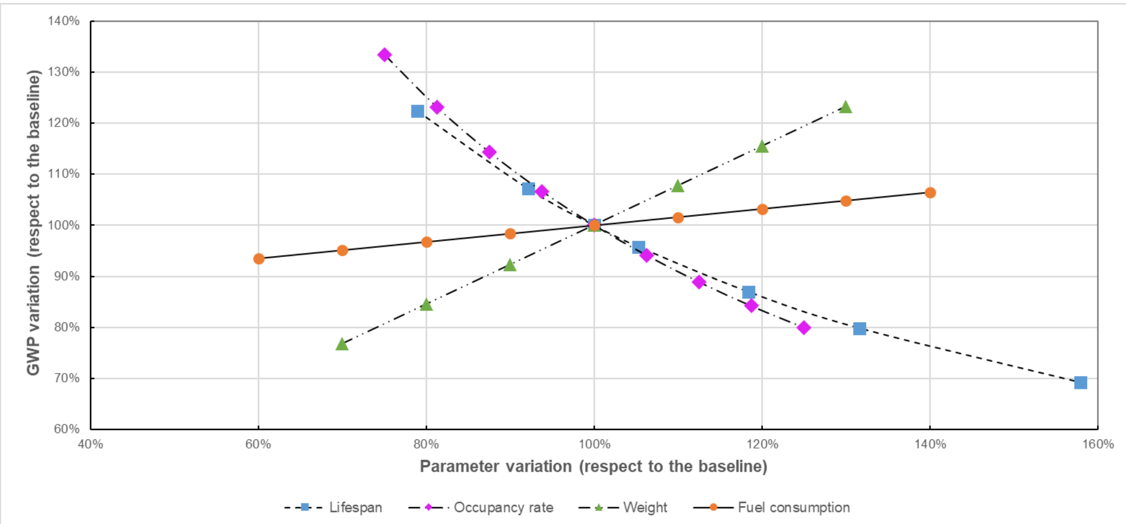

Figure 34. Influence of vehicle technical parameters on GWP impact, FCEV

Its achievement would mean that the FCEV durability would reach the technological parity with the conventional ICE vehicles. As shown in the figure this would also mean to strongly decrease the total life-cycle impact of a FCEV. The current situation is instead represented by the baseline (100% on both the x axis and the y axis), i.e. the point in the centre of the figure where all the curves cross.

Figure 35 depicts the results of the sensitivity analysis for the GWP of the H2-ICE vehicle.

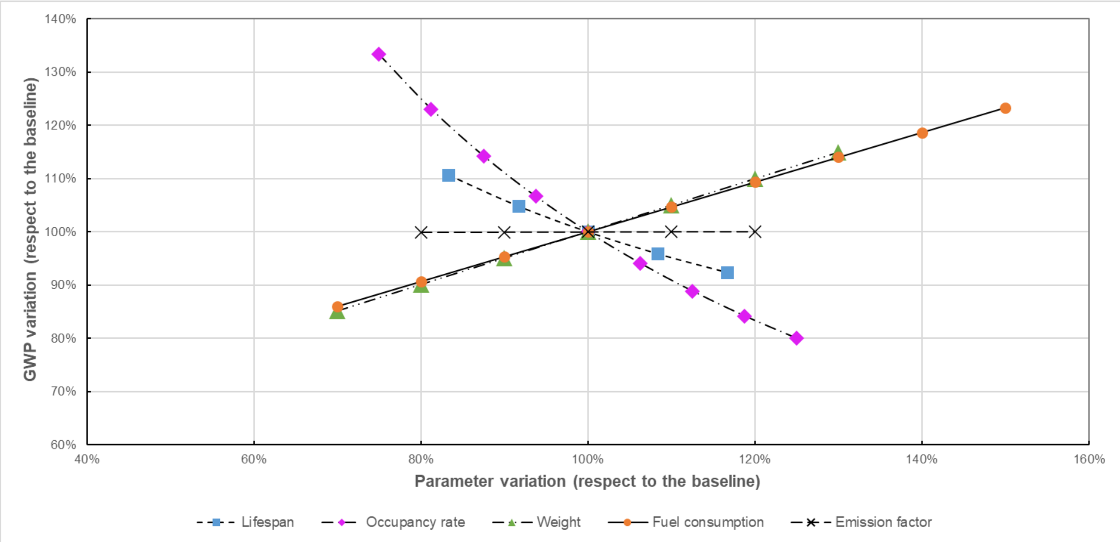

Figure 35. Influence of vehicle technical parameters on GWP impact, H2-ICE

In the case of the H2-ICE it was noticed a lower relevance of the lifespan when compared to a FCEV, confirmed not only by the curve slope, but also by the vehicle infrastructure in the impact breakdown (Figure 30). This is due both to the fact that the ICE is a mature technology, showing high durability and requiring less critical materials for the vehicle manufacturing, and to the fact that the fuel consumption has a greater incidence on the total impact, that is connected to the lower efficiency of the H2-ICE with respect to the FCEV and thus to higher hydrogen consumption. It can also be noticed that, while in the case of FCEV the tailpipe emissions were zero (being constituted only by water vapour), and so no curve was assessed for the emission factor variation, in the case of the H2-ICE the emission curve is almost flat, having the tailpipe emissions a negligible contribution on the total impact.

In the case of the GWP for the HEV H2-ICE (Figure 36) it can be noticed a greater vehicle efficiency with respect to the H2-ICE, that leads to a lower slope of the fuel consumption line and which again is related to the fuel production impact in the breakdown (Figure 82 in *Appendix B*). Contextually, this vehicle also shows a major impact contribution deriving from the vehicle infrastructure. This is due not only to the burden shifting given by the increased efficiency and diminished fuel consumption, but also to the partial electrification of the HEV that requires additional components (such as batteries, electric motor etc.) and impactful materials for its manufacturing. The greater impact contribution of the vehicle infrastructure also leads to a higher slope of the lifespan hyperbola. The presence of these additional powertrain components is also reflected in the vehicle weight, which assumes a greater relevance and thus a higher line slope. A greater vehicle weight also leads to higher non-exhaust PM emission due to wear of tyres, brakes and road, which affects (to a minor extent) the AP impact (see *Appendix B,* connected to use and maintenance impact). Even in this case the emission line is almost flat, being the tailpipe emissions even less than those of the H2-ICE.

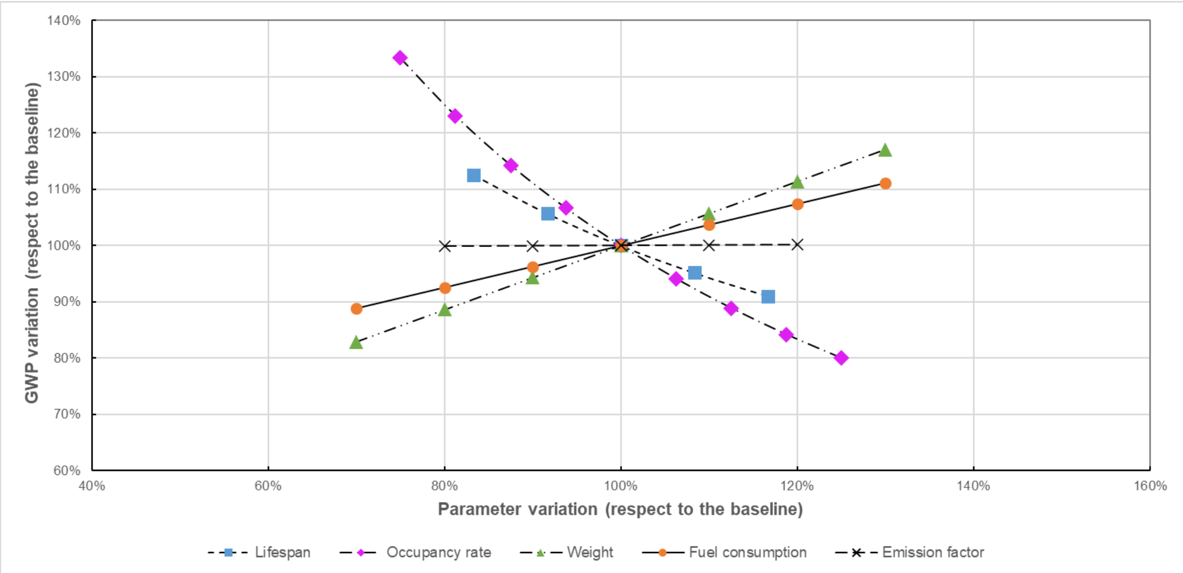

Figure 36. Influence of vehicle technical parameters on GWP impact, HEV H2-ICE

Finally, Figure 37 shows the results of the sensitivity analysis for the H2-Gasoline vehicle under the GWP impact category. For those vehicles that use blends of hydrogen with a fossil fuel (including the Hythane) it was found a major impact contribution deriving from the tailpipe emissions and thus a great sensitivity of the results to the variation of this parameter. This is particularly true for the GWP, in which the emission line shows a high slope that is mainly related to the tailpipe emissions of CO_2 and CO deriving from the combustion of a fossil fuel. A lower relevance of the emissions was found in the case of AP (see *Appendix B*), being the impact contribution deriving from tailpipe emissions much lower than in GWP and mainly related to NO_x emissions, (and to a minor extent to SO_x, considering that nowadays sulphur is almost totally removed from fuels at the refinery). Another critical parameter for the vehicle concepts that use blends was found to be the fuel consumption. This means that their impact could be potentially strongly reduced. In fact, being them still non-commercialised vehicles, they show important room for engine improvement and optimisation which could lead to decreased fuel consumption and emissions. In any case, the vehicles that use hydrogen blends already shows better fuel consumption and less emissions than their conventional counterpart.

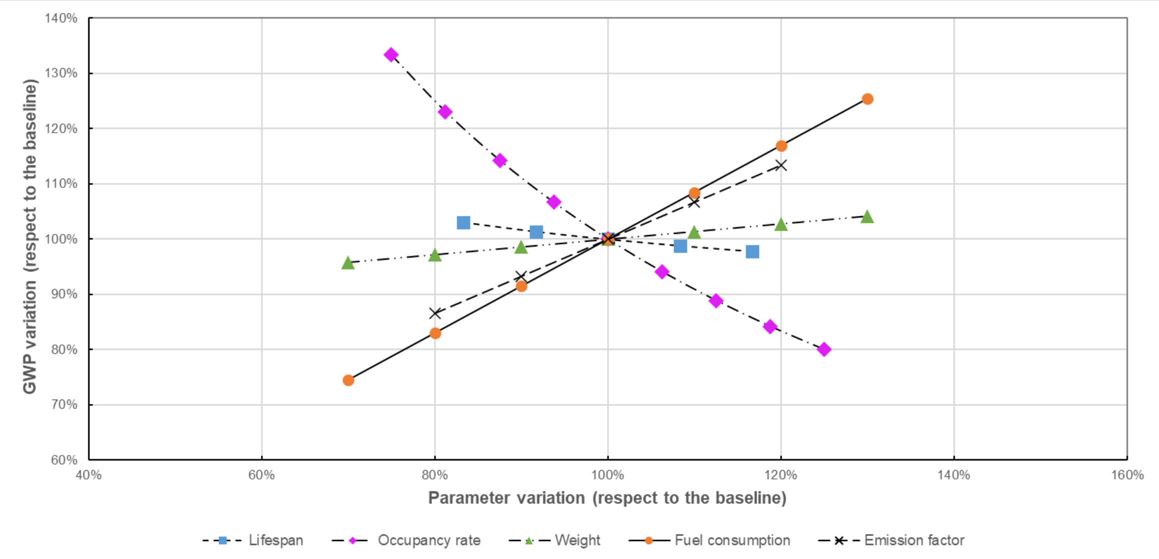

Figure 37. Influence of vehicle technical parameters on GWP impact, H2-Gasoline

Considering all the results obtained in the present analysis (for all the vehicles and the impact categories assessed), it was possible to identify the major environmental impact drivers, the critical technical parameters and the priority intervention areas on which research and development effort should be focused in order to reduce vehicles environmental impact. These results are summarised in Figure 38.

Vehicle	Parameter				
	Lifespan	Fuel consumption	Weight	Emission factor	Occupancy rate
FCEV	✔✔		✔		✔
H2-ICE		✔✔	✔		✔
HEV H2-ICE	✔	✔	✔✔		✔
Hythane		✔✔		✔	✔
H2-Gasoline		✔✔		✔	✔

Figure 38. Key findings on vehicle technical parameters and identification of priority intervention areas to reduce the environmental impact of vehicles

For instance, for the FCEV it would be crucial to improve its lifespan and the fuel cell stack durability in order to decrease the overall environmental impact, while for all those vehicles equipped with an ICE the fuel consumption reduction is paramount to improve their environmental profile.

In conclusion, the sensitivity analysis performed in this study allowed to check the robustness of the results obtained for the comparative LCA study addressed in *Publication 1*. For the FCEV the vehicle infrastructure impact (related to the lifespan) could be further reduced by taking into account eco-design aspects and using low-impact materials, but also by pursuing vehicle light-weighting, which in turn would improve also other aspects such as the fuel consumption and the non-exhaust PM emissions. Hydrogen-fuelled ICEs and HEVs can support the FCEVs but they need to reduce their fuel consumption as a priority for both increasing their driving range and further reducing their environmental footprint. Electrified vehicles (FCEV and HEV) showed a greater acidification footprint, mainly linked to the vehicle infrastructure and to electrical/electronic components. Fuel consumption is a highly uncertain parameter that depends on a multitude of factors, and the value chosen to perform the analysis could greatly affect the final result. Tailpipe emission reduction is crucial for vehicles that use hydrogen mixtures, and this could be pursued by ICE optimisation and aftertreatment system accurate design. Finally, the vehicle kerb weight was found to be related to PM non-tailpipe emissions, but indirectly also to maintenance, fuel consumption and vehicle infrastructure.

Overall, among the five explored technical parameters, lifespan and occupancy rate showed a hyperbolic trend (being connected with the FU), while fuel consumption, vehicle weight and emissions showed a linear trend. Fuel consumption and occupancy rate are found to be the most accentuate drivers to the environmental performance of vehicles. In this sense, potential actions to improve the environmental performance of vehicles could prioritise the improvement of these aspects. It should be noted that these actions not necessarily must be of technical or engineering nature; in some cases, also actions of social nature could be suggested. For instance, potential solutions for the occupancy rate improvement could involve informative campaigns targeted to end-users, promoting an increase of the average occupancy rates or the preferable use of car-sharing services, while fuel consumption could also be reduced by promoting the advantages of more efficient drive styles. The next steps and future expansion of the study could include the addition of the end-of-life stage, the conduction of a Montecarlo analysis to assess the uncertainty, or an assessment of the critical raw materials that, in addition with a Life Cycle Costing and a Social Life Cycle Assessment could lead to a better materials' social responsibility especially for those vehicles that showed a greater infrastructure impact.

3.4. Novel short-term national strategies to promote the use of renewable hydrogen in road transport: a life cycle assessment of passenger car fleets partially fuelled with hydrogen

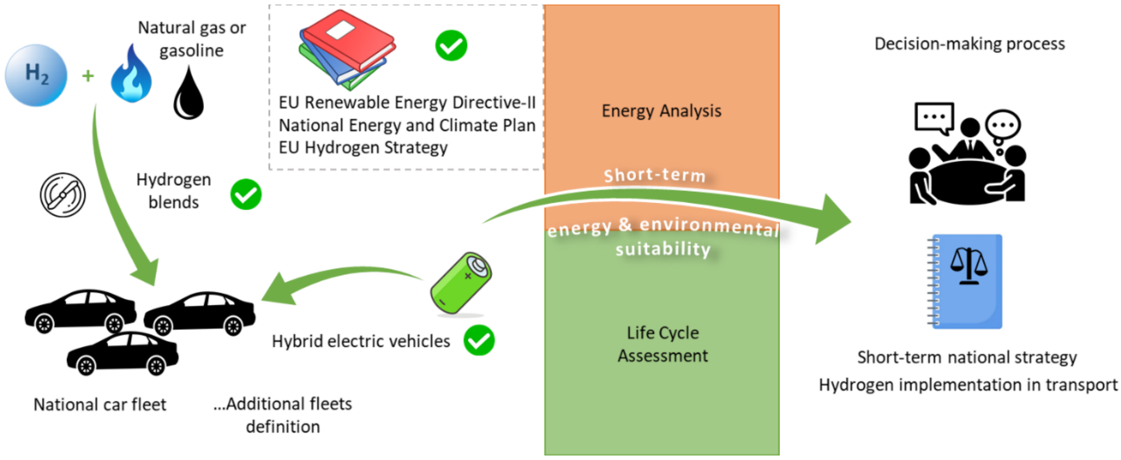

Figure 39. Graphical conceptualisation of the proposed scientific-assisted policy-making process leading to the implementation of national hydrogen strategies in road transport

Publication 4 addressed an energy analysis combined with a comparative environmental life cycle assessment of eight different passenger car fleets that use renewable hydrogen and a conventional fuel (natural gas or gasoline) under the same total energy input and the same hydrogen-to-mixture energy ratio. The fleets under comparison involve vehicles that use the two fuels separately or in a mixture. Using Italy as an illustrative country, this research work aims to help policy-makers implement well-supported strategies to promote the use of hydrogen in road transport in the short term. The proposed strategies achieved a carbon footprint reduction between 7% and 35% with respect to their conventional fleet benchmark. Within the current context, the results suggested the energy and environmental suitability of using hydrogen blends as short-term solutions, involving vehicles that require minor modifications with respect to current compressed natural gas vehicles and gasoline vehicles, while paving the way for pure hydrogen mobility.

3.4.1. Motivation and novelty

The European policy scenario regarding the implementation of renewable-based hydrogen in road transport was already addressed in Section 3.1 of this thesis. The main regulatory pillars considered relevant to the development of a hydrogen-based sustainable mobility were the RED-II, the NECPs and the NRRPs of different member states, as well as the European hydrogen strategy and the national hydrogen strategies of the different EU countries. Section

3.1. also highlighted which are the core barriers involved in a large-scale development of a hydrogen economy relevant to the transport sector, being the main one the need to start a massive production of renewable hydrogen from scratch and, therefore, a limited green hydrogen availability in the short term. Therefore, innovative strategies that circumvent these barriers while favouring the use of hydrogen in the short term should be explored.

On a national scale, in the short term, passenger car fleets would be fuelled only partially with hydrogen, as only relatively small amounts of renewable hydrogen would be available. On the other hand, it should be noted that (as already highlighted in other sections of this thesis) the use of hydrogen in pure form is not the only option and several studies have shown the possibility to inject it into the natural gas (NG) network to a certain extent [28,41,42,252] or use it in mixture, for vehicular applications, with other fuels such as NG [148,238,239], gasoline [240,253,254] or diesel [73]. It is therefore conceivable to propose different options of passenger car fleets that use both hydrogen and traditional fuels in diverse ways. However, to ensure an effective action, it is necessary to assess and compare the alternatives in terms of their energy and environmental performance. In order to conduct a comprehensive and sound comparison of the performance of different fleets involving hydrogen, a life-cycle approach is required. For this purpose, LCA is a consolidated methodology, as it allows analysts to compare different systems performing the same function and identify environmental hotspots.

In *Publication 1*, the life-cycle environmental performance of different passenger car options fuelled with pure hydrogen or hydrogen blends (H_2-NG and H_2-gasoline) was investigated, taking into account the life-cycle stages of vehicle production and maintenance in addition to the fuel-related ones. Renewable hydrogen produced through wind power electrolysis was considered in the study. The previous work showed that: (i) vehicles fuelled with pure hydrogen are excellent decarbonisation solutions; (ii) for pure renewable hydrogen vehicles, according to current technology levels, vehicle infrastructure is the main source of environmental burdens; and (iii) vehicles with internal combustion engine that use hydrogen mixed with fossil fuels (gasoline and NG) present an improved life-cycle environmental performance compared to traditional vehicles, arising as suitable short-term options temporarily circumventing major hydrogen storage and distribution issues.

Considering this background and the limited availability of hydrogen on a national scale, this work aims to give insight into environmentally-preferred passenger car fleets partially fuelled with hydrogen. Ultimately, the goal of this study is to provide policy actors with well-supported information in order to accelerate the resource-efficient implementation of renewable hydrogen in road transport. The main novelty lies in the proposal of innovative national strategies to promote the use of hydrogen in road passenger transport in the short term. The suitability of the proposals is evaluated by performing a comparative LCA of passenger car fleets that use hydrogen and traditional fuels either separately (in different vehicles) or in a mixture (in the same vehicle). In order to enable a fair comparison, fleet alternatives are defined under the same energy input. In addition, within the framework of the study, life-cycle inventories for two new vehicle types not available in the literature (hybrid electric vehicles that burn hydrogen blends in their ICE) are developed.

3.4.2. Definition of the case studies

This study addresses the definition and identification of passenger car fleets partially fuelled with hydrogen that could be both energy and environmentally convenient in the short term, under the constraint of a limited fixed amount of hydrogen available on a national scale. While Italy was taken as a reference country for some assumptions (Section 3.4.3), the proposed methodological approach could be applied to a large number of countries in a similar situation. Likewise, while –in accordance with previous work (*Publication 1*)– hydrogen from WPE was considered in this study, the analysis could be extended to other renewable hydrogen options with low environmental impacts. Nine types of vehicles were considered, which in turn were combined in eight different fleets. Four fleets are fuelled by hydrogen and NG, whereas the remaining ones by hydrogen and gasoline, with an energy equivalent amount. The fleets under analysis can use the two fuels separately or as a mixture inside the same vehicle. Other options such as diesel internal combustion engine vehicles or battery electric vehicles are out of the scope of this study. Furthermore, this study should be understood within the expected context of coexistence of complementary solutions for sustainable mobility such as hydrogen vehicles and battery electric vehicles [255,256].

Technical background on the different vehicle options was already provided in other sections of this thesis and further details can be found in *Publication 4*. This section however, focus on presenting the vehicle options considered in order to build the different fleets case studies. Figure 40 shows the vehicles considered in the present study for the definition of fleets. As regards pure hydrogen-fuelled solutions, only FCEVs were considered. On the other hand, vehicles equipped with ICE powertrain include: CNG vehicle, gasoline vehicle, hythane vehicle, and dual-fuel hydrogen-gasoline vehicle. For a fair comparison, the hydrogen-gasoline mixture was considered with an energy ratio of the mixture equal to that of hythane (i.e., H_2 provides 7.3% of the mixture energy).

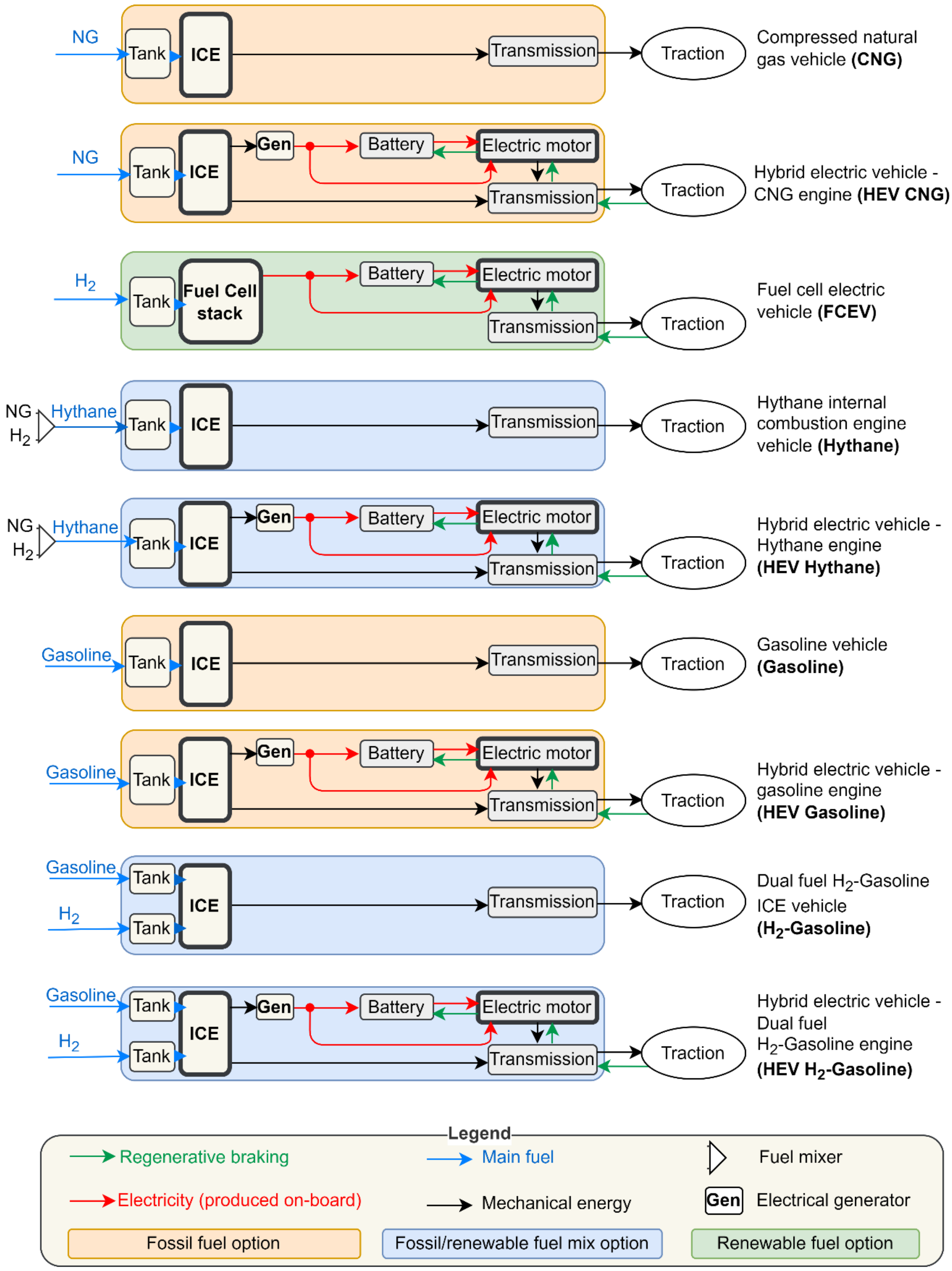

Figure 40. Vehicle concepts involved in fleet composition

HEVs of the full-hybrid, series/parallel type were also considered. These comprehend HEVs fuelled with compressed natural gas (HEV CNG) or gasoline (HEV Gasoline). In addition, for the first time, two novel HEVs were considered in the present study: an HEV fuelled with hythane (HEV Hythane), and an HEV fuelled with a hydrogen-gasoline mixture

(HEV H_2-Gasoline). An average European passenger car with a rated vehicle power of 80 kW was considered as reference, taking into account the different powertrain technologies to model each of the different vehicle options, as provided in Section 2.2.3.2 of this thesis. By using the above-mentioned vehicle options, the fleets subject to comparison were defined as follows: fleet F1 involving CNG vehicles and FCEVs; F2 involving Hythane; F3 with HEV CNG and FCEVs; F4 with HEV Hythane; F5 with Gasoline vehicles and FCEVs; F6 with H_2-Gasoline vehicles; F7 with HEV Gasoline and FCEVs; and F8 with HEV H_2-Gasoline. Hence, fleets from F1 to F4 are fuelled by NG and hydrogen, while fleets from F5 to F8 by gasoline and hydrogen. The number of vehicles in each fleet is not defined here because it derives from the energy analysis as an intermediate result (Section 3.4.5.).

3.4.3. Energy analysis and national contextualisation

In order to maximise the penetration of hydrogen-related vehicles in national fleets, it is necessary to promote fleets that use the available fuels with high efficiency. The aim of this energy analysis is to explore, given a fixed amount of fuel, which fleets can travel higher distances. In countries with a high number of passenger cars, even the achievement of a small hydrogen penetration (e.g., 1% of the national fleet) could be a challenging short-term target. For instance, Italy is the second country in the European Union with the largest number of passenger cars, 646 per thousand inhabitants [201]; according to the Italian Automobile Club [257], there were 39,717,874 cars in circulation on the Italian roads in 2020. Some constraints were set to carry out the energy analysis, mainly regarding the quantity of the two fuels available in each fleet in a year, fuel consumption and annual driving performance of each vehicle. The driving performance, namely the average distance travelled by one vehicle in a year, was assumed to be 15,000 km.

For comparative purposes, each fleet was fed with the same amount of total energy input, supplied in the form of two fuels. In particular, the amount of hydrogen available was set the same for all fleets, while the remaining part of the energy is supplied with CNG or gasoline. The amount of available hydrogen was assumed on the basis of NECPs and national hydrogen strategies, while the analysis is scalable to different hydrogen amounts. The amount of fossil fuel was subsequently calculated by considering an energy share of H_2 and fossil fuel of 7.3% and 92.7% of the available energy, respectively. This is the energy share fixed by hythane, and it was assumed to be the same in every case in order to put all fleets under the same conditions.

Regarding the hydrogen amount, the RED-II and the Italian NECP set the objectives to be achieved for Italy as a share of renewable energy sources in the final gross energy consumption of transport (RES-T) at 22% by 2030 and 14.4% by 2025 [204,210]. However, as part of the "Fit for 55" package proposed in July 2021 by the European Commission (2021), the RED-II is undergoing a review process and these objectives could become more ambitious in the coming years. According to the NECP [210], the preliminary guidelines for the Italian national hydrogen strategy [208] and the more recent national recovery and resilience plan (NRRP) [259], Italy plans to reach one percentage point of the RES-T target by 2030 through the use of green hydrogen. The NECP also suggests that a part of this hydrogen might be blended in the NG network or converted into renewable synthetic methane (0.8 percentage points of the RES-T target) while the remaining hydrogen might be used "as is" (i.e., in pure form) for direct use in cars, buses and trains (0.2 percentage points). As a 1% hydrogen-related target is set for 2030, a 0.5% short-term target was assumed for 2025.

According to the statistics of the Italian energy services operator (GSE), the national energy consumption in the transport sector amounted to 39,830 ktoe in 2019, with 83.2% of this value coming from road transport [260]. The energy consumption foreseen by the NECP and the GSE report for the Italian transport in 2025 is 28,851 ktoe, which corresponds to the denominator considered for the calculation of the targets according to the RED-II procedure. Taking into account the hydrogen-specific 0.5% target for 2025 and the calculation procedure shown in Figure 41, a hydrogen availability above 5 kt was estimated for Italian passenger cars in 2025. This is aligned with the national goals and the short-term perspective of the study, considering the need to start massive production of renewable hydrogen from scratch.

According to the previously defined energy ratio (7.3%), the amounts of CNG (168 kt) or gasoline (183.8 kt) available for each fleet in 2025, as well as the total energy (8.65 PJ), were derived. This means that, in energy terms for the year 2025, each fleet uses 8.65 PJ of energy: 0.63 PJ of hydrogen and 8.02 PJ of fossil fuel (NG or gasoline).

Finally, operational parameters for each vehicle, namely fuel consumption and tailpipe emissions, were based on *Publication 1*, where data from manufacturer declarations and technical datasheets are used along with scientific literature and databases such as GREET and Ecoscore [234,235].

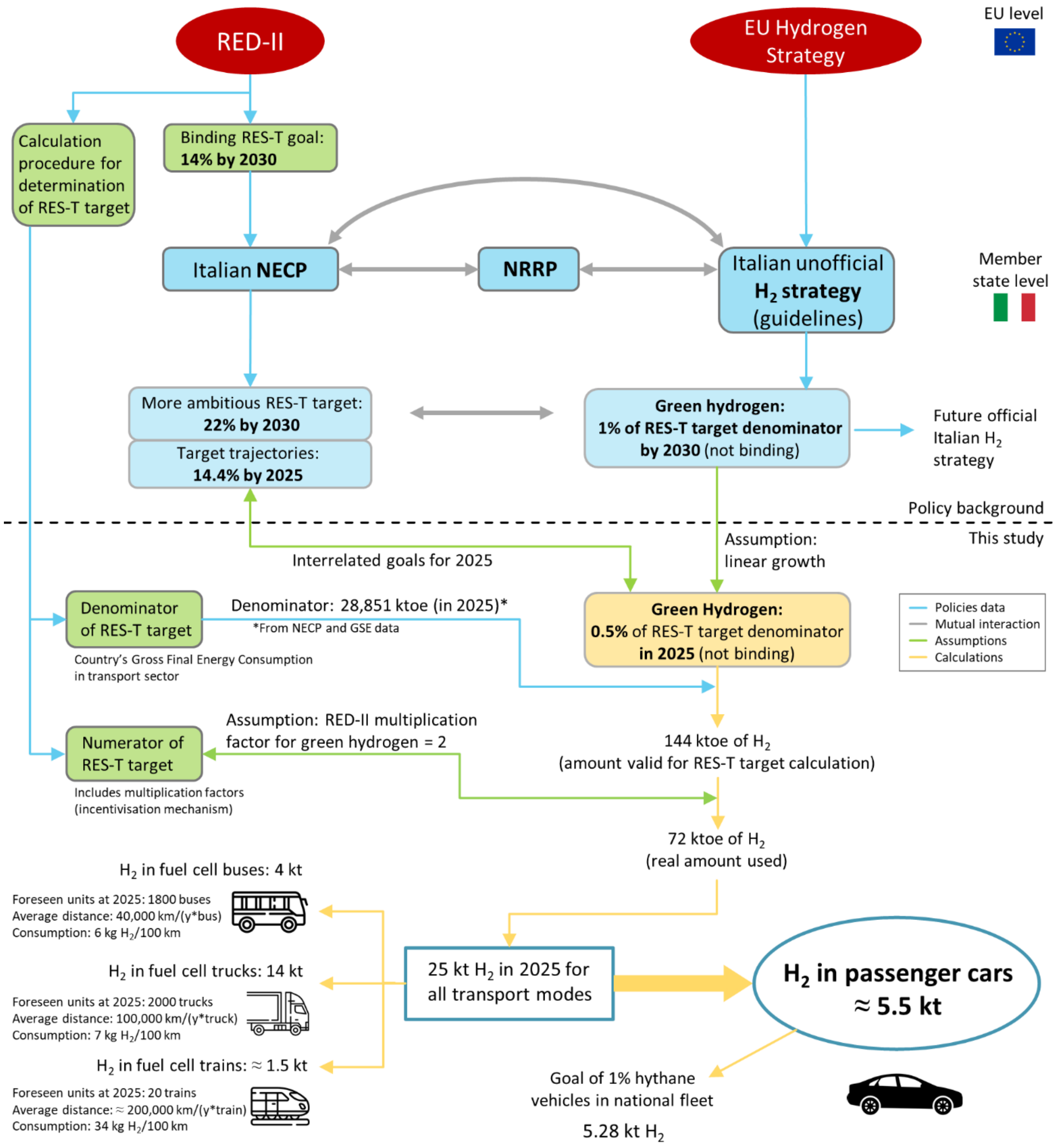

Figure 41. Calculation procedure for the target use of hydrogen in Italian passenger cars in 2025

Table 12 presents fuel economy (i.e., the reciprocal of fuel consumption), energy consumption and tailpipe emissions for each of the nine vehicles involved in fleets composition. For the sake of completeness, water emissions were included (as they could be relevant for other purposes, including the implementation of future progress in characterisation factors for water emissions) even though they do not currently affect the LCA results of this study. Values for fuel consumption refer to NEDC (New European Driving Cycle) under a combined cycle (urban/extra-urban route). The main considerations behind the energy analysis of fleets are summarised in Figure 42.

Table 12. Fuel economy and tailpipe emissions for the vehicles involved in fleets composition based on *Publication 1*.

Vehicle	Fuel economy [km/kg]	Energy consumption [a] [MJ/km]	CO_2 [g/km]	CO [mg/km]	HC [b] [mg/km]	NO_x [mg/km]	H_2O [c] [g/km]
FCEV	131.58	0.912	-	-	-	-	67.9
CNG	29.240	1.631	94	48.25	29.4	16.8	76.8
HEV CNG	44.303	1.077	66.888	32.33	20.1	4.9	50.7
Hythane	34.382	1.451	75.670	27.79	19.4	26.9	71.3
HEV Hythane	52.094	0.958	53.845	18.62	13.3	7.9	47.0
Gasoline	26.667	1.635	105.4	292.54	41.2	20.5	53.2
HEV Gasoline	40.404	1.079	75	196	28.2	6.0	35.1
H_2-Gasoline	31.352	1.459	87.146	102.27	25.8	33.7	52.0
HEV H_2-Gasoline	47.503	0.963	62.011	68.52	17.6	9.9	34.3

[a] Lower heating values of the fuels involved: 120 MJ/kg for hydrogen; 47.7 MJ/kg for CNG; 43.6 MJ/kg for gasoline; 49.9 MJ/kg for hythane; and 45.7 MJ/kg for H_2-Gasoline.
[b] HC: unburned hydrocarbons.
[c] Stoichiometric values; gasoline was considered as iso-octane.

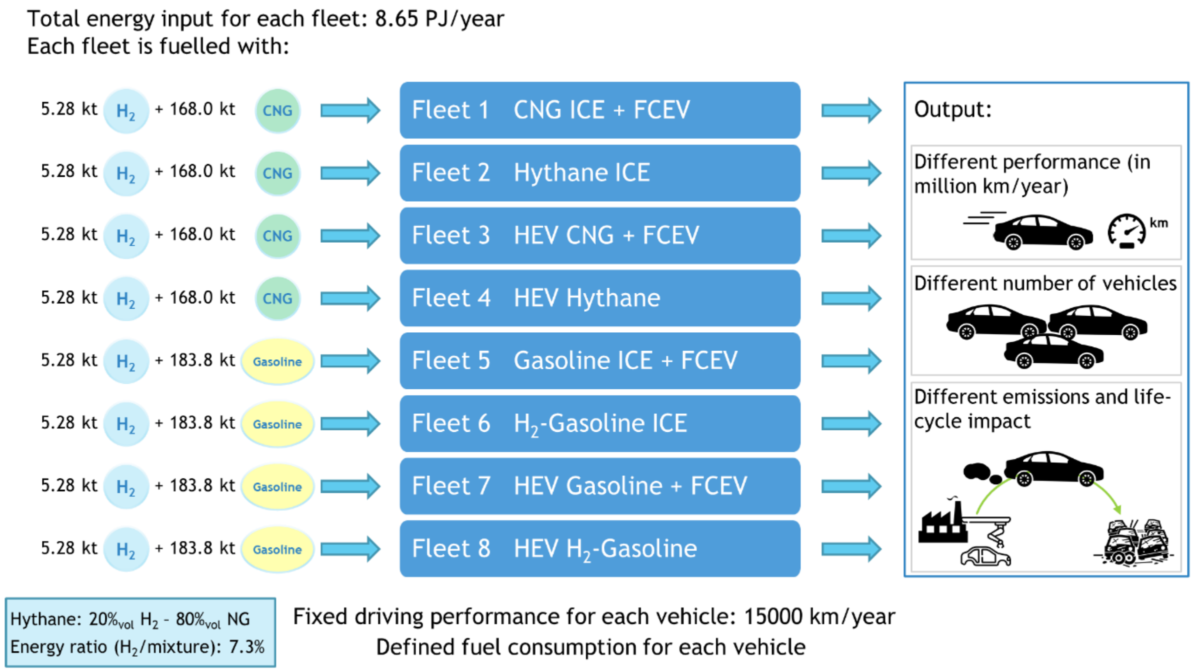

Figure 42. Main assumptions for the energy analysis of fleets

Altogether, Table 12, Figure 41 and Figure 42 present the key assumptions made for the study at the level of both national hydrogen availability (Figure 41) and technical features of vehicles (Table 12) and fleets (Figure 42).

3.4.4. LCA framework and data acquisition

In order to investigate the environmental suitability of the fleets under comparison, the LCA methodology was applied first to each vehicle system and then to each fleet (once vehicles were arranged into fleets by means of the energy analysis results). Figure 43a shows the system boundaries considered for each vehicle, involving both the fuel life cycle and the vehicle one [120]. The former includes the (WTW) stages of production, distribution and use of the fuel, including one or two fuels depending on the type of vehicle (whether it uses a mixture or not). "Fuel 1" refers to CNG or gasoline, while "Fuel 2" stands for hydrogen. The vehicle life-cycle involves here the stages of vehicle manufacturing, operation and maintenance. Vehicle end-of-life was not included due to the acknowledged need for robust inventory data on this stage [159,160]. The fuel and vehicle life cycles converge on the vehicle operation phase.

Figure 43b instead shows the system boundaries applied for a fleet system. Fleets were formed using different vehicles (in number and/or type). Inside a fleet, vehicles were homogeneously grouped by technology. In this regard, "Vehicle A" always refers to a type of vehicle that uses fossil fuel, pure or mixed with hydrogen, while "Vehicle B" (when present) always refers to FCEVs. The functional unit (FU) of the study was defined as 1 km travelled by each fleet.

The life-cycle environmental performance of each system was characterised in terms of global warming impact potential (GWP), acidification impact potential (AP) and cumulative non-renewable energy demand (CED) using the methods IPCC (2013), CML [215] and VDI (2012), respectively. The selection of these indicators was based on their specific relevance to hydrogen energy systems [109].

Concerning fuels, harmonised life-cycle indicators based on previous studies were used for hydrogen produced via WPE: carbon, acidification and non-renewable energy footprints [217–219] were adapted to the hydrogen pressure of 700 bar to comply with FCEV and H_2-Gasoline vehicle specifications (*Publication 1* and [211]). Hydrogen distribution from the production site to the refuelling point (100 km) by a tanker truck was considered [220]. Regarding CNG and gasoline production and distribution, background data from the ecoinvent database [181] were used. Regarding hythane, it was assumed that hydrogen is injected into the NG grid (blending) and distributed (100 km) via pipeline to the refuelling point [164,220].

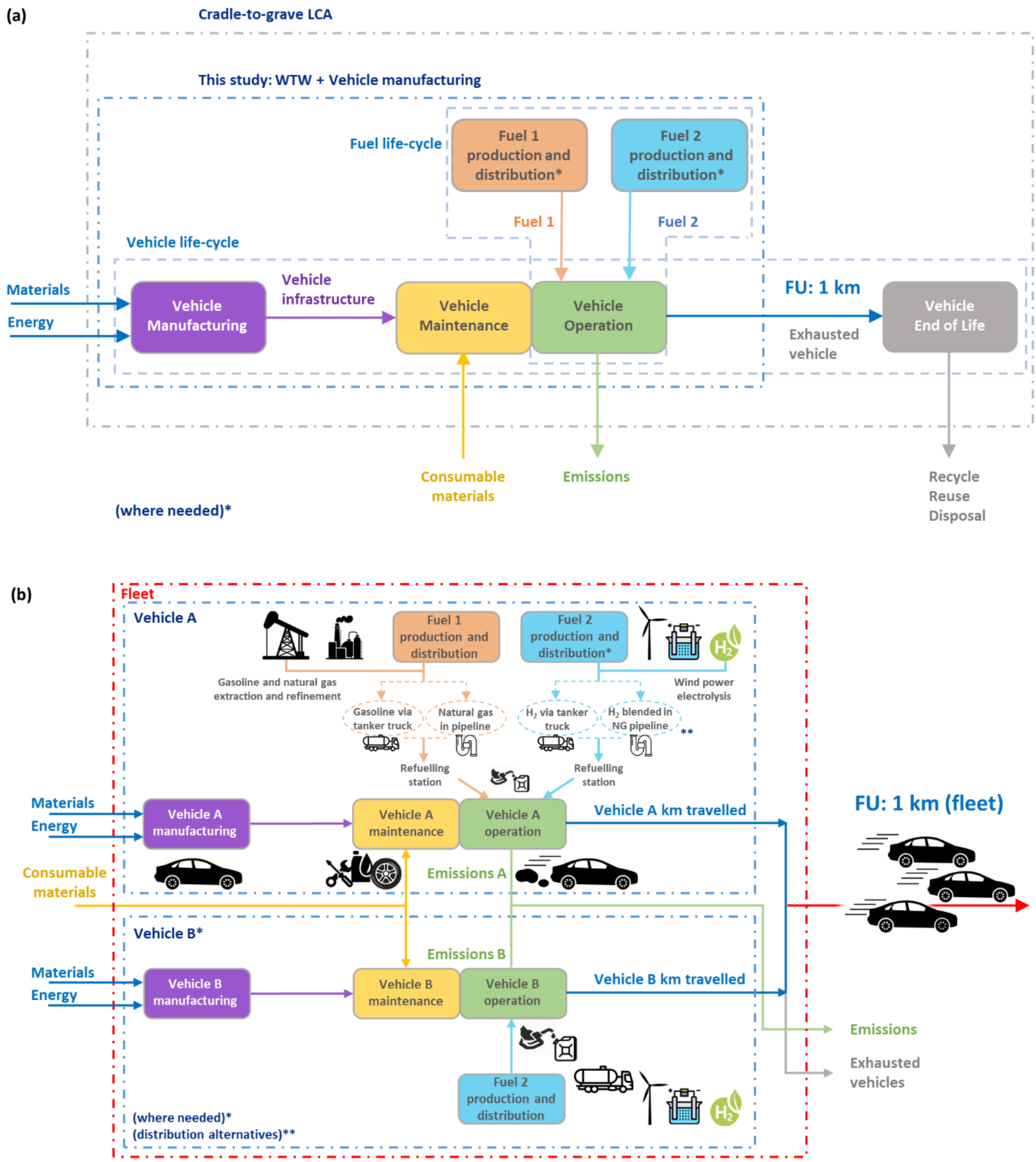

Figure 43. System boundaries: (a) single vehicle, and (b) fleet

For most of the vehicle types involved in fleets composition, inventory data for their manufacturing were directly retrieved from previous studies (*Publication 1* and [211]). On the other hand, those vehicles not previously considered are presented in Table 13. In particular, the inventories for the HEV Hythane and HEV H_2-Gasoline options constitute a novelty of this work. The technical feasibility of these options was not deemed a problem as they represent a combination of well-known technologies: internal combustion engines with soft modifications to run with hydrogen blends and common hybridisation by integration of an electrical propulsion system. However, the willingness to invest in these two innovative vehicle technologies to put them on the market will depend mainly on car manufacturers and policies.

Table 13. Main inventory data for vehicle production (values per one vehicle).

Item	Unit	HEV Hythane	HEV H_2-Gasoline	Gasoline	HEV Gasoline
Vehicle rated power	kW	80	80	80	80
Vehicle kerb weight	kg	1480	1425	1250	1400
Body and chassis	p	1	1	1	1
Fluids	p	1	1	1	1
ICE	kW	58.4	58.4	80	58.4
└Steel, low-alloyed	kg	36.80	37.86	50.41	36.80
└Aluminium	kg	30.22	31.28	41.40	30.22
└Polyphenylene sulphide	kg	18.02	20.14	24.68	18.02
└Lubricating oil	kg	6.37	6.37	8.73	6.37
Fuel system	p	1	1	1	1
└Copper	kg	3.94	3.94	-	-
└Polyvinylchloride	kg	0.92	0.92	-	-
└Reinforcing steel	kg	-	1.45	1.45	1.45
Gasoline tank	p	-	1	1	1
└High-density polyethylene, HDPE	kg	-	17.5	17.5	17.5
└Injection moulding	kg	-	17.5	17.5	17.5
Tank CNG-II	kg	80	-	-	-
└Steel, low-alloyed	kg	70	-	-	-
└Epoxy resin, liquid	kg	6	-	-	-
└Glass fibre	kg	4	-	-	-
Hydrogen tank (CNG-IV)	kg	-	18.60	-	-
└Aluminium	kg	-	1.42	-	-
└Carbon fibre	kg	-	3.96	-	-
└Epoxy resin, liquid	kg	-	5.93	-	-
└Glass fibre	kg	-	1.12	-	-
└High-density polyethylene, HDPE	kg	-	2.05	-	-
└Polyurethane, flexible foam	kg	-	0.93	-	-
└Steel, low-alloyed	kg	-	2.13	-	-
└Electricity	MJ	-	2.57	-	-
Exhaust system	p	1	1	1	1
└Reinforcing steel	kg	34.9	34.9	34.9	34.9
└Synthetic rubber	kg	1.45	1.45	1.45	1.45
└Talc	kg	1.4	1.4	1.4	1.4
└Steel, low-alloyed	kg	25.2	25.2	25.2	25.2
└Platinum	g	1.4	1.12	1.6	1.6
└Palladium	g	0.7	0.42	0.6	0.6
└Rhodium	g	0.64	0.48	0.3	0.3
└Cerium concentrate	kg	0.04	0.04	0.04	0.04
└Zirconium oxide	kg	0.14	0.14	0.14	0.14
└Aluminium oxide	kg	0.02	0.02	0.02	0.02
└Polyphenylene sulphide	kg	0.1	0.1	0.1	0.1
Li-ion battery	kWh	1.8	1.8	-	1.8
Electric motor	kW	48.6	48.6	-	48.6
Power control unit	kg	33.3	33.3	-	33.3
Gearbox	kg	80	80	80	80
Start system	p	1	1	1	1
Cooling system ICE	kg	29.1	29.1	29.1	29.1
Electronics for control units	kg	1.3	1.3	1.3	1.3
Tyres	p	4	4	4	4
Natural gas	MJ	1933	1933	1933	1933
Electricity	kWh	691	691	691	691

In addition, for the sake of completeness and traceability, the inventories for the Gasoline and HEV Gasoline options are also presented. The procedure and sources for the collection of the main inventory data for the stages of production, operation and maintenance of individual vehicles have been extensively covered in *Publication 1* and are based on well-established life cycle databases such as ecoinvent [181] and GREET [167], industry specifications, manufacturer statements, reports, and scientific literature.

For the options Gasoline and HEV Gasoline, data from technical datasheets released by manufacturers, as well as from literature and databases, were retrieved. On the other hand, for commercially unavailable vehicles (HEV Hythane and HEV H_2-Gasoline), data collection was based on specific literature combined with technical specifications regarding current HEVs. In particular, the ICE versions of Hythane and H_2-Gasoline vehicles from *Publication 1* were adapted to HEVs through the different sizing of the thermal and electrical subsystems that make up the vehicle powertrain. The overall rated power considered for individual HEVs is 80 kW (the same as all the other vehicles), which –for the degree of hybridisation and the assumptions made in *Publication 1*– is obtained through a 58.4 kW ICE and a 48.6 kW electric motor. In addition, HEVs present a 1.8 kWh Li-ion battery and a power control unit for smart management of electrical flows. HEVs and ICE vehicles were considered to involve the same glider, therefore the main differences in vehicle manufacturing are linked to powertrain configurations (additional components such as tanks, batteries, power control unit, etc.).

The HEV Hythane option is equipped with a 100-litre CNG-II tank (metal liner hoop-wrapped with glass fibre and epoxy resin), in which about 15 kg of hythane can be stored at 200 bar. It also involves a gaseous fuel distribution system and an exhaust gas system in which the amounts of platinum group metals (PGMs) in the catalytic converter are adjusted according to the emission characteristics of the vehicle.

Regarding the HEV H_2-Gasoline option, the differences in components (compared to HEV Gasoline) are closely linked to the presence of hydrogen. Being a dual-fuel vehicle, two separate tanks and fuel distribution systems are present on-board for each fuel: gasoline is stored in a common plastic tank paired with a traditional fuel distribution system, while pure hydrogen is stored in a composite cylinder at 700 bar (type-IV tank). The 25-litre hydrogen tank (18.6 kg) can store about 1 kg H_2. The small amount of hydrogen required by the vehicle mitigates hydrogen storage issues. Dedicated hydrogen supply (refuel filler neck, valves, special pipes) and distribution (pressure reducer, systems to prevent backfire, manifold/rail, gaskets, etc.) systems are also present, besides minor ICE modifications such as hydrogen injectors (in addition to gasoline injectors) and reinforced valve seats. Due to combustion improvements with respect to conventional gasoline vehicles, a lower load of PGMs was considered in the catalytic converter. Further details on the inventories of individual subsystems and components can be found in *Publication 1* and in Valente et al. [211].

Operational parameters regarding fuel consumption and tailpipe emissions are those presented in Table 12. The values for the new vehicle concepts (HEV Hythane and HEV H_2-Gasoline) were based on the H_2-blend vehicles in *Publication 1*, adapted to vehicle hybridisation. These, in turn, were based on specific literature about experimental tests and measures on ICEs according to the hydrogen percentage under examination for both NG [238,239] and gasoline [145,240–243] blends. The values considered for these two vehicle options correspond to a conservative approach and therefore present room for improvement through engine optimisation. Values from Table 12 were used to derive the amounts of fuel consumption and tailpipe emissions throughout the entire vehicle life. Inventory data for vehicle operation and maintenance are presented in Table 14.

Table 14. Main inventory data for vehicle operation and maintenance (values per total kilometres travelled by one vehicle during its useful life).

Item	Unit	HEV Hythane	HEV H_2-Gasoline	Gasoline	HEV Gasoline	Ref. for inventory
Operational inputs						
Vehicle infrastructure	p	1	1	1	1	Table 13
Hydrogen fuel	t	0.187	0.176	-	-	a
Natural gas	GJ	284	-	-	-	b
Gasoline (unleaded)	t	-	6.14	11.25	7.43	b
Maintenance inputs						
Lubricating oil	kg	34.6	34.6	34.6	34.6	b, c
Ethylene glycol	kg	12.9	12.9	12.9	12.9	b, c
Decarbonised water	kg	8.58	8.58	8.58	8.58	b, c
Tyres	p	12	12	12	12	c, d
Li-ion battery	kWh	1.8	1.8	-	1.8	e, f
Emissions						
Carbon dioxide	t	17.2	18.6	31.6	22.5	Table 12
Carbon monoxide	kg	5.96	20.6	87.8	58.8	Table 12
Hydrocarbons, unspecified	kg	4.24	5.28	12.4	8.46	Table 12
Nitrogen oxides	kg	2.52	2.96	6.15	1.8	Table 12
Brake wear emissions	g	436	380	334	374	b
Road wear emissions	kg	4.79	4.19	3.67	4.11	b
Tyre wear emissions	kg	28.05	24.50	21.49	24.07	b
Kilometres travelled	km	320,000	300,000	300,000	300,000	g

a: Valente et al. [211]; b: Frischknecht et al. [181]; c: Wang et al. [167]; d: Bras and Cobert [228];
e: Ellingsen et al. [221]; f: Majeau-Bettez et al. [222]; g: Candelaresi et al. *Publication 1*

The wear of tyres, brakes and road due to abrasion phenomena was taken into consideration, as it leads to emissions of particulate matter during the vehicle useful life. These emissions were calculated proportionally to each vehicle weight.

The life-cycle models presented in Tables 2 and 3 were implemented in SimaPro 9.4 using the ecoinvent database as the data source for background processes. The environmental characterisation was carried out by taking into account the selected life-cycle indicators and impact assessment methods. The combination of the LCA results for the individual vehicles with the results of the energy analysis allows the evaluation of the environmental performance of each fleet.

3.4.5. Energy analysis results

Table 15 presents the energy analysis results for each of the fleet systems under evaluation. According to the given energy input and vehicle fuel consumption, the annual kilometres travelled by each vehicle type (i.e., homogeneously grouped by technology) and the total annual kilometres travelled by each fleet were calculated. Additionally, taking into account the passenger transport function of a fleet by means of an occupancy rate of 1.6 for every vehicle (average number of passengers occupying a vehicle) [261,262], the total annual passenger-km (pkm) associated with each fleet were calculated.

Since the amount of energy entering the systems is the same, the fleets that exhibit the highest number in terms of total km or pkm are those that achieve the best energy performance. In this sense, Table 15 results show that the fleets that use blends outperform those with separate use of the two fuels (e.g., F2 vs F1 or F4 vs F3), and that HEV fleets behave better than those with simple ICEs (e.g., F3 vs F1, F4 vs F2 or F3 vs F2). The same is true for fleets involving the use of gasoline, where a gradual improvement was observed when switching from F5 to F8. This is due to an enhanced fuel economy of vehicles that use blends with respect to the separate use of fuels, and of HEVs compared to ICE vehicles. Thus, the fleets with the best performance were found to be F4 (involving only HEV Hythane) and F8 (involving only HEV H_2-gasoline). As another finding, fleets that involve the use of NG perform slightly better than their gasoline counterparts (e.g., F2 vs F6 or F3 vs F7). The worst strategies, among the analysed ones, would refer to the simple combination of FCEVs and existing gasoline or CNG cars (F5 and F1). In this sense, under specific circumstances hampering the use of hydrogen mixtures, HEVs (instead of conventional cars) are recommended to be deployed along with FCEVs.

Table 16 presents the results in terms of the number of vehicles that make up each fleet, penetration impact on the Italian fleet, and average fleet fuel economy, expressed as fleet efficiency. Taking into account the total kilometres travelled by each vehicle type and the fixed annual driving performance of each single vehicle (15,000 km), the number of vehicles within each fleet was calculated. Considering the total number of passenger cars circulating on Italian roads (presented in Section 3.4.3.), national fleet penetration for both the total number of vehicles in a fleet and only hydrogen-related vehicles were estimated. Fleet average efficiency was calculated as the inverse of the weighted average obtained by vehicle number in a fleet and vehicle specific energy consumption.

Results in Table 16 are aligned with those in Table 15. In this case, the greater the total number of vehicles that can be fuelled with the same energy input, the better the energy performance of the fleet. The same observations made for Table 15 regarding the fleets ranking are applicable. This trend is explained by the fleet average efficiency, with the favourable effect of a large number of medium-efficient vehicles exceeding that of high efficiency in a limited number of vehicles. The use of hydrogen-mixture vehicles leads to homogeneous fleets with a relatively high average efficiency. Since HEVs enjoy a more favourable fuel economy than their non-hybrid counterparts, the best performance was found for the combined use of hydrogen mixtures and HEVs (F4 and F8).

The amount of hydrogen taken into consideration would power only 0.12% of the national fleet if used in FCEVs. However, the same amount of hydrogen used in hythane vehicles would result in a penetration of 1% of the national fleet, and 1.52% if the mixture is used to fuel HEVs. This is due to the fact that each mixture-vehicle uses less hydrogen than an FCEV, as well as to higher average fleet efficiency. According to the Italian Automobile Club [257], the total number of CNG cars in circulation on Italian roads in 2020 amounted to 978,832 vehicles. Having 5.28 kt of renewable hydrogen annually available, it would be possible to convert 40.6% of the Italian CNG cars into hythane cars or 61.5% into HEV hythane cars. Therefore, by moderately increasing the assumed amount of renewable hydrogen available at the national level, the full Italian CNG car fleet could move to the use of mixtures containing hydrogen.

In order to sensibly understand the suitability of the proposed strategies, an environmental perspective is also needed. Contrary to the case in which hydrogen is used in FCEVs, the use of the same amount of hydrogen in vehicles fuelled with a mixture involves tailpipe exhaust emissions. Nevertheless, a fair environmental comparison between the fleets cannot be limited to tailpipe emissions, but a thorough LCA study is required. In this regard, for the subsequent LCA study, the results of the energy analysis were referred to one km travelled by each fleet (FU) and the fleets were represented as entities with a certain consumption of each of the fuels and a certain distance share associated with each type of vehicle (Table 17). As in Figure 43, “Fuel 1” refers to NG, hythane or gasoline depending on the fleet; “Fuel 2” corresponds to pure hydrogen; “Vehicle A” refers to a vehicle that uses fossil fuel, pure or mixed with hydrogen; and “Vehicle B” corresponds to an FCEV.

Table 15. Fleets' energy performance expressed as annual km travelled and annual passenger-km (pkm).

Fleet	Vehicles A [million km/year]	Vehicles B [million km/year]	Total km fleet [million km/year]	Vehicles A [million pkm/year]	Vehicles B [million pkm/year]	Total pkm fleet [million pkm/year]
F1: CNG + FCEV	4912.29	694.58	5606.87	7859.67	1111.33	8970.99
F2: Hythane	5957.68	-	5957.68	9532.29	-	9532.29
F3: HEV CNG + FCEV	7442.86	694.58	8137.45	11,908.58	1111.33	13,019.91
F4: HEV Hythane	9026.79	-	9026.79	14,442.86	-	14,442.86
F5: Gasoline + FCEV	4901.29	694.58	5595.88	7842.07	1111.33	8953.40
F6: H_2-Gasoline	5927.92	-	5927.92	9484.67	-	9484.67
F7: HEV Gasoline + FCEV	7426.20	694.58	8120.78	11,881.93	1111.33	12,993.25
F8: HEV H_2-Gasoline	8981.70	-	8981.70	14,370.72	-	14,370.72

Table 16. Number of vehicles, fleets composition and national fleet penetration.

Fleet	Number of Vehicles A [cars]	Number of Vehicles B [cars]	Total vehicle number in fleet [cars]	National fleet penetration [%]	Hydrogen-related vehicles national fleet penetration [%]	Fleet average efficiency [km/MJ]
F1: CNG + FCEV	327,486	46,305	373,791	0.941%	0.12%	0.648
F2: Hythane	397,178	-	397,178	1.000%	1.00%	0.689
F3: HEV CNG + FCEV	496,190	46,305	542,495	1.366%	0.12%	0.941
F4: HEV Hythane	601,785	-	601,785	1.515%	1.52%	1.044
F5: Gasoline + FCEV	326,752	46,305	373,057	0.939%	0.12%	0.647
F6: H_2-Gasoline	395,194	-	395,194	0.995%	0.99%	0.686
F7: HEV Gasoline + FCEV	495,080	46,305	541,385	1.363%	0.12%	0.939
F8: HEV H_2-Gasoline	598,779	-	598,779	1.508%	1.51%	1.039

Table 17. Consumption of fuels per km travelled by each fleet and distance travelled with each vehicle type.

Fleet	Fuel 1 [g/FU]	Fuel 2 [mg/FU]	km Vehicles A [km/FU]	km Vehicles B [km/FU]
F1: CNG + FCEV	29.963[a]	941.5[d]	0.876	0.124
F2: Hythane	29.085[b]	-	1	-
F3: HEV CNG + FCEV	20.645[a]	648.7[d]	0.915	0.085
F4: HEV Hythane	19.196[b]	-	1	-
F5: Gasoline + FCEV	32.845[c]	943.3[d]	0.876	0.124
F6: H_2-Gasoline	31.006[c]	890.5[d]	1	-
F7: HEV Gasoline + FCEV	22.633[c]	650.0[d]	0.914	0.086
F8: HEV H_2-Gasoline	20.464[c]	587.7[d]	1	-

[a] Amount of CNG required per each km travelled by the fleet.
[b] Amount of hythane required per each km travelled by the fleet.
[c] Amount of gasoline per each km travelled by the fleet.
[d] Amount of hydrogen per each km travelled by the fleet.

3.4.6. Environmental results

Figure 44 shows the carbon footprint per km travelled by each fleet, including its breakdown according to the main life-cycle stages and the type of vehicle. In agreement with the energy analysis results in Section 3.4.5, the most favourable profile was found for the fleet of HEVs fuelled with hythane (F4).

For comparative purposes, in Figure 44 the results are also benchmarked against two conventional fleets (B1 and B2) composed solely of either CNG or gasoline vehicles under the same assumptions used to define the other fleets (total input energy of 8.65 PJ). In this regard, the conventional CNG and gasoline fleets involve 353,373 and 352,582 cars, respectively. The comparison with conventional fleets allows evaluating the impact reduction achieved when applying the proposed fleet strategies.

The carbon footprint reduction was found to range from 7% to 35% when comparing either F1-F4 with the conventional CNG or F5-F8 with the conventional gasoline fleet. The fleets showing an impact reduction >30% compared to their conventional benchmark are F4 (HEV Hythane) and F8 (HEV H_2-Gasoline).

Regarding the carbon footprint breakdown, the emissions of the operational phase (TTW) from type-A vehicles (which burn fossil fuel solely or in mixture) were found to play the leading role, clearly ahead of vehicle manufacturing and fuel production.

Regarding FCEVs, while their fuel-use emissions are null, the role of vehicle manufacturing becomes more relevant. It should be noted that, in this regard, the infrastructure impact has to be read in light of the number of vehicles of each type.

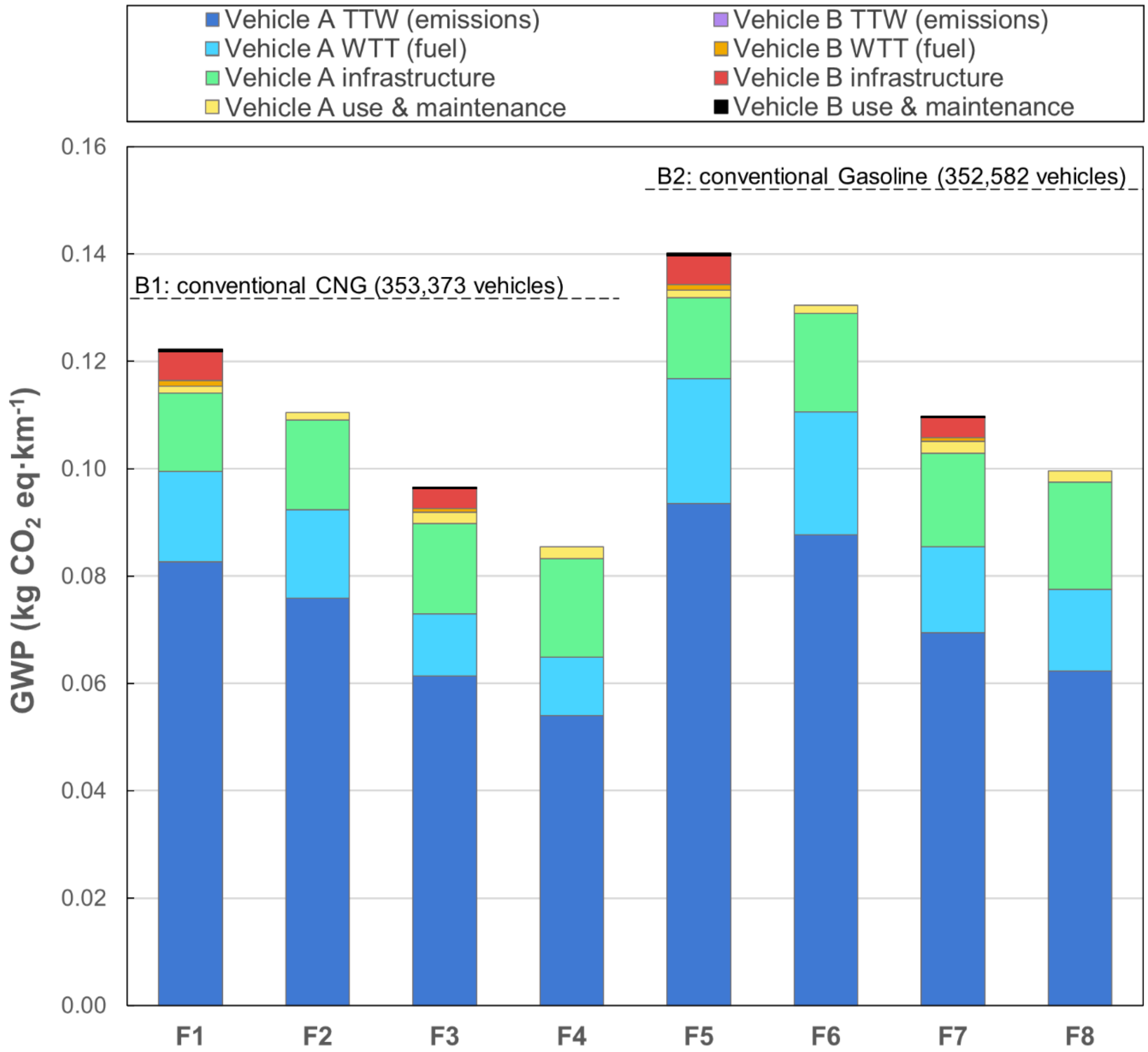

Number of Vehicle A	CNG 327,486	Hythane 397,178	HEV CNG 496,190	HEV Hythane 601,785	Gasoline 326,752	H_2-Gasoline 395,194	HEV Gasoline 495,080	HEV H_2-Gasoline 598,779
Number of Vehicle B	FCEV 46,305	-	FCEV 46,305	-	FCEV 46,305	-	FCEV 46,305	-
Total vehicle number	373,791	397,178	542,495	601,785	373,057	395,194	541,385	598,779

Figure 44. Breakdown of the carbon footprint of the proposed fleets per km travelled

The impact of renewable hydrogen, including production from WPE and distribution, was found to be negligible compared to the total fleet impact. This is true both in the case of pure hydrogen distributed via road (e.g., Vehicle B WTT in Figure 44) and in the case of hydrogen distributed via pipeline and/or mixed with other fuels (a fraction of Vehicle A WTT in Figure 44). Vehicle maintenance was also found to play a minor role.

Concerning fuel production, it should be noted that the NG/gasoline used in type-A vehicles was considered entirely of fossil origin. Some regions, such as Italy, aim for an increased use of biomethane, especially that produced from urban, agricultural or livestock waste, encouraging its injection into the gas grid [260]. If significant amounts of biomethane were injected into the NG network, this could reduce the fuel-related impact and methane-hydrogen blends would increase their renewable content.

As the purpose of this work is to help policy actors make well-supported decisions, the total result deriving from each strategy was also considered. To that end, Figure 45 shows the total carbon footprint of the proposed fleet strategies.

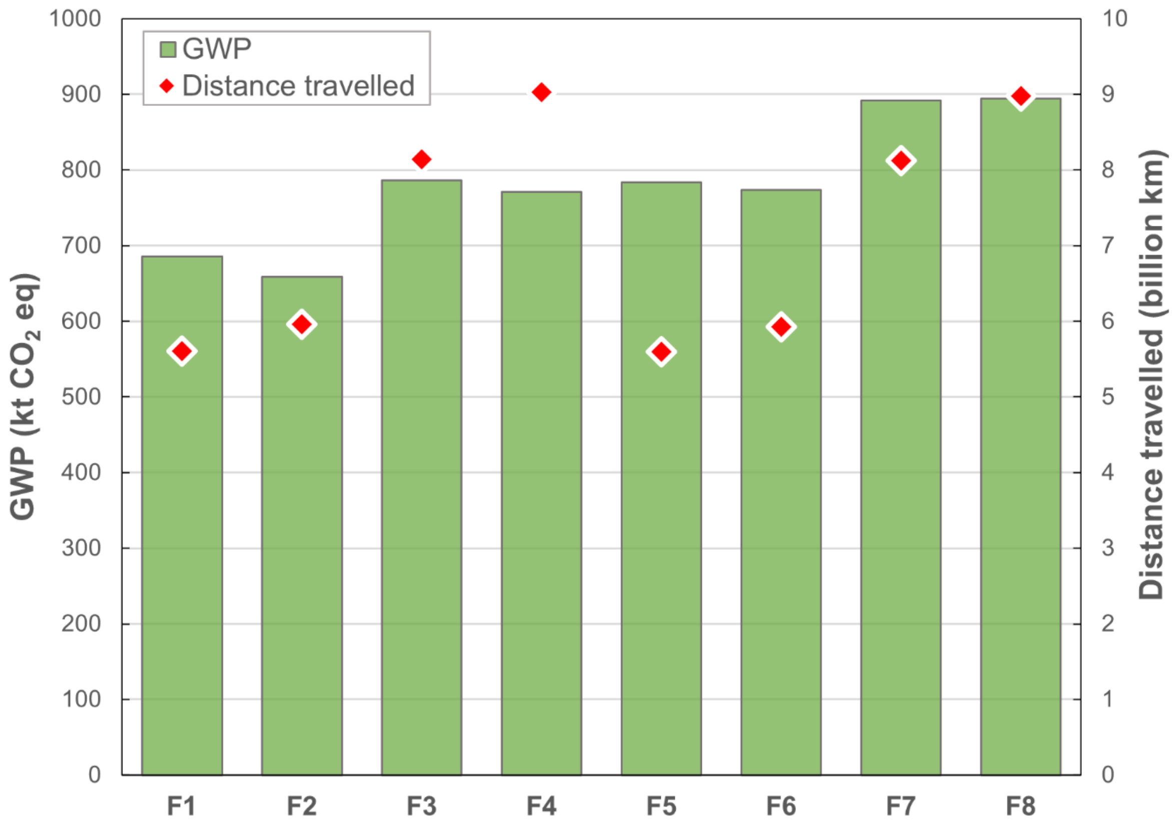

Figure 45. Total carbon footprint of the different fleet strategies proposed, and total distance travelled

However, it should be noted that each of the proposed fleets is composed of a different number of vehicles and involves a different number of kilometres, therefore the total carbon footprint must be interpreted accordingly. This means that some measures show a higher total carbon footprint but lead to travel more kilometres (or, in other words, to power more vehicles), whereas others show a lower impact but a poorer functional performance. Depending on whether the policy-maker prioritises only the carbon footprint, only the energy performance or both aspects, different fleet rankings are obtained. In the event that it is decided to prioritise both the carbon footprint and the energy performance, the best fleets would ideally be those with the lowest carbon footprint combined with the highest number of kilometres travelled.

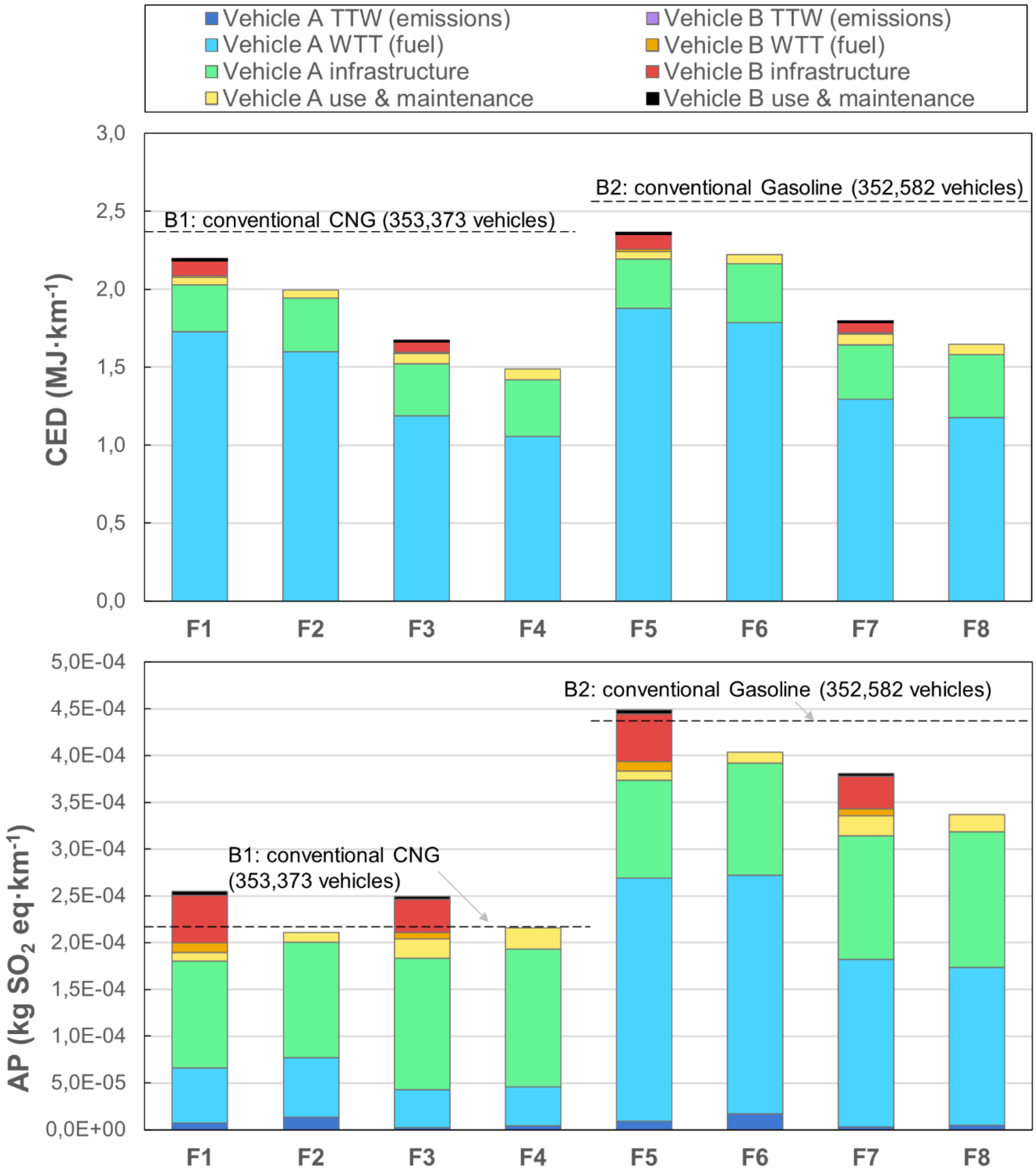

	F1	F2	F3	F4	F5	F6	F7	F8
Number of Vehicle A	CNG 327,486	Hythane 397,178	HEV CNG 496,190	HEV Hythane 601,785	Gasoline 326,752	H_2-Gasoline 395,194	HEV Gasoline 495,080	HEV H_2-Gasoline 598,779
Number of Vehicle B	FCEV 46,305	-	FCEV 46,305	-	FCEV 46,305	-	FCEV 46,305	-
Total vehicle number	373,791	397,178	542,495	601,785	373,057	395,194	541,385	598,779

Figure 46. Breakdown of the energy and acidification footprints of the proposed fleets per km travelled

Besides the carbon footprint, the non-renewable energy footprint and the acidification impact per km travelled by each fleet were assessed. Figure 46 shows the breakdown by life-cycle stage and vehicle type for the CED and AP results of the proposed fleets, including their benchmarking against conventional fossil fleets. Regarding CED, the results show a strong correlation with the carbon footprint ones, leading to the same ranking of fleet strategies. It should be clarified that CED encloses the energy consumption cumulated over the life-cycle stages, whereas the energy analysis in Section 3.4.5. focuses on fuel consumption.

On the other hand, the AP results show different hotspots and ranking in comparison with the previous results. From the breakdown in Figure 46, it can be observed that vehicle manufacturing plays a key role in terms of acidification, which is linked to the number and type of vehicles. Regarding single vehicles, the infrastructure contribution to AP is relatively low for vehicles equipped with ICEs, intermediate for HEVs, and very high for FCEVs [164]. This trend is associated with vehicle-specific aspects such as (i) electrification-related components such as batteries, electric motors, power control units and fuel cell stacks, (ii) materials contained in the above-mentioned components, such as platinum in fuel cells, and (iii) other vehicle components such as heavier car gliders or hydrogen tanks involving composite material. In HEVs and ICEs, especially CNG-fuelled ones, also the PGMs in the exhaust system show a certain AP incidence. For these reasons, in terms of acidification, there is a change in the ranking, with F2 performing slightly better than F4. The high contribution of infrastructure to AP in FCEVs leads the fleets F1 and F3 to a higher acidification impact than their CNG benchmark, while F2 and F4 remain slightly below the conventional CNG fleet. Finally, gasoline-related fleets show a higher acidification footprint than those related to NG, even though –apart from F5– they outperform their benchmark (conventional gasoline fleet).

3.4.7. Perspectives and final remarks

Overall, the results show that the use of hydrogen blends would be beneficial under different energy and environmental aspects to boost the hydrogen economy in the short term. While this result could be affected by important changes in technical aspects such as fuel consumption, lifespan, occupancy rate, weight and emission factors of each vehicle, the key findings in this work are deemed robust as the technical parameters considered in this paper are intended to give an average representation of each vehicle technology. In this regard, Candelaresi et al. [263,264] carried out a sensitivity analysis to technical parameters, showing the functional dependencies of the LCA results as the technical parameters vary. For instance, fuel consumption was found to have a linear influence on the impact indicators. By considering a realistic range of variation between worst and best cases of technical parameters, and its effect on LCA results, it was possible to represent each average vehicle technology in a robust way. Finally, rather than the numerical impact value of each vehicle or fleet, the key finding to be highlighted refers to the possible relationship between the different fleet options and the strategic opportunities that may arise from it.

Besides, other technical, economic and social co-benefits may derive from the use of hydrogen blends. For instance, the increased use of hydrogen would result in a large number of people acquainted with hydrogen energy systems, thereby favouring social acceptance.

From a techno-economic point of view, the use of mixtures would allow the immediate use of the available green hydrogen, relying on existing infrastructure and vehicles with minor modifications and thus starting up a market without gaps in the supply chain. In line with European goals, this would allow an initial concentration of investments in the production of hydrogen from renewable or low-carbon sources. At a later time, when green hydrogen production has already been scaled up, major investments related to pure-hydrogen infrastructure and end uses could be attracted. Alternatively, the hydrogen content in the mixture could be increased over time.

Among the opportunities derived from using blends, countries with a large number of CNG refuelling points such as Italy could start up hydrogen deployment with minor infrastructure modifications. Alternatively to hydrogen blending in pipeline, pure renewable hydrogen could be transported (e.g., by road) from the production point and used separately and/or mixed with CNG at the filling station. Regarding on-board storage, hythane can be stored at pressures similar to those already used for CNG (200 bar) and in very similar tanks, already suitable or adapted for containing small amounts of hydrogen. Storage pressure could be slightly raised to recover the loss of volumetric energy density due to hydrogen addition or further extend the driving range. Similarly, the combustion engine requires minimal modifications compared to a CNG engine.

As regards H_2-gasoline vehicles, in the absence of a dedicated hydrogen pipeline, pure hydrogen should be transported to the refuelling station by road. Since the amount of pure hydrogen stored in the vehicle is small, tank volume and weight issues associated with pure hydrogen storage are mitigated. The ICE presents minor modifications with respect to the conventional one, and the driving range is similar to that of a conventional gasoline vehicle. A more distributed use of pure hydrogen would allow the creation of several hydrogen refuelling stations of small size, which could be expanded at a later time to allow also refuelling FCEVs. The increased number of users would allow these stations to be exploited with high utilisation factors, thus accelerating the return on investment. Furthermore, the increased number of small filling stations would enable an enhanced coverage of the national road network, hastening action on the main transport arteries and points of national/European strategic interest such as big cities, main highways and the Trans-European Transport Network (TEN-T) core.

3.4.8. Conclusions

This study explored –from an energy and life-cycle environmental perspective– eight innovative fleet strategies for the short-term implementation of hydrogen in road transport (passenger cars) at the national level. The proposed strategies achieve a carbon footprint reduction ranging between 7% and 35% with respect to their conventional fleet benchmark. It is concluded that strategies using hydrogen mixtures in homogeneous fleets are more suitable than those separately using hydrogen and fossil fuels in heterogeneous fleets. In particular, strategies based on blends of natural gas and hydrogen (hythane) generally outperform those based on gasoline-hydrogen mixtures. Moreover, fleets involving hybrid electric vehicles perform better than those involving internal combustion engines. Thus, the best results were generally found for the fleet strategy based on the use of hythane in hybrid electric vehicles (35% reduction in carbon footprint with respect to its benchmark). Where this is not possible or under policy scenarios prioritising the separate use of hydrogen, it is advisable to encourage fleets involving both hybrid and fuel cell electric vehicles. The fleet strategies involving the use of hydrogen mixture and internal combustion engines could arise as a first step towards their hybrid versions as they would be preferred over those involving traditional vehicles alongside fuel cell electric vehicles. Overall, also taking into account potential technical, economic and social advantages, the use of hydrogen blends could facilitate the transition towards an environmentally sustainable transport while hastening the advent of the hydrogen economy.

Chapter 4

Modelling and environmental impact of renewable Substitute Natural Gas production pathways

4.1. Life cycle assessment of substitute natural gas production from biomass and electrolytic hydrogen

The synthesis of a Substitute Natural Gas (SNG) that is compatible with the gas grid composition requirements by using surplus electricity from renewable energy sources looks a favourable solution to store large quantities of electricity and to decarbonise the gas grid network while maintaining the same infrastructure. The most promising layouts for SNG production and the conditions under which SNG synthesis reduces the environmental impacts if compared to its fossil alternative is still largely untapped. *Publication 2* aimed at conducting an LCA on six different novel layouts for the coproduction of SNG and electricity, which have not been covered yet by previous literature. Whereas in previous papers from the co-authors [265,266] an energy analysis was carried out, the same layouts are hereby compared from an environmental point of view by means of LCA. In this work, an attributional LCA was performed. First, an impact assessment of the six analysed layouts was carried out for three selected impact categories, in a base-case scenario elaborated with the avoided burden approach. Moreover, in order to explore the role of key LCA methodological aspects and the influence of methodological choices on the results, a sensitivity analysis on the functional unit and on the approach to handle multifunctionality in polygenerative energy systems was also addressed, since five out of six layouts co-produce SNG and electricity. The results and discussion presented in this section are based on *Publication 2*.

4.1.1. Case studies

In a previous paper from the co-authors [265] different layouts were analysed to evaluate the energy balance of the production of SNG starting from biomass and electrolytic hydrogen. Two alternative scenarios were considered: (i) only the SNG is produced (Figure 47) and (ii) SNG and power are cogenerated (Figure 48). The efficiencies of the different analysed layouts range from 52.4% to 73.8% (Equation (4.1)) with chemical power (fuel) accounting for 73-100% of the total output.

$$\eta_{plant} = \frac{\dot{m}_{SNG} \cdot HHV_{SNG} + Electricity_{out}}{\dot{m}_{biomass} \cdot HHV_{biomass} + Electricity_{in}} \tag{4.1}$$

Different power units define different sub-scenarios: i) gas turbine (GT); ii) steam injected gas turbine (STIG); iii) internal combustion engine (ICE); iv) solid oxide fuel cell (SOFC) fed by syngas operated at 6 bar (SOFC6); v) SOFC fed by syngas operated at 30 bar (SOFC30); vi) the case of hydrogasification (HG) that does not involve the co-production of power.

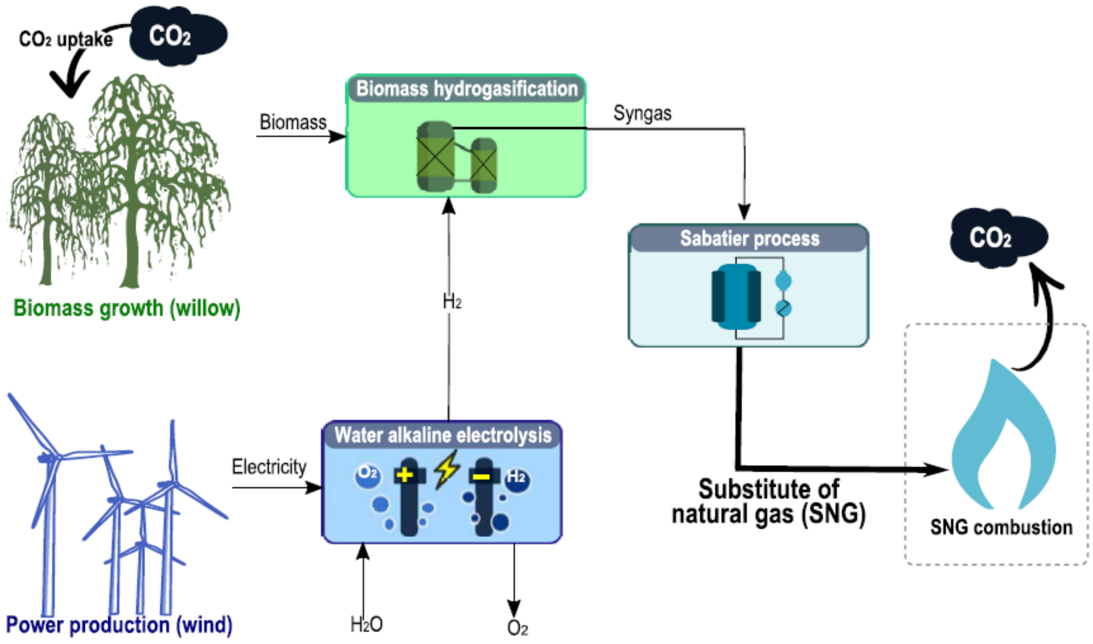

Figure 47. System diagram in case only SNG is produced (HG case)

All the considered plants are fed with lignocellulosic biomass, with an average composition of 40.32% carbon, 34.48% oxygen, 20.00% humidity, 4.88% hydrogen, 0.24% ash, 0.08% nitrogen, 64.87% volatile matter and 14.89% fixed carbon (weight %) and a HHV of 19 MJ/kg on a dry basis [265,266]. An alkaline electrolyser supplies the hydrogen that is necessary for the biomass hydrogasification in the first layout (HG, Figure 47) and the hydrogen employed for the methanation reaction in the cogenerative layouts (Figure 48). In the layouts involving cogeneration of SNG and electricity, electrolytic oxygen is used in the gasifier as the gasifying agent and in the power unit to perform an oxycombustion that allows to separate carbon dioxide from exhaust gases more easily. The amount of oxygen used into the gasifier is related to the considered power unit since each of them has particular requirements of feeding gas composition and temperature.

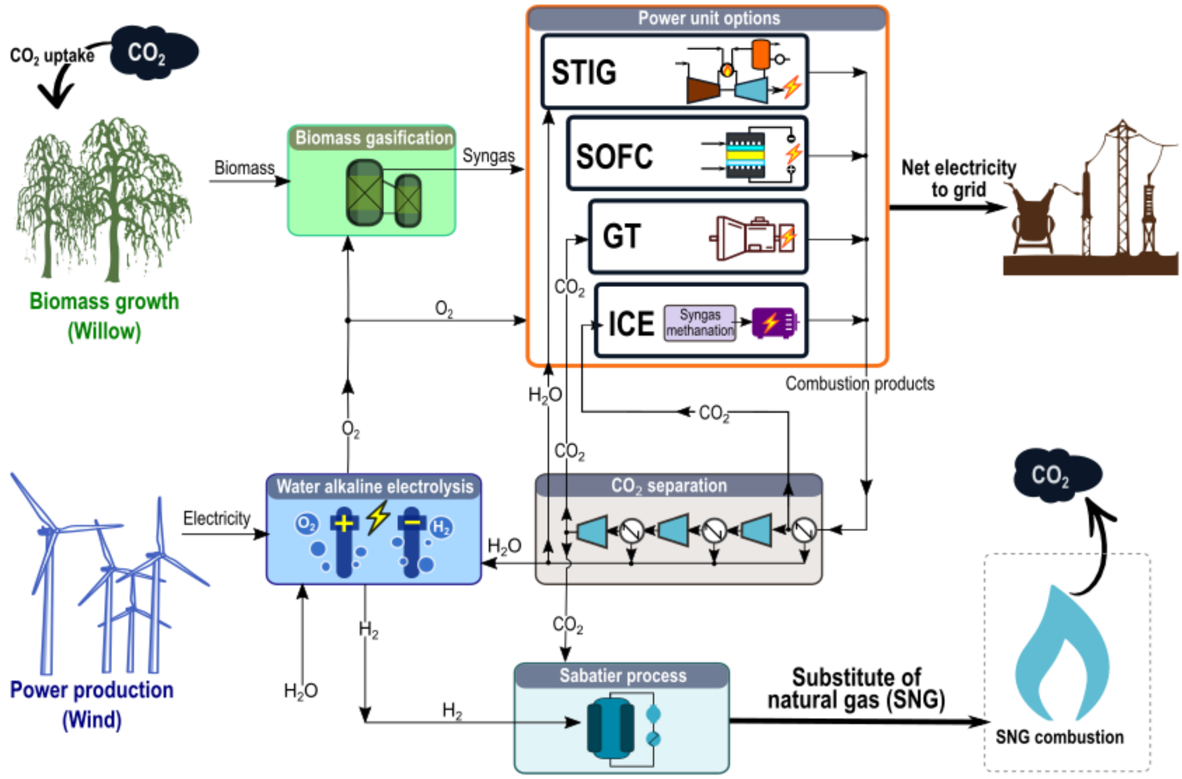

Figure 48. System diagram in case SNG and electricity are co-produced. The power unit varies in dependency of the chosen case study. SOFC refers to both SOFC6 and SOFC30 layouts

In the cases of STIG and SOFCs there is no recycle of carbon dioxide, while in the ICE and GT there is a partial recycle of carbon dioxide that acts as a temperature moderator agent, which occurs, respectively, at 1 bar and 30 bar (i.e., upstream or downstream of the compression line). Gas expanders are used to adjust pressures in different parts of the plant. Further and extensive details on the plant configurations can be found in Ref. [265]. The plants performances were analysed under the technical and efficiency point of views in several previous works by the co-authors. In *Publication 2*, the layouts were instead compared from the environmental point of view by means of LCA methodology. First, an impact assessment of the six analysed layouts was carried out for three impact categories, in a base-case scenario elaborated with the avoided burden approach. Since five out of six layouts simultaneously co-produce SNG and electricity, in order to explore the role of key LCA methodological aspects, a sensitivity analysis on the functional unit and on the methodology to handle multifunctionality was addressed.

4.1.2. Goal and scope

In this work, an attributional LCA was performed, according to the ISO 14040 and 14044 [105,106] guidelines presented in *Chapter 2*. For those systems performing more than one function or producing more than one product (i.e., the so-called multifunctional systems), the approach to deal with this multifunctionality has to be also defined in the goal and scope of the study. In this regard, the ISO standard prioritises the use of "system subdivision" (i.e., the subdivision of a multifunctional system into multiple monofunctional systems). When the application of system subdivision is not possible, the allocation of impacts should be avoided by the "system expansion" approach. This approach consists in discounting the environmental burdens associated with the co-function (or co-products) considered to be produced through the conventional pathway. When system expansion is not applicable, allocation procedures can be applied to redistribute the inputs and the outputs among the co-functions according to physical (e.g., mass, mole, energy, exergy) or economic bases.

The main scope of the present study was to compare different plant layouts, for the production of SNG starting from biomass and electrolytic hydrogen, from an environmental perspective. The comparative assessment was performed by exploring the effect of different methodological assumptions. The system is polygenerative since it co-produces SNG and electricity (in five of the six analysed cases); for this reason, different functional units (1 kg SNG, 1 MJ of total energy produced) were chosen to perform the assessment. It has to be remarked that in the first case (i.e. functional unit equal to 1 kg SNG) the main product SNG is considered to maintain the same composition in all the investigated layouts, as reported in [265], and producing SNG is the main function of the system. The system boundaries include the main steps for SNG production, from biomass growth and water extraction up to the SNG combustion (Cradle-to-Grave approach). The plant infrastructure was included in the study, with inventories detailed in Section 4.1.3. The life cycle environmental performance is characterised by quantifying the environmental impacts of global warming potential on a 100-years horizon (GWP), non-renewable cumulative energy demand (CEDnr) and acidification potential (AP) by employing the impact assessment methods of IPCC 2013 [5], VDI [216] and CML-IA baseline [215], respectively. The selection of the life cycle impact indicators is based on their relevance in energy systems involving hydrogen production [109]. The LCA tool used to implement the life cycle inventories was the SimaPro software.

4.1.3. Life cycle inventory

Materials and energy requirements and intermediate flows were calculated in previous studies by the co-authors, through simulation carried out by means of Aspen Plus software [265]. Table 18 shows the net inputs and outputs considered to build the LCI for the six SNG systems under analysis. It is important to note that the hydrogen (as an intermediate flow) needed in input to the methanation section to produce 1 kg of SNG corresponds to 0.262 kg for HG system while it is equal to 0.515 kg for the remaining case studies.

Table 18. Inventory data for the SNG technologies considered in this study. (Amount per kg of SNG produced)

	Flow	I/O	Unit	INV-HG	ICE-BS	STIG	GT	SOFC6	SOFC30
Electrolysis [1]									
	Wind electricity (to H_2)	i	kWh	12.85	25.22	25.24	25.24	25.23	25.27
	Wind electricity (H_2 compression)	i	kWh	$5.17\cdot10^{-2}$	$1.01\cdot10^{-2}$	$1.01\cdot10^{-2}$	$1.01\cdot10^{-2}$	$1.01\cdot10^{-2}$	$1.02\cdot10^{-2}$
	Deionised water	i	kg	2.94	5.77	5.77	5.77	5.77	5.78
	KOH	i	g	0.22	0.44	0.44	0.44	0.44	0.44
	Oxygen	o	kg	2.10	4.20	4.20	4.20	4.20	4.20
	Electrolyser (1 kW)	i	p	$1.60\cdot10^{-4}$	$3.20\cdot10^{-4}$	$3.20\cdot10^{-4}$	$3.20\cdot10^{-4}$	$3.20\cdot10^{-4}$	$3.20\cdot10^{-4}$
Methanation									
	Wastewater	o	kg	1.05	2.17	2.17	2.17	2.17	2.18
	Waste steel, recycling	o	kg	$9.12\cdot10^{-5}$	$9.12\cdot10^{-5}$	$9.12\cdot10^{-5}$	$9.12\cdot10^{-5}$	$9.12\cdot10^{-5}$	$9.12\cdot10^{-5}$
	Waste zeolite, landfilling	o	kg	$2.49\cdot10^{-4}$	$2.49\cdot10^{-4}$	$2.49\cdot10^{-4}$	$2.49\cdot10^{-4}$	$2.49\cdot10^{-4}$	$2.49\cdot10^{-4}$
	Rhodium, catalyst (GLO)	i	kg	$1.25\cdot10^{-6}$	$1.25\cdot10^{-6}$	$1.25\cdot10^{-6}$	$1.25\cdot10^{-6}$	$1.25\cdot10^{-6}$	$1.25\cdot10^{-6}$
	Aluminium oxide, catalyst (GLO)	i	kg	$2.48\cdot10^{-4}$	$2.48\cdot10^{-4}$	$2.48\cdot10^{-4}$	$2.48\cdot10^{-4}$	$2.48\cdot10^{-4}$	$2.48\cdot10^{-4}$
	Chromium steel 18/8 (GLO)	i	kg	$9.12\cdot10^{-5}$	$9.12\cdot10^{-5}$	$9.12\cdot10^{-5}$	$9.12\cdot10^{-5}$	$9.12\cdot10^{-5}$	$9.12\cdot10^{-5}$
Gasification									
	Biomass production, SRC	i	kg	1.79	1.79	1.79	1.79	1.79	1.79
	Water, deionised	i	kg	-	1.28	-	-	-	-
	Electricity	o	kWh	-	1.79	4.73	2.20	4.09	3.72
	Electricity (bottom cycle)	o	kWh	-	0.94	-	1.37	1.13	1.32
Capital Goods	Chemical factory, organic	i	p	$4.00\cdot10^{-10}$	$4.00\cdot10^{-10}$	$4.00\cdot10^{-10}$	$4.00\cdot10^{-10}$	$4.00\cdot10^{-10}$	$4.00\cdot10^{-10}$
Power unit									
	SOFC (230 kW) [2]	i	p	-	-	-	-	$6.81\cdot10^{-7}$	$4.04\cdot10^{-7}$
	Turbine (micro, 100 kW)	i	p	-		$1.83\cdot10^{-6}$	$1.98\cdot10^{-6}$	$2.31\cdot10^{-6}$	$2.01\cdot10^{-6}$
	Turbine (10 MW)	i	p	-	-	$2.78\cdot10^{-8}$	$1.66\cdot10^{-8}$	-	-
	Inverter (500 kW)	i	p	-	-	-	-	$1.57\cdot10^{-7}$	$1.86\cdot10^{-7}$
	Generator (200 kW)	i	p	-	$2.29\cdot10^{-7}$	$3.47\cdot10^{-7}$	$3.56\cdot10^{-7}$	$2.89\cdot10^{-7}$	$2.51\cdot10^{-7}$
	Compressor (300 kW)	i	p	-	$2.02\cdot10^{-7}$	$3.47\cdot10^{-7}$	$3.04\cdot10^{-7}$	$2.10\cdot10^{-7}$	$4.47\cdot10^{-7}$
	ICE + generator (160 kW)	i	p	-	$1.20\cdot10^{-7}$	-	-	-	-

[1] The life-cycle inventory for alkaline water electrolysis is taken from Valente et al. [211]

[2] The life-cycle inventory for solid oxide fuel cell (SOFC) is taken from Strazza et al. [267]

The production capacity is 559 kg SNG$\cdot$h^{-1} in all the systems under analysis. Inventory data for background processes are retrieved from ecoinvent database [181]. It should be noted that Strazza et al. [267] report in their inventory some material flows required in the SOFC that are not present in ecoinvent database. For this reason, nickel oxide inventory was based on [222,268], zirconium chloride and yttrium chloride inventories were modelled according to

[269] and [270–272], respectively. In particular, nickel oxide, as a precursor of metallic nickel at 99.5% purity, was obtained by considering an intermediate process in the nickel extraction and purification process. Similarly, zirconium oxide was considered as a precursor for zirconium chloride, adding the material and energy requirements for the chlorination process of ZrO_2 at 1200 °C. Regarding infrastructure and capital goods, the sections of methanation and gasification were included within a conventional chemical factory (organics) entry, while the power units and the electrolyser were separately considered as reported in Table 18. Apart from the built-in ones, all the inventory data were taken from ecoinvent 3.5 [273,274].

The biomass was willow wood chips and particles, from short rotation coppice, from ecoinvent database. The carbon balance was quantified by using the biomass composition reported in Section 4.1.1. In this regard, given the biomass input the same in each layout, a CO_2 uptake equal to -1.77 kg CO_2/kg biomass was applied. Regarding fuel combustion emissions, all the layouts adopt the same composition as conventional natural gas to which fossil characterisation factors were applied. Since the layouts refer to upcoming technologies, the electricity displaced by the plant was assumed from a 2030 scenario (Table 19) with a higher renewable share than current mixes, which is conservative for the purpose of this study. The electricity used for the electrolysis process and compression duties was assumed to be produced from wind power.

In this study, the assessment was performed to explore the effect of different methodological assumptions. Using 1 kg of SNG as the functional unit, avoided burdens approach was applied in the base scenario. As mentioned above, this multifunctionality approach consists in discounting the burdens associated with the co-product (i.e., electricity) that is considered to displace the production of the conventional Italian mix electricity (2030 base). In the second scenario, the burdens of the whole system were distributed between the two products (SNG and electricity) according to an energy allocation. Since each layout produces SNG and electricity in different proportions, allocation factors are different among layouts (see Table 20). The allocation factors (AF) for the i^{th} layout were calculated according to Equations (4.2) and (4.3), where the SNG energy content was calculated based on its lower heating value (LHV).

In order to further explore the effects of the sensitivity of the results to allocation factors, an extreme case in which the produced electricity is not dispatched is also discussed. In this case, the burdens are attributed only to the SNG production. In addition, when the main functional unit was 1 MJ of total energy in output, the system does not present co-functions; therefore, no multifunctionality approaches are followed.

Table 19. Italian 2030 energy mix for electricity production (TWh). Data from [275]

Installed Technology	Installed Capacity (TWh)	Share (%)
Gas	118.00	38.5
Gas, CC	36.09	11.8
Gas, conventional	9.69	3.2
Gas, CC, 400 MW	44.68	14.6
Gas, conventional, 100 MW	27.54	9.0
Coal	0.00	0.0
Oil and others	2.00	0.7
Oil, conventional	0.43	0.1
Oil, cogeneration	1.57	0.5
Geothermal	7.10	2.3
Bioenergy	15.70	5.1
Biogas, gas engine	11.96	3.9
Wood chips	3.74	1.2
Solar	74.50	24.3
PV, rooftop	30.15	9.8
PV, ground mounted	43.06	14.0
CSP	1.27	0.4
Wind	40.10	13.1
Onshore, <1 MW	10.70	3.5
Onshore, 1–3 MW	24.17	7.9
Onshore, >3 MW	3.27	1.1
Offshore	1.96	0.6
Hydro	49.30	16.1
Hydro, Pumped storage	1.43	0.5
Hydro, Reservoir	30.64	10.0
Hydro, Run-on	17.23	5.6
Tot	306.70	100.0
Tot RES	186.70	60.9

$$AF_{SNG,i} = \frac{FU_{SNG} \cdot LHV_{SNG}}{Electricity_{out} + FU_{SNG} \cdot LHV_{SNG}} \tag{4.2}$$

$$AF_{electricity,i} = \frac{Electricity_{out}}{Electricity_{out} + FU_{SNG} \cdot LHV_{SNG}} = 1 - AF_{SNG,i} \tag{4.3}$$

Table 20. Allocation factors for the two co-products (SNG and electricity) in the energy allocation scenario

Plant layout	SNG allocation factor	Electricity allocation factor
GT	80%	20%
ICE	84%	16%
HG	100%	-
SOFC30	74%	26%
SOFC6	73%	27%
STIG	75%	25%

4.1.4. Results and discussion

SNG mass as the functional unit

Based on the inputs and assumptions specified in the previous Sections 4.1.2. and 4.1.3, carbon footprint, acidification footprint and non-renewable energy footprint were calculated for the six analysed layouts (see Figure 49, Figure 50 and Figure 51 respectively).

The layout having the lowest GWP impact (-0.45 kg CO_2 eq/kg SNG) is the SOFC6 due to its higher production of electricity which results in higher credits (see Figure 49). The layouts with still negative or null GWP impact are the SOFC30, the STIG and the GT, with -0.42, -0.39 and 0.00 kg CO_2 eq/kg SNG, respectively. The highest GWP impacts are registered for the ICE (0.26 kg CO_2 eq/kg SNG) and the HG solutions (0.76 kg CO_2 eq/kg SNG). In the latter case, the lower impacts attributed to wind generation (51% lower than in the other configurations) do not compensate the lack of environmental credits for electricity fed to the grid.

The layout reporting the lowest AP footprint (0.0143 kg SO_2 eq/kg SNG) is the HG (see Figure 50), because of the low wind electricity consumption. The layouts STIG, SOFC6 and SOFC30 have similar AP footprint, accounting for 0.0171 ÷ 0.0173 kg SO_2 eq/kg SNG. The GT layout implies 0.0188 kg SO_2 eq/kg SNG. The ICE layout causes the highest AP footprint (0.0197 kg SO_2 eq/kg SNG) due to reduced electricity production and therefore lower environmental credits in the avoided burdens approach.

As far as the CEDnr is concerned, the SOFC30, SOFC6 and STIG layouts outperform the other solutions, reporting impacts of -14.75, -14.17 and -13.48 MJ/kg SNG, respectively. This is ascribable to the environmental credits given to the electricity fed to the grid. The GT and ICE layouts cause intermediate, but still negative CED impact (-7.21 and -3.07 MJ/kg SNG). The HG is the plant that has the most relevant CED impacts, accounting for 6.39 MJ/kg SNG. As for the carbon footprint, this layout is penalised by the lack of environmental credits for electricity production.

Impact breakdown

In all investigated layouts, the major GWP impact (38-49% on the total) is given by the SNG combustion (see Figure 49). Electricity production from wind power plants represents 4-6% over the total carbon footprint, and other processes (i.e., deionised water production and wastewater treatment account for only 3-4% of the share for all layouts.

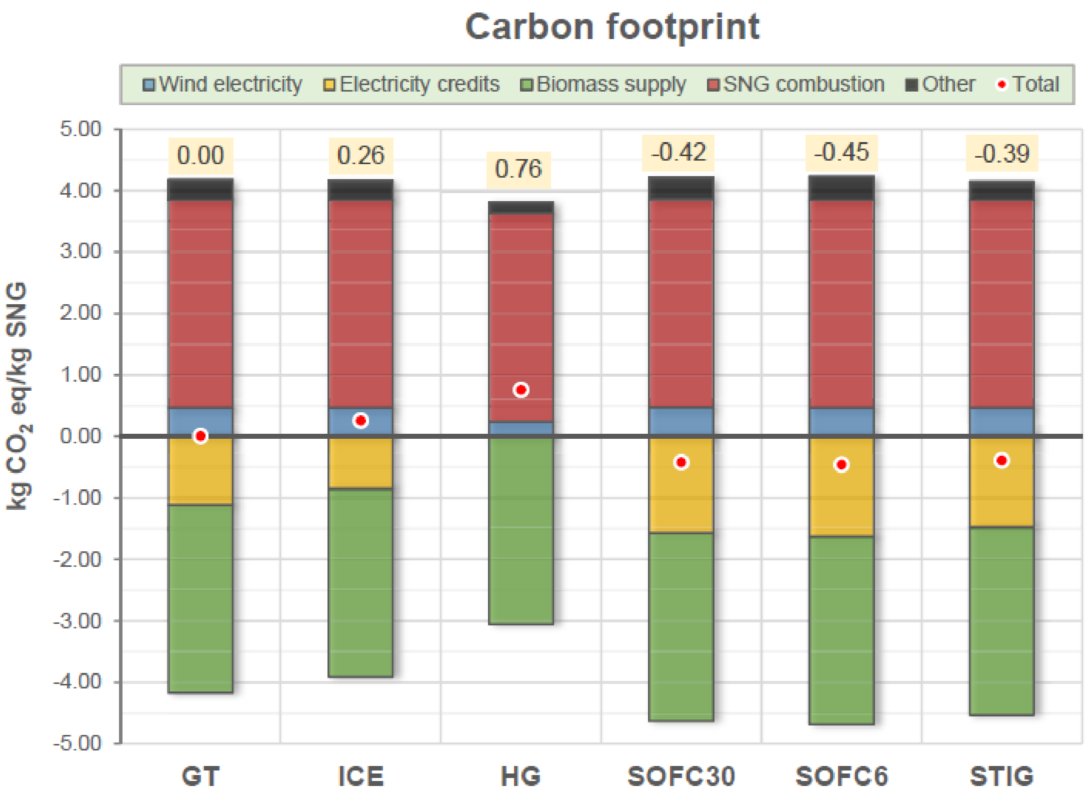

Figure 49. Impact breakdown for the GWP indicator for the six analysed layouts

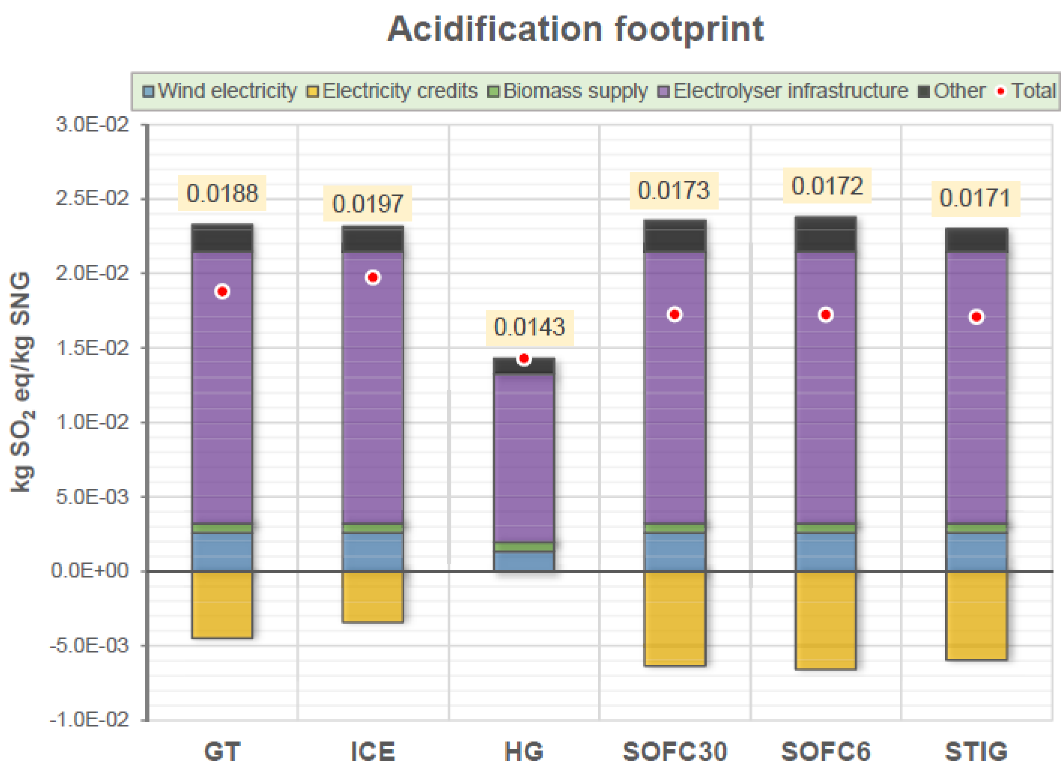

Figure 50. Impact breakdown for the AP indicator for the six analysed layouts

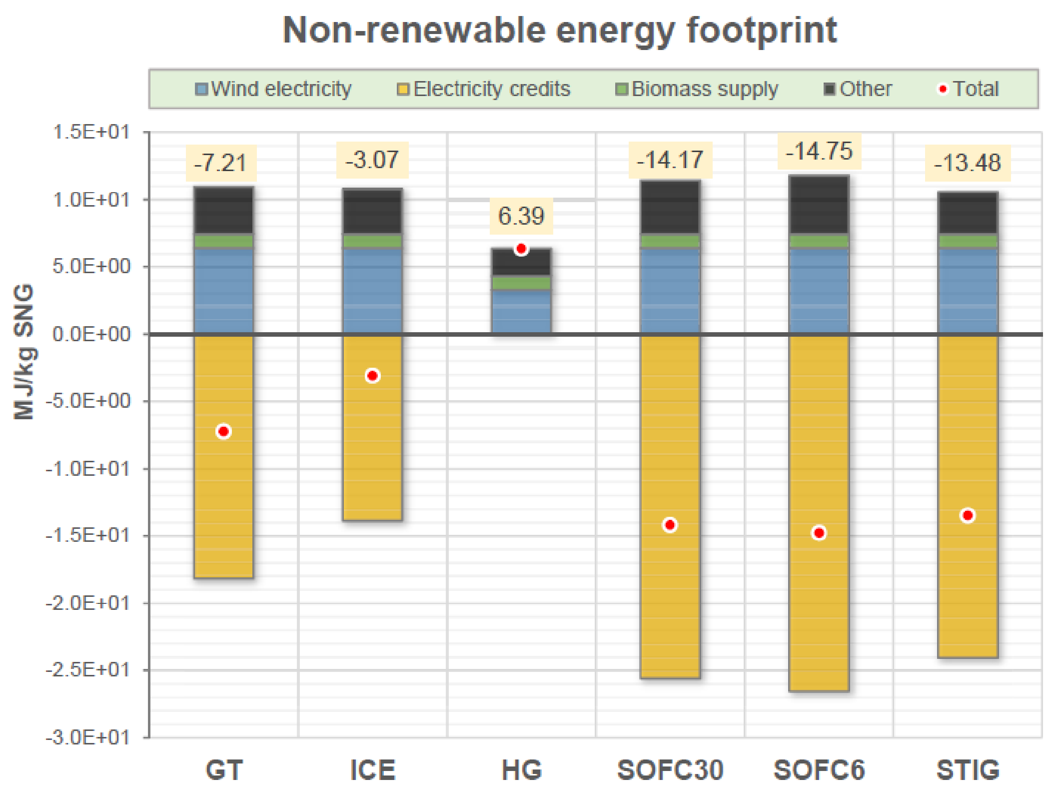

Figure 51. Impact breakdown for the CEDnr indicator for the six analysed layouts

With respect to the environmental credits, the higher benefit is given by the CO_2 uptake from the atmosphere by the biomass (between -45% and -35% of the total carbon footprint). With the energy mix employed in the present study, the environmental benefits related to the electricity production avoided emissions range between -18% (SOFC layouts) and 0% (HG layout).

The highest impact on AP is ascribable to the electrolyser infrastructure (60-79% of the overall impacts) for all considered layouts, as shown in Figure 50. In particular, the major contribution to AP is ascribable to the mining of catalyst metals (nickel and rhodium) for electrodes manufacturing. Wind electricity production, other processes and biomass supply account for 9%, 5-7% and 2-5% of the total impacts, namely. The environmental benefits for electricity production can contribute significantly (up to -21% in the SOFC and STIG layouts) to decrease the AP overall footprint. The HG layout shows a minor acidification footprint due to the lower amount of hydrogen required and proportionally lower burdens embodied in the electrolyser infrastructure per functional unit (Table 18).

With respect to the CEDnr, the major (negative) contribution is given by the electricity credits for the cogenerative layouts (-70% to -56%), while the most significant positive contribution is ascribable to electricity production from wind power (17%-26%) (see Figure 51). Other processes and biomass supply are responsible for 9-14% and 3-4% of the share, namely. Since the HG layout has no environmental credits from electricity production, the wind electricity production, other processes and the biomass supply account for 51%, 32% and 16% of the total CEDnr footprint.

4.1.5. Energy output as the functional unit

Since five out of six investigated layouts are cogenerative, it is worth investigating the sensitivity of the results to functional unit changes. Figure 52 shows the impact assessment for a functional unit of 1 MJ of energy output. The layout that implies the lowest GWP, AP and CED is the one with hydrogasification (HG). The highest GWP is found with the ICE layout, which also gives the highest impacts in terms of AP and CEDnr. The SOFC30, SOFC6 and STIG layouts report similar impacts on all the considered indicators, slightly lower than the GT layout. Conventional natural gas has higher impacts than the proposed layouts in terms of GWP and CEDnr but outperforms SNG in terms of AP. This found to be closely linked to the use of fertilisers and pesticides in the biomass growth stage in the six layouts producing SNG.

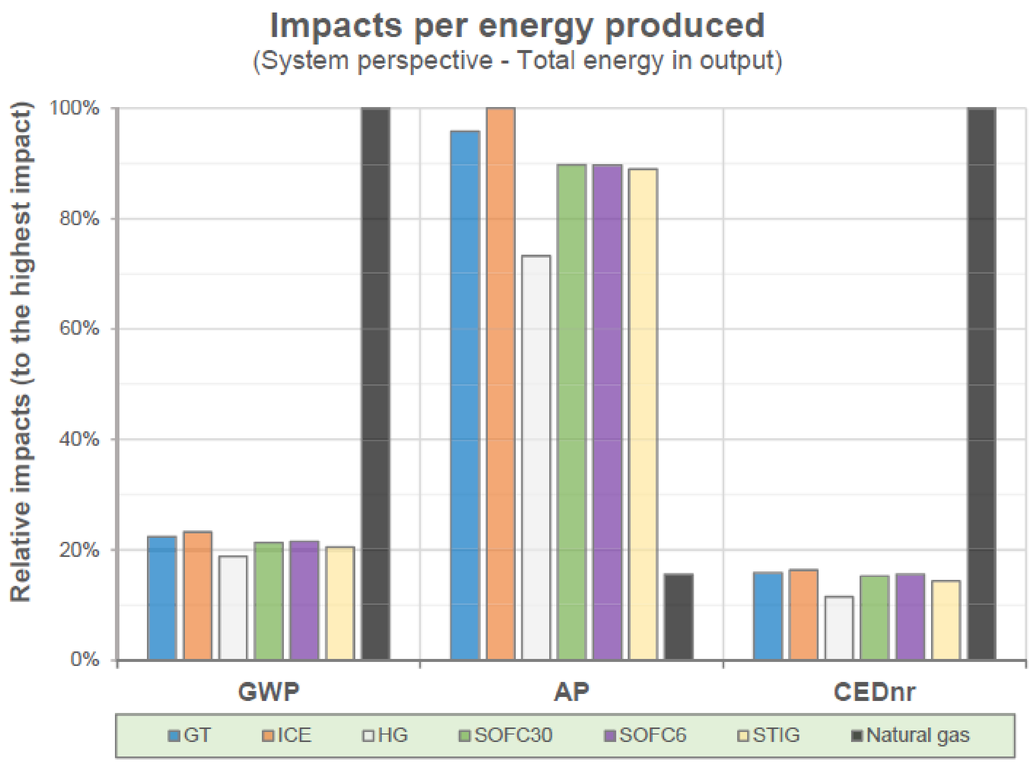

Figure 52. GWP, AP and CEDnr impacts for all investigated layouts

4.1.6. Multifunctionality handling

The impact assessment results and the ranking among the layouts change according to the chosen multifunctionality methodology. In the base-case scenario (avoided burdens approach), the SOFC6, SOFC30 and STIG layouts (in this order) outperform all the other layouts in the GWP and the CEDnr impacts, while the layout with the lowest impact on the AP is the HG (see Figure 53). The base-case results have been already deeply discussed in Section 4.1.4.

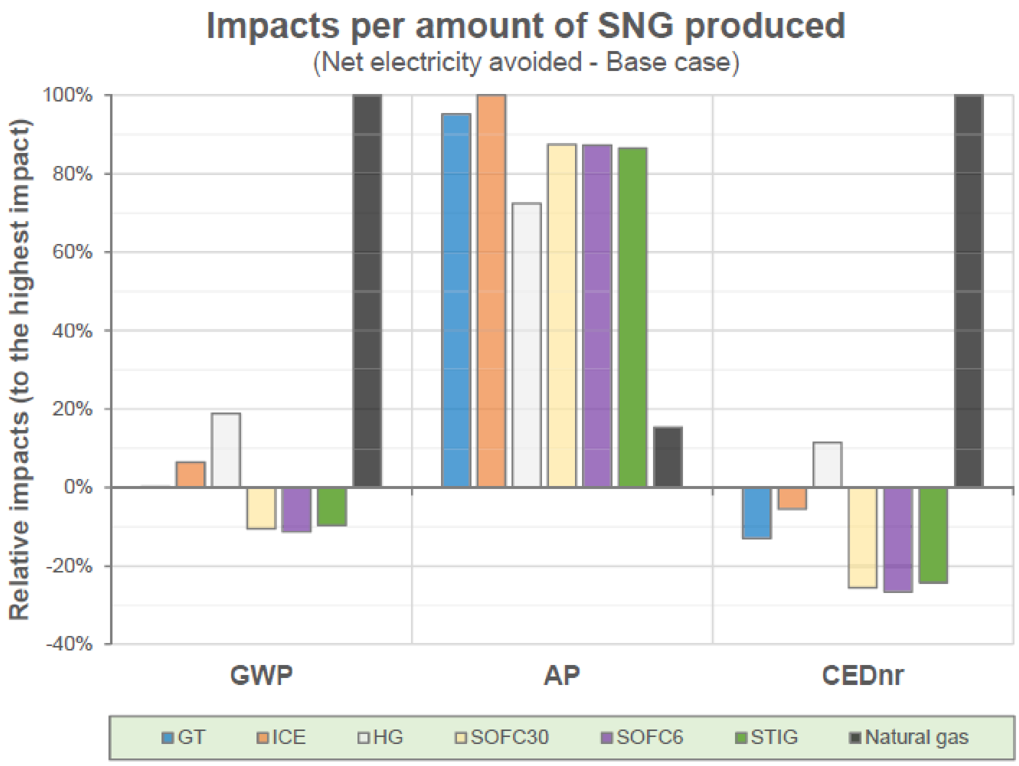

Figure 53. GWP, AP and CEDnr relative impacts for all investigated layouts, in the base-case scenario (avoided burdens approach)

On the contrary, when using an allocation approach (scenario 2) the layout with the lowest impacts on all considered indicators is the HG (see Figure 54). The layouts having the highest GWP impact are the SOFC6 and SOFC30 layouts. The rest of the ranking is completely overturned. Still in the energy allocation approach, the layouts with the most significant AP and CEDnr impacts are the ICE, and secondly, the GT. Regardless the multifunctionality approach applied, the overall GWP impacts of all layouts are significantly lower than in the case of NG, while the AP impacts of NG are much inferior than all the proposed layouts. With allocation approaches, the cogenerative solutions resulted penalised by the lack of credits from the co-produced electricity. Thus, although the ISO standards recommend avoiding allocation when possible, in this analysis allocation denotes a more conservative approach in contrast to the avoided burdens.

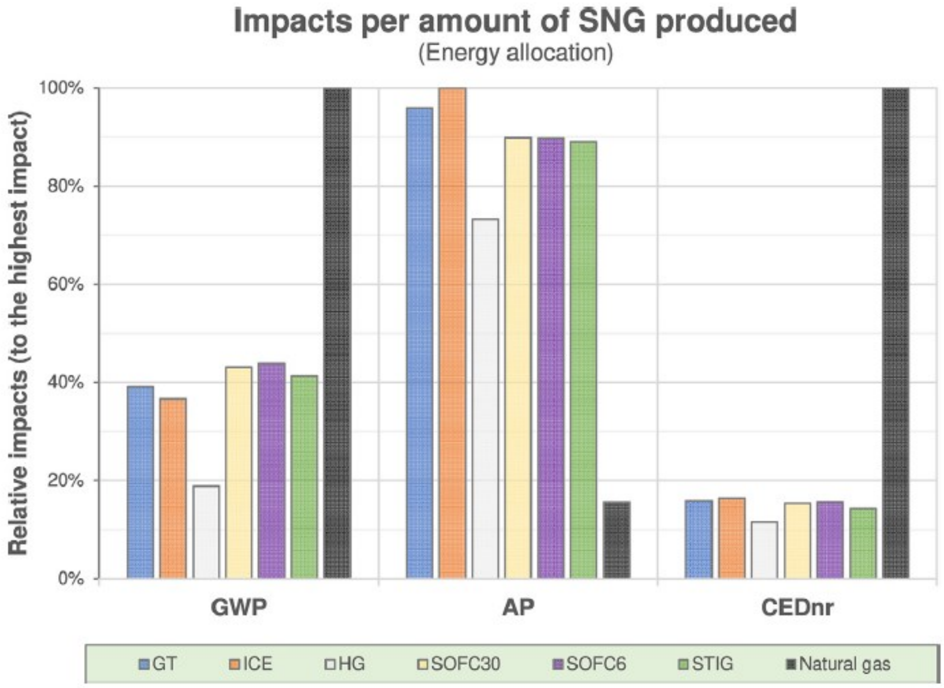

Figure 54. GWP, AP and CEDnr relative impacts for all investigated layouts, in the second scenario (energy allocation approach)

When exploring the effects of the uncertainty of allocation factors on the results, in the extreme case in which the produced electricity is not dispatchable, 100% of burdens and credits are attributed only to SNG. Counter-intuitively, in this case GWP impacts of the multifunctional systems are lower than their GWP impacts calculated using allocation factors (Table 20). This is due to the fact that the GWP impacts that are allocated are negative and, in absolute terms, the allocation factors reduce more benefits than impacts. In contrast to GWP, for AP and CEDnr indicators (impacts with positive value), a higher allocation factor to the SNG production corresponds to higher impacts. When looking at the comparison with NG impacts, in case the electricity is not fruitfully used and fed to the grid, the produced SNG gives higher AP and CEDnr impacts than the fossil alternative. Clearly, this last extreme scenario would be disadvantageous as for economic profitability but, being it the most conservative, it gives an immediate upper value to the calculated impacts for intermediate cases (i.e., electricity dispatched to the grid in a small number of hours per year). Overall, regardless layout configuration for the co-production of electricity (i.e., type of the power unit) and regardless LCA methodological aspects linked to multifunctionality approach and functional unit choice, the production of SNG using biomass and renewable electricity shows favourable performances under carbon and energy-related life cycle impact categories when comparing with the conventional NG. Impact trade-off is found for acidification potential, due to the water alkaline electrolysis. However, a shift from water alkaline to Proton Exchange Membrane (PEM) electrolysis technology could potentially bring environmental benefits also on acidification concerns. On the other hand, the most conservative scenario proves that the fruitful exploitation of the co-produced electricity is crucial in order to make SNG production from biomass more environmentally favourable than the fossil alternative, at least under CEDnr. Finally, the choice of the multifunctionality approach led to prioritise the monofunctional solution (HG layout) under environmental aspects over multifunctional layouts co-producing electricity.

4.1.7. Conclusions

In the present study, the LCA of six different layouts for the production of SNG from biomass and electrolytic hydrogen was performed according to three impact indicators (GWP, AP, CEDnr), and compared with the natural gas impacts. The analysis was carried out with different functional units and with two different approaches to deal with multifunctionality. The results showed that, with all the proposed layouts, SNG production from biomass and renewable electricity led to lower environmental burdens in terms of GWP and CEDnr with respect to conventional NG, although it presents a higher AP. The critical contribution identified for acidification is the alkaline electrolyser manufacturing, in particular associated with mining of the metals employed as electro-catalysts such as nickel and rhodium. The multifunctionality approach was found to determine the technology ranking among the investigated alternatives; nevertheless, it did not overturn the overall results in terms of suitability with respect to conventional NG. In this regard, under GWP and CEDnr indicators, systems involving electricity co-production showed lower impacts when addressing multifunctionality through avoided burdens approach. In contrast, the allocation approach led to prioritising monofunctional layouts under the three analysed environmental criteria. This result confirms the relevance of performing sensitivity analyses on multifunctionality approaches as an insightful practice in decision-making processes. Once the energy and environmental performance of all proposed layouts have been mapped, future works should investigate the economic performances or Life Cycle Costs (LCC), especially if in contrast with energy efficiency and environmental impacts.

4.2. Heat recovery from a PtSNG plant coupled with wind energy

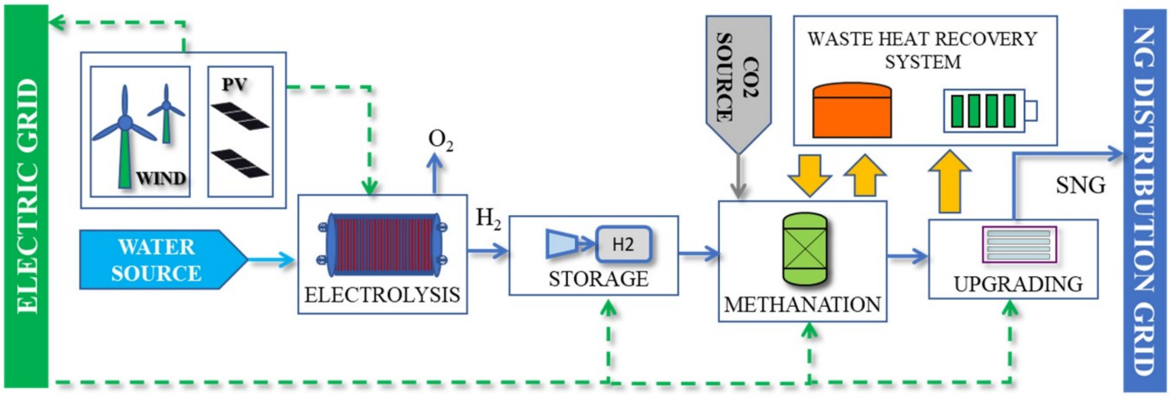

Figure 55. Conceptual scheme of the proposed waste heat recovery system for a PtSNG plant coupled with wind energy

Power to substitute natural gas (PtSNG) is a promising technology to store intermittent renewable electricity into a synthetic fuel. Power surplus on the electric grid is converted to hydrogen via water electrolysis and then to SNG via CO_2 methanation. The produced SNG can be directly injected in the natural gas infrastructure for long term and large-scale energy storage. Because of the fluctuating behaviour of the input energy source, the overall annual plant efficiency and SNG production are affected by the plant operation time and the standby strategy chosen. The re-use of internal (waste) heat for satisfying the energy requirements during critical moments can be crucial to achieve high annual efficiencies. In this study the heat recovery from a PtSNG plant coupled with wind energy, based on proton exchange membrane electrolysis, adiabatic fixed bed methanation and membrane technology for SNG upgrading, is investigated. The proposed thermal recovery strategy involves that the waste heat available from the methanation unit during the operation hours is accumulated by means of a two-tanks diathermic oil circuit. The stored heat is used to compensate the heat losses of methanation reactors, during the hot standby state. Two options to maintain the reactors at operating temperature have been assessed. The first requires that the diathermic oil transfers heat to a hydrogen stream which is used to flush the reactors in order to guarantee the hot standby conditions. The second option entails that the stored heat is recovered for electricity production through an Organic Rankine Cycle. The electricity produced is used to compensate the reactors heat losses by using electrical trace heating during the hot standby hours, as well as to supply energy to ancillary equipment.

The aim of the work presented in *Publication 3* was to evaluate the technical feasibility of the proposed heat recovery strategies and how they impact on the annual plant performances. The results showed that the annual efficiencies on LHV basis were found to be 44.0% and 44.3% for the thermal storage and electrical storage configurations, respectively.

4.2.1. Background and scope

The effective integration of wind energy in power system can be reached only by developing suitable storage technologies able to stabilise the electricity grids and increase flexibility. Owing to its intermittent and random nature, power production from non-programmable RESs generates critical issues in the balance between energy supply and demand, especially during overgeneration periods.

Power to Substitute Natural Gas (PtSNG) is one of the most promising storage technologies to support RESs integration in the energy system [276]. Exploiting the natural gas (NG) transmission and distribution networks, as well as the storage features of the existing NG infrastructure, the substitute natural gas produced from surplus renewable energy can be injected into the NG pipeline system, allowing to store large amounts of energy for long-term periods, thus offering balancing and regulation services to the electricity grid. However, a large-scale development of PtSNG technology is currently limited due to the relative low efficiency and high costs [277,278]. Both aspects significantly depend on the employment of the by-products derived from PtSNG process (e.g., oxygen, waste heat) [277].

In this sense, the use of waste heat from methanation process is crucial to increase the efficiency of PtSNG process chain [47,277,279]. CO_2 methanation reaction is a highly exothermic catalytic process operating typically at temperatures between 150 °C and 550 °C depending on the catalyst used [280]. The reaction heat released by the methanation of 1 mol of CO_2 is about equal to 165.1 kJ [281]. Furthermore, the outgoing SNG from methanation process requires to be dehydrated and cooled from an elevated temperature (i.e., 300 – 700 °C, depending on the reactor concept [277]) to be injected into the NG infrastructure. These processes represent sources of thermal energy at medium-high temperature level that can be exploited to reduce the overall PtSNG system energy input, and thus, increase its efficiency.

A literature review of scientific publications providing other possible solutions for the waste heat recovery from a power-to-SNG plant was provided in *Publication 3*.

In a previous work [282], the co-authors evaluated the energy storage potential and the technical feasibility of the PtSNG concept to store intermittent renewable sources. For this aim, different plant sizes (i.e., 1 MW, 3 MW, and 6 MW) were defined and investigated. The analysis results indicated that the annual overall plant efficiency decreases as plant size increases (i.e., from 43.7% to 41.6%) due to the growing impact of the energy required to balance the heat losses in the hot-standby mode (i.e., the standby period increases from 2713 hours to 4590 hours). However, the plant efficiencies were evaluated without taking into account the thermal energy management.

Owing to the fluctuating behaviour of the input energy source, the operation of the PtSNG plant sub-systems (i.e., electrolysis and methanation units) is characterised by frequent shutdowns, and consequently by frequent changeover of state (i.e., cold-standby, hot-standby and production with different loads) [279,282,283]. On the basis of the plant management strategy, the energy consumption required to restart the SNG production from the cold-standby state, as well as the energy consumption necessary for keeping the sub-systems in hot-standby state, could significantly increase the energy input required and therefore, negatively affect the annual performance of PtSNG plants.

In *Publication 3*, a novel thermal management strategy for a PtSNG plant coupled with a RES facility is presented. The concept involves employing the waste heat produced by methanation process to assure the hot-standby conditions of methanation unit itself, as well as to fulfil the ancillary equipment energy demand. The proposed strategy entails that the waste heat is accumulated by means of a two-tanks diathermic oil circuit during the operation hours of methanation unit and then, it is used to compensate the heat losses of methanation reactors during the hot-standby state. In particular, two different systems to maintain the reactors at operating temperature have been considered. The aim of this research activity was to evaluate the technical feasibility of the proposed heat recovery strategies and how they impact on the annual plant performances.

4.2.2. PtSNG plant description

The PtSNG plant, shown in Figure 56, is directly coupled with a 12 MW wind farm and is sized for 1 MW of electric power input. It consists of four sections: i) the hydrogen generation unit based on the proton exchange membrane (PEM) electrolyser, ii) the methanation unit based on the fixed-bed reactors technology, iii) the H_2 storage unit, in which gaseous hydrogen is stored into pressurised vessels and iv) the SNG upgrading unit based on the membrane technologies.

The demineralised water (1) is pumped and heated to the operative pressure and temperature of the PEM electrolysis unit where O_2 and H_2 are produced. On the basis of a specific control strategy, H_2 generated via electrolysis (stream 5) can be partially or totally sent to the methanation unit (6) and/or to the intercooled compressor C1 (8) to increase the pressure up to the maximum storage pressure. The compressed H_2 (9) is stored in high-pressure tanks. The H_2 streams from electrolysis unit and/or storage unit are mixed with the CO_2 stream (13) from the CO_2 storage unit. The CO_2 is assumed to be always available for the PtSNG plant (i.e., supplied by sequestration from other power plants or industrial processes) at the storage pressure of 200 bar.

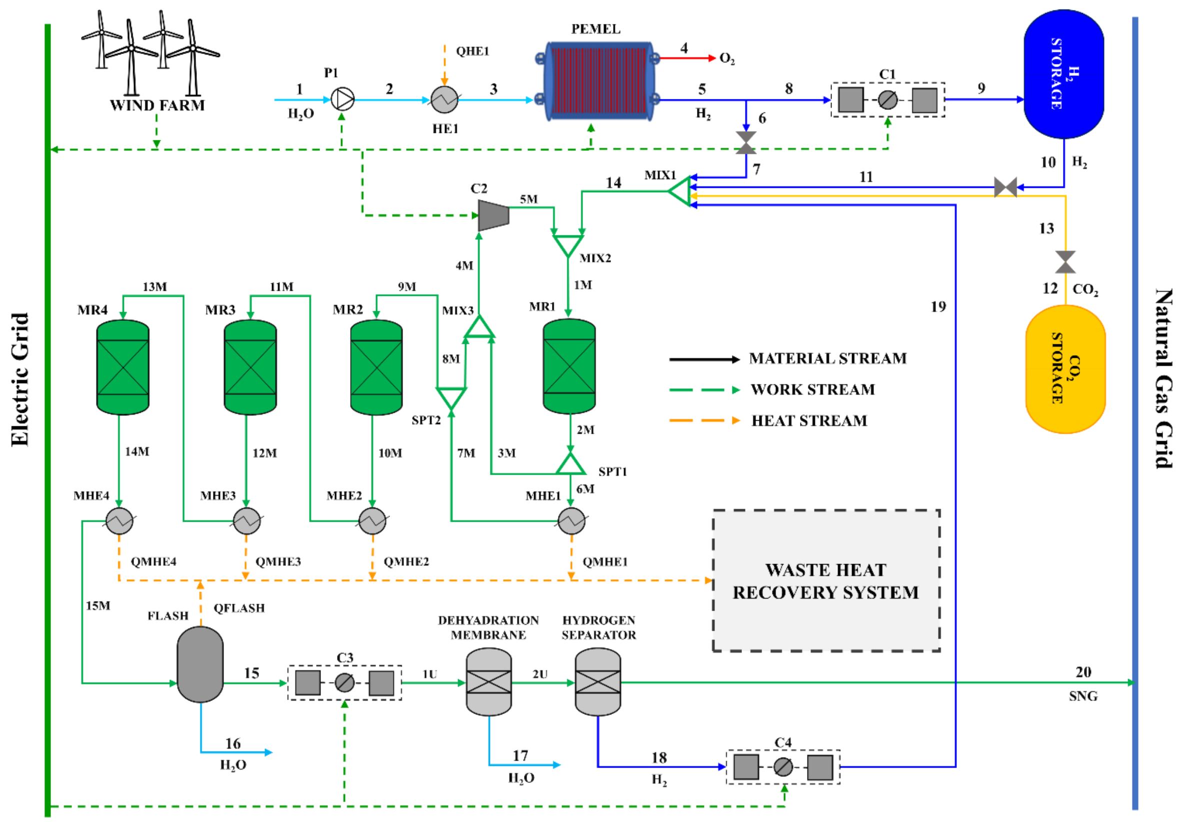

Figure 56. PtSNG plant layout

The methanation unit consists of four adiabatic fixed-bed reactors (MR1, MR2, MR3, MR4) connected in series with intermediate gas cooling (heat exchangers MHE1, MHE2, MHE3) for assuring the fixed inlet reactors temperatures. The H_2 and the CO_2 entering the methanation unit are mixed with the hydrogen (19) from the SNG upgrading unit and then preheated up to the inlet temperature of the methanation reactor MR1 (300 °C). This preheating is performed by mixing the reactant flow (14) with hot streams from the MR1 and MHE1 defined by specified recirculation ratios (stream 3M at the splitter SPT1 and stream 8M at the splitter SPT2). Thus, the syngas (9M) sent to the MR2 reactor is a fraction of the product gases leaving the first methanation reactor. In the following reactors (MR3 and MR4) the CO_2 hydrogenation is led at decreasing temperature levels, reaching the conversion of 94% at the exit of the last methanation reactor. During the methanation process a large amount of water is produced, so the raw SNG (14M) is cooled in the heat exchanger MHE4 and sent to the flash vapor-liquid separator (FLASH) for water removal. In order to meet the required grid specifications, the SNG (15) is further upgraded by means of a dehydration membrane (a commercial Pebax®-based membrane [284]) to eliminate the residual moisture to comply with the H_2O dew point requirements of the pipelines and of a H_2 separation membrane (polysolfone-based membrane).

The quality of the SNG exiting from the upgrading section (20) satisfies the current pipelines specifications effective in various European countries, as reported in Ref. [285] and therefore, can be directly injected into the low-medium pressure NG transmission network. If the country specific pipeline requirements are more stringent, additional CO_2 or H_2 removal systems should be considered. The hydrogen from the upgrading unit is recycled to the first methanation reactor, as mentioned above.

Finally, the waste heat available from the methanation unit and from the flash unit can be usefully recovered in the waste heat recovery system according to the concepts that will be described below.

The PtSNG plant is operated in input-oriented mode. In order to maximise the operating hours of the plant, a hydrogen storage unit is employed to decouple the H_2 generation and the SNG production. As management strategy, four operation modes are allowed for the methanation unit: i) full load, in which the hydrogen flow rate entering the methanation unit from the storage and/or the electrolyser is equal to the nominal value; ii) partial load, in which the hydrogen flow rate sent to methanation reactors varies from 40% to 100% of the nominal value, according to the specified minimum and maximum hydrogen storage pressures; iii) hot-standby mode, in which the reactors are kept at the minimum operating temperature of the catalysts to allow a quick restart; iv) cold-standby mode, in which no carbon dioxide and hydrogen feed the methanation unit. Even if the restart from cold-standby requires more energy than that required to maintain the hot-standby, this operation mode can be convenient when the number of hours from the shut-down to the restart is high. The parameter that controls the start of the plant and the operation modes of the methanation unit is the hydrogen storage pressure that follows the control strategy widely described in [282]. The mass and energy balances of the PtSNG plant in steady state conditions as well as the annual performance of the plant are performed by applying the thermochemical and electrochemical model (in Aspen Plus environment) and the dynamic model (in MATLAB environment) developed and described in [282]. The thermochemical and electrochemical model consists of sub-models for each plant section; the sub-model of the methanation unit in this study, was modified by considering the kinetics of the process and it was described in Appendix of *Publication 3*. The dynamic model based on the annual hourly energy input (the wind energy supplied to the plant) and on the storage control strategy allows forecasting the annual operation time (full and partial load hours, standby hours) and the annual performances (SNG production, energy consumption, efficiency) of the PtSNG plant.

4.2.3. Heat recovery management

The heat recovery management is based on the valorisation of the waste heat, generated during the plant operation in the methanation unit, to self-sustain, from an energetic point of view, the standby conditions. To this end, two heat recovery configurations based on different heat recovery concepts are proposed and investigated. In both configurations, the recovery of the waste heat coming from the methanation unit is performed by means of a heat transfer fluid (i.e., diathermic oil) stored in insulated tanks for thermal energy storage. Figure 57 shows the conceptual schemes of the two heat recovery systems.

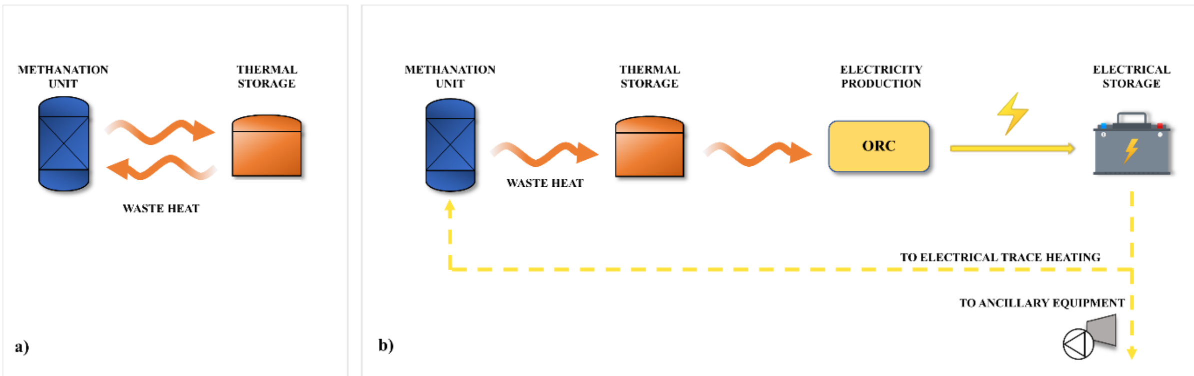

Figure 57. Conceptual schemes and energy flows of the two proposed waste heat recovery systems: (a) Thermal storage; (b) electrical storage

In the first one (Thermal storage configuration, Figure 57a), the stored thermal energy is used to satisfy the thermal energy demand of the reactors during the standby periods by means of a thermal carrier. In the second one (Electrical storage configuration, Figure 57b), the stored thermal energy is used to produce electricity by means of an Organic Rankine Cycle (ORC). This electrical energy is stored in batteries and it is used to meet the energy requirements of the electrical trace heating system of the methanation unit during the standby periods. In this case the stored electric energy is also used to satisfy the ancillary equipment electricity demand.

4.2.3.1. Thermal storage

In the thermal storage system, the waste heat is recovered and stored by means of a two-tanks diathermic oil circuit; the stored thermal energy is supplied, when required, to the methanation reactors by means of a thermal carrier. Hydrogen is used as thermal carrier because it removes the residual carbon dioxide preventing catalyst deactivation. Figure 58 shows the layout of the thermal storage configuration During the plant operation, the diathermic oil (stream 1HR) from the cold oil tank is pushed (2HR) by the pump P2 and sent to the methanation unit for heat recovering (heat exchangers MHE1, MHE2, MHE3, MHE4 and the FLASH unit) in such a way to minimise the temperature gradients and to optimise the heat transfer efficiencies; at the exit of the MHE1 the hot diathermic oil (7HR) is stored into the hot oil tank.

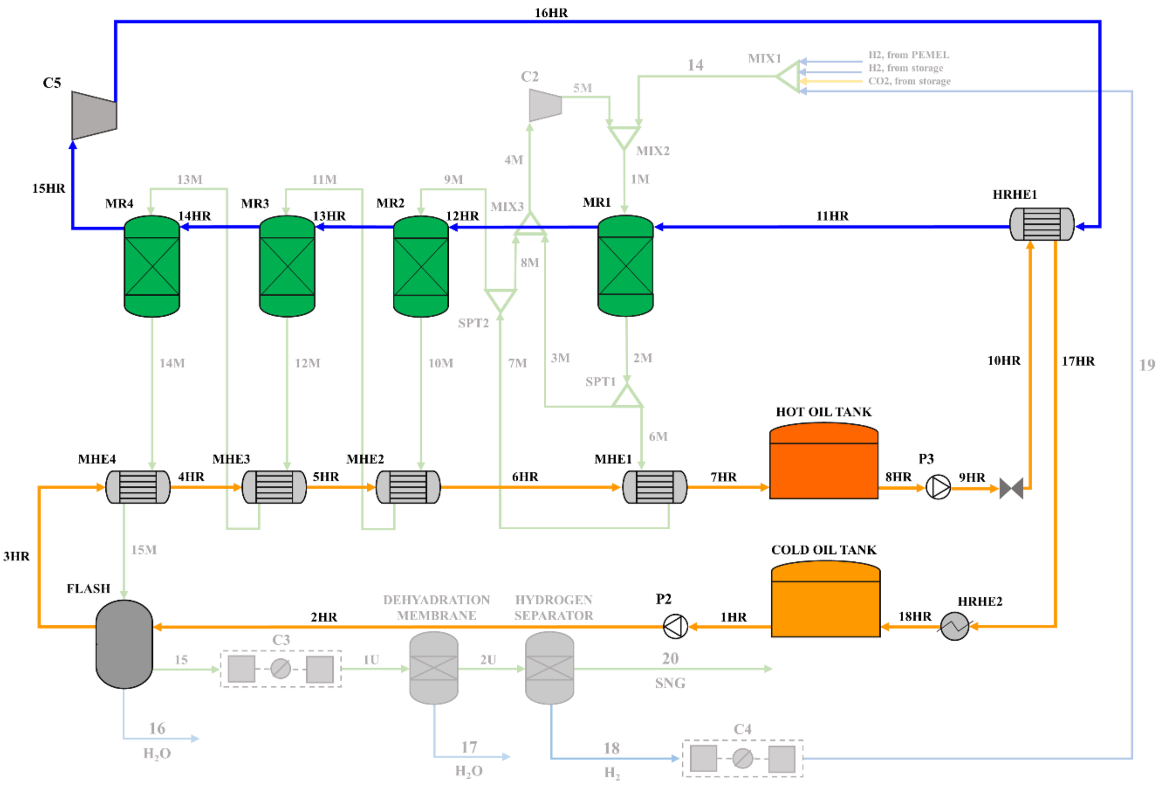

Figure 58. Schematic diagram of thermal storage system

When the reactors need to be heated, the diathermic oil from the hot oil tank is sent to the heat recovery heat exchanger (HRHE1) for heating the hydrogen used as thermal carrier. The diathermic oil leaving the HRHE1 is cooled down in the HRHE2 to the storage temperature of the cold oil tank. This cooling heat can be further recovered for external or internal use. The thermal power transferred by the hot hydrogen allows to compensate for the thermal losses in all the reactors and to keep the temperature of the catalysts within the activation range. The cold H_2 (15HR) is recovered downstream the last reactor MR4 to be recirculated again.

4.2.3.2. Electrical storage

In the electrical storage system, the waste heat is recovered by means of a two-tanks diathermic oil circuit (they are conceived as buffer tanks) and the stored thermal energy is used to generate electricity via an ORC. The oil tanks allow to ensure continuous and stable operation of the ORC by decoupling the heat storage (which depends on the methanation unit operation) from the electricity production. The produced electricity, stored in batteries, is supplied, when required, to the electrical trace heating system of the methanation unit and used for ancillary equipment. Figure 59 depicts the electrical storage configuration.

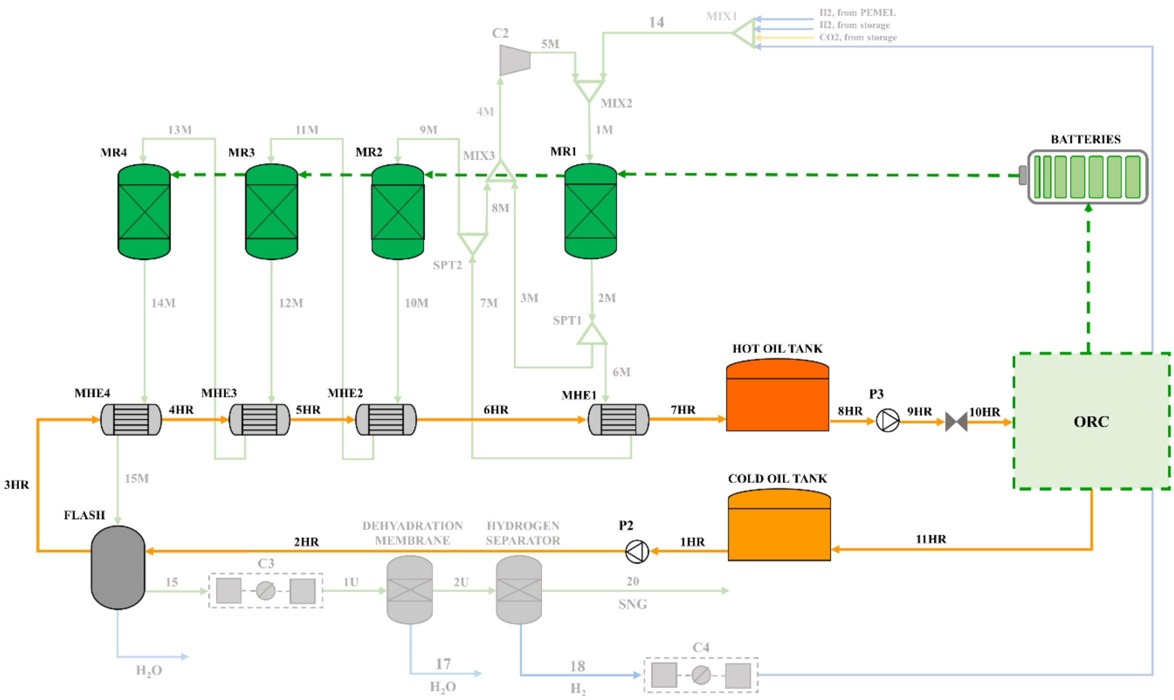

Figure 59. Schematic diagram of electrical storage system

The diathermic oil circuit works as described in the thermal storage configuration. When the hot oil tank is full, the diathermic oil (stream 8HR) is sent to the ORC unit for supplying the thermal power required by the ORC cycle. The returning cold oil (stream 11HR) is then stored in the cold oil tank.

With referring to the ORC power unit, by taking into account the heat sources temperatures as well as additional features (low toxicity, low global warming potential and ozone depletion potential, good compatibility and chemical stability in operation with other materials, etc.), the iso-butane (R600a) is selected as working fluid. In Figure 60, the functional scheme of the ORC power unit is shown.

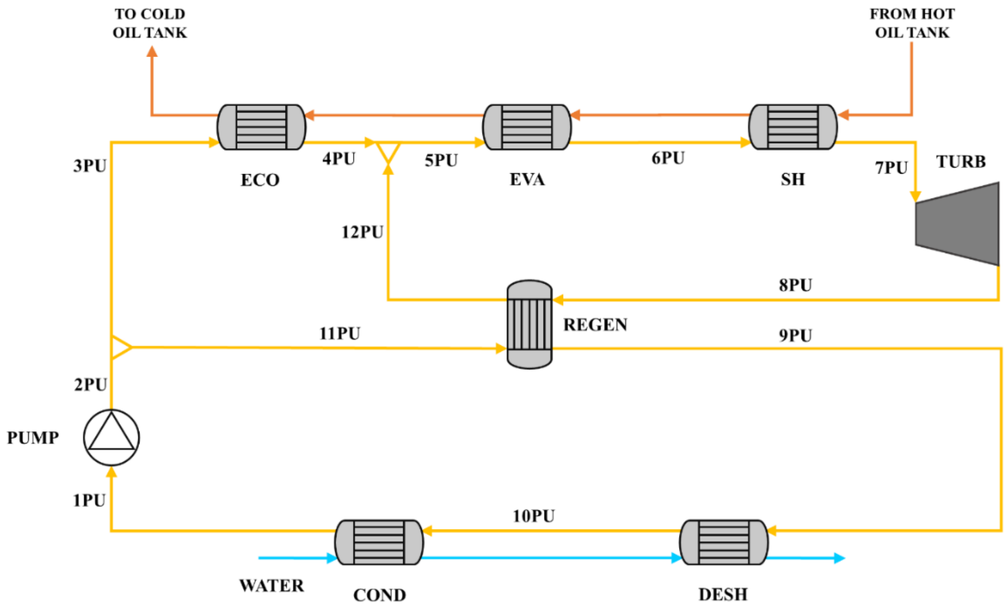

Figure 60. Functional scheme of the ORC

The organic fluid (stream 1PU, in Power Unit) leaving the condenser (COND) is pressurised up to the maximum pressure of the cycle (2PU). In order to optimise the use of the heat from the thermal storage and the heat internally available, it is split in two streams 3PU and 11PU. The first one (3PU) is sent to the economiser (ECO) where it is pre-heated up to the saturation condition (4PU) by the diathermic oil, while the second one is pre-heated (12PU) in the regenerator (REGEN) by the stream 8PU that exits the scroll expander, that is still in superheated condition (the iso-butane is a dry fluid). The streams 4PU and 12PU are mixed and the resulting is vaporised and superheated up to the turbine inlet temperature by the diathermic oil. The superheated vapour (7PU) expands in the scroll expander (TURB) down to the condenser pressure. The desuperheating of the iso-butane (9PU) is completed in the desuperheater heat exchanger (DESH) where it is cooled down to its dew-point temperature (10PU) and finally condensed in the condenser (COND).

4.2.4. Heat recovery system sizing criteria

Both the proposed heat recovery configurations are sized for assuring the thermal energy needed to maintain the hot-standby conditions of the methanation unit and the thermal energy needed for the cold restart.

The sizing procedure of the heat recovery systems is performed through the evaluation of: i) the thermal energy that can be recovered from the methanation unit (QMHE1, QMHE2, QMHE3, QMHE4) and the flash unit (QMHE5) and the temperatures at which they are available; ii) the thermal energy required by the methanation unit in the hot-standby status and that required for the restart after a cold-standby; iii) the optimal combination between the number of hot-standby hours and that of cold-standby. The thermal energy recoverable from the methanation unit and the flash unit as well as the temperatures at which it is available is assessed by the mass and energy balance of the plant. The thermal energy needed to maintain the hot-standby status (i.e., to maintain the reactors at the catalysts activation temperature) as well as that needed to warmup the reactors after a cold-standby (the thermal energy consumption to warm-up the reactors from ambient temperature to the catalysts activation temperature) has been calculated by considering convective and conductive heat transfer mechanisms. The standby hours are calculated by applying the dynamic model. The number hours of hot standby and, as a consequence, that of cold-standby, is evaluated by assuming the minimum capacity of the storage devices (the diathermic oil tanks for the thermal energy storage and the batteries for the electric energy storage) able to satisfy the energy requirements and, at the same time, to make economically feasible the plant. Thus, in order to identify the optimum combination between hot and cold standby hours a statistical analysis on the plant standby hours distribution is carried out in terms of average duration and frequency. It is worth noting that this analysis is site-specific and closely linked to the typical annual wind energy profile of the considered plant, therefore tailor-made considerations would be required for other plants.

4.2.5. Performance parameters

The PtSNG plant nominal efficiency is defined as the ratio between the useful output powers (i.e., the chemical power of the SNG) and the input powers. The input powers for the PtSNG plant are represented by the electric power consumption for electrolyser and the ancillary equipment, namely the hydrogen compressor for hydrogen storage, the blowers for the methanation unit and the raw SNG compressor and the hydrogen compressor for the upgrading unit. The efficiencies are calculated taking into account both the lower heating value (LHV) and the higher heating value (HHV) for the calculation of the chemical powers.

The nominal overall efficiency of the PtSNG plant is calculated using the following equation:

$$\eta_{PtSNG} = \frac{\Phi_{SNG}}{P_{el,RES} + P_{el,H2} + P_{el,MU} + P_{el,UU}} \tag{4.4}$$

In the above equation, Φ_{SNG} is the chemical power of the generated SNG, $P_{el,RES}$ is the wind power supply to the electrolysis unit in alternate current (AC), $P_{el,H2}$ is the power consumption of the hydrogen compressor for the H_2 storage, $P_{el,MU}$ is the electric power consumption of recirculation blower in the methanation unit, $P_{el,UU}$ is the power consumption of the upgrading unit, that includes the power consumption of the SNG compressor and that of the hydrogen compressor downstream the hydrogen membrane separation. The thermal power available from the methanation unit heat exchangers is not accounted in this calculation.

Because of the fluctuating behaviour of the input energy source, the nominal efficiencies are not sufficient to evaluate the effectiveness of the plant, but it is necessary to evaluate the annual performance [279]. This is defined as the ratio of the usable system energy output to the overall system energy input (electricity and possibly heat) [279,286]. Therefore, the overall annual efficiency of the PtSNG plant is calculated as the nominal efficiency, by replacing the power with the energy (electric or chemical) consumed or generated in one year of operation. However, in this case, the thermal energy required to maintain the plant equipment in hot-standby during the no production hours, as well as that required to restart the reactors after a cold-standby, should be added as energy input:

$$\varepsilon_{PtSNG} = \frac{E_{SNG} + E_{H2,storage}}{E_{el,RES} + E_{el,H2} + E_{el,MU} + E_{el,UU} + E_{th,MU,HS} + E_{th,MU,CS}} \tag{4.5}$$

where $E_{th,MU,HS}$ is the thermal energy required to maintain the methanation reactors in hot-standby during the no production hours, $E_{th,MU,CS}$ is the thermal energy required to warm up the reactors after a cold standby and $E_{H2,storage}$ is the chemical energy of the remaining hydrogen in the storage tank. For the purposes of calculating the efficiencies for the proposed configurations, having carried out the heat recovery necessary to make the plant self-sufficient from the point of view of the energy demands of the standby periods, the terms relating to the standby thermal requirements ($E_{th,MU,HS}$ and $E_{th,MU,CS}$) are considered null. Indeed, these energy requirements are satisfied by re-using internal energy.

4.2.6. Results and discussion

4.2.6.1. PtSNG mass and energy balance results

Table 21 summarises the main operating parameters of the PtSNG plant. The 1 MW_{DC} PEM electrolysis unit consists of three stacks with nominal operating conditions, in terms of current density and average cell voltage for each stack, equal to 2.99 A/cm^2 and 2.17 V, respectively.

Table 21. Operational data of the PtSNG plant.

Plant Sections and Components	
PEM Electrolysis Unit	
Nominal power (MW)	1
AC/DC rectifier efficiency (%)	95
Stacks number/Cells number per stack	3/50
Active cell area (cm^2)	1000
Cell pressure/temperature (bar/°C)	20/55
Water utilization factor, UF	0.45
Current density (A/cm^2) @Average cell voltage (V) at rated power	2.17
Auxiliaries (% of rated power)	2.8
H_2 Compressor (C1)	
Pressure ratio	2.25
Isentropic efficiency (%)	70
H_2 Storage Unit	
Maximum Storage pressure (bar)	45
Minimum Storage pressure (bar)	22
Storage temperature (°C)	30
Methanation Unit	
Pressure (bar)	10
H_2/CO_2 (mol/mol)	4
Recycle ratio to MR1	0.70
Recycle ratio from SPT1 to MIX3	0.30
Recycle ratio from SPT2 to MIX3	0.57
MR1 in/out temperature (°C)	300/585
MR2 in/out temperature (°C)	300/468
MR3 in/out temperature (°C)	350/409
MR4 in/out temperature (°C)	350/365
Recycle blower (C2) isentropic efficiency (%)	85
SNG Upgrading Unit	
Dehydration membrane efficiency (%)	90
H_2 separation membrane efficiency (%)	90
SNG compressor (C3) pressure ratio	1.75
H_2 recycle compressor (C4) pressure ratio	10
Isentropic efficiency (%)	85

The power consumption of the unit auxiliaries is set to 2.8% of the rated power. At nominal conditions, the hydrogen generated is equal to 16.8 kg/h with a specific energy consumption of 59.6 kWh/kg of the produced hydrogen. To contain the hydrogen storage tank capacity, the methanation unit is sized for processing the maximum hydrogen flow generated by the electrolysis unit. With this assumption the decoupling between the dynamics of the electrolysis unit and that of the methanation unit is less effective, but the plant capital costs (based on the storage pressure of 50 bar, the cost is estimated 375 €/kg [282]) are reduced. Furthermore, the hydrogen storage unit is sized to assure the full load operation of the methanation unit for about 6.5 h.

In Table 22 the mass and energy balances under nominal conditions are reported. The composition of the produced SNG is 92.5% mol CH_4, 2.2% mol H_2, 5.3% mol CO_2, and traces of H_2O, and its lower heating value (LHV) is 43.4 MJ/kg, whereas the calculated Wobbe Index is 43.9 MJ/Nm^3.

Table 22. Mass and energy balances under nominal conditions

PtSNG plant capacity (Electrical power input) (MW_{DC})	1 MW
Wind Energy supply (kW_{AC})	1051
Plant Sections and Components	
Water Pump (P1)	
Water pump power consumption (kW)	0.11
PEM Electrolysis Unit	
Number of power modules	1
H_2O consumption (kg/h)	150.3
H_2 production (kg/h)	16.8
Thermal power consumption (kW)	5.96
Electric power consumption (kW_{DC})	998.9
H_2 Compressor (C1)	
Compressor power consumption (kW)	7.74
H_2 Storage Unit	
Storage capacity (kg of H_2)	110
Storage volume (m^3) at 30 °C	30
Methanation Unit	
Carbon dioxide mass flow (kg/h)	96.8
H_2 mass flow (kg/h)	17.74
H_2 recycle mass flow (kg/h)	0.912
Recycle blower (C2) power consumption (kW)	0.34
Raw SNG composition (mol %)	76.7 CH_4, 18.5 H_2, 4.4 CO_2, 0.3 H_2O
SNG upgrading	
SNG compressor (C3) power consumption (kW)	3.05
H_2 recycle compressor (C4) power consumption (kW)	1.08
Plant Performances	
SNG production (kg/h)	38.52
SNG composition (mol %)	92.5 CH_4, 2.2 H_2, 5.3 CO_2, traces H_2O
SNG LHV/HHV basis (MJ/kg)	43.4/48.2
SNG LHV/HHV (MJ/Nm^3)	30.5/33.9
SNG Plant nominal efficiency, LHV/HHV basis (%)	43.9/48.8

This value fill with the quality foreseen by the ongoing work on European standardisation of power-to-hydrogen applications, for which most of the European natural gas infrastructure can withstand a volume concentration 10% of hydrogen. The SNG production is equal to 38.52 kg/h while the maximum amount of the stored hydrogen is 110 kg. By considering the storage conditions (45 bar and 30 °C), the tank capacity is 30 m^3. The PtSNG plant efficiency on LHV basis is 43.9%.

Table 23 reports the thermal powers recoverable from the methanation unit and the flash unit as well as the range of temperature at which they are available. It is worth nothing that, due to the water condensation, a large amount of heat is available in the flash unit, albeit at a low temperature. In heat exchanger MHE4, the thermal energy is available at relatively low temperature levels compared to the other ones (the temperature level increases towards the MHE1).

Table 23. Thermal powers available from the methanation unit and SNG inlet and outlet temperatures in the heat exchangers

	MHE1	**MHE2**	**MHE3**	**MHE4**	**FLASH**
Q (kW)	58.1	9.9	4.8	15.8	59.1
T_{in} (°C)	585	468	409	365	158
T_{out} (°C)	300	350	350	158	25

Thus, considering these temperature levels, the commercial Therminol-VP1, a diathermic oil capable of operating at high temperatures (up to 400 °C), has been chosen as heat transfer fluid for both the proposed heat recovery systems. The oil is kept at a pressure of 10 bar to allow its operation at high temperatures while preventing the formation of vapours. Finally, the plant operation time is listed in Table 24.

Table 24. Annual operation time of the 1 MW PtSNG plant.

Operation time (hours)	6047
Full load (hours)	2500
Partial load (hours)	3547
Standby (hours)	2255
Transient (hours)	458

4.2.6.2. Thermal energy requirement

The reactors are multitube type and are insulated by means of a microporous material with reinforcing filaments in pyrogenic silica (Steelflex-1100®) with a thermal conductivity at 300 °C of about 0.035 W/m·K and a thickness of 2 cm. Table 25 reports the thermal energy requirement (kWh/h) during the hot-standby and the thermal energy (kWh) required to restart the reactors after the cold-standby. The thermal energy required during the hot standby have been calculated by assuming for each reactor a minimum working temperature of 250 °C (the minimum temperature for catalysts activation), while the thermal energy required to warm up the reactors after a cold standby, up to the catalysts' activation temperature, has been calculated by assuming 20 °C as reference ambient temperature

Table 25. Thermal energy requirements of the methanation unit

	MHE1	MHE2	MHE3	MHE4	Total
Hot-standby (kWh/h)	1.01	0.74	0.74	0.56	3.06
Cold-standby (kWh)	7.78	4.60	3.18	1.94	17.79

By comparing the total energy requirement of the two standby options due to reactors' characteristics, it can be noted that if no heat recovery system is coupled to the plant the hot standby is cheaper than cold-standby if its duration is less than 6 consecutive hours. In this case the energy consumption would be covered by energy coming from outside the plant, representing a cost. Furthermore, hot standby is preferable to avoid thermal stress and for reasons of flexibility, i.e. for restarting SNG production as soon as conditions return favourable [287]. Moreover, it is clear that the amount of energy that has to be stored in the storage devices (the oil tanks in the case of the thermal storage configuration and the batteries in the case of electrical storage configuration) depends on the number of hot-standby hours, being fixed the thermal energy (17.79 kWh) required to restart the methanation unit from the cold standby.

Thus, in order to in order to identify the optimum combination between hot and cold standby hours when the plant is coupled with energy recovery systems, a statistical analysis on the plant standby hours distribution is carried out in terms of average duration and frequency. It is worth noting that this analysis is site-specific and closely linked to the typical annual wind energy profile of the considered RES facility, therefore tailor-made considerations would be required for other plants. Figure 61 shows the distribution of the standby periods in terms of duration and frequency in the year.

It can be noted that most of the standby periods have a duration less than 20 hours and few occurrences have longer standby durations (the maximum is 62 hours). By designing the energy storage in an appropriate way, it is possible to extend the hot-standby duration without requiring any additional external energy.

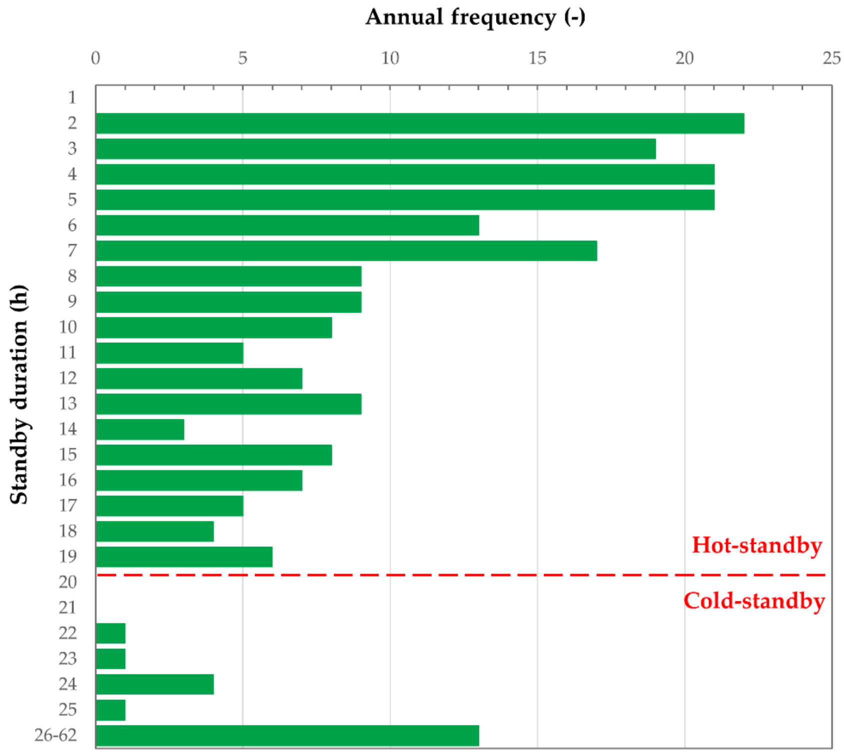

Figure 61. Results of the statistical analysis and distribution of the standby periods

Although extending the hot standby for a greater number of hours results in a higher energy consumption, in this case the latter is covered with recovered waste energy, therefore it does not represent an operational cost. Thus, the duration of the standby periods and their frequency allow to identify a threshold value for the maximum desirable duration of the hot-standby also useful for the storage sizing. Beyond this threshold value, the control strategy switches the operation mode of the methanation unit to cold-standby. In this case, when the plant is coupled with heat recovery systems, the selected threshold value is 19 h, as reported in Table 26 that summarises the results of the statistical analysis.

Table 26. Results of the statistical analysis and distribution of the standby periods

Total number of methanation unit standby hours (h)	2255
Longest standby (h)	62
Total number of standby periods	213
Average annual standby duration (h)	10.6
Threshold value (h)	19
Number of hot-standby	193
Total hours of hot-standby (h)	1521
Number of cold-standby	20
Total hours of cold-standby (h)	734

Finally, according to the data reported in Table 25, the total energy that has to be stored in the storage devices is equal to 75.9 kWh (58.1 kWh to cover the energy consumption of the 19 hour hot-standby and 17.8 kWh, to cover the energy consumption related to the restart from the cold-standby).

4.2.6.3. Thermal storage results

Results of the thermal storage model showed that the hydrogen flow rate needed to maintain the temperature of the methanation reactors at least at the minimum catalysts activation temperature (250 °C) is equal to 6.5 kg/h and its temperature at the inlet of the first reactor (MR1) is equal to 367 °C. The temperature of the hydrogen exiting the last reactor (MR4) is 250 °C (stream 15HR in Figure 58). Then, in order to ensure the cyclic operation, the hydrogen is re-heated by the diathermic oil from the hot oil tank (in the heat exchanger HRHE1) up to 367 °C. With referring to the two tanks oil circuit, the hot oil flow (8HR) is equal to 31.5 kg/h and it is stored at 387 °C. Because the diathermic oil leaves the HRHE1 heat exchanger at 281 °C, it has to be cooled down to the storage temperature of the cold oil tank (30 °C). This cooling heat (from the HRHE2) can be further recovered for external or internal use. The mass of diathermic oil necessary to store the required thermal energy (75.9 kWh) is equal to 1067.3 kg (the specific heat is 2.416 kJ/kg·K) and the hot oil tank volume results in 1.50 m^3 (the density at 387 °C is 713.2 kg/m^3).

4.2.6.4. Electrical storage results

The ORC operating parameters have been chosen in order to maximise the waste heat recovery and the ORC efficiency. These constraints are conflicting. In fact, to maximise the waste heat recovery, a high flow rate of diathermic oil is required due to the large amount of heat available from the flash unit, while a high turbine inlet temperature, necessary to obtain a high ORC efficiency, cannot be reached due to the temperature of the hot oil which decreases as its flow rate increases. Therefore, a compromise has been found by assuming the oil flow rate equal to 827 kg/h. The temperature of the hot oil exiting the last heat exchanger is about 300 °C. Figure 62 shows the energy balance of the oil circuit. The total amount of waste heat recovered and supplied to the ORC is therefore equal to 145.2 kW, out of a total of 148 kW that were recoverable from the methanation unit.

With respect to the operating parameters of the ORC cycle, the minimum and maximum pressures and the inlet turbine temperature are set to 3 bar, 30 bar and 183 °C, respectively.

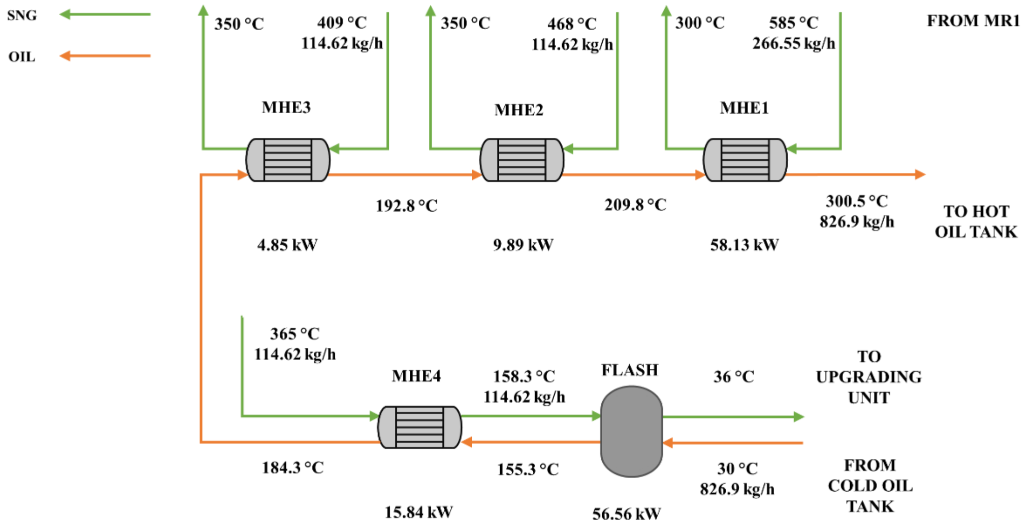

Figure 62. Diathermic oil circuit for waste heat recovery from the methanation unit, sized for coupling with the ORC power unit

Table 27 summarises the main operating conditions and performance of the ORC unit. Results details concerning streams' temperatures, pressures and flow rates are also given in Figure 63.

Table 27. Operating conditions and performance of the ORC unit

ORC Operating parameter	
Isobutane flow rate (kg/h)	1200
Condenser pressure (bar)	3
Pressure ratio	10
Turbine inlet temperature (°C)	183
Split to ECO (kg/h)	499.6
Pump efficiency	0.70
Scroll expander efficiency	0.65
ORC Performance	
Compression power (kW)	2.47
Expansion power (kW)	26.57
Net mechanical power (kW)	24.1
Provided heat power (kW)	145.2
Overall ORC efficiency (%)	16.6

Regarding the sizing of the oil tanks necessary to decouple the heat recovery from the electricity generation allowing more continuous operation of the ORC, the thermal energy stored is 435.6 kWh (3 h of operation in full load). Therefore 2481 kg of diathermic oil are stored at 300 °C. Since the diathermic oil density at 300 °C is 817 kg/m^3, the volume of the hot oil tank results equal to about 3 m^3. Referring to the batteries sizing, by assuming the electrical efficiency equal to 0.95, the battery is designed for a capacity of 80 kWh. When the methanation unit is in operation and the ORC produces electrical energy, part of this is used for plant auxiliaries (12.3 kWh at full load operation for 1h) so that the electrical energy useful to charge the batteries is equal to 11.8 kWh, resulting in a battery charge time of around 6.8 hours.

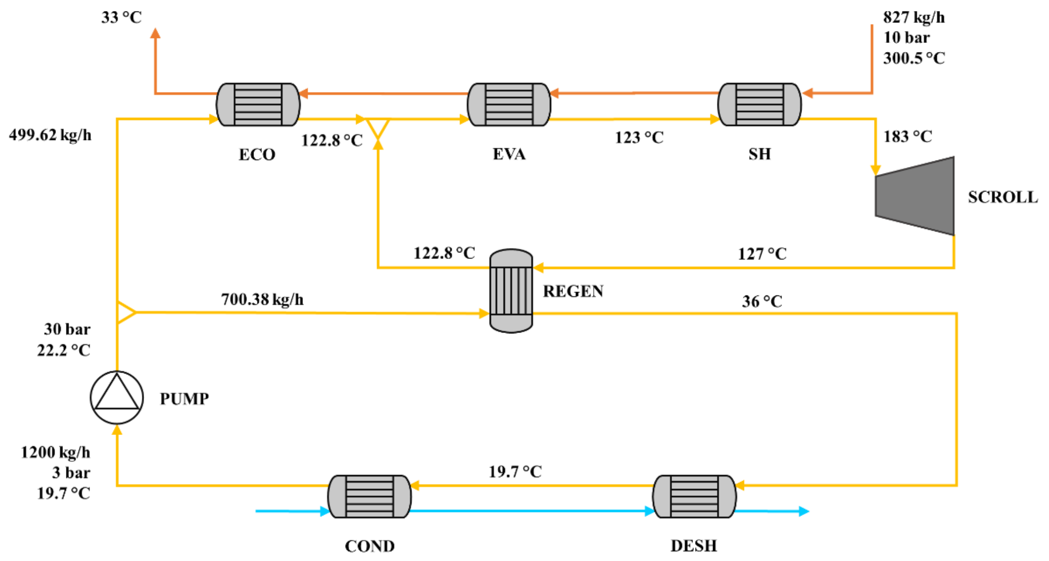

Figure 63. Results for the ORC power unit

4.2.6.5. Annual performances results

Table 28 reports the annual energy balance as well as the annual performances of the PtSNG plant. The annual water, hydrogen and carbon dioxide consumptions are equal to 790 Nm^3, 999,000 Nm^3 and 261,286 Nm^3, respectively. The SNG production is equal to 265,287 Nm^3.

Table 28. Annual mass and energy balance and annual performances

PtSNG plant capacity (electrical power input DC)	1 MW	
Energy (MWh/year)		
Annual electric energy consumption of the electrolysis unit (AC/DC)	5483/5209	
Annual electric energy consumption for compressors and auxiliaries	29.8	
Annual energy consumption for hot-standby	4.7	
Annual energy consumption for cold-standby	0.36	
Annual SNG chemical energy (LHV basis)	2424	
Chemical energy of the remaining hydrogen* (LHV basis)	3.6	
Plant Performances		
Waste Heat recovery configuration	***Thermal storage***	***Electrical storage***
PtSNG Plant annual efficiency, LHV basis (%)	44.0	44.3
PtSNG Plant annual efficiency, HHV basis (%)	48.9	49.2

*The remaining hydrogen in the storage tank is the difference between the annual hydrogen production and the annual hydrogen consumption

From the data in the Table 28 it can be noted that the energy consumption for hot and cold standby states (5.06 MWh/year in total) is only a small percentage (0.09%) of the total energy required to operate the plant (electric energy in AC for the electrolyser and that for ancillary equipment). As regards the annual efficiencies, the PtSNG plant in the base case, without any heat recovery systems, shows efficiencies of 43.9% on an LHV basis and 48.8% on an HHV basis. The results for the thermal storage and electrical storage configurations show that the energy recovery intended to satisfy internal consumption only is beneficial for a PtSNG plant, albeit slightly. Compared to the base case (in which no energy recovery is carried out), the increase in the annual efficiency was proportional to the annual energy savings achieved by the two proposed systems, equal to 5.06 MWh/year and 34.86 MWh/year for the thermal storage and the electrical storage respectively. In the base case, it would be reasonable to expect a decrease in the annual efficiency with respect to the nominal efficiency, due to shutdowns and to the fluctuating plant behaviour. However, the annual efficiency remains close to the nominal efficiency values in the case in which waste energy is recovered for internal uses. Moreover, the electrical storage configuration shows a slightly higher annual efficiency with respect to the thermal storage configuration because in the first case, the ancillary equipment power consumption is also satisfied by waste energy recovered. If the surplus electricity produced by the ORC were also valued or sold externally, slightly higher annual efficiencies could be achieved. A rough discussion on costs is also tried to be given. In principle, the proposed energy recovery systems should present very low operating expenditures, linked mainly to their maintenance as they are operated with waste energy, while the capital costs should be carefully evaluated. This will be the subject of future investigation in greater detail. Capital expenditures are expected to be low in the case of thermal storage (purchase of diathermic oil tanks and heat transfer fluid), and higher in the case of electrical storage (higher volumes of diathermic oil, ORC and batteries). However, electrical storage could lead to greater annual savings, avoiding the expense of electricity to be supplied to ancillary equipment, and providing a faster return on investment. In reality, considering the heat recovery only to satisfy the internal demands of the plant is probably not convenient, but it can become interesting if one considers the possibility of being able to sell all the recoverable waste energy, whether it is heat (for example for district heating) or electricity that can be sold to the grid. Meeting the internal energy demand of the plant with recovered waste energy could also lead to environmental benefits, where previously the additional external energy was provided by the electric grid (affected by the energy mix) or by natural gas. Finally, it is emphasised that in this work, the heat recovery systems have been designed only to ensure the self-sustain of the plant regarding the standby periods and ancillary equipment energy requirements. However, the plant internal energy consumption is significantly lower than the waste energy available from methanation process.

A remarkable further improvement of the PtSNG plant performance can be reached if this surplus is employed for external thermal or electrical utilities.

4.2.7. Conclusions

In this study, two heat recovery systems for a 1 MW (the DC wind power to the electrolysis unit) PtSNG plant coupled with a 12 MW wind farm have been presented. The common approach is based on the valorisation of the waste heat generated during the plant operation to self-sustain, from an energetic point of view, the standby conditions (hot-standby and cold-standby).

In the first one (Thermal storage configuration), the recovered thermal energy is used to satisfy the thermal energy demand of the reactors during the standby periods by means of a thermal carrier (hydrogen).

In the second one (Electrical storage configuration), the stored thermal energy is used to produce electricity by means of an Organic Rankine Cycle (ORC) where iso-butane is used as working fluid. This electrical energy is then stored in batteries and it is used to meet the energy requirements of the electrical trace heating system of the methanation unit during the standby periods.

The analysis has been performed by means of thermochemical and electrochemical model developed in Aspen Plus environment to define the mass and energy balances in steady state conditions and integrated with a dynamic model built (by the co-authors) in Matlab language to forecast the plant operation time and the annual performance. The main constraint for the thermal recovery systems sizing is the minimisation of the storage devices (oil tanks for the thermal storage configuration or batteries for the electrical storage configuration) achieved by identifying the optimum combination between the hot and cold standby hours.

To this end, a statistical analysis on the plant standby hours distribution in terms of average duration and frequency and has been carried out. For the specific energy input profile, the maximum duration of the hot standby has been found equal to 19 h.

Results of the thermal storage configuration have shown that the hydrogen flow rate needed to maintain the methanation reactors at the minimum catalysts temperature (250 °C) is equal to 6.5 kg/h at 367 °C, while the hot oil flow rate required to heat the hydrogen is equal to 31.5 kg/h and it is stored at 387 °C.

Results on the electric storage configuration have shown that the electric power generated is equal to 24 kW and the ORC cycle efficiency is 16.6%. The battery is sized for a capacity of 80 kWh, guaranteeing 19 hours of hot standby and a cold restart by means of electrical trace heating. When the methanation unit is in operation and the ORC produces electrical energy, part of this is used for plant auxiliaries (12.3 kWh at full load operation for 1h) so that the electrical energy useful to charge the battery is equal to 11.8 kWh, resulting in a battery charge time of 6.8 hours.

The overall nominal efficiencies of the PtSNG plant obtained are equal to 43.9% and 48.8% on LHV and HHV basis, respectively. When heat recovery systems are coupled to the plant, the annual efficiencies on LHV basis have been found to be 44.0% and 44.3% for the thermal storage and electrical storage configurations, respectively. The results showed that the internal heat recovery system positively impacted on the annual efficiency. It is expected that this could lead to a decrease of the plant operational costs with an associated initial capital expenditure relatively low. Furthermore, the amount of waste heat recoverable from the methanation unit resulted significantly higher than the energy needed for the self-sustainment of the plant. Therefore, to achieve a considerable increase of the plant efficiency it is necessary to couple the plant with other thermal or electrical utilises (e.g., district heating, cogeneration of SNG and power, etc.). In the event that it is decided to carry out cogeneration of electricity to sell it to the grid, this could also be produced with more efficient systems than the ORC (e.g., steam turbine), but careful cost assessments are required both on initial investments and on possible revenues.

4.3. Production of substitute natural gas integrated with Allam cycle for power generation

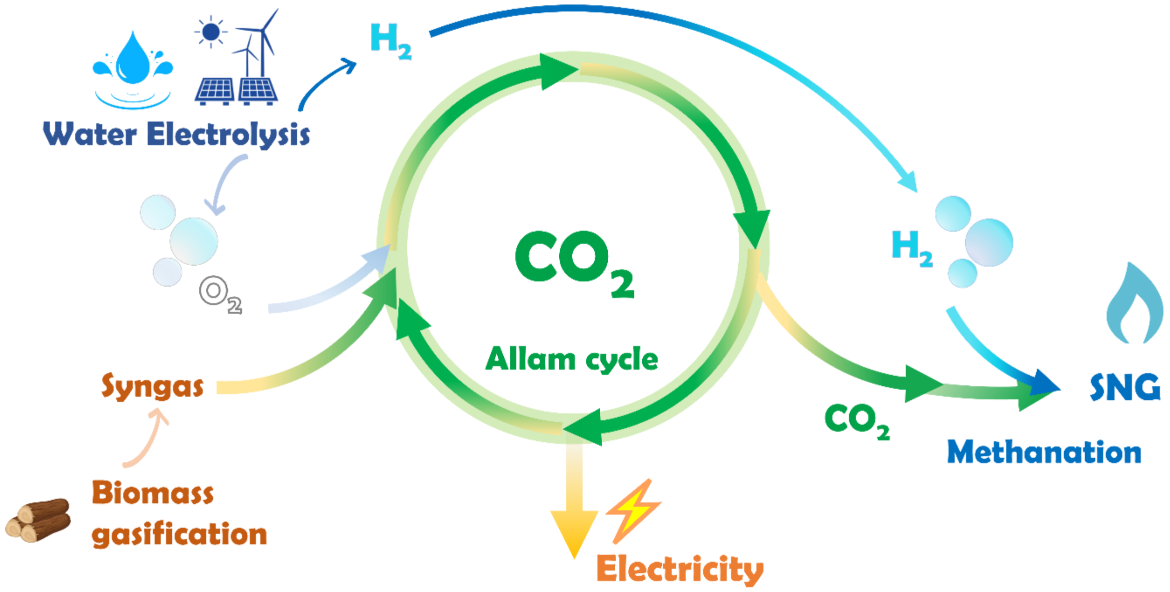

Figure 64. Conceptual scheme of the proposed system. Electricity and SNG are cogenerated starting from water, renewable electricity surplus and biomass

The accumulation of energy from non-programmable renewable sources is a crucial aspect for the energy transition. Using surplus electricity from renewable energy sources, power-to-gas plants allow to produce a substitute natural gas (SNG) that can be injected in the existing infrastructure for large-scale and long-term energy storage, contributing to gas grid decarbonisation. The plant layout, the method used for carbon dioxide capture and the possible cogeneration of electricity can increase the efficiency and convenience of SNG synthesis plants. In the work presented in *Publication 5*, a system for the simultaneous production of SNG and electricity starting from biomass and fluctuating electricity from renewables was proposed, using a plant based on the Allam thermodynamic cycle as the power unit. The Allam power cycle uses supercritical CO_2 as evolving fluid and is based on the oxycombustion of gaseous fuels, thus greatly simplifying CO_2 capture. In the proposed system, oxycombustion is performed using biomass syngas and electrolytic oxygen. The CO_2 generated by means of oxycombustion is captured, and it is subsequently used together with renewable hydrogen for the production of SNG through thermochemical methanation. The system is also coupled with a solid oxide electrolyser and a biomass gasifier. The whole plant was analysed from an energy-related point of view. The results show overall plant efficiency of 67.6% on an LHV basis (71.6% on an HHV basis) and the simultaneous production of significant amounts of electricity and of high-calorific-value SNG, whose composition could be compatible with the existing natural gas network.

4.3.1. Background and motivation

SNG is one of the most promising synthetic carbon-neutral fuels that can be produced starting from renewable energy source and a carbon source. Taking advantage of the capillarity and the extension of the natural gas distribution network, SNG – mainly consisting of methane – could be directly injected into the grid, representing a good solution in the short term and favouring the transition to pure hydrogen in the long term [47,277,288].

The production of SNG requires the availability of hydrogen and carbon, where the latter can be obtained from several sources. In power-to-fuel systems, therefore, the electrolysers for renewable hydrogen production are often coupled with carbon capture utilisation and storage (CCUS) systems. The latter usually make it possible to capture CO_2 that can be further used within a chemical reactor together with (renewable) hydrogen for subsequent conversion to fuels or chemicals. When it comes to synthetic fuels, the carbon source is essential to determining the environmental sustainability of the final product [289]. Fossil-based carbon dioxide can be captured in a concentrated form from industrial sources; however, cleaner fuel can be obtained when the carbon source is biomass or waste materials. Biomass can make its carbon content available in several ways, depending on the type of biomass and the process used to elaborate it. Through the gasification process, lignocellulosic biomass can be converted into an easily usable combustible gas (called syngas) mainly composed of hydrogen and carbon oxides. On the other hand, anaerobic digestion is suitable for humid biomass and produces biogas mainly composed of methane and carbon dioxide.

One of the main disadvantages of common CCUS systems lies in the great energy consumption required to separate and capture carbon dioxide from the rest of the gases and for sorbents regeneration. This is particularly true for CO_2 direct air capture, while capture from industrial sources is less energy intensive, as the energy consumption is related to the carbon dioxide concentration in the gas [290]. In order to obtain energy, environmental and possibly also economic convenience, it is, therefore, essential to investigate CO_2 capture processes that consume as little energy as possible. In this regard, the oxycombustion of a carbon-containing fuel is one of the methods that can greatly simplify the process of CO_2 separation and capture, as oxycombustion allows to obtain mainly carbon dioxide and water vapour as final products in exhaust gases, where water can be easily separated by condensation [291,292].

Oxycombustion can be also used for syngas obtained by means of biomass gasification, and the derived exhaust gas is almost exclusively composed of carbon dioxide and steam, with trace amounts of other substances. The same could apply to biogas produced by means of anaerobic digestion, almost exclusively composed of methane and carbon dioxide. Furthermore, at the same time, the oxycombustion of a fuel allows electricity to be produced with better programmability and continuity than renewable sources. Finally, in the case of a plant equipped with an electrolyser, oxycombustion allows the electrolytic oxygen produced to be valorised.

The study presented in *Publication 5*, therefore, proposed a system that cogenerates SNG and electricity starting from biomass and electricity surplus from RESs. This system is to be intended as an integrated energy storage system that allows to increase the flexibility and interconnection of the gas network and the electricity network. As a power-to-gas system, the proposed system can act as a bridge that connects the electricity grid and the gas grid. By accepting storable chemicals produced starting from excess electricity, the gas grid can act as a huge energy storage pool, helping to achieve electricity grid balancing and the match between electricity demand and production. The produced SNG can be injected into the gas grid, thus also enabling the seasonal or annual balancing of the overall energy system. Moreover, if the various reactants are stored in suitable tanks, electricity could be produced by the power plant in a more programmable and flexible way than electricity from variable RESs. The proposed integrated system, therefore, consists of: (i) an electrolyser powered by renewable electricity, (ii) a biomass processing system (lignocellulosic biomass gasification), (iii) a power unit based on oxycombustion that allows the production of electricity and simultaneous CO_2 sequestration to be achieved and (iv) a thermochemical methanation system for the production of SNG.

4.3.2. Definition of the proposed system

Figure 65 depicts a conceptual scheme of the proposed system. Electricity from RESs and water are fed to an electrolyser, which, thanks to an electrochemical reaction, splits water into hydrogen and oxygen. Biomass is sent to a gasifier together with a part of the oxygen produced by the electrolyser, since oxygen is used as a gasifying agent. In the gasifier, the solid biomass undergoes thermal degradation, which converts it into a gaseous fuel called syngas, which is mainly composed of carbon monoxide and hydrogen, with lower contents of other gaseous substances. Syngas coming from the biomass gasifier is fed to a power plant based on oxycombustion together with a part of the oxygen produced by the electrolyser. The power plant produces electric power and, at the same time, makes it possible to easily capture the carbon dioxide produced by means of oxycombustion. The carbon dioxide captured from the power plant is sent to a Sabatier process together with the hydrogen produced by the electrolyser. Here, carbon dioxide and hydrogen react together according to the methanation reactions to produce raw SNG mainly composed of methane and water. Finally, the raw SNG is upgraded by removing water via condensation, in order to obtain SNG with high calorific value. Overall, electric power surplus from variable RESs, water and biomass enter the system boundaries, while SNG and net electric power exit from the system. SNG and stable electric power can then be injected in their respective gas and electricity grids.

A system such as the one shown in Figure 65 has been analysed in previous articles by the co-authors, where a gas turbine, a steam-injected gas turbine, an internal combustion engine and a high-temperature fuel cell were considered as alternative power units [265,293,294]. The same systems have also been analysed in *Publication 2* from an environmental impact point of view to evaluate the sustainability of the SNG produced [295]. The goal of such a system is to co-generate electricity and a renewable fuel, starting from biomass and the surplus of electricity from renewable sources. The main novelty in this research work then, was that a plant based on the Allam thermodynamic cycle was considered as the power unit.

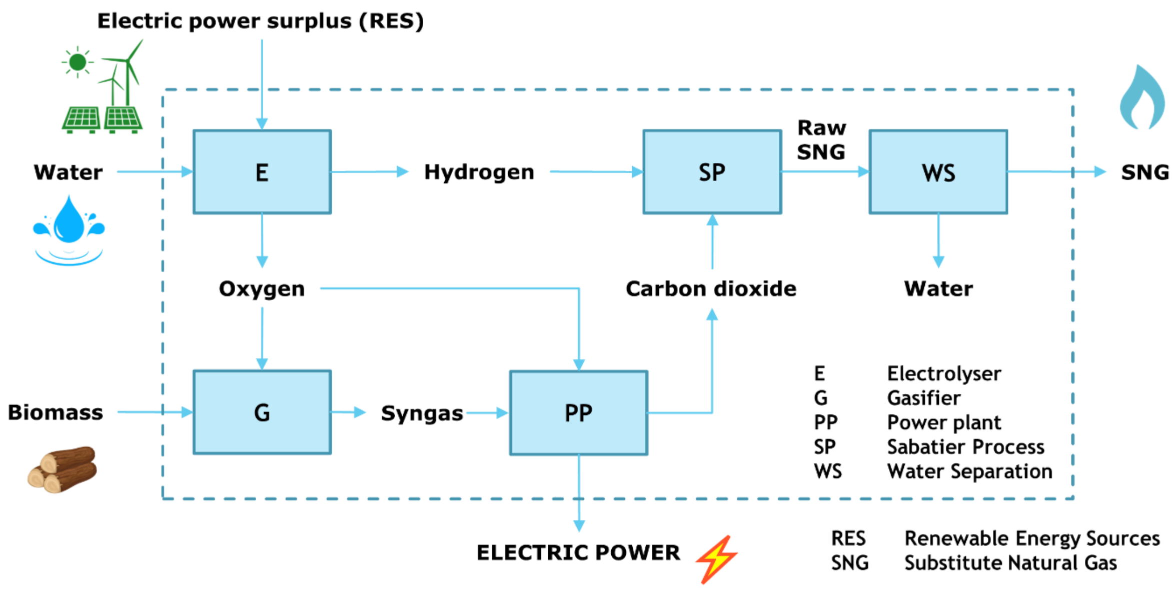

Figure 65. Simplified scheme of the proposed system

4.3.3. Allam cycle

The Allam cycle, also known as NET Power cycle, was first patented in 2011 [296] and subsequently updated by the same authors [297–301]. This innovative thermodynamic cycle is similar to a high-pressure Brayton cycle, but uses CO_2 under supercritical conditions as the main evolving fluid, and it is based on the oxycombustion of a gaseous fuel to obtain heat adduction within the fluid itself. The cycle was initially thought for the combustion of syngas obtained from coal gasification, and later, the use of natural gas was also considered [300]. However, it seems that only few literature studies have coupled the Allam cycle with a biomass gasifier or with an electrolyser for oxygen demand. The conventional Allam cycle is shown in Figure 66 and described below.

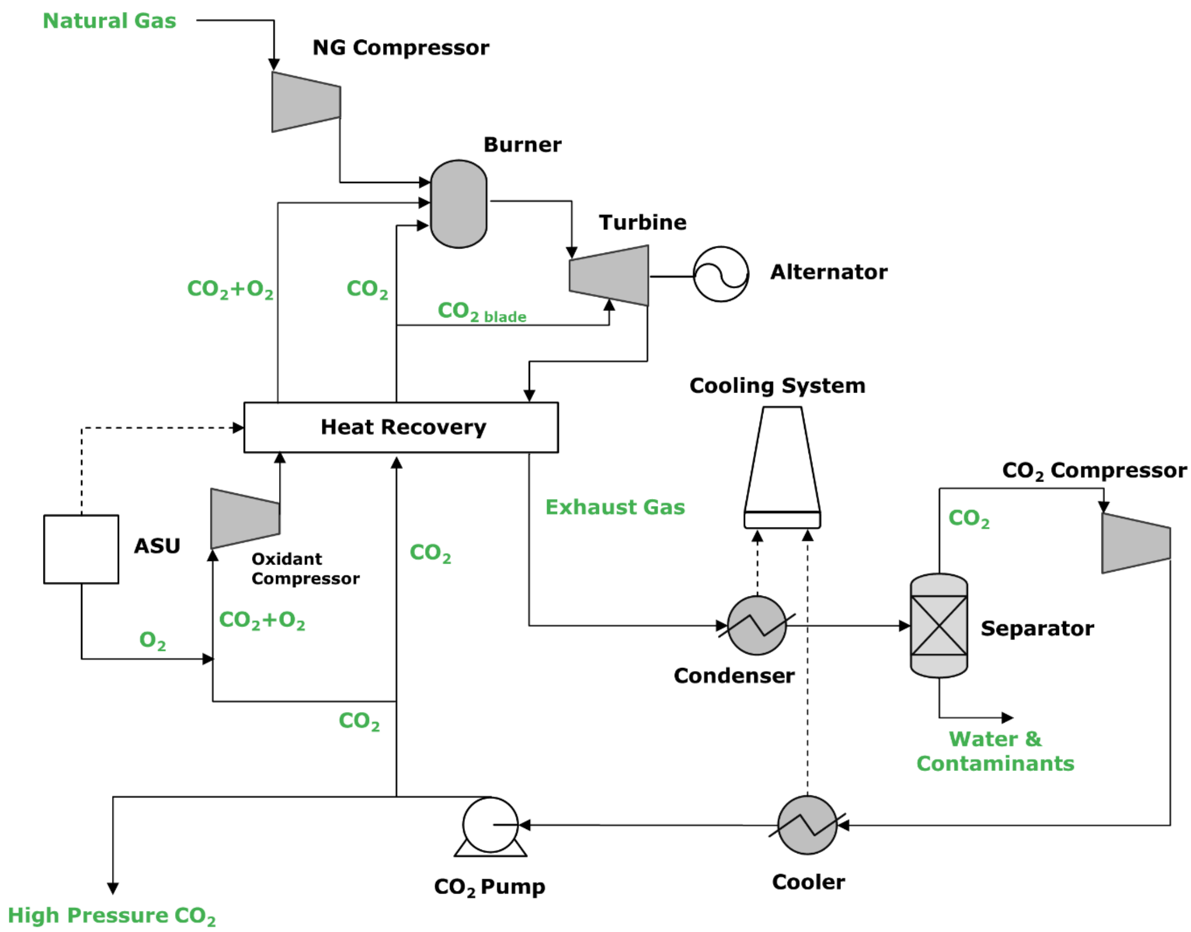

Figure 66. Conventional Allam cycle fuelled by natural gas

To provide the oxygen needed for oxycombustion, the starting point of the conventional cycle is the air separation unit (ASU), which supplies oxygen at 99.5% purity at a pressure of 120 bar. The pure oxygen, to be sent to the combustion chamber in an overstoichiometric amount of 3%, is at first mixed with a CO_2 stream recirculated from the end of the cycle, obtaining, overall, an oxidant mixture with a molar fraction of 13.34% O_2 [302,303]. This preliminary blending is useful to avoid corrosion problems of the metallic walls of the heat recuperator. This oxidant flow is compressed up to the highest pressure of the cycle and then preheated in a heat recovery unit up to 720 °C to be subsequently fed to the combustion chamber.

The fuel, methane or coal syngas in the conventional cycle [297] and the oxidant are fed in the combustion chamber at a pressure between 200 and 400 bar. A second CO_2 flow is sent to the combustion chamber with the double task of limiting the combustion temperature (to avoid material resistance problems) and obtaining a working fluid (exhaust gas) that is almost completely composed of CO_2, with small percentages of H_2O vapour derived from combustion and some traces of unburned O_2. The resulting temperature of the exhaust gases is about 1150-1200 °C, and it corresponds to the turbine inlet temperature.

The high-pressure gaseous stream leaving the combustion chamber expands in a turbine having an expansion ratio between 6 and 12. The exhaust gases at the turbine outlet, which are at a temperature of about 740 °C and a pressure of 34 bar [302], enter a multi-flow heat exchanger, where they transfer their energy content to various flows for energy recovery purposes. In particular, exhaust gases give part of their thermal energy to the CO_2 flow used as a combustion temperature moderator, to the oxidant flow composed of CO_2 and O_2, and to a third CO_2 flow used as a cooling fluid for the turbine blades. At the outlet of the heat exchanger, the exhaust gases are cooled down to room temperature, allowing the condensation and the extraction of water vapour to be achieved.

The residual gaseous flow, essentially composed of CO_2, is compressed and cooled in several stages, entering into supercritical state. Finally, it is sent to a multistage centrifugal pump, which again increases its pressure up to that of the combustion chamber.

To close the loop and ensure the mass balance of the CO_2 circulating in the system, it is necessary to extract from the cycle an amount of carbon dioxide equal to the net product derived from the combustion reaction between the fuel and oxygen previously added to the combustion chamber. Thus, as additional output besides electricity, a high-purity, compressed CO_2 flow, is obtained, ready for storage or industrial use. Obviously, CO_2 can be extracted before or after compression, depending on the intended use. The creators of the cycle have estimated that a natural gas-fired power plant with carbon capture based on this technology can achieve theoretical conversion efficiency (on an LHV basis) of around 58.9% (comparable with combined cycle power plants fuelled by natural gas and without CO_2 capture) or about 51.44% if the plant is fed with coal-derived syngas. A 50 MW plant based on the Allam cycle and fuelled by natural gas has already been built and successfully tested in Texas [299], while the construction of a new 300 MW plant is expected to start in 2023 and its full operation in 2026, together with similar announced projects in other locations or countries [299,304]. Since its presentation, the Allam cycle has become a subject of research for academics, who have focused on the thermodynamic analysis of the operating parameters [302,305–307], on new operating modes aimed at increasing plant efficiency [308,309] or on investigating the integration of a gasifier within the plant to use solid fuels rather than natural gas [310–312].

4.3.4. Description of the proposed cogeneration plant

As shown in Figure 67, four fundamental sections compose the proposed system:

- An electrolysis section;
- A gasification section;
- A power section;
- A methanation section.

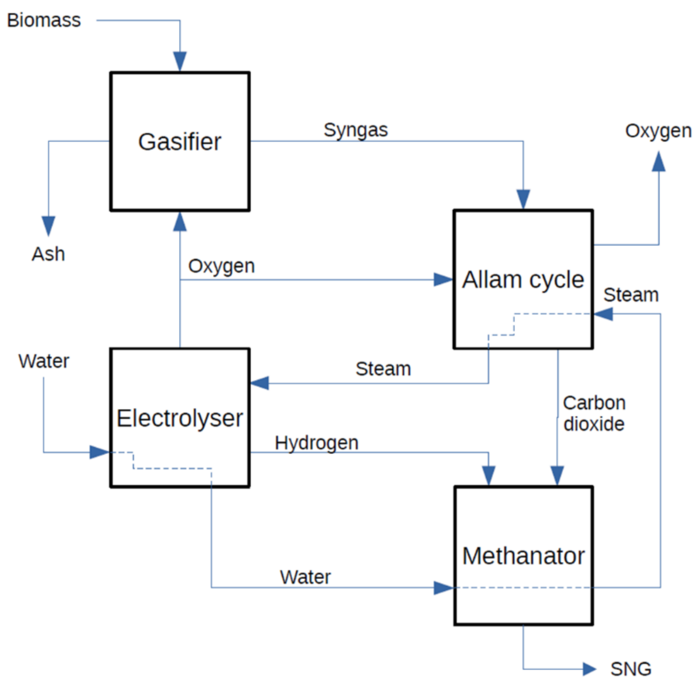

Figure 67. Scheme of the proposed cogeneration plant

The gasifier is a chemical reactor in which a solid fuel (biomass, in this case) undergoes thermal degradation (pyrolysis) and partial combustion so that it is transformed into a gaseous fuel known as syngas, mainly composed of carbon monoxide and hydrogen, with lower contents of other gaseous substances. The electrolyser is an electrochemical device capable of splitting water into hydrogen and oxygen using electricity. The methanator is a catalytic thermochemical reactor in which carbon dioxide, carbon monoxide and hydrogen can react together to produce methane and water.

Using the power surplus from RESs, a water stream is split into hydrogen and oxygen in the electrolysis section. Water electrolysis can be carried out either at low temperature or at high temperature. In this case, a solid oxide electrolyser (SOEC) working at an average temperature of 800 °C has been selected. The conversion ratio from electric power to hydrogen has been assumed equal to 85%, thanks to the fact that thermal power also contributes to the process. To reduce the compression work, the electrolysis process is carried out at 30 bar. The gases at the outlet of the cell are then cooled, transferring the high-temperature heat to the feed water.

The same pressure has also been adopted for the gasification section, which converts biomass into syngas. A lignocellulosic biomass with negligible quantities of sulphur or chlorine compounds has been selected (Table 29) in order to avoid the need for an acid gas removal unit; however, it is possible to include it in the layout when required. A part of the electrolytic oxygen is used as gasifying agent for the biomass, in order to obtain a syngas with high calorific value and, overall, with a minimum content of nitrogen (deriving from the biomass). The obtained syngas is cooled in a heat regenerator to reduce its temperature and condense its water content before compression. The highest operating pressure of the Allam cycle selected in this study is 305 bar, so that the syngas is compressed to such a pressure before entering the combustion chamber. In order to save energy, such compression is carried out using four intercooled compressors. Finally, syngas is sent back to the heat regenerator to increase its temperature.

Table 29. Composition and calorific values of the selected biomass [293]

Proximate Analysis (w%)		**Ultimate Analysis (w%)**	
Fixed carbon	14.89	C	50.4
Volatile matter	64.87	H	6.1
Moisture	20	N	0.1
Ash	0.24	O	43.1
		Ash	0.3
LHV		MJ/kg	12.480
HHV		MJ/kg	14.078

The power section receives syngas and a stoichiometric amount of oxygen and produces electricity and a flow essentially consisting of water and carbon dioxide, with a few traces of nitrogen, oxygen, carbon monoxide and hydrogen. These traces do not pose purity problems or separation needs, as the captured CO_2 flow is sent to the methanation unit. In the proposed system, syngas is burnt with a stoichiometric amount of oxygen inside the combustion chamber and not with an overstoichiometric amount, as in the original Allam cycle, thus achieving slightly less complete combustion. The stoichiometric oxygen amount was selected in order to obtain a very low oxygen content in the exhaust gas and thus in the captured CO_2 flow, since introducing a higher oxygen content in the methanator would lower the methane yield, while carbon monoxide deriving from incomplete combustion is converted into methane inside the methanator. Being the combustion between syngas and oxygen an oxycombustion, the temperature would be too high for usual materials; therefore, a recycled carbon dioxide stream that acts as a temperature moderator is fed to the combustion chamber. Another effect of this additional flow is to increase the total mass flow rate entering the turbine, thus increasing the mechanical power obtained. A second flow of recycled carbon dioxide is fed to the turbine through its blades in order to cool them. Overall, the gas is expanded in the turbine from the pressure of 305 bar down to 34 bar. The gas resulting from combustion is almost exclusively composed of carbon dioxide, and steam, which can be easily removed by means of cooling and condensation. The resulting gas after water separation is almost pure carbon dioxide and corresponds to the recycled flow plus that generated by means of syngas combustion. In a traditional Allam cycle, after expansion, this last amount could be extracted from the plant and vented into the atmosphere with no environmental impact when the carbon content comes from biomass. However, it could also be captured to obtain a negative carbon footprint; indeed, in the proposed plant, this CO_2 is captured and fed to the methanation section. After expansion, the recycled carbon dioxide flow needs to be recompressed to the Allam cycle higher operating pressure. In this case, the compression is carried out with six intercooled steps, i.e., three compressors and three pumps, since at a pressure higher than 73.8 bar, carbon dioxide becomes liquid or supercritical fluid, depending on the temperature. After compression, the recycled carbon dioxide stream is heated by the gas exiting from the turbine inside a recovery heat exchanger.

The last section, i.e., the methanation unit, receives carbon dioxide from the power section and hydrogen from the electrolysis section. It is based on the Sabatier reaction, and a TREMP layout has been adopted. It consists of a series, three in this case, of adiabatic reactors operating at 30 bar and at gradually reduced temperature. The first reactor receives the flows of carbon dioxide and hydrogen plus a flow recycled upstream of the second reactor. Such a flow has the goal to control the reaction temperature, which would become too high for catalysts in the absence of methane. The catalysts used by the TREMP process can work in the range of 250–700 °C. No recycling is required by the second and third reactors, since they receive a flow already containing a high percentage of methane. As the reaction is exothermic and the reactors are adiabatic, there is the need to reduce the gas temperature before sending the gas to the next reactor. Therefore, downstream of each reactor, a recovery heat exchanger has been introduced to transfer heat to the water fed to the electrolysis section. Finally, a condenser has also been included downstream of the third reactor with the task to dry the SNG.

4.3.5. Model

The proposed system was analysed by means of a simulation carried out using Aspen Plus software. The method used to calculate the properties of the species involved was that of Peng–Robinson [302,303]. First, an Aspen Plus model of the natural gas-fuelled conventional Allam cycle alone was validated against literature data [303]. This model was then slightly modified to consider biomass syngas, instead of natural gas, and electrolytic oxygen, instead of oxygen produced by an ASU, analysing the differences with respect to the conventional model. Finally, this Allam cycle model was integrated with the rest of the proposed plant.

All compressors and pumps were modelled with isentropic efficiency of 0.85 and mechanical efficiency of 0.98. All turbines were modelled with isentropic efficiency of 0.93 and mechanical efficiency of 0.98. The isentropic efficiency of the water pump in the electrolysis section was set to 0.7. No pressure drops were considered for the heat exchangers. All intercoolers were modelled with an exit temperature of 33 °C, with the only exception of the coolers in the Allam cycle before the CO_2 pumps, which were set to 31 °C. Figure 68 shows the model of the SOEC used in the proposed system.

The electrolyser was modelled as a stoichiometric reactor performing a 0.85 conversion of the water split reaction (CELL) followed by a separator (SEP). The electric power required for the electrolysis process (W-SOEC) was supplied to the electrolyser as a heat power input. Two flows at 30 bar and 825 °C exit from the separator: oxygen and a mix of hydrogen and residual steam. Both are cooled (O2-HEX and H2-HEX), transferring heat to the feed water, which also receives heat from the methanation (MET-HEX1 and MET-HEX2) and power (ALL-HEX) sections and becomes superheated steam at 775 °C before entering the cathode. The oxygen flow, cooled down to 33 °C, is split in two flows: the first one (O2-GAS) is fed to the biomass gasifier, whereas the second one (O2-ALL) enters the power section. The flow of hydrogen and residual steam (MIX-MET) is fed to the methanation section at 255 °C.

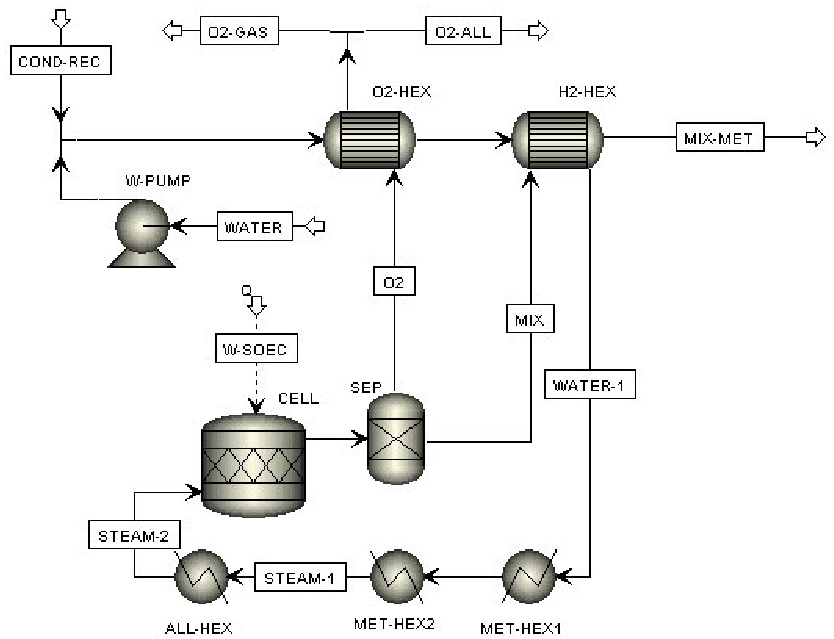

Figure 68. Model of the solid oxide electrolyser section

Figure 69 shows the model of the biomass gasifier section. An updraft gasifier was selected in such a way that biomass was directly dried by the syngas exiting from the gasifier. It was modelled as a couple of reactors and separators. The first reactor (DECOMP) is a Yield reactor with the task to decompose biomass in its elementary components plus humidity and ash, as shown in Table 29. This is followed by a separator (WAT-SEP) in which the syngas exiting the gasifier extracts the humidity. The second reactor (GASIF) is a Gibbs reactor fed by the dried flow coming from the separator and by part of the electrolytic oxygen coming from the electrolysis section, so that the biomass undergoes partial oxidation. In the Aspen Plus model, a heat stream connects DECOMP and GASIF in order to achieve an automatic heat balance that takes into account both the enthalpy of decomposition and that of gasification. The gasifier operates at 30 bar and about 800 °C. The syngas produced crosses a separator (ASH-SEP), which removes the ash and finally absorbs the humidity. The syngas needs to be compressed at 305 bar, which is the operating pressure of the Allam cycle. In order to minimise the power consumption, the syngas is first cooled inside a regenerative heat exchanger (R-HEX) down to 190.3 °C and finally in a condenser (GAS-COND), which makes it possible to separate the water. The dry syngas is then supplied to four intercooled compression stages and finally re-enters the regenerative heat exchanger in such a way to recover heat before leaving the gasifier section at 455 °C.

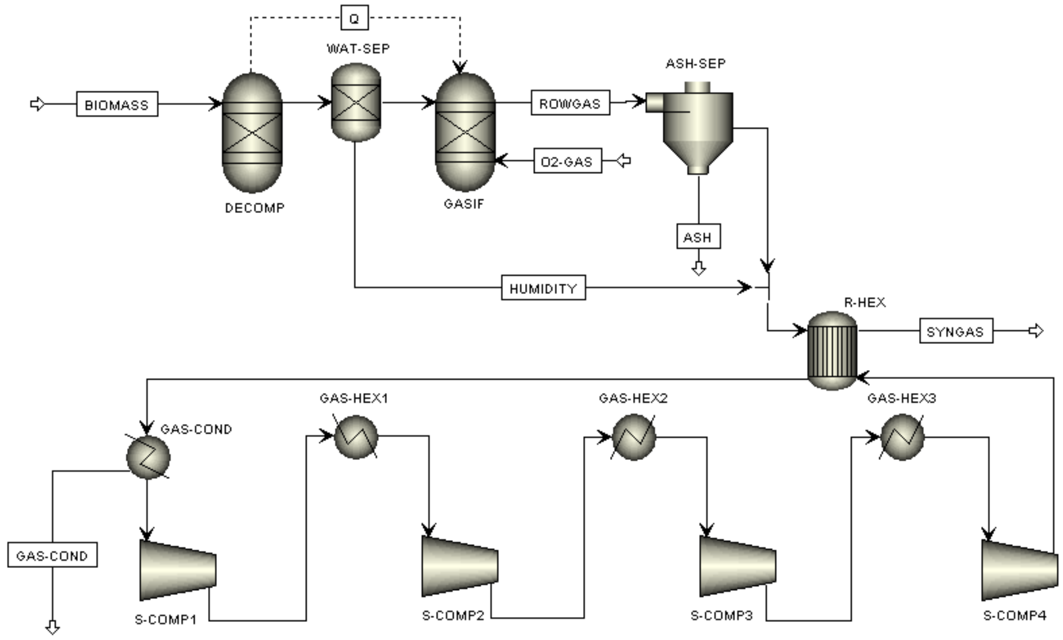

Figure 69. Model of the biomass gasifier section

The power section was modelled based on an Allam cycle plant (Figure 70), which makes it possible to obtain both mechanical power on the turbine axis for electricity production and an output flow consisting of high-purity carbon dioxide, suitable for being sent to the methanation section for the production of SNG.

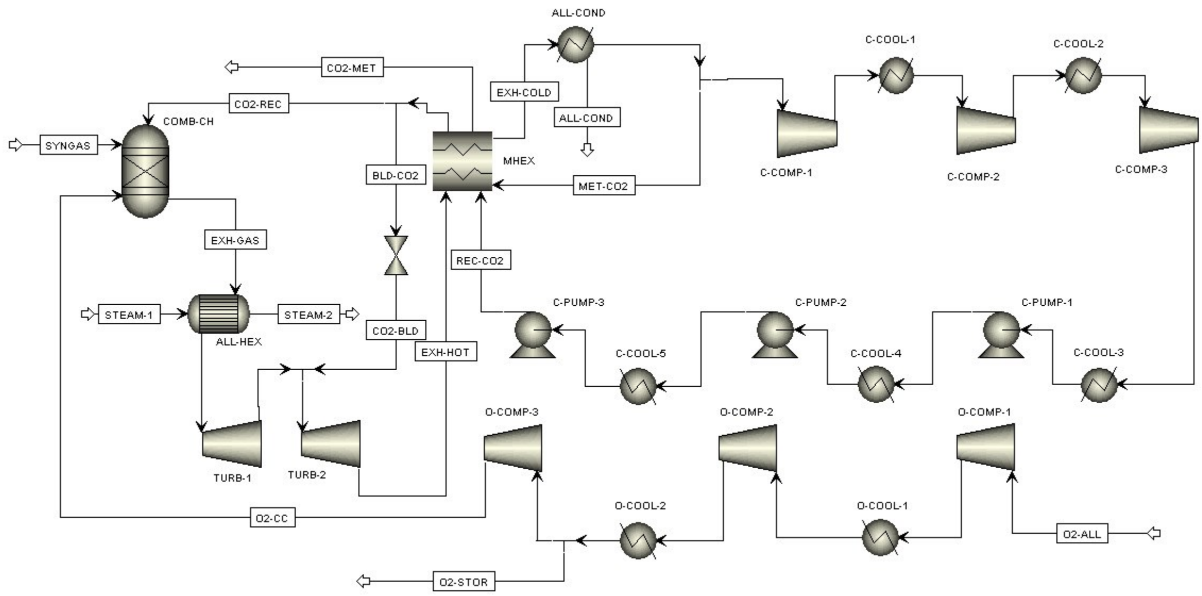

Figure 70. Model of the Allam cycle power section

The combustion chamber (COMB-CH) was modelled with a Gibbs reactor operating at 305 bar and fed with the syngas coming from the gasifier section (SYNGAS) and the oxygen coming from the electrolysis section (O2-CC). The latter needs to be compressed from 30 bar up to

305 bar, and this has been achieved using three intercooled compressors. A flow of oxygen (O2-STOR) exceeding the amount required by the syngas combustion is separated at 200 bar after the second intercooler; this might be accumulated to be sold, given its high purity.

The exhaust gas leaving the burner at 1213 °C is supplied to a heat exchanger (ALL-HEX) which receives from the methanation section steam at 582 °C (STEAM-1) which then goes to the electrolyser at 775 °C (STEAM-2). After the heat exchange with steam, exhaust gas enters the turbine at 1150 °C. In addition to the reactants, a temperature moderator consisting of a recycled flow of carbon dioxide (CO2-REC) at 720 °C is supplied to the combustion chamber in order to obtain a turbine inlet temperature of 1150 °C. The gas turbine also receives further carbon dioxide blown through the turbine blades in order to cool the blades themselves. To simplify the model, a couple of gas turbines (TURB-1 and TURB-2) were utilised with the total cooling flow (CO2-BLD) at 717 °C added between the two turbines. The cooling flow added is such that the final temperature of the exhaust gas exiting the turbine is 774 °C, approximately the same as in the original Allam cycle.

Therefore, the gas exiting at 34 bar from the turbine (EXH-HOT) is composed of the product of syngas combustion, almost-pure steam and carbon dioxide, and recycled carbon dioxide. Steam has to be condensed. A flow of carbon dioxide corresponding to the combustion product has to be fed to the methanation unit, whereas the residual flow has to be recompressed and recycled.

The first step is the cooling of exhaust gas inside a multi-flux heat exchanger (MHEX), which elaborates three different flows. Then, the exhaust gas (EXH-COLD) at 51.1 °C is sent to a condenser (ALL-COND) to condense and remove water. At this point, the almost-pure carbon dioxide flow is split to separate the carbon dioxide produced during combustion (MET-CO2), which is heated up to 300 °C inside the above-mentioned multi-flux heat exchanger and supplied to the methanation section (CO2-MET).

The residual flow (REC-CO2) is recompressed using three intercooled compressors and three pumps up to the pressure of 305 bar. Then, the flow is heated up to 720 °C inside the above-mentioned multi-flux heat exchanger and finally split to separate the stream for turbine cooling (BLD-CO2) from the stream sent to the combustion chamber (CO2-REC).

The part of the plant devoted to the Sabatier process (Figure 71) consists of three adiabatic methanation units operating at 30 bar.

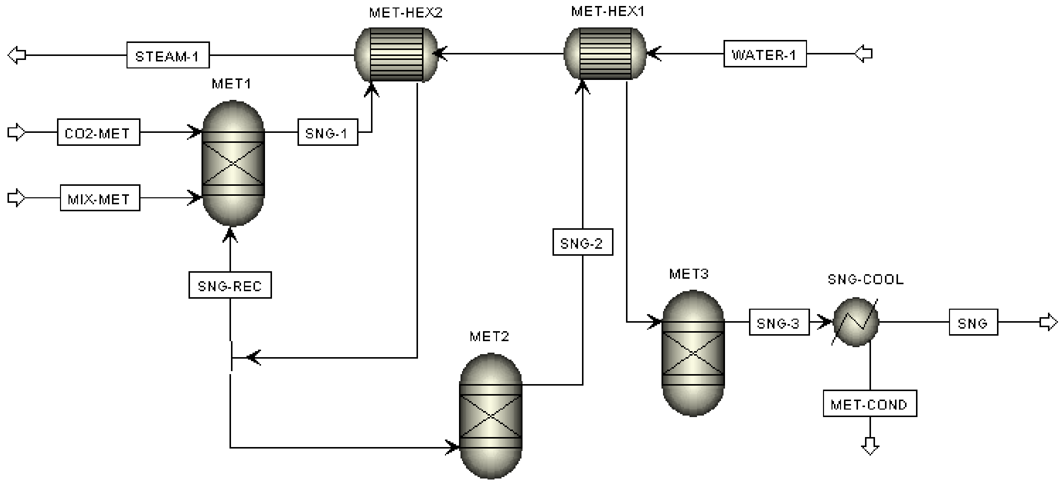

Figure 71. Model of the methanation section for SNG production

The first consists of a Gibbs reactor (MET1) fed with a flow of electrolytic hydrogen mixed with a residual amount of water (MIX-MET) at 255 °C and with a flow of carbon dioxide extracted at 300 °C from the power section (CO2-MET). In addition, there is a partial recycling of the outgoing gas (SNG-REC), according to the TREMP layout designed by Haldor Topsoe. The reactor is followed by a countercurrent, two-stream heat exchanger (MET-HEX2) having the task to recover heat from the flow exiting the reactor and transfer it to the steam entering the Allam section (STEAM-1) at 582 °C.

The second unit is almost identical to the first one, with a Gibbs reactor (MET2) and a countercurrent, two-stream heat exchanger (MET-HEX1) having the task to recover heat from the flow exiting the reactor and transfer it to the water coming from the SOEC section (WATER-1). In this case, there is no recycling, and the reactor is only fed with the gas stream from the first unit after splitting for recycling.

Finally, the third unit receives the gas from the second unit. It is composed of a Gibbs reactor (MET3) and a cooler with no heat recovery (SNG-COOL) for the refrigeration and dehumidification of the SNG produced, which mainly consists of methane and is suitable for storage or injection into the natural gas distribution network.

4.3.6. Results

A flow rate of 1 kmol/s of water fed to the electrolyser was considered. This corresponded to an input to the gasifier of 6.3 kg/s of the biomass defined in Table 29. The electrolytic oxygen used for gasification (O2-GAS) amounted to 2.584 kg/s, supplied at 33 °C and 30 bar.

Figure 72 shows a detail of the syngas flows in the gasification section. The biomass is dehumidified by the syngas produced to facilitate the gasification process; therefore, the moisture present in the biomass is found in the syngas (5-SYN4). It is removed by means of condensation, since the syngas is refrigerated (5-SYN6) before being brought to the operating pressure of the Allam cycle. This compression is carried out in four intercooled stages, downstream of which the syngas (5-SYN13) is heated in a regenerative exchanger, countercurrent with respect to the flow leaving the cyclone (5-SYN4). Finally, the resulting syngas is sent to the power unit (5-SYN14).

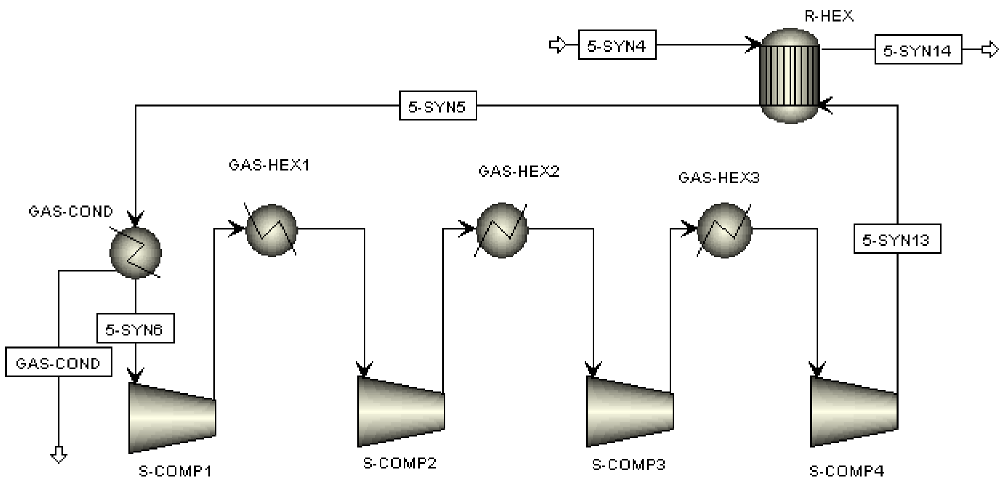

Figure 72. Detail of the syngas flows in the gasification section

The characteristics of the main syngas flows in the gasification section are shown in Table 30.

Table 30. Characteristics of the main flows of the gasification section

Molar Flow (mol/s)	5-SYN4	5-SYN5	5-SYN6	5-SYN13	5-SYN14
H_2O	108.0		0.6		
H_2	57.2				
CO	106.6				
CO_2	76.3				
CH_4	28.6				
N_2	0.2				
Total flow (mol/s)	376.9		269.4		
Temperature (°C)	474.9	190.3	33.0	86.7	454.9
Pressure (bar)	30			305	
Vapor fraction	1				

The syngas is then fed to the combustion chamber together with a flow of oxygen that comes from the SOEC section. The features of the main flows of the electrolysis section are shown in Table 31. The electrolysis section receives a flow of water (WATER) at room temperature, which, after compression, is mixed with the water recovered from the other sections (COND-REC). This flow is partially evaporated by recovering heat from the products coming out of the electrolyser (O2 and MIX) and then by completing evaporation and overheating at the expense of the heat recovered from other sections. The flow of hydrogen and residual water (MIX-MET) is sent to the methanation section. The oxygen flow is divided into two flows, where the first (O2-GAS) is sent to the gasification section, while the second (O2-ALL) is sent to the Allam section.

Table 31. Characteristics of the main flows of the electrolysis section

Molar Flow (mol/s)	WATER	WATER-1	STEAM-2	MIX	MIX-MET	O2	O2-GAS	O2-ALL
H_2O	1000.0			150.0		0		
H_2	0			850.0		0		
O_2	0			0		425.0	80.8	344.2
Total flow (mol/s)	1000.0			1000.0		425.0	80.8	344.2
Temperature (°C)	20	233.9	775.0	825.0	255.0	825.0	33.0	
Pressure (bar)	30							
Vapor fraction	0	0.398	1					
Liquid fraction	1	0.602	0					

The latter flow exceeds the flow rate required by the burner; therefore, it is split in two streams after being compressed to 200 bar. This first compression is carried out with a couple of intercooled compressors. After the second cooling process, the exceeding flow (O2-STOR) is separated; it may be available for selling or for other applications. The remaining flow is finally compressed to 305 bar and fed (O2-CC) to the combustion chamber.

The features of the main flows of the Allam section are shown in Table 32 and Table 33. The burnt gas from the combustion chamber (EXH-GAS) enter the heat exchanger (ALL-HEX) and then the gas turbine, whose blades are cooled by a carbon dioxide flow (CO2-BLD). After expansion down to 34 bar, the gas flow (EXH-HOT) at 774 °C enters the multi-flux heat exchanger and leaves it at 51.1 °C (EXH-COLD). With further cooling to 33 °C, almost all steam is condensed and separated (ALL-COND).

Table 32. Main oxygen, exhaust gas and condensed water flows of the Allam section

Molar Flow (mol/s)	O2-STOR	O2-CC	EXH-GAS	EXH-HOT	EXH-COLD	ALL-COND
H_2O	0		119.0	119.1		114.5
H_2	traces					
O_2	205.1	139.1	traces			
CO	0		0.2			0
CO_2	0		2038.5	2076.0		0
N_2	0		2			0
Total flow (mol/s)	205.2	139.1	2156.1	2193.5		114.5
Temperature (°C)	33.0	76.4	1212.7	774.0	51.1	33.0
Pressure (bar)	200	305		34		
Vapor fraction	1				0.951	0
Liquid fraction	0				0.049	1

After condensation, the almost-pure stream of carbon dioxide is split into two flows. The first one (MET-CO2) corresponds to the product of combustion and is sent to the multi-flux heat exchanger, from which it exits at 300 °C (CO2-MET) to be fed to the methanation section. The captured CO_2 flow that is sent to methanation presents a purity of 99.67%. The second flow (REC-CO2) corresponds to the recirculation flow and is recompressed to 305 bar. After recompression, the flow is sent to the multi-flux heat exchanger to be heated up to 720 °C and is finally split to be sent to the combustion chamber (CO2-REC) to moderate the temperature and to the turbine (CO2-BLD) for blades cooling.

Table 33. Main carbon dioxide flows of the Allam section

Molar Flow (mol/s)	**MET-CO2**	**CO2-MET**	**REC-CO2**	**CO2-BLD**	**CO2-REC**
H_2O	0.5		4.2	0.1	4.1
H_2	traces				
O_2	traces				
CO	0.2				
CO_2	211.4		1864.4	37.3	1827.1
N_2	0.2		1.6	traces	1.6
Total flow (mol/s)	212.1		1870.4	37.4	1832.8
Temperature (°C)	33	300	43.3	717.4	720
Pressure (bar)	34		305	100	305
Vapor fraction	1				
Liquid fraction	0				

The features of the main flows of the methanation section are shown in Table 34.

Table 34. Characteristics of the main flows of the methanation section

Molar Flow (mol/s)	**SNG-1**	**SNG-REC**	**SNG-2**	**SNG-3**	**SNG**	**MET-COND**
H_2O	1211.4	726.8	539.0	565.2	0.5	564.7
H_2	470.4	282.2	74.0	20.4		0
CO	15.8	9.5	0.4	traces		0
CO_2	103.0	61.9	17.2	4.1		0
CH_4	409.7	245.8	193.9	207.4		0
N_2	0.5	0.3	0.2			0
Total flow (mol/s)	2210.9	1326.5	824.3	797.3	232.6	564.7
Temperature (°C)	606.3	305.0	467.5	333.2	33.0	
Pressure (bar)	30					
Vapor fraction	1					0
Liquid fraction	0					1

The stream of hydrogen (and water) coming from the electrolysis section (MIX-MET) and that of carbon dioxide coming from the Allam section (CO2-MET) are fed to the first methanation reactor together with the recycled SNG flow (SNG-REC). The product gas (SNG-1) exits from the first reactor at 606.3 °C with a methane concentration of about 18.5%. After refrigeration down to about 300 °C and splitting for recycling, the gas is fed to the second reactor, which increases the methane concentration up to about 23.5% and the temperature to 467.5 °C (SNG-2). After a new refrigeration process, the gas is fed to the third reactor for the final conversion. The methane concentration reaches the value of 26.1% (SNG-3), which is not very high due to the significant formation of water during the methanation process. The final cooling down to 33 °C allows to condensate and separate almost all water (MET-COND), so that the composition of the SNG results to be 89.2% CH_4, 8.8% H_2, 1.7% CO_2, 0.2% H_2O and 0.1% N_2 (LHV = 48.072 MJ/kg; HHV = 53.466 MJ/kg). The obtained SNG flow rate resulted to be 3.56 kg/s. The sequence of SNG composition obtained downstream of each methanation reactor and after final drying is graphically shown in Figure 73.

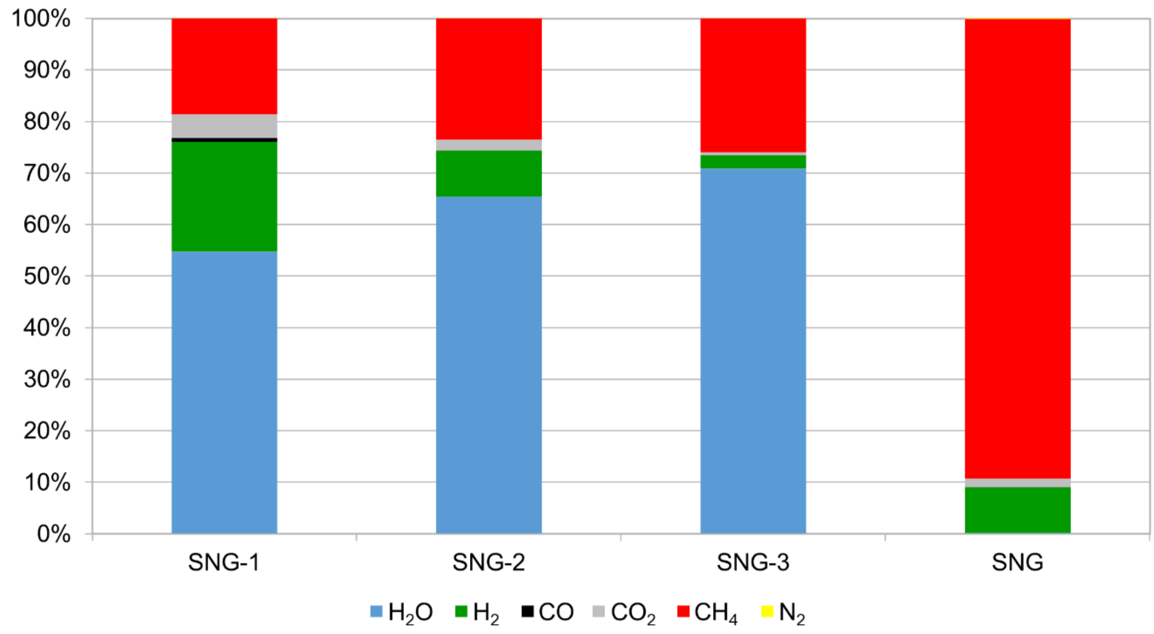

Figure 73. Sequence of the obtained SNG composition

Finally, the global energy balance is reported in Table 35. The electrolysis section required an input of 222.398 MW as electric power for electrolysis, plus the thermal power input recovered from other sections and 0.016 MW of mechanical power for the water pump.

The gasification section required an input of 1.995 MW as mechanical power for gas compression and an input of 78.625 MW as chemical power of the biomass consumed. The turbines in the Allam section produced 45.343 MW, while the CO_2 and the O_2 compression lines required 7.653 MW and 2.503 MW of mechanical power, respectively. Overall, the Allam section required chemical power coming from the gasification section and generated 35.186 MW of net mechanical power. By also taking into consideration the mechanical power required by the water pump and the gasification section, the net mechanical power produced by the whole plant was 33.174 MW. Assuming an electric efficiency value of 0.985, the electric power generated was 32.677 MW.

Finally, the methanation section required an input of chemical power corresponding to the hydrogen produced by the electrolysis section and generated a chemical power of 170.805 MW, based on LHV, or 189.970 MW, based on HHV, as SNG. It is possible to calculate the overall plant efficiency using Equation (4.1), using LHV or HHV depending on the desired calorific value basis.

Table 35. Global energy balance of the proposed system

	Input	Output
Chemical power (MW)	78.625	170.805
Electric power (MW)	222.398	32.677
Total power (MW)	301.023	203.482
Efficiency, LHV basis (%)	67.60	
Efficiency, HHV basis (%)	71.57	

The results show global plant efficiency of 67.60% on an LHV basis and 71.57% on an HHV basis. Finally, this paper mainly deals with the proof of concept and with the integration of the various sections of the plant. Future studies should focus on the sizing of the proposed system to a size compatible with the coupling with RES plants (especially regarding the electrolyser) and the further optimization of the various plant sections. Nevertheless, different types of input biomass or of synthetic fuels and green chemicals as outputs could be explored, while the environmental suitability could be checked using a life-cycle approach.

4.3.7. Conclusions

Publication 5 proposed a novel integrated system for the cogeneration of electricity and the simultaneous production of substitute natural gas, starting from lignocellulosic biomass, water and renewable electricity. Through the production of renewable fuel, this system could serve as energy storage, helping to increase the flexibility and interconnection of natural gas and electricity grids as well as the share of renewable sources in the energy mix. The main novelty of this study lies in the coupling of a power unit based on the Allam thermodynamic cycle with a water electrolyser, a biomass gasifier and a methanation section. The Allam power cycle uses supercritical CO_2 as evolving fluid and is based on the oxycombustion, of a biomass syngas in this case, allowing carbon dioxide capture and utilisation to be more easily achieved. Electrolytic oxygen can be valorised and used for oxycombustion, while the CO_2 captured from the power cycle (simply by means of water condensation) can be used for the production of renewable fuel (SNG in this case). In addition, electricity is simultaneously produced by the power cycle with better programmability and continuity than wind or solar power. The results show an efficiency value of the proposed system of around 68% on an LHV basis, producing almost 33 MW of net electrical power and 171 MW of SNG chemical power, against an energy input of 222 MW renewable electricity and 78.6 MW of biomass. The composition of the produced SNG showed contents of 89.2% CH_4 and 8.8% H_2, resulting in a gas with high calorific value that could be injected into the existing natural gas grid. The current barriers to the injection of SNG with similar composition in the natural gas grid are mostly of legislative rather than technical nature. However, higher methane contents could also be obtained by means of the further optimisation of the methanation section. For realistic coupling with renewable energy sources, it would be essential to scale the system to a size compatible with those of common wind and photovoltaic plants. Future studies could explore the further optimisation of the plant and waste heat recovery, the use of different types of biomass, the coupling of anaerobic digestion systems with the Allam cycle and the production of different fuels, such as methanol. Finally, an analysis of the environmental impacts (for example, through life-cycle assessment) would be crucial to evaluate the environmental sustainability of the gas produced compared with conventional systems.

References

[1] Della Volpe R. Macchine. Liguori Editore; 2011.

[2] British Petroleum. BP Statistical Review of World Energy 2022. London: 2022.

[3] IEA. Key World Energy Statistics 2021. Paris: International Energy Agency; 2021.

[4] Nasa Earth Observatory. Global Patterns of Carbon Dioxide 2013. https://earthobservatory.nasa.gov/images/82142/global-patterns-of-carbon-dioxide (accessed January 5, 2023).

[5] IPCC. Climate change 2013: the physical science basis - contribution of working group I to the fifth assessment report of the Intergovernmental Panel on Climate Change. Cambridge: Cambridge University Press; 2013.

[6] Ritchie H, Roser M, Rosado P. CO_2 and Greenhouse Gas Emissions - Emissions by sector. Our World Data 2020. https://ourworldindata.org/emissions-by-sector (accessed December 28, 2022).

[7] Climate Watch. Greenhouse Gas (GHG) Emissions | Historical GHG emissions by sector 2022.https://www.climatewatchdata.org/ghg-emissions?breakBy=sector&end_year=2019&source=Climate Watch&start_year=1990 (accessed January 5, 2023).

[8] IEA. Global Energy Review: CO_2 Emissions in 2021 - Global emissions rebound sharply to highest ever level. Paris: International Energy Agency; 2022.

[9] UNFCCC. Adoption of the Paris Agreement. Paris: United Nations Framework Convention on Climate Change; 2015.

[10] IPCC. Global Warming of 1.5°C. An IPCC Special Report on the impacts of global warming of 1.5°C above pre-industrial levels and related global greenhouse gas emission pathways, in the context of strengthening the global response to the threat of climate change, sustainable development, and efforts to eradicate poverty. Cambridge: Intergovernmental Panel on Climate Change; 2018.

[11] European Commission. The European Green Deal. Communication from the Commission to the European Parliament, the European Council, the Council, the European Economic and Social Committee and the Committee of the regions. COM(2019) 640 final. Brussels: 2019.

[12] European Council. European Green Deal - Fit for 55 2021. https://www.consilium.europa.eu/en/policies/green-deal/ (accessed March 13, 2023).

[13] European Commission. European Climate Law. Regulation (EU) 2021/1119 of the European Parliament and of the Council of 30 June 2021 establishing the framework for achieving climate neutrality and amending Regulations (EC) No 401/2009 and (EU) 2018/1999. 2021.

[14] UNFCCC. Glasgow Climate Pact. Glasgow: United Nations Framework Convention on Climate Change; 2021.

[15] IEA. Renewables 2022 - Analysis and forecast to 2027. Paris: International Energy Agency; 2022.

[16] IRENA. Renewable Capacity Statistics 2022. Abu Dhabi: International Renewable Energy Agency; 2022.

[17] United Nations. Renewable energy – powering a safer future; 2022. https://www.un.org/en/climatechange/raising-ambition/renewable-energy (accessed March 13, 2023).

[18] IEA. World Energy Outlook 2022. Paris: International Energy Agency; 2022.

[19] Shafiul Alam M, Al-Ismail FS, Salem A, Abido MA. High-level penetration of renewable energy sources into grid utility: Challenges and solutions. IEEE Access 2020;8:190277–99. https://doi.org/10.1109/ACCESS.2020.3031481.

[20] Saha S, Saleem MI, Roy TK. Impact of high penetration of renewable energy sources on grid frequency behaviour. Int J Electr Power Energy Syst 2023;145:108701. https://doi.org/https://doi.org/10.1016/j.ijepes.2022.108701.

[21] Dalala Z, Al-Omari M, Al-Addous M, Bdour M, Al-Khasawneh Y, Alkasrawi M. Increased renewable energy penetration in national electrical grids constraints and solutions. Energy 2022;246:123361. https://doi.org/https://doi.org/10.1016/j.energy.2022.123361.

[22] Zhang Z, Ding T, Zhou Q, Sun Y, Qu M, Zeng Z, et al. A review of technologies and applications on versatile energy storage systems. Renew Sustain Energy Rev 2021;148:111263. https://doi.org/10.1016/j.rser.2021.111263.

[23] Blanco H, Faaij A. A review at the role of storage in energy systems with a focus on Power to Gas and long-term storage. Renew Sustain Energy Rev 2018;81:1049–86. https://doi.org/10.1016/j.rser.2017.07.062.

[24] Candelaresi D, Spazzafumo G. Introduction: the power-to-fuel concept. In: Spazzafumo G, editor. Power to Fuel - How to Speed Up a Hydrogen Economy 1st ed., Academic Press; 2021, p. 1–15. https://doi.org/https://doi.org/10.1016/B978-0-12-822813-5.00005-9.

[25] Barron AR. 2.1: Discovery of Hydrogen - Chemistry LibreTexts. Chem Libr 2021. https://chem.libretexts.org/Bookshelves/Inorganic_Chemistry/Chemistry_of_the_Main_Group_Elements_(Barron)/02%3A_Hydrogen/2.01%3A_Discovery_of_Hydrogen (accessed March 15, 2023).

[26] Perry RH, Green DW. Perry's Chemical Engineers' Hanbook. McGraw-Hill; 1998.

[27] Zhang JZ, Li J, Li Y, Yiping Z. Established Methods Based on Compression and Cryogenics. In: Zhang JZ, Li J, Li Y, Yiping Z, editors. Hydrogen Generation, Storage and Utilization. First edition, John Wiley & Sons; 2014, p. 75–90. https://doi.org/10.1002/9781118875193.ch5.

[28] IEA. The Future of Hydrogen - Seizing today's opportunities - Report prepared for the G20, Japan. Paris: International Energy Agency; 2019.

[29] H21 Northern Gas Networks. H21 North of England. 2018. Available at:

https://www.h21.green/app/uploads/2019/01/H21-NoE-PRINT-PDF-FINAL-1.pdf

[30] U.S. Department of Energy. Hydrogen Tube Trailers 2022. https://www.energy.gov/eere/fuelcells/hydrogen-tube-trailers (accessed March 13, 2023).

[31] U.S. Department of Energy. Gaseous Hydrogen Delivery 2022. https://www.energy.gov/eere/fuelcells/gaseous-hydrogen-delivery (accessed March 13, 2023).

[32] Hydrogen Europe. HYDROGEN EUROPE-TECH [Overview] Hydrogen Transport & Distribution. 2021. Available at: https://hydrogeneurope.eu/wp-content/uploads/2021/11/Tech-Overview_Hydrogen-Transport-Distribution.pdf

[33] Hydrogen Central. Germany To Join Mediterranean Hydrogen Pipeline Project H2Med - Hydrogen Central 2023. https://hydrogen-central.com/germany-join-mediterranean-hydrogen-pipeline-project-h2med/ (accessed March 14, 2023).

[34] van Rossum R, Jens J, La Guardia G, Wang A, Kühnen L, Overgaag M. European Hydrogen Backbone. A European hydrogen infrastructure covering 28 countries. 2022. Available at: https://ehb.eu/files/downloads/ehb-report-220428-17h00-interactive-1.pdf

[35] Sadler D, Cargill A, Crowther M, Rennie A, J. W, Burton S, et al. H21 Leeds City Gate Project. 2016. Available at: https://h21.green/projects/h21-leeds-city-gate/

[36] Melaina M, Antonia O, Penev M. Blending Hydrogen into Natural Gas Pipeline Networks: A Review of Key Issues. Contract 2013;303:275–3000. https://doi.org/10.2172/1068610.

[37] NaturalHy. NaturalHy project 2010. http://66.39.116.196/scientific_papers.htm (accessed August 21, 2020).

[38] Anstrom JR, Collier K. Blended hydrogen–natural gas-fueled internal combustion engines and fueling infrastructure. Compend. Hydrog. Energy, Elsevier Ltd.; 2016, p. 219–32. https://doi.org/10.1016/b978-1-78242-363-8.00008-6.

[39] SNAM. Snam: hydrogen blend doubled to 10% in Contursi trial 2020. https://www.snam.it/en/Media/news_events/2020/Snam_hydrogen_blend_doubled_in_Contursi_trial.html (accessed November 25, 2020).

[40] SNAM. Snam and Baker Hughes test world's first hydrogen blend turbine for gas networks 2020. https://www.snam.it/export/sites/snam-rp/repository/ENG_file/Media/Press_releases/2020/PR_Baker-Hughes-Snam-Hydrogen-Test.pdf (accessed October 1, 2020).

[41] Kippers MJ, De Laat JC, Hermkens RJM, Overdiep JJ, Van Der Molen A, Van Erp WC, et al. Pilot project on hydrogen injection in natural gas on island of Ameland in The Netherlands. vol. 2. Apeldoorn, Netherlands: 2011. Available at: http://members.igu.org/old/IGU Events/igrc/igrc2011/igrc-2011-proceedings-and-presentations/poster paper-session 1/P1-34_Mathijs Kippers.pdf

[42] Altfeld K, Pinchbeck D. Admissible hydrogen concentrations in natural gas systems. Gas for Energy 2013;March/2013:1–16. www.gas-for-energy.com

[43] Verhelst S, Wallner T. Hydrogen-fueled internal combustion engines. Prog Energy Combust Sci 2009;35:490–527. https://doi.org/10.1016/j.pecs.2009.08.001.

[44] USDrive (DOE). Fuel Cell Technical Team Roadmap. 2013. Available at: http://www.osti.gov/servlets/purl/1220127/. https://doi.org/10.2172/1220127.

[45] U.S. Department of Energy Fuel Cell Technologies Office. Fy 2017 Budget At-a-Glance 2017. Available at: https://www.energy.gov/sites/prod/files/2016/03/f30/At_A_GLANCE %28FCTO%29.pdf

[46] U.S. Department of Energy Fuel Cell Technologies Office. 3.4 Fuel Cells 2016 - Multi-Year Research, Development, and Demonstration Plan. Dep Energy, Multi-Year Res Dev Demonstr Plan 2016;2015:1–58.

[47] Schaaf T, Grünig J, Schuster MR, Rothenfluh T, Orth A. Methanation of CO_2 - storage of renewable energy in a gas distribution system. Energy Sustain Soc 2014;4:1–14. https://doi.org/10.1186/s13705-014-0029-1.

[48] Monash University. Australian researchers set record for carbon dioxide capture 2020. https://www.monash.edu/news/articles/australian-researchers-set-record-for-carbon-dioxide-capture2 (accessed October 2, 2020).

[49] Repsol. Repsol to develop two major emissions-reductions projects in Spain 2020. https://www.repsol.com/en/press-room/press-releases/2020/repsol-to-develop-two-major-emissions-reductions-projects-in-spain.cshtml (accessed October 2, 2020).

[50] Environmental Protection Agency. Understanding Global Warming Potentials | Greenhouse Gas (GHG) Emissions | US EPA 2020. https://www.epa.gov/ghgemissions/understanding-global-warming-potentials (accessed August 22, 2020).

[51] Mitsubishi Gas Chemical. Dimethyl ether | Products | Mitsubishi Gas Chemical Company, Inc. 2020. https://www.mgc.co.jp/eng/products/nc/dimethyl-ether.html (accessed July 27, 2020).

[52] Dahmen N, Abeln J, Eberhard M, Kolb T, Leibold H, Sauer J, et al. The bioliq process for producing synthetic transportation fuels. Wiley Interdiscip Rev Energy Environ 2017;6. https://doi.org/10.1002/wene.236.

[53] Maus W. Zukünftige Kraftstoffe - Energiewende des Transports als ein weltweites Klimaziel. Berlin: Springer Vieweg, Berlin, Heidelberg; 2019. https://doi.org/https://doi.org/10.1007/978-3-662-58006-6.

[54] Semmel M, Ali RE, Ouda M, Schaadt A, Sauer J, Hebling C. Power-to-DME: a cornerstone towards a sustainable energy system. In: Spazzafumo G, editor. Power to Fuel - How to Speed Up a Hydrogen Economy, Academic Press; 2021, p. 123–51. https://doi.org/10.1016/B978-0-12-822813-5.00010-2.

[55] Semelsberger TA, Borup RL, Greene HL. Dimethyl ether (DME) as an alternative fuel. J Power Sources 2006;156:497–511. https://doi.org/10.1016/j.jpowsour.2005.05.082.

[56] Matzen M, Demirel Y. Methanol and dimethyl ether from renewable hydrogen and

carbon dioxide: Alternative fuels production and life-cycle assessment. J Clean Prod 2016;139:1068–77. https://doi.org/10.1016/j.jclepro.2016.08.163.

[57] Arcoumanis C, Bae C, Crookes R, Kinoshita E. The potential of di-methyl ether (DME) as an alternative fuel for compression-ignition engines: A review. Fuel 2008;87:1014–30. https://doi.org/https://doi.org/10.1016/j.fuel.2007.06.007.

[58] Kashyap D, Teller H, Schechter A. Dimethyl Ether Oxidation on an Active SnO_2/Pt/C Catalyst for High-Power Fuel Cells. ChemElectroChem 2019;6:2407–14. https://doi.org/10.1002/celc.201900216.

[59] Fúnez Guerra C, Reyes-Bozo L, Vyhmeister E, Jaén Caparrós M, Salazar JL, Clemente-Jul C. Technical-economic analysis for a green ammonia production plant in Chile and its subsequent transport to Japan. Renew Energy 2020;157:404–14. https://doi.org/10.1016/j.renene.2020.05.041.

[60] Perl A. Power to ammonia and urea. In: Spazzafumo G, editor. Power to Fuel - How to Speed Up a Hydrogen Economy, Academic Press; 2021, p. 153–67. https://doi.org/10.1016/B978-0-12-822813-5.00007-2.

[61] Boggs BK, King RL, Botte GG. Urea electrolysis: direct hydrogen production from urine. Chem Commun 2009:4859–61. https://doi.org/10.1039/b905974a.

[62] Lan R, Tao S, Irvine JTS. A direct urea fuel cell - power from fertiliser and waste. Energy Environ Sci 2010;3:438–41. https://doi.org/10.1039/b924786f.

[63] Chatterjee S, Dutta I, Huang KW. Power to formic acid. In: Spazzafumo G, editor. Power to Fuel - How to Speed Up a Hydrogen Economy, Academic Press; 2021, p. 169–210. https://doi.org/10.1016/B978-0-12-822813-5.00006-0.

[64] Ye L, Nayak-luke R, Banares-Alcàntara R, Tsang E. Reaction : ‘“ Green ”’ Ammonia Production. Chem 2017;3:709–714.

[65] Market Research Future. Ammonia Market by Size, Share, Type and Research Analysis – 2028 2020. https://www.marketresearchfuture.com/reports/ammonia-market-2405 (accessed December 21, 2020).

[66] Grand View Research. Methanol Market Size, Share & Trends Analysis Report By Application (Formaldehyde, Acetic Acid, MTBE, DME, Fuel Blending, MTO, Biodiesel), By Region, And Segment Forecasts, 2019 - 2025 2019. https://www.grandviewresearch.com/industry-analysis/methanol-market (accessed December 24, 2020).

[67] Wang T, Tang X, Huang X, Qian W, Cui Y, Hui X, et al. Conversion of methanol to aromatics in fluidized bed reactor. Catal Today 2014;233:8–13. https://doi.org/10.1016/j.cattod.2014.02.007.

[68] Tian P, Wei Y, Ye M, Liu Z. Methanol to olefins (MTO): From fundamentals to commercialization. ACS Catal 2015;5:1922–38. https://doi.org/10.1021/acscatal.5b00007.

[69] Hsieh J. U.S. Patent 4160663A - Method for the direct reduction of iron ore. 1979.

[70] Krüger A, Andersson J, Grönkvist S, Cornell A. Integration of water electrolysis for

fossil-free steel production. Int J Hydrogen Energy 2020;45:29966–77. https://doi.org/10.1016/j.ijhydene.2020.08.116.

[71] HYBRIT Project. HYBRIT - Towards fossil-free steel 2019. http://www.hybritdevelopment.com/ (accessed September 21, 2020).

[72] Valera-Medina A, Xiao H, Owen-Jones M, David WIF, Bowen PJ. Ammonia for power. Progress in Energy and Combustion Science 2018;69:63–102. https://doi.org/10.1016/j.pecs.2018.07.001.

[73] Vavra J, Bortel I, Takats M. A Dual Fuel Hydrogen - Diesel Compression Ignition Engine and Its Potential Application in Road Transport. SAE Tech. Pap., SAE International; 2019. https://doi.org/10.4271/2019-01-0564.

[74] IVECO. Natural Gas Powered Vehicles 2010. https://www.iveco.com/en-us/press-room/kit/Pages/E3-NaturalGasPoweredVehicles.aspx (accessed December 22, 2020).

[75] Towoju OA, Dare A. Di-Methyl Ether (DME) as a substitute for Diesel fuel in compression ignition engines. Int J Adv Res Eng Manag 2017:39–47.

[76] IEA. World Energy Balances. Paris: IEA; 2019.

[77] EIA. International Energy Outlook 2019 - with projections to 2050. Washington, DC 20585: U.S. Energy Information Administration; 2019.

[78] Snam. Agreement between Alstom and Snam for the development of hydrogen trains in Italy 2020. https://www.snam.it/en/Media/Press-releases/Agreement_Alstom_and_Snam_hydrogen_trains_in_Italy.html (accessed December 22, 2020).

[79] Global Railway Review. Alstom awarded Germany contract for supply of 30 Coradia Lint trains 2020. https://www.globalrailwayreview.com/news/98798/alstom-germany-contract-coradia-lint-trains/ (accessed December 22, 2020).

[80] International Maritime Organization. Adoption of Initial IMO Strategy on Reduction of GHG Emissions from Ships. 2018.

[81] MAN Energy Solutions. Engineering the future two-stroke green-ammonia engine 2019.

[82] Dimitriou P, Javaid R. A review of ammonia as a compression ignition engine fuel. Int J Hydrogen Energy 2020;45:7098–118. https://doi.org/10.1016/j.ijhydene.2019.12.209.

[83] ANT Energy Solutions. Renewable Hydrogen Market Report 2013.

[84] Asian Rehub. Asian Renewable Energy Hub Project 2020. https://asianrehub.com/ (accessed December 22, 2020).

[85] ICAO. Sustainable Aviation Fuels Guide. International Civil Aviation Organisation; 2018.

[86] McKinsey & Company, Clean Sky 2 JU, Fuel Cell and Hydrogen 2 JU. Hydrogen-powered aviation. A fact-based study of hydrogen technology, economics, and climate impact by 2050. Belgium: 2020. https://doi.org/10.2843/766989.

[87] European Commission. Liquid hydrogen fuelled aircraft - system analysis (CRYOPLANE project) 2002. https://cordis.europa.eu/project/id/G4RD-CT-2000-00192/it (accessed December 22, 2020).

[88] CNN. Bill Gates, Amazon and British Airways are backing a hydrogen plane startup 2020. https://edition.cnn.com/2020/12/16/business/zeroavia-hydrogen-planes/index.html (accessed December 22, 2020).

[89] Nagashima M. Japan's hydrogen strategy and its economic and geopolitical implications. Ifri: 2018.

[90] Nielsen ER, Prag CB. Learning points from demonstration of 1000 fuel cell based micro-CHP units - Summary of analysis from the ene.field project. 2017.

[91] ENE-FARM. Panasonic Launches New "ENE-FARM" Product, a Fuel Cell for Condominiums - FuelCellsWorks 2020. https://fuelcellsworks.com/news/panasonic-launches-new-ene-farm-product-a-fuel-cell-for-condominiums/ (accessed November 30, 2020).

[92] Spazzafumo G. An Overview of Thermodynamic Cycles Based on Direct Stoichiometric Combustion of Hydrogen and Oxygen. J Sci Ind Res 2003;62:71–80.

[93] Goldmeer J. Fuel flexible gas turbines as enablers for a low or reduced carbon energy ecosystem 2018.

[94] Mitsubishi Power. Hydrogen Power Generation Handbook. 2019.

[95] EUTurbines. The gas turbine industry commitments to drive Europe's transition to a decarbonised energy mix (press release). 2019.

[96] Ditaranto M, Heggset T, Berstad D. Concept of hydrogen fired gas turbine cycle with exhaust gas recirculation: Assessment of process performance. Energy 2020;192:116646. https://doi.org/10.1016/j.energy.2019.116646.

[97] Shiozawa B. "SIP Energy Carriers " Updates and Establishment of Green Ammonia Consortium 2019.

[98] Ballard, GSMA. Fuel Cell Systems for Telecom Backup Power. 2013.

[99] GenCell. Adrian Kenya Selects New GenCell A5 Fuel Cell Solution to Provide Green, Off-Grid Power to 800 Telecom Base Stations 2018. https://www.gencellenergy.com/news/adrian-kenya-800-telecom-base-stations/ (accessed December 23, 2020).

[100] GSMA. Case Study: GenCell 2019. https://www.gsma.com/futurenetworks/wiki/case-study-gencell/ (accessed December 23, 2020).

[101] Fuel Cells Bulletin. Intelligent Energy fuel cells showcased in S. Africa. Fuel Cells Bull 2006:1. https://doi.org/https://doi.org/10.1016/S1464-2859(06)70995-6.

[102] Fuel Cells Bulletin. South African clinic using fuel cell power to benefit TB patients. Fuel Cells Bull 2015;2015:5. https://doi.org/10.1016/s1464-2859(15)30308-4.

[103] Fuel Cells Bulletin. SA supports Ballard, Anglo American fuel cells deployment. Fuel

Cells Bull 2013;2013:6. https://doi.org/10.1016/s1464-2859(13)70255-4.

[104] ESI Africa's Power Journal. Methanol Fuel Cells trialled to power rural South African towns 2014. https://www.esi-africa.com/top-stories/methanol-fuel-cells-trialled-to-power-rural-south-african-towns/ (accessed December 23, 2020).

[105] ISO. ISO 14040:2006 Environmental Management - Life Cycle Assessment - Principles and Framework. Geneva: International Organization for Standardization; 2006.

[106] ISO. ISO 14044:2006 Environmental Management - Life Cycle Assessment - Requirements and Guidelines. Geneva: International Organization for Standardization; 2006.

[107] Lozanovski A, Schuller O, Faltenbacher M. Guidance document for performing LCA on hydrogen production systems. Brussels, Belgium: 2011.

[108] Masoni P, Zamagni A. Guidance document for performing LCA on fuel cells. Brussels, Belgium: 2011.

[109] Valente A, Iribarren D, Dufour J. Life cycle assessment of hydrogen energy systems: a review of methodological choices. Int J Life Cycle Assess 2017;22:346–63. https://doi.org/10.1007/s11367-016-1156-z.

[110] European Commission, Joint Research Centre. International Reference Life Cycle Data system (ILCD) Handbook - General guide for Life Cycle Assessment - Detailed guidance. Luxembourg: Publications Office of the European Union; 2010. https://doi.org/doi:10.2788/38479.

[111] Zampori L, Pant R. Suggestions for updating the Product Environmental Footprint (PEF) method. Luxembourg: Publications Office of the European Union; 2019. https://doi.org/10.2760/424613.

[112] European Commission, Joint Research Centre. International Reference Life Cycle Data System (ILCD) Handbook - Framework and requirements for Life Cycle Impact Assessment models and indicators. Luxembourg: Publications Office of the European Union; 2010. https://doi.org/10.2788/38719.

[113] IPCC. The Earth's Energy Budget, Climate Feedbacks, and Climate Sensitivity. Chapter 7 in Climate Change 2021: the physical science basis. Contribution of Working Group I to the Sixth Assessment Report of the Intergovernmental Panel on Climate Change (AR6). Cambridge, United Kingdom and New York, NY, USA: Cambridge University Press; 2021. https://doi.org/10.1017/9781009157896.009.923.

[114] ecoinvent. Impact Assessment - ecoinvent 2022. https://ecoinvent.org/the-ecoinvent-database/impact-assessment/ (accessed May 29, 2023).

[115] ecoinvent. UPR, LCI & LCIA - ecoinvent 2022. https://ecoinvent.org/the-ecoinvent-database/upr-lci-lcia/#!/life (accessed May 29, 2023).

[116] Orsi F, Muratori M, Rocco M, Colombo E, Rizzoni G. A multi-dimensional well-to-wheels analysis of passenger vehicles in different regions: Primary energy consumption, CO_2 emissions, and economic cost. Appl Energy 2016;169:197–209. https://doi.org/10.1016/j.apenergy.2016.02.039.

[117] Torchio MF, Santarelli MG. Energy, environmental and economic comparison of different powertrain/fuel options using well-to-wheels assessment, energy and external costs - European market analysis. Energy 2010;35:4156–71. https://doi.org/10.1016/j.energy.2010.06.037.

[118] Yazdanie M, Noembrini F, Dossetto L, Boulouchos K. A comparative analysis of well-to-wheel primary energy demand and greenhouse gas emissions for the operation of alternative and conventional vehicles in Switzerland, considering various energy carrier production pathways. J Power Sources 2014;249:333–48. https://doi.org/10.1016/j.jpowsour.2013.10.043.

[119] Wang MQ. GREET 1.5 - Transportation Fuel-Cycle Model - Vol. 1 : methodology, development, use, and results. 9700 South Cass Avenue, Argonne, Illinois 60439: Argonne National Laboratory - Center for Transportation Research; 1999. https://doi.org/10.2172/14775.

[120] Ricardo E&E. Determining the environmental impacts of conventional and alternatively fuelled vehicles through LCA - Final Report for the European Commission. Brussels: Ricardo Energy & Environment; 2020. https://doi.org/10.2834/91418.

[121] Zamel N, Li X. Life cycle analysis of vehicles powered by a fuel cell and by internal combustion engine for Canada. J Power Sources 2006;155:297–310. https://doi.org/10.1016/j.jpowsour.2005.04.024.

[122] Zamel N, Li X. Life cycle comparison of fuel cell vehicles and internal combustion engine vehicles for Canada and the United States. J Power Sources 2006;162:1241–53. https://doi.org/10.1016/j.jpowsour.2006.08.007.

[123] Kobayashi O, Teulon H, Osset P, Morita Y. Life cycle analysis of a complex product, application of ISO 14040 to a complete car. SAE Tech Pap 1998. https://doi.org/10.4271/982187.

[124] JEC. JEC Well-to-Wheels Analysis: well-to-wheels analysis of future automotive fuels and powertrains in the European context. JEC: Joint Research Centre-EUCAR-CONCAWE collaboration; 2014. https://doi.org/10.2790/95533.

[125] EU JRC. Well-to-Wheels Analyses | EU Science Hub 2016 https://ec.europa.eu/jrc/en/jec/activities/wtw (accessed September 17, 2020).

[126] Dinex. Well-to-Wheel Insights 2020. https://www.dinex.net/news-and-events/news/202006-well-to-wheel-insights (accessed March 18, 2023).

[127] Wikipedia. Petroleum - Wikipedia 2022. https://en.wikipedia.org/wiki/Petroleum (accessed May 29, 2023).

[128] Wikipedia. Extraction of petroleum - Wikipedia 2022. https://en.wikipedia.org/wiki/Extraction_of_petroleum (accessed May 29, 2023).

[129] American Petroleum Institute. Industry Sectors 2011. https://web.archive.org/web/20120125195548/http://www.api.org/aboutoilgas/sectors/ (accessed May 29, 2023).

[130] Wikipedia. Upstream (petroleum industry) - Wikipedia 2022.

https://en.wikipedia.org/wiki/Upstream_(petroleum_industry) (accessed May 29, 2023).

[131] ISO. ISO 14224:2016 - Petroleum, petrochemical and natural gas industries — Collection and exchange of reliability and maintenance data for equipment. 2016.

[132] Wikipedia. Midstream - Wikipedia 2022. https://en.wikipedia.org/wiki/Midstream (accessed May 29, 2023).

[133] ISO. ISO 20815:2018 - Petroleum, petrochemical and natural gas industries — Production assurance and reliability management. 2018.

[134] Wikipedia. Downstream (petroleum industry) - Wikipedia 2022. https://en.wikipedia.org/wiki/Downstream_(petroleum_industry) (accessed May 29, 2023).

[135] Eni Scuola. Oil - Extraction and uses. 2022.

[136] Eni Scuola. Natural Gas - Extraction and distribution. 2022.

[137] Eni Scuola. Petrolio 2022. https://eniscuola.eni.com/it-IT/energia/petrolio.html (accessed May 29, 2023).

[138] Eni Scuola. Gas naturale 2022. https://eniscuola.eni.com/it-IT/energia/gas-naturale.html (accessed May 29, 2023).

[139] Wikipedia. Natural gas - Wikipedia 2022. https://en.wikipedia.org/wiki/Natural_gas (accessed May 29, 2023).

[140] IVECO. Iveco at the 12th International Natural Gas Vehicle Conference and Exhibition in Rome 2010. https://www.iveco.com/en-us/press-room/release/Pages/Ivecoatthe12thInternationalNaturalGasVehicleConferenceandExhibitioninRome.aspx (accessed August 2, 2021).

[141] Il Sole 24 Ore. La Fiat Panda sperimenta l'idro-metano 2012. https://st.ilsole24ore.com/art/motori/2012-04-26/la-fiat-panda-sperimenta-idro-metano-085930.shtml?uuid=ADsF86c (accessed August 2, 2021).

[142] NGV Journal. Lombardy introduces ten hydrogen/CNG Fiat Panda | NGV Journal 2011. http://www.ngvjournal.com/s1-news/c7-lng-h2-blends/lombardy-introduces-ten-hydrogencng-fiat-panda/ (accessed August 2, 2021).

[143] Genovese A, Villante C. Environmental analysis of hydrogen-methane blends for transportation. In: Gugliuzza A, Basile A, editors. Membr. Clean Renew. Power Appl., Woodhead Publishing Limited; 2013, p. 218–34. https://doi.org/10.1533/9780857098658.3.218.

[144] Pana C, Negurescu N, Popa MG, Cernat A, Soare D. An investigation of the hydrogen addition effects to gasoline fueled spark ignition engine. SAE Tech Pap 2007. https://doi.org/10.4271/2007-01-1468.

[145] Shi W, Yu X, Zhang H, Li H. Effect of spark timing on combustion and emissions of a hydrogen direct injection stratified gasoline engine. Int J Hydrogen Energy 2017;42:5619–26. https://doi.org/10.1016/j.ijhydene.2016.02.060.

[146] Luo S, Ma F, Mehra RK, Huang Z. Deep insights of HCNG engine research in China. Fuel 2020;263:116612. https://doi.org/10.1016/j.fuel.2019.116612.

[147] Anstrom JR. Hydrogen as a fuel in transportation. Adv. Hydrog. Prod. Storage Distrib., Woodhead Publishing Limited; 2014, p. 499–524. https://doi.org/10.1533/9780857097736.3.499.

[148] Çeper BA. Use of Hydrogen-Methane Blends in Internal Combustion Engines. In: Dragica Minić, editor. Hydrog. Energy - Challenges Perspect., 2012. https://doi.org/10.5772/50597.

[149] Bauer CG, Forest TW. Effect of hydrogen addition on the performance of methane-fueled vehicles. Part I: Effect on S.I. engine performance. Int J Hydrogen Energy 2001;26:55–70. https://doi.org/10.1016/S0360-3199(00)00067-7.

[150] Mariani A, Morrone B, Unich A. A Review of Hydrogen-Natural Gas Blend Fuels in Internal Combustion Engines. Foss Fuel Environ 2012. https://doi.org/10.5772/37834.

[151] Mehra RK, Duan H, Juknelevičius R, Ma F, Li J. Progress in hydrogen enriched compressed natural gas (HCNG) internal combustion engines - A comprehensive review. Renew Sustain Energy Rev 2017;80:1458–98. https://doi.org/10.1016/j.rser.2017.05.061.

[152] Ferrari G. Internal combustion engines. 2nd ed. Società Editrice Esculapio; 2014.

[153] Kanari N, Pineau JL, Shallari S. End-of-Life Vehicle Recycling in the European Union. Jom 2003;55:15–9. https://doi.org/10.1007/s11837-003-0098-7.

[154] Simic V. End-of-life vehicle recycling - a review of the state-of-the-art . Recikliranje Vozila Na Kraj Životnog Ciklusa - Pregl Najsuvremnijih Znan Rad 2013;20:371–80.

[155] Kosacka-Olejnik M. How manage waste from End-of-Life Vehicles? - method proposal. IFAC-PapersOnLine 2019;52:1733–7. https://doi.org/10.1016/j.ifacol.2019.11.451.

[156] Li W, Bai H, Yin J, Xu H. Life cycle assessment of end-of-life vehicle recycling processes in China - Take Corolla taxis for example. J Clean Prod 2016;117:176–87. https://doi.org/10.1016/j.jclepro.2016.01.025.

[157] European Union. End-of-life vehicles (ELV) Directive (EU). Directive 2000/53/EC of the European Parliament and of the council of 18 September 2000 on end-of-life vehicles. 2000.

[158] BMU - German Federal Ministry for the Environment Nature Conservation and Nuclear Safety. Annual report on end-of-life vehicle reuse/recycling/recovery rates in Germany for 2017. 2019.

[159] Funazaki A, Taneda K, Tahara K, Inaba A. Automobile life cycle assessment issues at end-of-life and recycling. JSAE Rev 2003;24:381–6. https://doi.org/10.1016/S0389-4304(03)00081-X.

[160] Karagoz S, Aydin N, Simic V. End-of-life vehicle management: a comprehensive review. J Mater Cycles Waste Manag 2020;22:416–42. https://doi.org/10.1007/s10163-019-00945-y.

[161] European Commission. Merger Procedure Article 6 (1)(b) of Council Regulation (EEC) No 4064/89 - Decision on Case No IV/M.1406. HYUNDAI/KIA. Brussels: 1999.

[162] Thiel C, Schmidt J, Van Zyl A, Schmid E. Cost and well-to-wheel implications of the vehicle fleet CO_2 emission regulation in the European Union. Transp Res Part A Policy Pract 2014;63:25–42. https://doi.org/10.1016/j.tra.2014.02.018.

[163] Trost T, Sterner M, Bruckner T. Impact of electric vehicles and synthetic gaseous fuels on final energy consumption and carbon dioxide emissions in Germany based on long-term vehicle fleet modelling. Energy 2017;141:1215–25. https://doi.org/10.1016/j.energy.2017.10.006.

[164] Candelaresi D, Valente A, Iribarren D, Dufour J, Spazzafumo G. Comparative life cycle assessment of hydrogen-fuelled passenger cars. Int J Hydrogen Energy 2021;46:35961–73. https://doi.org/10.1016/j.ijhydene.2021.01.034.

[165] Ha J, Min SK, Hur T, Kim S. Practical life cycle assessment methodology for a whole automobile. SAE Tech Pap 1998. https://doi.org/10.4271/982188.

[166] Scullino D. Meccanica dell'automobile. Sandit; 2012.

[167] Wang M, Wu Y, Elgowainy A. Operating Manual for GREET: Version 1.7. Argonne: Argonne National Laboratory; 2007.

[168] UN/ECE. Regulation No 115 of the Economic Commission for Europe of the United Nations (UN/ECE). Brussels, Belgium: Official Journal of the European Union; 2014.

[169] U.S. DOE. Alternative Fuels Data Center: Natural Gas Vehicles 2022. https://afdc.energy.gov/vehicles/natural_gas.html (accessed May 29, 2023).

[170] U.S. DOE. Alternative Fuels Data Center: How Do Natural Gas Vehicles Work? 2022. https://afdc.energy.gov/vehicles/how-do-natural-gas-cars-work (accessed May 29, 2023).

[171] Landi Renzo. CNG vehicle systems | Landi Renzo 2022. https://landirenzo.com/en/natural-gas-vehicle-systems (accessed May 29, 2023).

[172] Bosch. CNG systems for passenger cars and light commercial vehicles 2022. https://www.bosch-mobility.com/en/solutions/powertrain/gas/compressed-natural-gas/ (accessed May 30, 2023).

[173] Shivaprasad KV, Raviteja S, Chitragar P, Kumar GN. Experimental Investigation of the Effect of Hydrogen Addition on Combustion Performance and Emissions Characteristics of a Spark Ignition High Speed Gasoline Engine. Procedia Technol 2014;14:141–8. https://doi.org/10.1016/j.protcy.2014.08.019.

[174] Yip HL, Srna A, Yuen ACY, Kook S, Taylor RA, Yeoh GH, et al. A review of hydrogen direct injection for internal combustion engines: Towards carbon-free combustion. Appl Sci 2019;9:1–30. https://doi.org/10.3390/app9224842.

[175] Szwabowski SJ, Hashemi S, Stockhausen WF, Natkin RJ, Kabat DM, Reams L, et al. Ford P2000 Hydrogen Engine Powered P2000 Vehicle 2002.

[176] Stockhausen WF, Natkin RJ, Kabat DM, Reams L, Tang X, Hashemi S, et al. Ford P2000

hydrogen engine design and vehicle development program. SAE Tech Pap 2002. https://doi.org/10.4271/2002-01-0240.

[177] Hollinger T, Bose T. Hydrogen Technology - Chapter 7 Status on Existing Technologies - Hydrogen Internal Combustion Engine. In: Aline Léon, editor. Hydrog. Technol., Springer, Berlin, Heidelberg; 2008, p. 207–33. https://doi.org/10.1007/978-3-540-69925-5_7.

[178] Yamagata H. Science and technology of materials in automotive engines - Chapter 1 Engines. Woodhead Publishing; 2005. https://doi.org/https://doi.org/10.1533/9781845690854.1.

[179] Saborío-González M, Rojas-Hernández I. Review: Hydrogen Embrittlement of Metals and Alloys in Combustion Engines. Rev Tecnol En Marcha 2018;31. https://doi.org/10.18845/tm.v31i2.3620.

[180] Dai Q, Lastoskie CM. Life cycle assessment of natural gas-powered personal mobility options. Energy and Fuels 2014;28:5988–97. https://doi.org/10.1021/ef5009874.

[181] Frischknecht R, Jungbluth N, Althaus H, Doka G, Dones R, Heck T, et al. Overview and Methodology – ecoinvent report no. 1. Dübendorf: Swiss Centre for Life Cycle Inventories; 2007.

[182] Fornalczyk A, Saternus M. Removal of Platinum Group Metals from the used auto catalytic converter. METALURGIJA 2009;48:133–6.

[183] Jimenez De Aberasturi D, Pinedo R, Ruiz De Larramendi I, Ruiz De Larramendi JI, Rojo T. Recovery by hydrometallurgical extraction of the platinum-group metals from car catalytic converters. Miner Eng 2011;24:505–13. https://doi.org/10.1016/j.mineng.2010.12.009.

[184] Twigg M V. Catalytic control of emissions from cars. Catal Today 2011;163:33–41. https://doi.org/10.1016/j.cattod.2010.12.044.

[185] Zeng F, Hohn KL. Modeling of three-way catalytic converter performance with exhaust mixture from natural gas-fueled engines. Appl Catal B Environ 2016;182:570–9. https://doi.org/10.1016/j.apcatb.2015.10.004.

[186] Hussain M, Deorsola FA, Russo N, Fino D, Pirone R. Abatement of CH4 emitted by CNG vehicles using Pd-SBA-15 and Pd-KIT-6 catalysts. Fuel 2015;149:2–7. https://doi.org/10.1016/j.fuel.2014.12.024.

[187] Matam SK, Otal EH, Aguirre MH, Winkler A, Ulrich A, Rentsch D, et al. Thermal and chemical aging of model three-way catalyst Pd/Al 2O 3 and its impact on the conversion of CNG vehicle exhaust. Catal Today 2012;184:237–44. https://doi.org/10.1016/j.cattod.2011.09.030.

[188] Singh S, Bathla VK, Mathai R, Subramanian KA. Development of Dedicated Lubricant for Hydrogen Fuelled Spark Ignition Engine. SAE Tech Pap 2019:1–9. https://doi.org/10.4271/2019-28-2511.

[189] Simons A, Bauer C. A life-cycle perspective on automotive fuel cells. Appl Energy 2015;157:884–96. https://doi.org/10.1016/j.apenergy.2015.02.049.

[190] Evangelisti S, Tagliaferri C, Brett DJL, Lettieri P. Life cycle assessment of a polymer electrolyte membrane fuel cell system for passenger vehicles. J Clean Prod 2017;142:4339–55. https://doi.org/10.1016/j.jclepro.2016.11.159.

[191] Usai L, Hung CR, Vásquez F, Windsheimer M, Burheim OS, Strømman AH. Life cycle assessment of fuel cell systems for light duty vehicles, current state-of-the-art and future impacts. J Clean Prod 2021;280. https://doi.org/10.1016/j.jclepro.2020.125086.

[192] Toyota Motor Corporation. Toyota Mirai Technical Specifications 2017. https://media.toyota.co.uk/wp-content/files_mf/1444919532151015MToyotaMiraiTechSpecFinal.pdf (accessed September 17, 2020).

[193] Wikipedia. Hybrid electric vehicle - Wikipedia 2022. https://en.wikipedia.org/wiki/Hybrid_electric_vehicle (accessed May 29, 2023).

[194] U.S. DOE. Alternative Fuels Data Center: Hybrid Electric Vehicles 2022. https://afdc.energy.gov/vehicles/electric_basics_hev.html (accessed May 29, 2023).

[195] Lo Faro M, Barbera O, Giacoppo G. Hybrid Technologies for Power Generation. 1st edition. Academic Press; 2021. https://doi.org/10.1016/C2020-0-00513-X.

[196] Govardhan OM. Fundamentals and Classification of Hybrid Electric Vehicles. Int J Eng Tech 2017;3:194–8.

[197] Hu X, Han J, Tang X, Lin X. Powertrain Design and Control in Electrified Vehicles: A Critical Review. IEEE Trans Transp Electrif 2021;7:1990–2009. https://doi.org/10.1109/TTE.2021.3056432.

[198] IEA. Key World Energy Statistics 2020. Paris: International Energy Agency; 2020.

[199] British Petroleum. BP Energy Outlook 2018. 2018. https://doi.org/10.1088/1757-899X/342/1/012091.

[200] EEA. Climate change - driving forces - Statistics Explained 2019. https://ec.europa.eu/eurostat/statistics-explained/index.php?title=Climate_change_-_driving_forces (accessed July 14, 2021).

[201] Eurostat. Energy, transport and environment statistics - 2020 edition. Luxembourg: Publications Office of the European Union; 2020. https://doi.org/10.2785/522192.

[202] EEA. Greenhouse gas emissions from transport in Europe 2018. https://www.eea.europa.eu/data-and-maps/indicators/transport-emissions-of-greenhouse-gases-7/assessment (accessed July 13, 2021).

[203] EEA. Final energy consumption in Europe by mode of transport 2018. https://www.eea.europa.eu/data-and-maps/indicators/transport-final-energy-consumption-by-mode/assessment-10 (accessed July 13, 2021).

[204] European Union. Directive (EU) 2018/2001 of the European Parliament and of the Council on the promotion of the use of energy from renewable sources. Strasbourg: European Parliament and Council; 2018.

[205] European Commission. National energy and climate plans (NECPs) 2018.

https://ec.europa.eu/energy/topics/energy-strategy/national-energy-climate-plans_en (accessed July 14, 2021).

[206] European Commission. A hydrogen strategy for a climate-neutral Europe. Communication from the Commission to the European Parliament, the Council, the European Economic and Social Commitee and the Committee of the regions - COM(2020) 301 final. Brussels: 2020.

[207] BMWi. The National Hydrogen Strategy. Berlin: German Federal Ministry for Economic Affairs and Energy (Bundesministerium für Wirtschaft und Klimaschutz); 2020.

[208] MiSE. Strategia Nazionale Idrogeno - Linee Guida Preliminari. Rome: Italian Ministry of Economic Development (Ministero dello Sviluppo Economico); 2020.

[209] MITERD. Hoja de Ruta del Hidrógeno: Una apuesta por el hidrógeno renovable. Madrid: Ministerio para la Transición Ecológica y el Reto Demográfco (MITERD); 2020.

[210] MiSE. Integrated National Energy and Climate Plan. Rome: Italian Ministry of Economic Development (Ministero dello Sviluppo Economico); 2019.

[211] Valente A, Iribarren D, Candelaresi D, Spazzafumo G, Dufour J. Using harmonised life-cycle indicators to explore the role of hydrogen in the environmental performance of fuel cell electric vehicles. Int J Hydrogen Energy 2020;45:25758–65. https://doi.org/10.1016/j.ijhydene.2019.09.059.

[212] Sealy C. The problem with platinum. Mater Today 2008;11:65–8. https://doi.org/10.1016/S1369-7021(08)70254-2.

[213] U.S. Department of Energy. 3.4 Fuel Cells - Fuel Cell Technologies Office Multi-Year Research, Development, and Demonstration Plan. Washington: U.S. Department of Energy; 2016.

[214] Lopes PP, Li D, Lv H, Wang C, Tripkovic D, Zhu Y, et al. Eliminating dissolution of platinum-based electrocatalysts at the atomic scale. Nat Mater 2020. https://doi.org/10.1038/s41563-020-0735-3.

[215] Guinée J, Gorrée M, Heijungs R, Huppes G, Kleijn R, de Koning A, et al. Life cycle assessment - an operational guide to the ISO standards. Leiden: Centre of Environmental Science; 2001.

[216] VDI. VDI guideline 4600: cumulative energy demand (KEA) - terms, definitions, methods of calculation. Düsseldorf: Verein Deutscher Ingenieure; 2012.

[217] Valente A, Iribarren D, Dufour J. Harmonised life-cycle global warming impact of renewable hydrogen. J Clean Prod 2017;149:762–72. https://doi.org/10.1016/j.jclepro.2017.02.163.

[218] Valente A, Iribarren D, Dufour J. Harmonising methodological choices in life cycle assessment of hydrogen: A focus on acidification and renewable hydrogen. Int J Hydrogen Energy 2019:19426–33. https://doi.org/10.1016/j.ijhydene.2018.03.101.

[219] Valente A, Iribarren D, Dufour J. Harmonising the cumulative energy demand of renewable hydrogen for robust comparative life-cycle studies. J Clean Prod

2018;175:384–93. https://doi.org/10.1016/j.jclepro.2017.12.069.

[220] Sergeant N, Boureima FS, Matheys J, Timmermans JM, Van Mierlo J. An environmental analysis of FCEV and H2-ICE vehicles using the Ecoscore methodology. World Electr Veh J 2009;3:635–46. https://doi.org/10.3390/wevj3030635.

[221] Ellingsen LAW, Majeau-Bettez G, Singh B, Srivastava AK, Valøen LO, Strømman AH. Life Cycle Assessment of a Lithium-Ion Battery Vehicle Pack. J Ind Ecol 2014;18:113–24. https://doi.org/10.1111/jiec.12072.

[222] Majeau-Bettez G, Hawkins TR, Strømman AH. Life cycle environmental assessment of lithium-ion and nickel metal hydride batteries for plug-in hybrid and battery electric vehicles. Environ Sci Technol 2011;45:5454. https://doi.org/dx.doi.org/10.1021/es103607c.

[223] Habermacher F. Modeling Material Inventories and Environmental Impacts of Electric Passenger Cars - Comparison of LCA results between electric and conventional vehicle scenarios - Master Thesis. Zurich: Department of Environmental Sciences, ETH; 2011.

[224] Notter DA, Gauch M, Widmer R, Wäger P, Stamp A, Zah R, et al. Contribution of li-ion batteries to the environmental impact of electric vehicles. Environ Sci Technol 2010;44:6550–6. https://doi.org/10.1021/es1029156.

[225] Schweimer G, Levin M. Life Cycle Inventory of the Golf A4. Research Environment and Transport Volkswagen AG, Wolfsburg and Center of Environmental System Research, University of Kassel, Germany; 2000.

[226] Del Duce A, Gauch M, Althaus HJ. Electric passenger car transport and passenger car life cycle inventories in ecoinvent version 3. Int J Life Cycle Assess 2016;21:1314–26. https://doi.org/10.1007/s11367-014-0792-4.

[227] Leuenberger M, Frischknecht R. Life cycle assessment of battery electric vehicles and concept cars. Report, ESU-Services Ltd 2010;2.

[228] Bras B, Cobert A. Life-Cycle Environmental Impact of Michelin Tweel® Tire for Passenger Vehicles. SAE Int J Passeng Cars - Mech Syst 2011;4:32–43. https://doi.org/10.4271/2011-01-0093.

[229] Boureima FS, Vincent W, Nele S, Heijke R, Messagie M, Mierlo J Van. Clean Vehicles Research: LCA and Policy Measures (LCA report). Renew Energy 2009.

[230] Toyota Motor Corporation. Toyota Yaris Hybrid - Technical specifications. 2017.

[231] Tagliaferri C, Evangelisti S, Acconcia F, Domenech T, Ekins P, Barletta D, et al. Life cycle assessment of future electric and hybrid vehicles: A cradle-to-grave systems engineering approach. Chem Eng Res Des 2016;112:298–309. https://doi.org/10.1016/j.cherd.2016.07.003.

[232] Hua TQ, Ahluwalia RK, Peng JK, Kromer M, Lasher S, McKenney K, et al. Technical assessment of compressed hydrogen storage tank systems for automotive applications. Int J Hydrogen Energy 2011;36:3037–49. https://doi.org/10.1016/j.ijhydene.2010.11.090.

[233] International Organization for Standardization. ISO 11439:2013 Gas cylinders - High

pressure cylinders for the on-board storage of natural gas as a fuel for automotive vehicles. Geneva: ISO; 2013.

[234] Vrije Universiteit Brussel. Ecoscore Database 2006. https://ecoscore.be/en/home (accessed September 18, 2020).

[235] Timmermans J, Matheys J, Mierlo J Van, Lataire P. Environmental rating of vehicles with different fuels and drive trains : a univocal and applicable methodology 2006.

[236] Rašić D, Rodman Oprešnik S, Seljak T, Vihar R, Baškovič UŽ, Wechtersbach T, et al. RDE-based assessment of a factory bi-fuel CNG/gasoline light-duty vehicle. Atmos Environ 2017;167:523–41. https://doi.org/10.1016/j.atmosenv.2017.08.055.

[237] Bielaczyc P, Woodburn J, Szczotka A. An assessment of regulated emissions and CO_2 emissions from a European light-duty CNG-fueled vehicle in the context of Euro 6 emissions regulations. Appl Energy 2014;117:134–41. https://doi.org/10.1016/j.apenergy.2013.12.003.

[238] Genovese A, Contrisciani N, Ortenzi F, Cazzola V. On road experimental tests of hydrogen/natural gas blends on transit buses. Int J Hydrogen Energy 2011;36:1775–83. https://doi.org/10.1016/j.ijhydene.2010.10.092.

[239] Yan F, Xu L, Wang Y. Application of hydrogen enriched natural gas in spark ignition IC engines: From fundamental fuel properties to engine performances and emissions. Renew Sustain Energy Rev 2017:1–32. https://doi.org/10.1016/j.rser.2017.05.227.

[240] Akif Ceviz M, Sen AK, Küleri AK, Volkan Öner I. Engine performance, exhaust emissions, and cyclic variations in a lean-burn SI engine fueled by gasoline-hydrogen blends. Appl Therm Eng 2012;36:314–24. https://doi.org/10.1016/j.applthermaleng.2011.10.039.

[241] Conte E, Boulouchos K. Hydrogen-enhanced gasoline stratified combustion in SI-DI engines. J Eng Gas Turbines Power 2008;130:1–9. https://doi.org/10.1115/1.2795764.

[242] Du Y, Yu X, Liu L, Li R, Zuo X, Sun Y. Effect of addition of hydrogen and exhaust gas recirculation on characteristics of hydrogen gasoline engine. Int J Hydrogen Energy 2017;42:8288–98. https://doi.org/10.1016/j.ijhydene.2017.02.197.

[243] Du Y, Yu X, Wang J, Wu H, Dong W, Gu J. Research on combustion and emission characteristics of a lean burn gasoline engine with hydrogen direct-injection. Int J Hydrogen Energy 2016;41:3240–8. https://doi.org/10.1016/j.ijhydene.2015.12.025.

[244] Benitez A, Wulf C, de Palmenaer A, Lengersdorf M, Röding T, Grube T, et al. Ecological assessment of fuel cell electric vehicles with special focus on type IV carbon fiber hydrogen tank. J Clean Prod 2021;278. https://doi.org/10.1016/j.jclepro.2020.123277.

[245] Miotti M, Hofer J, Bauer C. Integrated environmental and economic assessment of current and future fuel cell vehicles. Int J Life Cycle Assess 2017;22:94–110. https://doi.org/10.1007/s11367-015-0986-4.

[246] Bauer C, Hofer J, Althaus HJ, Del Duce A, Simons A. The environmental performance of current and future passenger vehicles: Life Cycle Assessment based on a novel scenario analysis framework. Appl Energy 2015;157:871–83.

https://doi.org/10.1016/j.apenergy.2015.01.019.

[247] Desantes JM, Molina S, Novella R, Lopez-Juarez M. Comparative global warming impact and NOX emissions of conventional and hydrogen automotive propulsion systems. Energy Convers Manag 2020;221. https://doi.org/10.1016/j.enconman.2020.113137.

[248] Dun C, Horton G, Kollamthodi S. Improvements to the definition of lifetime mileage of light duty vehicles – Report for European Commission – DG Climate Action. Didcot: Ricardo-AEA; 2015.

[249] Fiorello D, Martino A, Zani L, Christidis P, Navajas-Cawood E. Mobility Data across the EU 28 Member States: Results from an Extensive CAWI Survey. Transp. Res. Procedia, vol. 14, Elsevier B.V.; 2016, p. 1104–13. https://doi.org/10.1016/j.trpro.2016.05.181.

[250] U.S. EPA. Fuel Economy Guide. Washington, D.C.: U.S. Department of Energy; 2020.

[251] Toyota Motor Corporation. Toyota Yaris technical sheet 2021.

[252] European Commission. NATURALHY - Using the existing natural gas system for hydrogen - Preparing for the Hydrogen Economy by Using the Existing Natural Gas System as a Catalyst - Project Contract No.: SES6/CT/2004/502661. 2009.

[253] Niu R, Yu X, Du Y, Xie H, Wu H, Sun Y. Effect of hydrogen proportion on lean burn performance of a dual fuel SI engine using hydrogen direct-injection. Fuel 2016;186:792–9. https://doi.org/10.1016/j.fuel.2016.09.021.

[254] Yu X, Du Y, Sun P, Liu L, Wu H, Zuo X. Effects of hydrogen direct injection strategy on characteristics of lean-burn hydrogen–gasoline engines. Fuel 2017;208:602–11. https://doi.org/10.1016/j.fuel.2017.07.059.

[255] Valente A, Tulus V, Galán-Martín Á, Huijbregts MAJ, Guillén-Gosálbez G. The role of hydrogen in heavy transport to operate within planetary boundaries. Sustain Energy Fuels 2021;5:4637–49. https://doi.org/10.1039/d1se00790d.

[256] Staffell I, Scamman D, Velazquez Abad A, Balcombe P, Dodds PE, Ekins P, et al. The role of hydrogen and fuel cells in the global energy system. Energy Environ Sci 2019;12:463–91. https://doi.org/10.1039/c8ee01157e.

[257] ACI. ACI Studi e ricerche - Annuario Statistico 2021 - Capitolo 3 - Consistenza Parco Veicoli 2021. https://www.aci.it/laci/studi-e-ricerche/dati-e-statistiche/annuario-statistico.html (accessed July 26, 2021).

[258] European Commission. European Green Deal: Commission proposes transformation of EU economy and society to meet climate ambitions 2021. https://ec.europa.eu/commission/presscorner/detail/en/IP_21_3541 (accessed July 14, 2021).

[259] Italian Council of Ministers. Piano nazionale di ripresa e resilienza. Rome: 2021.

[260] GSE. Energia nel settore trasporti - 2005-2020. Rome: Gestore dei Servizi Energetici; 2021.

[261] EEA. Occupancy rates - Are we moving in the right direction? Indicators on transport and environmental integration in the EU: TERM 2000 2016. https://www.eea.europa.eu/publications/ENVISSUENo12/page029.html (accessed February 15, 2022).

[262] Archer G, Earl T, Bannon E, Poliscanova J, Muzi N, Alexandridou S. CO_2 Emissions From Cars: The facts. Transport & Environment; 2018.

[263] Candelaresi D, Valente A, Bargiacchi E, Spazzafumo G. Life cycle assessment of hybrid passenger electric vehicle. Hybrid Technol Power Gener 2021:475–95. https://doi.org/10.1016/B978-0-12-823793-9.00017-6.

[264] Candelaresi D, Valente A, Bargiacchi E, Iribarren D, Dufour J, Spazzafumo G. Life Cycle Assessment of hydrogen passenger cars and sensitivity to technical parameters. 12th Int. Conf. Hydrog. Prod. (ICH2P-2021 - Online Conf. Sept. 19-23, 2021, 2021.

[265] Frigo S, Spazzafumo G. Comparison of different system layouts to generate a substitute of natural gas from biomass and electrolytic hydrogen. Int J Hydrogen Energy 2020;45:26166–78. https://doi.org/10.1016/j.ijhydene.2020.03.205.

[266] Bargiacchi E, Frigo S, Spazzafumo G. From biomass and electrolytic hydrogen to substitute natural gas and power: The issue of intermediate gas storages. Int J Hydrogen Energy 2019;44:21045–54. https://doi.org/10.1016/j.ijhydene.2019.03.028.

[267] Strazza C, Del Borghi A, Costamagna P, Gallo M, Brignole E, Girdinio P. Life Cycle Assessment and Life Cycle Costing of a SOFC system for distributed power generation. Energy Convers Manag 2015;100:64–77. https://doi.org/10.1016/j.enconman.2015.04.068.

[268] Mistry M, Gediga J, Boonzaier S. Life cycle assessment of nickel products. Int J Life Cycle Assess 2016;21:1559–72. https://doi.org/10.1007/s11367-016-1085-x.

[269] Gediga J, Morfino A, Finkbeiner M, Schulz M, Harlow K. Life cycle assessment of zircon sand. Int J Life Cycle Assess 2019;24:1976–84. https://doi.org/10.1007/s11367-019-01619-5.

[270] Navarro J, Zhao F. Life-cycle assessment of the production of rare-earth elements for energy applications: A review. Front Energy Res 2014;2:1–17. https://doi.org/10.3389/fenrg.2014.00045.

[271] Lee JCK, Wen Z. Rare Earths from Mines to Metals: Comparing Environmental Impacts from China's Main Production Pathways. J Ind Ecol 2017;21:1277–90. https://doi.org/10.1111/jiec.12491.

[272] Zaimes GG, Hubler BJ, Wang S, Khanna V. Environmental life cycle perspective on rare earth oxide production. ACS Sustain Chem Eng 2015;3:237–44. https://doi.org/10.1021/sc500573b.

[273] Wedema BP, Bauer C, Hischier R, Mutel C, Nemecek T, Reinhard J, et al. Data quality guideline for the ecoinvent database version 3. Ecoinvent Report 1 (v3). Swiss Cent Life Cycle Invent 2013;3.

[274] Swiss Centre for Life Cycle Inventories. Ecoinvent data version 3.5. Ecoinvent Data

Version 35 n.d.

[275] Bargiacchi E, Thonemann N, Geldermann J, Antonelli M, Desideri U. Life cycle assessment of synthetic natural gas production from different CO2 sources: A cradle-to-gate study. Energies 2020;13. https://doi.org/10.3390/en13174579.

[276] Mazza A, Bompard E, Chicco G. Applications of power to gas technologies in emerging electrical systems. Renew Sustain Energy Rev 2018;92:794–806. https://doi.org/10.1016/j.rser.2018.04.072.

[277] Götz M, Lefebvre J, Mörs F, McDaniel Koch A, Graf F, Bajohr S, et al. Renewable Power-to-Gas: A technological and economic review. Renew Energy 2016;85:1371–90. https://doi.org/10.1016/j.renene.2015.07.066.

[278] van Leeuwen C, Zauner A. D8.3— Report on the costs involved with PtG technologies and their potentials across the EU. Brussels, Belgium: EU Horizon 2020 Project STORE&GO; 2018.

[279] Frank E, Gorre J, Ruoss F, Friedl MJ. Calculation and analysis of efficiencies and annual performances of Power-to-Gas systems. Appl Energy 2018;218:217–31. https://doi.org/10.1016/j.apenergy.2018.02.105.

[280] Uchida H, Harada MR. Application of hydrogen by use of chemical reactions of hydrogen and carbon dioxide. In: de Miranda PE V., editor. Sci. Eng. Hydrog. Energy Technol. Hydrog. Prod. Pract. Appl. Energy Gener., Amsterdam, The Netherlands: Elsevier; 2019, p. 279–89. https://doi.org/10.1016/B978-0-12-814251-6.00013-7.

[281] Sabatier P, Senderens JB. New synthesis of Methane. Comptes Rendus Hebd Des Seances Acad Des Scrences 1902:514–6.

[282] Perna A, Moretti L, Ficco G, Spazzafumo G, Canale L, Dell'isola M. SNG generation via power to gas technology: Plant design and annual performance assessment. Appl Sci 2020;10:1–23. https://doi.org/10.3390/app10238443.

[283] Gorre J, Ortloff F, van Leeuwen C. Production costs for synthetic methane in 2030 and 2050 of an optimized Power-to-Gas plant with intermediate hydrogen storage. Appl Energy 2019;253:113594. https://doi.org/10.1016/j.apenergy.2019.113594.

[284] Chauvy R, Dubois L, Lybaert P, Thomas D, De Weireld G. Production of synthetic natural gas from industrial carbon dioxide. Appl Energy 2020;260. https://doi.org/10.1016/j.apenergy.2019.114249.

[285] Fendt S, Buttler A, Gaderer M, Spliethoff H. Comparison of synthetic natural gas production pathways for the storage of renewable energy. Wiley Interdiscip Rev Energy Environ 2016;5:327–50. https://doi.org/10.1002/wene.189.

[286] Salomone F, Giglio E, Ferrero D, Santarelli M, Pirone R, Bensaid S. Techno-economic modelling of a Power-to-Gas system based on SOEC electrolysis and CO_2 methanation in a RES-based electric grid. Chem Eng J 2019;377. https://doi.org/10.1016/j.cej.2018.10.170.

[287] Inkeri E, Tynjälä T, Karjunen H. Significance of methanation reactor dynamics on the annual efficiency of power-to-gas -system. Renew Energy 2021;163:1113–26.

https://doi.org/10.1016/j.renene.2020.09.029.

[288] Bargiacchi E, Candelaresi D, Spazzafumo G. Power to methane. In: Spazzafumo G, editor. Power to Fuel - How to Speed Up a Hydrog. Econ. 1st ed., Academic Press; 2021, p. 75–101. https://doi.org/10.1016/B978-0-12-822813-5.00001-1.

[289] Koj JC, Wulf C, Zapp P. Environmental impacts of power-to-X systems - A review of technological and methodological choices in Life Cycle Assessments. Renew Sustain Energy Rev 2019;112:865–79. https://doi.org/10.1016/j.rser.2019.06.029.

[290] Dahiru AR, Vuokila A, Huuhtanen M. Recent development in Power-to-X: Part I - A review on techno-economic analysis. J Energy Storage 2022;56:105861. https://doi.org/10.1016/j.est.2022.105861.

[291] Stanger R, Wall T, Spörl R, Paneru M, Grathwohl S, Weidmann M, et al. Oxyfuel combustion for CO_2 capture in power plants. Int J Greenh Gas Control 2015;40:55–125. https://doi.org/10.1016/j.ijggc.2015.06.010.

[292] Basile A, Gugliuzza A, Iulianelli A, Morrone P. Membrane technology for carbon dioxide (CO_2) capture in power plants. Adv. Membr. Sci. Technol. Sustain. Energy Environ. Appl., Woodhead Publishing Series in Energy; 2011, p. 113–59. https://doi.org/10.1533/9780857093790.2.113.

[293] Spazzafumo G. Storing renewable energies in a substitute of natural gas. Int J Hydrogen Energy 2016;41:19492–8. https://doi.org/10.1016/j.ijhydene.2016.05.209.

[294] Spazzafumo G. Cogeneration of power and substitute of natural gas using electrolytic hydrogen, biomass and high temperature fuel cells. Int J Hydrogen Energy 2018;43:11811–9. https://doi.org/10.1016/j.ijhydene.2018.02.078.

[295] Bargiacchi E, Candelaresi D, Valente A, Frigo S, Spazzafumo G. Life Cycle Assessment of Substitute Natural Gas production from biomass and electrolytic hydrogen. Int J Hydrogen Energy 2021;46:35974–84. https://doi.org/10.1016/j.ijhydene.2021.01.033.

[296] Allam RJ, Palmer M, Brown GW. System and method for high efficiency power generation using a carbon dioxide circulating working fluid. US Patent: US 2011/0179799 A1. US 2011/0179799 A1, 2011.

[297] Allam RJ, Palmer MR, Brown GW, Fetvedt J, Freed D, Nomoto H, et al. High efficiency and low cost of electricity generation from fossil fuels while eliminating atmospheric emissions, including carbon dioxide. Energy Procedia 2013;37:1135–49. https://doi.org/10.1016/j.egypro.2013.05.211.

[298] Allam RJ, Fetvedt JE, Forrest BA, Freed DA. The Oxy-Fuel, Supercritical CO_2 Allam Cycle: New Cycle Developments To Produce Even Lower-Cost Electricity From Fossil Fuels without Atmospheric Emissions. Proc ASME Turbo Expo 2014 Turbine Tech Conf Expo 2014. https://doi.org/https://doi.org/10.1115/GT2014-26952.

[299] Allam R, Martin S, Forrest B, Fetvedt J, Lu X, Freed D, et al. Demonstration of the Allam Cycle: An update on the development status of a high efficiency supercritical carbon dioxide power process employing full carbon capture. Energy Procedia 2017;114:5948–66. https://doi.org/10.1016/j.egypro.2017.03.1731.

[300] Martin S, Forrest B, Rafati N, Lu X, Fetvedt J, McGroddy M, et al. Progress Update on the Allam Cycle: Commercialization of Net Power and the Net Power Demonstration Facility. SSRN Electron J 2018. https://doi.org/10.2139/ssrn.3366370.

[301] Allam RJ, Forrest BA, Fetvedt JE. Method and system for power production with improved efficiency. US patent US010711695B2. US010711695B2, 2020.

[302] Scaccabarozzi R, Gatti M, Martelli E. Thermodynamic analysis and numerical optimization of the NET Power oxy-combustion cycle. Appl Energy 2016;178:505–26. https://doi.org/10.1016/j.apenergy.2016.06.060.

[303] IEAGHG. Oxy-Combustion Turbine Power Plants. Cheltenham, UK: 2015.

[304] Powermag. NET Power's First Allam Cycle 300-MW Gas-Fired Project Will Be Built in Texas n.d. https://www.powermag.com/net-powers-first-allam-cycle-300-mw-gas-fired-project-will-be-built-in-texas/ (accessed January 3, 2023).

[305] Penkuhn M, Tsatsaronis G. Exergy Analysis of the Allam Cycle. 5th Int. Symp. – Supercrit. CO_2 Power Cycles, 2016.

[306] Scaccabarozzi R, Gatti M, Martelli E. Thermodynamic Optimization and Part-load Analysis of the NET Power Cycle. Energy Procedia 2017;114:551–60. https://doi.org/10.1016/j.egypro.2017.03.1197.

[307] Wimmer K, Sanz W. Optimization and comparison of the two promising oxy-combustion cycles NET Power cycle and Graz Cycle. Int J Greenh Gas Control 2020;99:103055. https://doi.org/10.1016/j.ijggc.2020.103055.

[308] Mitchell C, Avagyan V, Chalmers H, Lucquiaud M. An initial assessment of the value of Allam Cycle power plants with liquid oxygen storage in future GB electricity system. Int J Greenh Gas Control 2019;87:1–18. https://doi.org/10.1016/j.ijggc.2019.04.020.

[309] Zhu Z, Chen Y, Wu J, Zhang S, Zheng S. A modified Allam cycle without compressors realizing efficient power generation with peak load shifting and CO_2 capture. Energy 2019;174:478–87. https://doi.org/10.1016/j.energy.2019.01.165.

[310] Lu X, Forrest B, Martin S, Fetvedt J, McGroddy M, Freed D. Integration and optimization of coal gasification systems with a near-zero emissions supercritical carbon dioxide power cycle. Proc. ASME Turbo Expo 2016 Turbomach. Tech. Conf. Expo., 2016. https://doi.org/doi: 10.1115/GT2016-58066.

[311] Lu X, Beauchamp D, Laumb J, Stanislowski J, Swanson M, Dunham D, et al. Coal drying study for a direct syngas fired supercritical CO_2 cycle integrated with a coal gasification process. Fuel 2019;251:636–43. https://doi.org/10.1016/j.fuel.2019.04.050.

[312] Zhu Z, Chen Y, Wu J, Zheng S, Zhao W. Performance study on s-CO_2 power cycle with oxygen fired fuel of s-water gasification of coal. Energy Convers Manag 2019;199:112058. https://doi.org/10.1016/j.enconman.2019.112058.

[313] Toyota Motor Corporation. The Toyota Mirai (first generation) 2015. https://media.toyota.co.uk/wp-content/uploads/sites/5/pdf/Gen1-Mirai-archive-press-pack.pdf (accessed May 28, 2023).

[314] Liu CY, Sung CC. A review of the performance and analysis of proton exchange

membrane fuel cell membrane electrode assemblies. J Power Sources 2012;220:348–53. https://doi.org/10.1016/j.jpowsour.2012.07.090.

[315] Klose C, Breitwieser M, Vierrath S, Klingele M, Cho H, Büchler A, et al. Electrospun sulfonated poly(ether ketone) nanofibers as proton conductive reinforcement for durable Nafion composite membranes. J Power Sources 2017;361:237–42. https://doi.org/10.1016/j.jpowsour.2017.06.080.

[316] Busby C, W. L. Gore & Associates. Manufacturing of low-cost, durable membrane electrode assemblies engineered for rapid conditioning. 2013.

[317] Gasik M. Materials for Fuel Cells. Woodhead Publishing; 2008. https://doi.org/10.1533/9781845694838.1.

[318] Odgaard M. The Use of Per-Fluorinated Sulfonic Acid (PFSA) Membrane as Electrolyte in Fuel Cells. Adv. Fluoride-Based Mater. Energy Convers., Elsevier; 2015, p. 325–74. https://doi.org/10.1016/B978-0-12-800679-5.00014-2.

[319] Kumbur EC, Mench MM. Fuel cells – Proton-exchange membrane fuel cells | Water Management. Encycl Electrochem Power Sources 2009:828–47. https://doi.org/10.1016/B978-044452745-5.00862-5.

[320] Standard Fluoromers Pvt. Ltd. Production Process of PTFE Polymer 2015. http://www.standard-ptfe.com/production-process-of-ptfe.php (accessed May 28, 2023).

[321] Ebnesajjad S. Expansion of Polytetrafluoroethylene Resins. Expand. PTFE Appl. Handb., William Andrew Publishing; 2017, p. 99–127. https://doi.org/10.1016/B978-1-4377-7855-7.00005-5.

[322] Battelle. Manufacturing cost analysis of 10 kW and 25 kW direct hydrogen polymer electrolyte membrane (PEM) fuel cell for material handling applications. Prepared for U.S. Department of Energy. U.S. Department of Energy; 2013.

[323] Polymer Science Learning Center. Free Radical Vinyl Polymerization 2015. https://pslc.ws/macrog/radical.htm (accessed May 28, 2023).

[324] Rahaman MSA, Ismail AF, Mustafa A. A review of heat treatment on polyacrylonitrile fiber. Polym Degrad Stab 2007;92:1421–32. https://doi.org/10.1016/j.polymdegradstab.2007.03.023.

[325] De Vegt OM, Haije WG. Comparative Environmental Life Cycle Assessment of Composite Mate. 1997.

[326] Gallo Stampino P, Molina D, Omati L, Turri S, Levi M, Cristiani C, et al. Surface treatments with perfluoropolyether derivatives for the hydrophobization of gas diffusion layers for PEM fuel cells. J Power Sources 2011;196:7645–8. https://doi.org/10.1016/j.jpowsour.2011.04.039.

Appendix A
Life Cycle Inventories of considered vehicle options

1. Glider life cycle inventory

Table A1: Body and Chassis, material composition, weight, kg

Using a vehicle kerb weight of 1250 kg for ICEV and HEV (reference case, European average car) and 1800 kg for FCEV, and vehicle components composition (% by weight) from GREET [167], the total weight of body and chassis is obtained. Using GREET material composition for each vehicle component (in % by weight), the material composition weight for each component is calculated.

Table A1. Body and Chassis, material composition, weight, kg

Vehicle component, material composition	ICEV and HEV	FCEV
Body	576.80	852.11
Steel	393.96	582
Wrought Aluminium	4.04	5.96
Cast Aluminium	0.00	0.00
Copper/Brass	10.96	16.19
Zinc	0.00	0.00
Magnesium	0.23	0.34
Glass Fibre-Reinforced Plastic	0.00	0.00
Glass	37.49	55.39
Carbon Fibre-Reinforced Plastic	0.00	0.00
Average Plastic	104.40	154.23
Rubber	2.88	4.26
Others*	22.84	33.74
Chassis	298.75	449.94
Steel	251.25	378.40
Cast Iron	20.61	31.05
Wrought Aluminium	0.00	0.00
Cast Aluminium	2.99	4.50
Copper/Brass	3.59	5.40
Zinc	0.00	0.00
Magnesium	0.00	0.00
Glass Fibre-Reinforced Plastic	0.00	0.00
Average Plastic	5.38	8.10
Rubber	13.15	19.80
Others**	1.793	2.70

Others* in Body is inventoried as:

Process	kg (ICEV and HEV)	kg (FCEV)	% with respect to Others	% with respect to Body
Alkyd paint, white, 60% in solvent, at plant/RER	4.16	6.15	18.21%	0.72%
Chromium, at regional storage/RER	2.4	3.55	10.51%	0.42%
Textile, woven cotton, at plant/GLO	2.2	3.25	9.63%	0.38%
Aluminium, production mix, at plant/RER	2.8	4.14	12.26%	0.49%
Polyethylene, HDPE, granulate, at plant/RER	3.06	4.52	13.40%	0.53%
Polyvinylchloride, at regional storage/RER	1.881	2.78	8.24%	0.33%
Steel, low alloyed, at plant/RER	3.99	5.89	17.47%	0.69%
Natural rubber-based sealing, at plant/DE	2.35	3.47	10.29%	0.41%
	total			
	22.841	33.74	100.00%	3.96%

Others in Chassis is inventoried as:**

Process	kg (ICEV and HEV)	kg (FCEV)	% with respect to Others	% with respect to Chassis
Steel, low alloyed, at plant/RER	0.326	0.492	18.21%	0.11%
Aluminium, production mix, at plant/RER	1.466	2.208	81.79%	0.49%
	total			
	1.793	2.70	100%	0.60%

Processes for “Others” were modelled based on ecoinvent’s passenger car dataset [181,225].

2. Fluids

Table A2: Vehicle fluids, weight, kg

Table A2. Vehicle fluids, weight, kg

	Engine Oil	Power Steering Fluid	Brake Fluid	Transmission Fluid	Powertrain Coolant	Windshield Fluid	Adhesives
ICEV and HEV	3.86	0.0	0.91	10.90	10.43	2.72	13.61
FCEV	0.0	0.0	0.91	0.84	7.15	2.72	13.61

This process takes into account fluids needed for vehicle operation, already supplied from the first use, when the vehicle leaves the factory. Data are taken from GREET [167] and ecoinvent passenger car [181,225].

Engine oil, brake fluid and transmission fluid were modelled as lubricating oil, powertrain coolant and windshield fluid were modelled as a mixture of 40% decarbonised water and 60% ethylene glycol, adhesives as adhesive for metals.

3. Internal combustion engine

Table A3: Internal combustion engine for ICE vehicles

Table A3. Internal combustion engine for ICE vehicles

Internal Combustion Engine for ICEV				
Inputs	***Amount***	***Unit***	***Remarks***	***Comments***
Steel, low-alloyed, at plant/RER	21.8	kg	G=80/55=1.45 ; proportion based on engine power [224]	15*G ; Crankcase
Aluminium, production mix, at plant/RER	21.8	kg		15*G ; Crankcase
Steel, low-alloyed, at plant/RER	11.6	kg		8*G ; Crankshaft
Steel, low-alloyed, at plant/RER	8.73	kg		6*G ; Flywheel
Steel, low-alloyed, at plant/RER	0.727	kg		0.5*G ; Ring gear
Steel, low-alloyed, at plant/RER	2.18	kg		1.5*G ; Connecting rod (4 pcs)
Aluminium, production mix, at plant/RER	11.6	kg		8*G ; Cylinder head
Steel, low-alloyed, at plant/RER	2.91	kg		2*G ; Camshaft
Steel, low-alloyed, at plant/RER	0.291	kg		0.2*G ; Intake valve (4 pcs)
Steel, low-alloyed, at plant/RER	0.436	kg		0.3*G ; Hydraulic valve lifter (8 pcs)
Steel, low-alloyed, at plant/RER	0.291	kg		0.2*G ; Exhaust valves (4 pcs)
Aluminium, production mix, at plant/RER	0.727	kg		0.5*G ; Pistons (4 pcs)
Aluminium, production mix, at plant/RER	5.82	kg		4*G ; Intake Manifold
Steel, low-alloyed, at plant/RER	1.45	kg		1*G ; Injection System
Aluminium, production mix, at plant/RER	1.45	kg		1*G ; Injection system
Polyphenylene sulfide, at plant/GLO	2.91	kg		2*G ; Injection system
Polyphenylene sulfide, at plant/GLO	7.27	kg		5*G ; Air filter
Polyphenylene sulfide, at plant/GLO	14.5	kg		10*G ; others
Lubricating oil, at plant/RER	8.73	kg		6*G ; Lubricating oil
Output	***Amount***	***Unit***	***Remarks***	
Internal combustion engine for ICEV	80	kW	Final Product	based on Notter [224]

Internal combustion engine for H2-ICE, CNG, Hythane and H2-Gasoline vehicles is based on Notter et al. [224] adapting the original inventory with respect to the engine power (55 kW to 80 kW).

From an inventory modelling point of view, internal combustion engines fed with hydrogen (pure or mixed), should take into account some structural modifications with respect to common gasoline or CNG engines, to allow the use of hydrogen. For instance, hardened valve seats are required to limit valve wear, due to reduced lubricating effect of the fuel. Small quantities of tungsten carbide are required to harden the valve seats surface, together with steels in which the alloying elements are slightly different. Very small amounts of these materials do not have a significant effect on the final results, while different steels needed can continue to be classified as low-alloyed steel. For these reasons very slight differences between a common engine and a hydrogen engine have not been modelled in this inventory (*cut-off criteria*).

It should also be noted that hydrogen embrittlement does not represent a limitation for the use of hydrogen in the combustion chamber since the commonly used materials already offer good resistance to this phenomenon. For example, aluminium with its various alloys is often used for pistons, mainly AlSi alloys with different concentrations of silicon (generally from 12 to 21%), AlCu alloys, or pistons in ceramic materials [43,177–179]. For these reasons, the inventory of internal combustion engine for hydrogen, hythane and hydrogen-gasoline blend, is identical to that of CNG engine.

Table A4: Internal combustion engine for HEVs

Table A4. Internal combustion engine for HEVs

Internal Combustion Engine for HEV				
Inputs	***Amount***	***Unit***	***Remarks***	***Comments***
Steel, low-alloyed, at plant/RER	15.9	kg	G=58.4/55=1.06 ; proportion based on engine power [224]	15*G ; Crankcase
Aluminium, production mix, at plant/RER	15.9	kg		15*G ; Crankcase
Steel, low-alloyed, at plant/RER	8.49	kg		8*G ; Crankshaft
Steel, low-alloyed, at plant/RER	6.37	kg		6*G ; Flywheel
Steel, low-alloyed, at plant/RER	0.531	kg		0.5*G ; Ring gear
Steel, low-alloyed, at plant/RER	1.59	kg		1.5*G ; Connecting rod (4 pcs)
Aluminium, production mix, at plant/RER	8.49	kg		8*G ; Cylinder head
Steel, low-alloyed, at plant/RER	2.12	kg		2*G ; Camshaft
Steel, low-alloyed, at plant/RER	0.212	kg		0.2*G ; Intake valve (4 pcs)
Steel, low-alloyed, at plant/RER	0.319	kg		0.3*G ; Hydraulic valve lifter (8 pcs)
Steel, low-alloyed, at plant/RER	0.212	kg		0.2*G ; Exhaust valves (4 pcs)
Aluminium, production mix, at plant/RER	0.531	kg		0.5*G ; Pistons (4 pcs)
Aluminium, production mix, at plant/RER	4.25	kg		4*G ; Intake Manifold
Steel, low-alloyed, at plant/RER	1.06	kg		1*G ; Injection System
Aluminium, production mix, at plant/RER	1.06	kg		1*G ; Injection system
Polyphenylene sulfide, at plant/GLO	2.12	kg		2*G ; Injection system
Polyphenylene sulfide, at plant/GLO	5.31	kg		5*G ; Air filter
Polyphenylene sulfide, at plant/GLO	10.6	kg		10*G ; others
Lubricating oil, at plant/RER	6.37	kg		6*G ; Lubricating oil
Output	***Amount***	***Unit***	***Remarks***	
Internal combustion engine for HEV	58.4	kW	Final Product	based on Notter [224] and [230]

Internal combustion engine for HEV H2-ICE and HEV CNG vehicles is based on Notter et al. [224] adapting the original inventory with respect to the engine power (55 kW to 58.4 kW)

4. Fuel System

Table A5: CNG fuel system

Table A5. CNG fuel system

Fuel system for CNG and HEV CNG, High Pressure Piping				
Inputs	***Amount***	***Unit***	***Remarks***	***Comments***
Copper, at regional storage/RER	1.97	kg		
Polyvinylchloride, at regional storage/RER	0.46	kg		
Output	***Amount***	***Unit***	***Remarks***	
CNG fuel system	1	p	Final Product	based on [180,181] and own calculations

Fuel system for CNG and HEV CNG vehicles consist of copper high-pressure piping (from the filler neck to the tank and from the CNG tank to the pressure reducer), valves, gaskets and pressure reducer. Pipes from the pressure reducer to the injectors are of the conventional type.

Table A6: Hydrogen fuel system

Table A6. Hydrogen fuel system

Fuel system hydrogen and hythane, High Pressure Piping				
Inputs	***Amount***	***Unit***	***Remarks***	***Comments***
Copper, at regional storage/RER	3.94	kg		
Polyvinylchloride, at regional storage/RER	0.92	kg		
Output	***Amount***	***Unit***	***Remarks***	
Hydrogen fuel system	1	p	Final Product	own calculations

Fuel system for H2-ICE, HEV H2-ICE and Hythane vehicles and the hydrogen fuel system in H2-Gasoline vehicle are similar to that of CNG vehicle, with some additional safety components to prevent backfire or hydrogen leakages.

Table A7: Gasoline fuel system

Table A7. Gasoline fuel system

Fuel System Gasoline				
Inputs	***Amount***	***Unit***	***Remarks***	***Comments***
Reinforcing steel, at plant/RER	1.45	kg	G=80/55=1.45 ; proportion based on engine power [224]	1*G ; Tubes, fuel pump, fittings
Output	***Amount***	***Unit***	***Remarks***	
Fuel System Gasoline	1.45	kg	Final Product	based on [224]

A gasoline fuel system is also present in the H2-Gasoline vehicle. Data for inventory are from [224].

5. Gasoline Tank

Table A8: Gasoline tank

Table A8. Gasoline tank

Gasoline Tank				
Inputs	***Amount***	***Unit***	***Remarks***	***Comments***
Polyethylene, HDPE, granulate, at plant/RER	17.5	kg	G=80/55=1.45 ; proportion based on engine power [224]	12*G
Injection moulding	17.5	kg	processing HDPE	
Output	***Amount***	***Unit***	***Remarks***	
Gasoline Tank	17.5	kg	Final Product	based on [224]

6. CNG Tank

Table A9: CNG-II tank

Table A9. CNG-II tank

CNG-II Tank				
Inputs	*Amount*	*Unit*	*Remarks*	*Comments*
Steel, low-alloyed, at plant/RER	70	kg	based on [180]	liner, base material
Epoxy resin, liquid, at plant	6	kg	3/5 of epoxy resin, based on [233]	wrap, proportion for composite based on hydrogen tank
Glass fibre, at plant/RER	4	kg	based on [233]	wrap, proportion for composite based on hydrogen tank
Output	*Amount*	*Unit*	*Remarks*	
CNG-II Tank	80	kg	Final Product	100-litre tank, (same capacity but lighter than CNG-I and resistant to higher pressures. Liner in metallic material (steel or aluminium), hoop-wrapped with composite material (epoxy resin + glass fibre); 100 litre=80 kg (CNG-II)

As CNG, Hythane® can be stored in CNG-I or CNG-II tanks, even if it contains some hydrogen. In fact, up to 200 bar, even pure hydrogen can be transported in appropriate steel cylinders without the occurrence of hydrogen embrittlement; however, this can be solved with suitable internal lining materials.

Table A10: CNG-I tank

Table A10. CNG-I Tank

CNG-I Tank				
Inputs	*Amount*	*Unit*	*Remarks*	*Comments*
Steel, low-alloyed, at plant/RER	100	kg	Dai and Lastoskie [180]	100 litres =100 kg (CNG-I)
Output	*Amount*	*Unit*	*Remarks*	
CNG-I Tank	100	kg	Final Product	100-litre tank, full-metal

7. Hydrogen Tank (CNG-IV)

Table A11: Hydrogen tank for FCEV, H2-ICE and HEV H2-ICE

Table A11. Hydrogen tank for FCEV, H2-ICE and HEV H2-ICE

Hydrogen Tank (CNG-IV)				
Inputs	*Amount*	*Unit*	*Remarks*	*Comments*
Aluminium, primary, at plant/RER	7.09	kg	based on [190]	
Carbon fibre cloth	19.78	kg		
Electricity	12.87	MJ		
Epoxy resin, liquid, at plant/RER	29.67	kg		
Glass fibre, at plant/RER	5.6	kg		
Polyethylene, HDPE, granulate, at plant/RER	10.26	kg		
Polyurethane, flexible foam, at plant/RER	4.67	kg		
Steel, low-alloyed, at plant/RER	10.64	kg		
Output	*Amount*	*Unit*	*Remarks*	
Hydrogen Tank (CNG-IV)	93	kg	Final product	Based on [190,192,229,232] Type-IV tank with HDPE, capacity:122 litre, fuel storage: about 5 kg H_2 @ 700 bar

Table A12: Hydrogen tank for H2-Gasoline

Table A12. Hydrogen tank for H2-Gasoline

Hydrogen Tank (CNG-IV) for H2-Gasoline				
Inputs	***Amount***	***Unit***	***Remarks***	***Comments***
Aluminium, primary, at plant/RER	1.418	kg	based on [190]	
Carbon fibre cloth	3.956	kg		
Electricity	2.574	MJ		
Epoxy resin, liquid, at plant/RER	5.934	kg		
Glass fibre, at plant/RER	1.12	kg		
Polyethylene, HDPE, granulate, at plant/RER	2.052	kg		
Polyurethane, flexible foam, at plant/RER	0.934	kg		
Steel, low-alloyed, at plant/RER	2.128	kg		
Output	***Amount***	***Unit***	***Remarks***	
Hydrogen Tank (CNG-IV)	18.6	kg	Final product	Based on [190,192,229,232] Type-IV tank with HDPE, capacity:25 litre, fuel storage: about 1 kg H_2 @ 700 bar

8. Exhaust system

For each vehicle equipped with an internal combustion engine, the exhaust system is mainly composed by a three-way catalytic converter (TWC) and other components such as the exhaust manifold, exhaust pipes and muffler. Differences in platinum group metal loads in the TWC are taken into account for each vehicle, accordingly with tailpipe emissions generated by the engine.

Table A13: Catalytic converter for CNG and HEV CNG

Table A13. Catalytic converter for CNG and HEV CNG

Three Way Catalytic Converter (TWC) CNG and HEV CNG				
Inputs	***Amount***	***Unit***	***Remarks***	***Comments***
Talc, in ground	1.4	kg	(in ground)	input from nature
Steel, low-alloyed, at plant/RER	25.2	kg		Coat
Platinum, at regional storage/RER	2	g	based on [182–187]	catalyst for oxidation reactions HC, CO higher than in gasoline vehicle, to increase oxidation of unburned CH4
Palladium, at regional storage/RER	1	g	based on [182–187]	catalyst for oxidation reactions HC, CO Pt:Pd=2:1
Rhodium, at regional storage/RER	0.4	g	based on [182–187]	catalyst for NOx reduction reactions Pt:Rh= 5:1
Cerium concentrate, 60% cerium oxide, at plant/CN	0.04	kg		accumulates oxygen in lean cycles and releases it in rich cycles, helps catalysts, improves abatement efficiency
Zirconium oxide, at plant/AU U	0.14	kg		ceramic material
Aluminium oxide, at plant/RER	0.02	kg		alumina, a paste spread on the ceramic channels and containing the catalysts, increases the active surface in contact with the exhaust gases
Polyphenylene sulfide, at plant/GLO	0.1	kg		gaskets
Output	***Amount***	***Unit***	***Remarks***	
Three Way Catalytic Converter (TWC) CNG and HEV CNG	1	p	Final Product	based on Boureima [229] and Dai [180]

Table A14: Exhaust system for CNG and HEV CNG

Table A14. Exhaust system for CNG and HEV CNG

Exhaust System CNG and HEV CNG				
Inputs	***Amount***	***Unit***	***Remarks***	***Comments***
Reinforcing steel, at plant/RER	11.6	kg	based on [224]	8*G ; Exhaust Manifold
Reinforcing steel, at plant/RER	23.3	kg	based on [224]	16*G ; Exhaust pipes, Muffler
Synthetic rubber, at plant/RER	1.45	kg	based on [224]	1*G ; Exhaust pipes, Muffler
Three Way Catalytic Converter (TWC) CNG	1	p	Table S13	
Output	***Amount***	***Unit***	***Remarks***	
Exhaust System CNG and HEV CNG	1	p	Final Product	

Table A15: Catalytic converter for Hythane vehicle

Table A15. Catalytic converter for Hythane vehicle

Three Way Catalytic Converter (TWC) Hythane				
Inputs	***Amount***	***Unit***	***Remarks***	***Comments***
Talc, in ground	1.4	kg	(in ground)	input from nature
Steel, low-alloyed, at plant/RER	25.2	kg		Coat
Platinum, at regional storage/RER	1.4	g	based on [182–187]	catalyst for oxidation reactions HC, CO CO emissions reduction (with respect to CNG): 42,4% HC emissions reduction (with respect to CNG): 34%; Pt load assumed 30% lower than CNG;
Palladium, at regional storage/RER	0.7	g	based on [182–187]	catalyst for oxidation reactions HC, CO Pt:Pd=2:1 CO emission reduction (with respect to CNG): 42,4% HC emission reduction (with respect to CNG): 34%; Pd load assumed 30% lower than CNG;
Rhodium, at regional storage/RER	0.64	g	based on [182–187]	catalyst for NOx reduction reactions NOx emissions increase (with respect to CNG): 60% Rh load assumed 60% greater than CNG
Cerium concentrate, 60% cerium oxide, at plant/CN	0.04	kg		accumulates oxygen in lean cycles and releases it in rich cycles, helps catalysts, improves abatement efficiency
Zirconium oxide, at plant/AU	0.14	kg		ceramic material
Aluminium oxide, at plant/RER	0.02	kg		alumina, a paste spread on the ceramic channels and containing the catalysts, increases the active surface in contact with the exhaust gases
Polyphenylene sulfide, at plant/GLO	0.1	kg		gaskets
Output	***Amount***	***Unit***	***Remarks***	
Three Way Catalytic Converter (TWC) Hythane	1	p	Final Product	based on Boureima [229] and Dai [180]

Table A16: Exhaust system for Hythane vehicle

Table A16. Exhaust system for Hythane vehicle

Exhaust System Hythane				
Inputs	***Amount***	***Unit***	***Remarks***	***Comments***
Reinforcing steel, at plant/RER	11,6	kg	based on [224]	8*G ; Exhaust Manifold
Reinforcing steel, at plant/RER	23,3	kg	based on [224]	16*G ; Exhaust pipes, Muffler
Synthetic rubber, at plant/RER	1,45	kg	based on [224]	1*G ; Exhaust pipes, Muffler
Three Way Catalytic Converter (TWC) Hythane	1	p	Table S15	
Output	***Amount***	***Unit***	***Remarks***	
Exhaust System Hythane	1	p	Final Product	

Table A17: Catalytic converter for H2-ICE and HEV H2-ICE vehicles

Table A17. Catalytic converter for H2-ICE and HEV H2-ICE vehicles

Three Way Catalytic Converter (TWC) H2-ICE and HEV H2-ICE				
Inputs	***Amount***	***Unit***	***Remarks***	***Comments***
Talc, in ground	1.4	kg	(in ground)	input from nature
Steel, low-alloyed, at plant/RER	25.2	kg		Coat
Platinum, at regional storage/RER	1.4	g	based on [182–187]	catalyst for oxidation reactions HC, CO Pt load assumed as in Hythane, conservative approach; CO and HC emissions reduction is greater than in hythane vehicle
Palladium, at regional storage/RER	0.7	g	based on [182–187]	catalyst for oxidation reactions HC, CO Pd load assumed as in Hythane; conservative approach; CO and HC emissions reduction is greater than in hythane vehicle
Rhodium, at regional storage/RER	0.64	g	based on [182–187]	catalyst for NOx reduction reactions Rh load assumed 60% as in Hythane; conservative approach
Cerium concentrate, 60% cerium oxide, at plant/CN	0.04	kg		accumulates oxygen in lean cycles and releases it in rich cycles, helps catalysts, improves abatement efficiency
Zirconium oxide, at plant/AU U	0.14	kg		ceramic material
Aluminium oxide, at plant/RER	0.02	kg		alumina, a paste spread on the ceramic channels and containing the catalysts, increases the active surface in contact with the exhaust gases
Polyphenylene sulfide, at plant/GLO	0.1	kg		gaskets
Output	***Amount***	***Unit***	***Remarks***	
Three Way Catalytic Converter (TWC) H2-ICE and HEV H2-ICE	1	p	Final Product	based on Boureima [229] and Dai [180]

Table A18: Exhaust system for H2-ICE and HEV H2-ICE vehicles

Table A18. Exhaust system for H2-ICE and HEV H2-ICE vehicles

Exhaust System H2-ICE and HEV H2-ICE				
Inputs	***Amount***	***Unit***	***Remarks***	***Comments***
Reinforcing steel, at plant/RER	11.6	kg	based on [224]	8*G ; Exhaust Manifold
Reinforcing steel, at plant/RER	23.3	kg	based on [224]	16*G ; Exhaust pipes, Muffler
Synthetic rubber, at plant/RER	1.45	kg	based on [224]	1*G ; Exhaust pipes, Muffler
Three Way Catalytic Converter (TWC) Hythane	1	p	Table S17	
Output	***Amount***	***Unit***	***Remarks***	
Exhaust System H2-ICE and HEV H2-ICE	1	p	Final Product	

Table A19: Catalytic converter for H2-Gasoline vehicle

Table A19. Catalytic converter for H2-Gasoline vehicle

Three Way Catalytic Converter (TWC) H2-Gasoline				
Inputs	***Amount***	***Unit***	***Remarks***	***Comments***
Talc, in ground	1.4	kg	(in ground)	input from nature
Steel, low-alloyed, at plant/RER	25.2	kg		Coat
Platinum, at regional storage/RER	1.12	g	based on [182–187]	catalyst for oxidation reactions HC, CO CO emissions reduction (with respect to gasoline vehicle): 65% HC emissions reduction (with respect to gasoline vehicle): 37%; Pt load assumed 30% lower than gasoline vehicle;
Palladium, at regional storage/RER	0.42	g	based on [182–187]	catalyst for oxidation reactions HC, CO CO emission reduction (with respect to gasoline vehicle): 65% HC emission reduction (with respect to gasoline vehicle): 37%; Pd load assumed 30% lower than gasoline vehicle;
Rhodium, at regional storage/RER	0.48	g	based on [182–187]	catalyst for NOx reduction reactions NOx emissions increase (with respect to gasoline vehicle): 60% Rh load assumed 60% greater than gasoline vehicle
Cerium concentrate, 60% cerium oxide, at plant/CN	0.04	kg		accumulates oxygen in lean cycles and releases it in rich cycles, helps catalysts, improves abatement efficiency
Zirconium oxide, at plant/AU U	0.14	kg		ceramic material
Aluminium oxide, at plant/RER	0.02	kg		alumina, a paste spread on the ceramic channels and containing the catalysts, increases the active surface in contact with the exhaust gases
Polyphenylene sulfide, at plant/GLO	0.1	kg		gaskets
Output	***Amount***	***Unit***	***Remarks***	
Three Way Catalytic Converter (TWC) H2-Gasoline	1	p	Final Product	based on Boureima [229] and Dai [180]

Table A20: Exhaust system for H2-Gasoline

Table A20. Exhaust system for H2-Gasoline

Exhaust System H2-Gasoline				
Inputs	***Amount***	***Unit***	***Remarks***	***Comments***
Reinforcing steel, at plant/RER	11.6	kg	based on [224]	8*G ; Exhaust Manifold
Reinforcing steel, at plant/RER	23.3	kg	based on [224]	16*G ; Exhaust pipes, Muffler
Synthetic rubber, at plant/RER	1.45	kg	based on [224]	1*G ; Exhaust pipes, Muffler
Three Way Catalytic Converter (TWC) Hythane	1	p	Table S19	
Output	***Amount***	***Unit***	***Remarks***	
Exhaust System H2-Gasoline	1	p	Final Product	

9. Li-ion battery

The Li-ion battery (NCM type) is based on [221,222] and adapted from the original inventory from the capacity of 26.6 kWh to that of 1.8 kWh. The liquid cooling system of the battery is not included, as for small batteries the air cooling is considered sufficient.

10. Electric Motor

Table A21: Electric motor for FCEV

Table A21. Electric motor for FCEV

Electric Motor (FCEV)				
Inputs	***Amount***	***Unit***	***Remarks***	***Comments***
Steel, low-alloyed, at plant/RER	36.4	kg	based on [224] ; A=80/55 proportion based on motor power	A*25 ; Magnetic circuit sheet
Steel, low-alloyed, at plant/RER	2.91	kg		A*2 ; Shaft
Ferrite, at plant/GLO	1.67	kg		A*1.15 ; Permanent magnet
Neodymium oxide, at plant/CN	0.611	kg		A*0.42 ; Permanent magnet
Boron carbide, at plant/GLO	0.0291	kg		A*0.02 ; Permanent magnet
Copper, at regional storage/RER	14.5	kg		A*10 ; Windings
Aluminium, production mix, at plant/RER	20.4	kg		A*14 ; Housing
Polyphenylene sulfide, at plant/GLO	1.6	kg		A*1.10 ; Housing
Cable, three-conductor cable, at plant/GLO	4.54	m		A*3.12 ; high power 3x16 mm^2 cables
Output	***Amount***	***Unit***	***Remarks***	
Electric Motor (FCEV)	80	kW	Final Product	based on [223,224]

The electric motor is of the alternate current (AC), synchronous, with permanent magnet type. Electric motor for FCEV is based on [224] and adapted from the original inventory from a rated power of 55 kW to 80 kW.

Table A22: Electric motor for HEVs

Table A22. Electric motor for HEVs

Electric Motor (HEV)				
Inputs	***Amount***	***Unit***	***Remarks***	***Comments***
Steel, low-alloyed, at plant/RER	22.1	kg	based on [224] ; A=48.6/55 proportion based on motor power	A*25 ; Magnetic circuit sheet
Steel, low-alloyed, at plant/RER	1.77	kg		A*2 ; Shaft
Ferrite, at plant/GLO	1.02	kg		A*1.15 ; Permanent magnet
Neodymium oxide, at plant/CN	0.371	kg		A*0.42 ; Permanent magnet
Boron carbide, at plant/GLO	0.0177	kg		A*0.02 ; Permanent magnet
Copper, at regional storage/RER	8.84	kg		A*10 ; Windings
Aluminium, production mix, at plant/RER	12.4	kg		A*14 ; Housing
Polyphenylene sulfide, at plant/GLO	0.972	kg		A*1.10 ; Housing
Cable, three-conductor cable, at plant/GLO	2.76	m		A*3.12 ; high power 3x16 mm^2 cables
Output	***Amount***	***Unit***	***Remarks***	
Electric Motor (HEV)	48.6	kW	Final Product	based on [223,224,230]

Electric motor for HEV H2-ICE and HEV CNG is based on [224] and adapted from the original inventory from a rated power of 55 kW to 48.6 kW.

11. Power control unit

Power control unit is an electronic intelligent system for managing the electricity flows from the battery to the electric motor/generator and vice versa. Comprehends AC/DC inverter, DC/DC converter, battery charger and management system and power distribution unit and is based on [189,190,221,223].

12. Balance of plant

Table A23: Balance of plant for FCEV

Table A23. Balance of plant for FCEV

Balance of plant (FCEV)				
Inputs	***Amount***	***Unit***	***Remarks***	***Comments***
Steel, low-alloyed, at plant/RER	2.5	kg		
Reinforcing steel, at plant/RER	43.5	kg		
Aluminium, production mix, at plant/RER	2.5	kg		
Polyphenylene sulfide, at plant/GLO	5.5	kg		
Synthetic rubber, at plant/RER	1	kg		
Tetrafluoroethylene film, on glass/RER	0.4568	kg		
Transport, lorry>16t, fleet average/RER	5.5457	tkm		
Transport, freight, rail/RER	13.874	tkm		
Output	***Amount***	***Unit***	***Remarks***	
Balance of plant (FCEV)	55	kg	Final Product	based on [180,190]

13. Gearbox

Table A24: Gearbox

Table A24. Gearbox

Gearbox				
Inputs	***Amount***	***Unit***	***Remarks***	***Comments***
Aluminium, production mix, at plant/RER	24.7	kg	G=80/55=1.45 ; proportion based on engine power [224]	17*G ; Casing 100% secondary AlSi9
Steel, low-alloyed, at plant/RER	10.2	kg		7*G ; Input shaft with gears
Steel, low-alloyed, at plant/RER	11.6	kg		8*G ; Output shaft with gears
Steel, low-alloyed, at plant/RER	13.1	kg		9*G ; Differential
Steel, low-alloyed, at plant/RER	1.45	kg		1*G ; Shift parts
Steel, low-alloyed, at plant/RER	11.6	kg		8*G ; Others
Steel, low-alloyed, at plant/RER	7.27	kg		5*G ; Clutch
Output	***Amount***	***Unit***	***Remarks***	
Gearbox	80	kg	Final Product	takes into account the gearbox mechanism, differential, clutch, components for mechanical power transmission from the engine to the wheels based on [167,181,224]

14. Starting System

The starting system serves to start the internal combustion engine by overcoming the initial inertia. It is present in all vehicles equipped with an internal combustion engine and is composed by three main subsystems: the alternator, the starter battery and the starter motor. Inventory based on [224].

Table A25: Alternator

Table A25. Alternator

Alternator				
Inputs	***Amount***	***Unit***	***Remarks***	***Comments***
Steel, low alloyed, at plant/RER	5.82	kg	G=80/55=1.45 ; proportional to engine power [224]	4*G
Aluminium, production mix, at plant/RER	1.45	kg		1*G
Copper, at regional storage/RER	1.45	kg		1*G
Wire drawing, copper/RER	1.45	kg	processing copper	1*G
Output	***Amount***	***Unit***	***Remarks***	
Alternator	8.73	kg	Final Product	based on [181,224]

Table A26: Starter battery (Pb-H_2SO_4)

Table A26. Starter battery (lead acid)

Starter Battery (Pb-H_2SO_4)				
Inputs	***Amount***	***Unit***	***Remarks***	***Comments***
Polyphenylene sulfide, at plant/GLO	5.82	kg	G=80/55=1.45 ; proportion based on engine power [224]	4*G
Lead, at regional storage/RER	18.9	kg		13*G
Sulphuric acid, liquid, at plant/RER	1.45	kg		1*G
Output	***Amount***	***Unit***	***Remarks***	
Starter Battery (Pb-H_2SO_4)	26.2	kg	Final Product	based on [181,224]

Table A27: Starter motor

Table A27. Starter motor

Starter Motor				
Inputs	***Amount***	***Unit***	***Remarks***	***Comments***
Steel, low alloyed, at plant/RER	5.82	kg	G=80/55=1.45 ; proportion based on engine power [224]	4*G
Aluminium, production mix, at plant/RER	1.45	kg		1*G
Copper, at regional storage/RER	1.45	kg		1*G
Wire drawing, copper/RER	1.45	kg	processing copper	1*G
Output	***Amount***	***Unit***	***Remarks***	
Starter Motor	8.73	kg	Final Product	based on [181,224]

Table A28: Starting system for ICE

Table A28. Starting system for ICE

Starting System				
Inputs	***Amount***	***Unit***	***Remarks***	***Comments***
Starter Motor	8.73	kg	G=80/55=1.45 ; proportion based on engine power [224]	4*G
Starter Battery (Pb-H2SO4)	26.2	kg		1*G
Alternator	8.73	kg		1*G
Output	***Amount***	***Unit***	***Remarks***	
Starting System	1	p	Final Product	based on [181,224]

15. Cooling system ICE

Table A29: Cooling system for ICE

Table A29. Cooling system for ICE

Cooling System ICE				
Inputs	***Amount***	***Unit***	***Remarks***	***Comments***
Reinforcing steel, at plant/RER	2.91	kg	G=80/55=1.45 ; proportion based on engine power [224]	2*G ; water cooler
Aluminium, production mix, at plant/RER	2.91	kg		2*G ; water cooler
Polyethylene, HDPE, granulate, at plant/RER	1.45	kg		1*G ; water cooler
Ethylene glycol, at plant/RER	10.2	kg		7*G ; water cooler
Reinforcing steel, at plant/RER	1.45	kg		1*G ; ventilator
Polyethylene, HDPE, granulate, at plant/RER	1.45	kg		1*G ; ventilator
Polyphenylene sulfide, at plant/GLO	5.82	kg		4*G ; piping
Synthetic rubber, at plant/RER	2.91	kg		2*G ; piping
Output	***Amount***	***Unit***	***Remarks***	
Cooling System ICE	29.1	kg	Final Product	based on [181,224]

16. Electronics for control unit (ECU)

Table A30: Electronics for control unit

Table A30. Electronics for control unit

ECU				
Inputs	***Amount***	***Unit***	***Remarks***	***Comments***
Electronics for control units/RER	1.3	kg		
Output	***Amount***	***Unit***	***Remarks***	
ECU	1	p	Final Product	based on [181]

The ECU is a set of electronic components that controls different electronic subsystems and aspects of the vehicle such as many engine parameters, including the instant of spark ignition or the instant and duration of fuel injection, but some modules also deal with braking or mechanical power transmission.

17. Tyres

Table A31: Inventory for the production of 1 tyre

Table A31. Inventory for the production of 1 tyre

Tyre (production) 14 kg				
Inputs	***Amount***	***Unit***	***Remarks***	***Comments***
Synthetic rubber, at plant/RER	3.46	kg		
Natural rubber based sealing, at plant/DE	2.62	kg		
Carbon black, at plant/GLO	2.66	kg		
Silica sand, at plant/DE	1.35	kg		
Secondary sulphur, at refinery/RER	0.179	kg		
Zinc oxide, at plant/RER	0.221	kg		
Petroleum coke, at refinery/RER	0.857	kg		
Viscose fibres, at plant/GLO	2.25	kg		
Steel, low-alloyed, at plant/RER	4	kg		
Electricity, medium voltage, production RER, at grid/RER	1.1	kWh		
Output	***Amount***	***Unit***	***Remarks***	
Tyre (production) 14 kg	1	p	Final Product	based on [228]

18. Vehicle specifications

Table A32: Vehicles kerb weight, kg

Table A32. Vehicles kerb weight, kg

Vehicle	Kerb Weight [kg]
Gasoline (reference case)	1250
HEV Gasoline (reference)	1400
CNG V	1330
HEV CNG	1480
Hythane	1380
H2-Gasoline	1335
H2-ICE	1380
HEV-H2	1550
FCEV	1800

Table A33: Vehicle components composition, % by weight (from GREET [167])

Table A33. Vehicle Components Composition, % by weight (from GREET)

	ICEV: Conventional Material	FCV: Conventional Material	HEV: Conventional Material
Powertrain System (including BOP)	24.7%	8.3%	22.5%
Transmission System	5.3%	2.8%	5.0%
Chassis (w/o battery)	23.9%	25.0%	24.5%
Traction Motor	0.0%	4.2%	2.1%
Generator	0.0%	0.0%	2.1%
Electronic Controller	0.0%	3.7%	1.8%
Fuel Cell Onboard Storage	0.0%	8.7%	0.0%
Body: including BIW, interior, exterior, and glass	46.1%	47.3%	41.9%

Material composition for vehicle components (from GREET)

Table A34: Material composition for each component, % by weight

Table A34. Material composition for each component, % by weight

	ICEV: Conventional Material	FCV: Conventional Material
Body		
Steel	68.3%	68.3%
Wrought Aluminium	0.7%	0.7%
Cast Aluminium	0.0%	0.0%
Copper/Brass	1.9%	1.9%
Zinc	0.0%	0.0%
Magnesium	0.04%	0.04%
Glass Fibre-Reinforced Plastic	0.0%	0.0%
Glass	6.5%	6.5%
Carbon Fibre-Reinforced Plastic	0.0%	0.0%
Average Plastic	18.1%	18.1%
Rubber	0.5%	0.5%
Others	3.96%	3.96%
Chassis (w/o battery)		
Steel	84.1%	84.1%
Cast Iron	6.9%	6.9%
Wrought Aluminium	0.0%	0.0%
Cast Aluminium	1.0%	1.0%
Copper/Brass	1.2%	1.2%
Zinc	0.0%	0.0%
Magnesium	0.0%	0.0%
Glass Fibre-Reinforced Plastic	0.0%	0.0%
Average Plastic	1.8%	1.8%
Rubber	4.4%	4.4%
Others	0.6%	0.6%
Transmission System/Gearbox		
Steel	30.0%	
Copper	0.0%	
Cast Iron	30.0%	
Magnesium	0.0%	
Wrought Aluminium	30.0%	
Cast Aluminium	0.0%	
Carbon Fibre-Reinforced Plastic	0.0%	
Average Plastic	5.0%	
Rubber	5.0%	
Others	0.0%	

19. Results

Table A35: GWP Results, absolute values

Table A35. GWP results, absolute values

Vehicle	GWP kg CO2 eq / km				
	TTW (emissions)	WTT (fuel)	Infrastructure	Use & Maintenance	Total
CNG	0.094314322	0.019218381	0.01673515	0.001451474	1.317E-01
HEV CNG	0.067099343	0.012683954	0.019184849	0.001451595	1.004E-01
FCEV	0	0.009019680	0.044724564	0.002268851	5.601E-02
H2-ICE	0.000270362	0.020034182	0.021573079	0.001548368	4.343E-02
HEV H2-ICE	0.000270363	0.015025636	0.024186092	0.001548368	4.103E-02
Hythane	0.075860028	0.016505967	0.01673503	0.001451595	1.106E-01
H2-Gasoline	0.087663476	0.023007912	0.017865944	0.001548238	1.301E-01

Table A36: CED Results, absolute values

Table A36. CED results, absolute values

Vehicle	CED MJ / km				
	TTW (emissions)	WTT (fuel)	Infrastructure	Use & Maintenance	Total
CNG	0	1.970636751	0.342519264	0.053625723	2.367E+00
HEV CNG	0	1.300602047	0.379288877	0.053629612	1.734E+00
FCEV	0	0.110785200	0.803183861	0.077305492	9.913E-01
H2-ICE	0	0.246072016	0.441738077	0.057204920	7.450E-01
HEV H2-ICE	0	0.184554012	0.480958997	0.057204920	7.227E-01
Hythane	0	1.600180717	0.342516302	0.053629612	1.996E+00
H2-Gasoline	0	1.785218032	0.368640191	0.057200771	2.211E+00

Table A37: AP Results, absolute values

Table A37. AP results, absolute values

Vehicle	AP kg SO2 eq / km				
	TTW (emissions)	WTT (fuel)	Infrastructure	Use & Maintenance	Total
CNG	8.40013E-06	6.69887E-05	0.000130054	1.06231E-05	2.161E-04
HEV CNG	2.45683E-06	4.42119E-05	0.000165604	1.06235E-05	2.229E-04
FCEV	0	8.64941E-05	0.000430363	1.63387E-05	5.332E-04
H2-ICE	1.02571E-05	0.000192117	0.000148089	1.13317E-05	3.618E-04
HEV H2-ICE	8.61600E-06	0.000144088	0.000186008	1.13317E-05	3.500E-04
Hythane	1.34400E-05	6.38455E-05	1.23436E-04	1.06235E-05	2.113E-04
H2-Gasoline	1.68670E-05	2.55536E-04	1.18142E-04	1.13313E-05	4.019E-04

FCEV inventory

Table A38. Technical datasheet of the FCEV (based on Toyota Mirai)

			Comments – How it is calculated – References
Rated power	80	kW	Average European car [44,163]
Dimensions	1m x 19.5 cm x 19.5 cm		Hypothesized from Toyota Mirai data [313]
Weight	40	kg	[1/(Specific power)]*(kW stack)= (1/2)*80 =0,5 kg/kW *80 kW
Power density	3.1	kW/l	Toyota Mirai data, DOE Target 3 kW/l achieved in 2012 [44] (volume basis)
Specific power	2	kW/kg	Toyota Mirai data, DOE Target 2 kW/kg achieved in 2012 [44] (weight basis)
Operating temperature	80	°C	Average temperature used in PEM fuel cells [44]
Operating pressure	2.5	bar	Data from [189] for a typical automotive PEM fuel cell
Active area	250	cm^2	Calculated from Toyota Mirai data, compared with data in [189]
Cell area	380	cm^2	Calculated from Toyota Mirai data, assuming 19,5 cm*19,5 cm [313]
Number of cells per kW	3.246	cells/kW	Calculated from Toyota Mirai data (370 cells/114 kW) [313]
Power per individual cell	308	W/cell	Calculated from Toyota Mirai data (1000 W/ 3,246 cells) [313]
Required number of cells (for 80 kW)	260	cells	Same power density as Mirai was assumed: power density = 308 W/cell, Number of required cells = 80,000 W/308 (W/cell)
Cell Voltage at rated power	0.615	V	The rated power was assumed equal to the operating point at maximum power (in the polarization curve) of the fuel cell of Toyota Mirai (typical assumption in automotive, also used for ICE rated power). Rated power operating point = (0.6 V @ 2000 mA/cm^2), compared with data in [314–316] for polarization curves and performance of membranes NRE-211, NRE-212 and composite membranes Gore-Select. Calculated as V=W/I where W=308 W, I=J*active area = 2 A/cm^2*250 cm^2 = 500 A
Current density at rated power	2000	mA/cm^2	Same assumptions used for the rated cell voltage, reference: composite membrane Gore-Select, thickness: 12 micron (0.85 V @ 1200 mA/cm^2 @ 80°C) [314–316]
Platinum loading	0.15	mg/cm^2	[189,314,315] DOE Target achieved in 2012 [44]
Stack Voltage at rated power	160	V	Calculated as: V cell * Number of cells = 0.615*260
Current per individual cell	500	A	(Power per individual cell)/(Cell Voltage at rated power) = 308 W / 0,615 V = 500 A
Stack Current at rated power	500	A	Cells are connected in series, same current as the individual cell. Calculable also as I=J*active area = 2 A/cm^2 *250 cm^2
Stack rated power	80,000	W	Calculated as: V stack*I stack = 160 V*500 A
Platinum content (per kW of stack)	0.122	g/kW	(Platinum loading)/(Cell power density) = (mg/cm^2)/(W/cm^2) = mg/W = g/kW
Cell power density	1.23	W/cm^2	(W/cell)/(Active area)= 308 W/250 cm^2, compared with data in [314–316]; (per unit of active area)

The first vehicle, analysed in a previous study from Valente, Candelaresi et al. is the FCEV [211]. A new inventory was created, in particular for the fuel cell stack, based on the technical data of the few FCEV vehicles commercially available at the time of data collection (Toyota Mirai 1st generation, Honda FCX Clarity, Hyundai ix35), and on inventories present in scientific literature (mainly by Simons and Bauer [189] and Evangelisti [190]).

In the initial stage, technical data regarding commercial vehicles were collected, in order to understand which subsystems to consider, the powers, weights, dimensions and in general various ratios between the quantities involved (Figure 74). The main reference for the FCEV is represented by the Toyota Mirai. From the technical data of the Toyota Mirai fuel cell stack, through calculations concerning the electrochemical characteristics, it was possible to define a technical data sheet of a generic fuel cell stack for a power of 80 kW. Table A38 shows the technical sheet used to define the stack inventory.

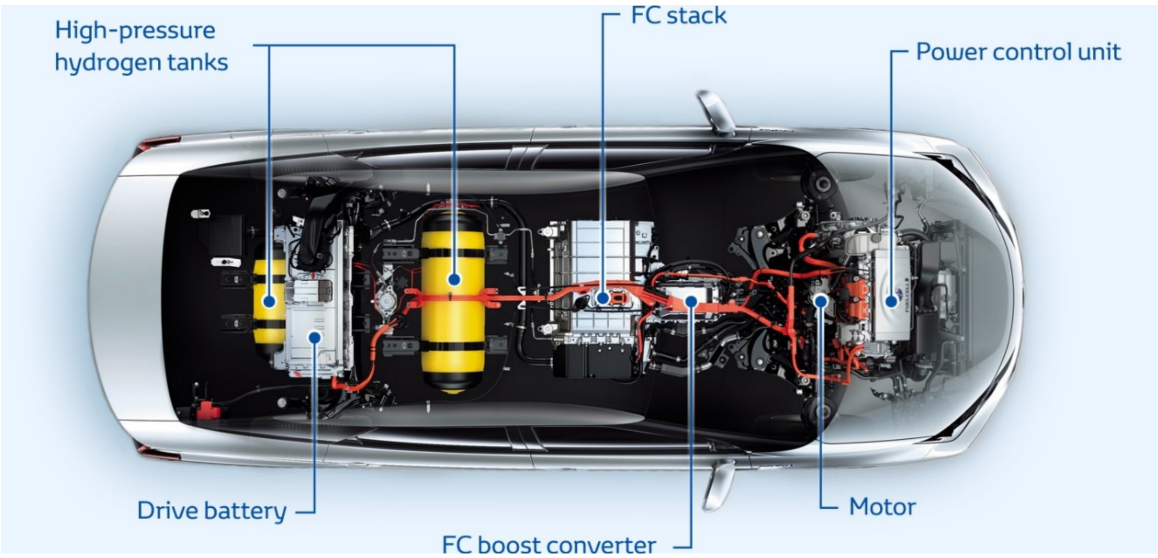

Figure 74. Toyota Mirai cutaway. In the initial phase of the study, the various propulsion subsystems present inside each vehicle were analysed, starting from the architectures of commercial vehicles

The collection of real technical data has made it possible to model an inventory more in line with the current industrial situation regarding the automotive sector. Indeed, inventories of fuel cell stacks retrieved in the literature presented clear differences in terms of performance when compared to commercial fuel cells vehicles. The main reason for this difference seems to be attributable mainly to the membrane performance, as well as to some materials used in other components of the stack. For the purpose of a better understanding of the subsequent inventory, it is useful to previously carry out a classification of the proton exchange membranes on the market and a distinction between the materials commonly used for generic proton exchange membrane fuel cells and those currently most quoted in the automotive sector.

The fuel cells typically used for automotive traction are all of the proton exchange membrane type (PEMFC), as their characteristics are particularly suitable for this application. In fact, in the automotive industry, compared to stationary power generation, weights, dimensions, start-up times, response to transients, durability, etc. take on considerable importance.

The most widely used polymer for making proton exchange membranes for fuel cells goes under the commercial name of Nafion, produced by DuPont.

Nafion is a fluoropolymer-PFSA copolymer or an acid perfluorosulphonic polymer molecule, mainly consisting of polytetrafluoroethylene (Teflon or PTFE) with the addition of sulphonic groups.

As a synthetic polymer with ionic conductivity properties, it can be defined as an ionomer. Its porous structure and the characteristics conferred by the SO_3H group allow the passage of protons, provided that the membrane is kept within the right levels of hydration. For this reason, the humidification of the membrane inside a fuel cell is of fundamental importance. The low electronic conductivity of the membrane instead prevents the passage of electrons. In addition to the high proton conductivity, Nafion has excellent characteristics of thermal, mechanical and chemical stability, and is permeable to water.

There are various types of Nafion membranes commercially available, with different thicknesses, suitable for making PEMFCs. In particular, a first distinction is made between:

- Non-reinforced membranes
- Reinforced membranes

The non-reinforced membranes are made in Nafion only, and can be manufactured with the extrusion-cast or with the dispersion-cast method, with thicknesses ranging between 25 and 254 μm. These are the most commonly used membranes in the fabrication of PEMFCs. These include N-111 (25.4 μm), N-112 (50.8 μm), N-115 (127 μm), and N-117 (183 μm). Nafion membranes are commonly categorized and named in terms of their EW (Equivalent Weight) and thickness, as well as the manufacturing method. For instance, in the acronym N-117, the "N-" indicates an extrusion-cast membrane, with "11" being 1100 g/mol EW, while the last number refers to the thickness in "thou" or "mils" (one thousandth of an inch), so that the "7" means 7 thou or 0.007 inches in thickness. The new types NRE-211 and NRE-212, where "NRE" indicate a dispersion-cast membrane, replace the previous ones N-111 and N-112, presenting the same thicknesses, but with better electrochemical characteristics [317,318]. The inventories of fuel cell stacks found in literature all use these two types of membrane (extrusion or dispersion).

In the automotive sector, however, thinner membranes, with a thickness of less than 20 μm, but which require mechanical reinforcement, are preferable and actually used in the most innovative solutions. Indeed, a very significant improvement in PEMFC performance, especially in power densities, was achieved by reducing the membrane thickness. The thinner membranes increase the efficiency of the performances in part thanks to a lower (ionic/electrical) resistance offered by the cell (due to the reduced thickness), but they also present a lower mechanical resistance, that can negatively affect the membrane durability. For this reason, (mechanically) reinforced membranes were conceived. Improving the durability of fuel cells is considered one of the key research and development objectives, in anticipation of the future widespread diffusion of such devices. In a motor vehicle, the membranes must therefore be chemically stable for thousands of hours, for thousands of cycles of start and stop, of humidification and dehumidification, in a corrosive environment and subjected to vibrations. The advantage gained with thinner membranes, combined with a basic understanding of the mechanisms of proton exchange membrane degradation, has led to novel approaches for the production of thin perfluorinated membranes using mechanical and chemical reinforcement. "Gore and Associates" was the first company to introduce a new process for producing reinforced membranes, by impregnating a micro-porous or macro-porous expanded polytetrafluoroethylene (ePTFE) support with a Nafion-based solution, obtaining membranes with thicknesses between 10 and 15 microns, with high mechanical and durability characteristics. This type of membrane is commercially available under the name Gore-Select.

Subsequently, DuPont also introduced reinforced membranes that combine the advantages of mechanical reinforcement with greater chemical stability, under the name of Nafion XL. Also, the reinforced membranes, thanks to the reduction in thickness, facilitate the water-management i.e. the humidification of the membrane, through the so-called mechanism of water back-diffusion [319], i.e. the diffusion and migration of the water molecules produced on the cathode, towards the anode. Better wetting is another reason for increased performance in a reinforced membrane.

Ultimately, all models of commercial fuel cell vehicles considered, such as the Toyota Mirai, use Gore-Select membranes. Through the data sheet shown in Table A38 and the information reported, an effort has been made in the present thesis work to model a fuel cell stack inventory based on a composite reinforced type membrane.

Other details that increase stack performance in commercial vehicles concern various components and materials. Titanium bipolar plates were considered, used in automotive applications for their lightness, thinner gas-diffusion layers (GDL), and a better catalysis of cathode reactions offered by cobalt in combination with platinum.

Figure 75 shows (in red) the polarization curves of a Gore-Select membrane, while the other curves refer to experimental reinforced membranes (not used in the present study) obtained by combining direct membrane deposition techniques with high conductivity (SPEK) or reinforced with chemically inert nanofibers (PVDF) [315]. It should be noted the high cell power density, current density and cell potential obtained with thin reinforced membrane when compared with conventional ones. The technical data sheet of the stack, previously defined through calculations starting from the electrochemical characteristics of commercial vehicles, is in agreement with these experimental curves. These polarization curves show that the selected operating point at maximum (or rated) power, including voltage > 0.6 V and power density of 1.23 W·cm^{-2} at 2 A·cm^{-2} current density, are easily achievable with this type of membranes.

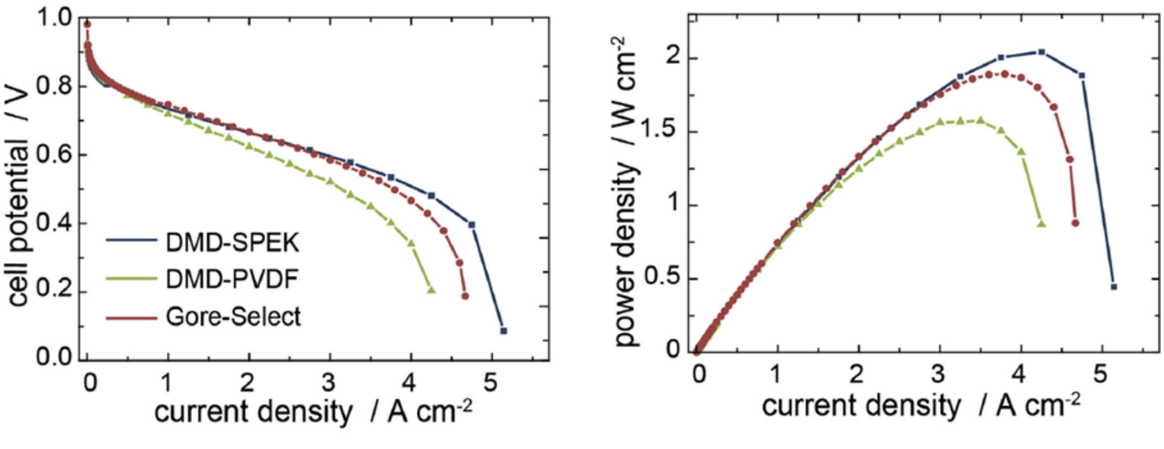

Figure 75. Polarization curves for a cell with Gore-Select membrane (in red). The other curves refer to experimental membranes with high proton conductivity nanofibre reinforcements [315]

FCEV inventory

From membrane to Fuel Cell stack

Reinforced membrane PFSA/ePTFE

In the following dissertation, the life cycle inventories for the fuel cell stack are presented.

Table A39. Nafion base material and Nafion solution

Nafion Base				
Inputs	***Amount***	***Unit***	***Remarks***	***How it is calculated***
Tetrafluoroethylene, at plant/RER U	0.574	kg	From Simons and Bauer,2015 (TFE) [189]	Nafion precursors. Composition: 57.4 wt% TFE, 42.6 wt% PSF
Sulphuric acid, liquid, at plant/RER U	0.426	kg	[189]	Nafion precursors. Composition: 57.4 wt% TFE, 42.6 wt% PSF
Output	***Amount***	***Unit***	***Remarks***	
Nafion Base	1	kg	Intermediate product	
Nafion Solution				
Inputs	***Amount***	***Unit***	***Remarks***	
Nafion base	0.05	kg	Based on Du Pont (2015) [190]	5 wt%
Water, deionised, at plant/CH U	0.19	kg	Based on Du Pont (2015) [190]	Water-isopropanol=4/1 w/w
Isopropanol, at plant/RER U	0.76	kg	Based on Du Pont (2015) [190]	Water-isopropanol=4/1 w/w
Output	***Amount***	***Unit***	***Remarks***	
Nafion Solution	1	kg	Intermediate product	

For the production of the membrane, a solution based on Nafion is prepared. The production process of Nafion is not well known, due to confidentiality issues, however in various scientific articles it is inventoried through the proportions of tetrafluoroethylene (TFE) and sulfuric acid used as a precursor of the sulphonic groups. The Nafion base material thus prepared is added in certain doses to deionised water and isopropanol, an alcohol that acts as a solvent, to form a Nafion-based solution.

Table A40. PTFE, Polytetrafluoroethylene

PTFE, Polytetrafluoroethylene				
Inputs	***Amount***	***Unit***	***Remarks***	***How it is calculated***
Water, deionised, at plant/CH U	0.03	kg	From Standard Fluoromers Pvt.Ltd [320]	
Tetrafluoroethylene, at plant/RER U	0.97	kg		
Boric Oxide, at plant/GLO U	4.26E-4	kg		Precursor for boron trioxide
Ammonium sulphate, as N, at regional storehouse/RER U	0.057	kg		
Output	***Amount***	***Unit***	***Remarks***	
PTFE	1	kg	Intermediate product	

Since in the version of ecoinvent used neither PTFE nor ePTFE are present, these have been modelled using literature data and added manually. The manufacturing processes of tetrafluoroethylene and expanded tetrafluoroethylene are well known in the chemical industry. PTFE is produced by polymerization of the monomer TFE, by adding water, boron trioxide (the simple boron oxide is used as a precursor here) and ammonium sulphate (Table A40).

Table A41. Expanded Polytetrafluoroethylene, ePTFE

Expanded Polytetrafluoroethylene, ePTFE				
Inputs	***Amount***	***Unit***	***Remarks***	***How it is calculated***
PTFE, Polytetrafluoroethylene	1	kg	See PTFE production	
Extrusion, plastic film/RER U	1	kg	Expanded PTFE Applications Handbook. [321]	
Thermoforming, with calendering/RER U	1	kg	Expanded PTFE Applications Handbook. [321]	Productive process: Calendering (stretching) The process "thermoforming with calendering" present in ecoinvent was used
Natural gas, burned in industrial furnace low-NOx>100kW/ RER U	2.66	MJ	Expanded PTFE Applications Handbook. [321]	Heat (sintering), passage in the oven while it is "stretched" on rolls. It was assumed: heat = cp air*(ΔT) = 1.005 * (380 °C -20 °C) =J/kg * m^3 air, air density =1 kg/m^3
Output	***Amount***	***Unit***	***Remarks***	
ePTFE	1	kg	Intermediate product	

ePTFE is produced starting from PTFE through a thermomechanical expansion process which makes it particularly elastic and porous at the end of the process. The PTFE is first extruded in the form of a thin film, then it is laminated and kept in tension on some rolls. Finally, it is stretched as it passes through an oven kept at temperatures around 380 °C.

Table A42. Reinforced membrane Nafion/ePTFE

Reinforced Membrane Nafion/ePTFE				
Inputs	***Amount***	***Unit***	***Remarks***	***How it is calculated***
Expanded Polytetrafluoroethylene, ePTFE	0.133	g	Mechanical reinforce (support) for a single membrane	ePTFE layer thickness for one membrane: (5 micron) =0.0005 cm; ePTFE layer volume = ePTFE layer thickness* * Cell area= 0.0005 cm*(380 cm^2)= 0.19 cm^3; ePTFE mass= Volume* e-PTFE density= 0.19 cm^3 * 0.7 g/cm^3= 0.133 g
Nafion Solution	1.927	g	Amount to impregnate ePTFE, plus coating layers, account for evaporation [314]	12:1 vol/vol, ratio solution/ePTFE, (3 cm^3 of solution are needed to impregnate 0.25 cm^3 of ePTFE). ePTFE layer volume=0.19 cm^3; Solution volume = (0.19 cm^3)*12=2.28 cm^3 ; Solution density = 0.845 g/cm^3 ; Solution mass = 0.845 g/cm^3*2.28 cm^3= 1.927 g.
Natural gas, burned in industrial furnace low-NOx>100kW/ RER U	0.004	MJ	From Evangelisti [190]	Heat (Drying)
Output	***Amount***	***Unit***	***Remarks***	
Reinforced Membrane	1	p	Final Product	Considering a final thickness of the membrane = 15 micron, the membrane is made of a central layer of ePTFE 5 microns thick, impregnated with Nafion (pores are also filled) and covered with two layers of Nafion 5 microns thick each, on the two faces of the mechanical support: Membrane weight = 0.9038 g/membrane

The reinforced membrane is then produced. A 5-micron thick ePTFE mechanical support is impregnated with the previously prepared Nafion solution. A part of the solution occupies the pores of the ePTFE, a part evaporates and a part solidifies forming two layers of 5-micron thickness on each face of the support. The membrane can also be sprayed with solution, hot laminated or simply dried using heat. The functional unit of the process is defined in product units (indicated with the letter "p", abbreviation for pieces). The final product is a 15-micron thick Nafion/ePTFE reinforced membrane.

MEA: Membrane Electrode Assembly (CCM type: Catalyst Coated Membrane)

Catalyst Layer

The membrane considered is of the CCM (Catalyst Coated Membrane) type. In this type of manufacturing method, the membrane is sprayed on both sides with a catalyst ink solution which gives the characteristics of electrochemical activity to each electrode. Another possible constructive typology is represented by the GDE (Gas Diffusion Electrode) in which the catalyst ink is sprayed onto the gas-diffusion layer, from the side which will then come into contact with the membrane. Various studies demonstrate the achievement of higher cell efficiency using the CCM method.

Table A43. Catalyst ink, for PEMFC for automotive applications

Catalyst Ink						
Inputs	***Amount***	***Unit***	***Per kW of stack***	***Unit***	***Remarks***	***How it is calculated***
Platinum, market mix, at regional storage/RER U	9.756	g	0.122	g/kW	Based on a Pt loading of 0.15 mg/cm^2 in 2012 [44,189]	Platinum content = (0.15 mg/cm^2)/(1.23 W/cm^2) = platinum loading/ cell power density = 0.122 g/kW
Carbon black, at plant/GLO U	14.634	g	0.183	g/kW	Used to represent the activated carbon Pt support. Value based on weight ratio of 4:6 Pt to C [189]	catalyst support 0.122/4*6= 0.183 g/kW
Tetrafluoroethylene, at plant/RER U	0.7	g	0.0088	g/kW	Constituent part of the Nafion solution, added at 5wt% (Pt+C) [189]	Nafion for ink solution: 57.4% TFE*(0.122+0.183)* *0.05 = 0.0088 g/kW
Sulphuric acid, liquid, at plant/RER U	0.52	g	0.0065	g/kW	Representing the PSF part of the Nafion solution, added at 5wt% (Pt+C) [189]	Nafion for ink solution: 42.6% PSF *(0.122+0.183)* *0.05 = 0.0065 g/kW
Ethylene glycol, at plant/RER U	1.22	g	0.015	g/kW	Used to form the catalyst ink. Also added at 5wt% (Pt+C). [189]	glycol for ink solution: (0.122+0.183)*0.05= 0.015 g/kW
Water, ultrapure, at plant/GLO U	12.195	g	0.152	g/kW	Used to form the catalyst ink. Assumed to be added at 50wt% (Pt+C) [189]	water for ink solution, (0.122+0.183) *0.5 = 0.152 g/kW
Cobalt, at plant/GLO U	1.63	g	0.020	g/kW	Using a Co-loading at the cathode of 0,025 mg/cm^2 [189] Co-loading = Cathode Pt/3 assuming Pt/Co = 3:1	Cobalt content= (0.025 mg/cm^2)/(1.23 W/cm^2) = 0.020 g/kW Cobalt loading/Power density
Electricity, medium voltage, production RER, at grid/RER U	33.874	MJ			Electricity for mixing, ball milling, Based on Battelle (2013) [322] and Evangelisti [190]	Process energy = 473.32 MJ/0.568 kg = 833.3 MJ/kg= 0.8333 MJ/g Total mass = 40.65 g Energy required = 0.8333 MJ/g*40.65 g=33.874 MJ
Output	***Amount***	***Unit***			***Remarks***	
Catalyst Ink	40.65	g			Final Product	Ink amount for 80 kW stack

The catalyst ink is then prepared through a complicated process shown in Table A43. First a carbon support is prepared for the catalyst, on which platinum or cobalt is deposited. The catalysts are then inserted into a solution based on Nafion, distilled water and ethylene glycol, in order to form the ink which will be sprayed on the membrane. Electricity is involved in various stages of the process, from ball milling to mixing of the solution.

The amount and type of catalysts are also different between the anode and the cathode. The anode in general has faster chemical kinetics, and requires only platinum, in a smaller amount (about 1/3 of the total platinum of a cell). The cathode, on the other hand, has slower kinetics, which needs to be speeded up with the remaining platinum (about 2/3) and with the addition of cobalt. It was found that cobalt addition is significant for improving performance in automotive fuel cells.

The previously prepared reinforced membrane is finally sprayed with the catalyst ink and laminated, involving electricity in the process (Table A44). From this process a catalysed reinforced membrane is obtained.

Table A44. Catalysed reinforce membrane, roll calendering of catalyst ink and membrane

Catalysed reinforced membrane, (application of catalyst ink to membrane and roll calendering)						
Inputs	***Amount***	***Unit***	***Per kW of stack***	***Unit***	***Remarks***	***How it is calculated***
Electricity, medium voltage, production RER, at grid/RER U	0.041	MJ			Based on Battelle (2013) [322] and Evangelisti [190]	Process energy = 39.18 MJ/1 kg coated membrane = 0.03918 MJ/g; Energy required for a membrane = process energy (MJ/g) *1.06 g= 0.041 MJ
Reinforced Membrane Nafion/ePTFE	1	p				
Catalyst Ink	0.156	g				
Output	***Amount***	***Unit***			***Remarks***	
Catalysed Reinforced Membrane	1	p			Final Product	1.06 g

GDL: Gas Diffusion Layers

Table A45. Polyacrylonitrile fibre (PAN fibre)

Polyacrylonitrile fibre (PAN fibre)				
Inputs	***Amount***	***Unit***	***Remarks***	***How it is calculated***
Acrylonitrile, at plant/RER U	1	kg	Monomer: forms polyacrylonitrile by free radical polymerization (needs an initiator) [323]	By adding an initiator, the molecules begin to aggregate on their own. Initiator unknown, assumed negligible.
Extrusion, plastic pipes/RER U	1	kg	Fibre extrusion process (Wet Spinning) [324]	
Output	***Amount***	***Unit***	***Remarks***	
Polyacrylonitrile fibre (PAN fibre)	1	kg	Intermediate Product	PAN fibre is a precursor of carbon fibre.

The GDL, through their porosity, act as mediators between the flow-fields, i.e. the channels engraved on the bipolar plates and the MEA, with the aim of homogeneously diffusing the gases over the entire active area of the cell, thus allowing the passage from the macroscopic scale of the channels, to the micrometric scale of the membrane, through gradually decreasing porosity.

The most commonly used material for the realization of the GDL is the carbon fibre, woven or non-woven, which confers a high electrical conductivity and a porosity higher than 70%, while presenting at the same time high stability and resistance to corrosion. There is a natural trade-off between the porosity and conductivity of a GDL material; as the porosity of the layer increases, the substances flows improve, but at the same time the electrical resistance increases. For the purposes of this study, a woven carbon fibre mesh is used which, unlike carbon paper, does not require a resin binder. Unlike the membrane, which needs a hydrophilic treatment to maintain hydration even at higher temperatures, the carbon mesh needs to be treated hydrophobically, in order to avoid flooding of the electrodes which would result in a reduction of the diffusion capacity of gases. The hydrophobic treatment is carried out using a PTFE hydrophobic ink.

The large contrast between the relatively large pore size of GDL (10-30 µm) and the small size of the catalyst particles (10-100 nm) is commonly neutralised by the use of a microporous layer (MPL) of approximately 20-50 µm thick, which is made to adhere to the GDL. This brings further advantages in improving both the electrical contact and the water transport. MPL for current technology consists of carbon or graphite particles, mixed with a PTFE binder, i.e. the same basic materials as GDL. Carbon fibre is currently widely produced from polyacrylonitrile fibres and the production of carbon fibre mesh from the fibres uses an industrial weaving process.

However, carbon fibres are not present in the ecoinvent version used, therefore their production process was first considered. Starting from their precursor, i.e. the acrylonitrile monomer, polyacrylonitrile is formed by free radical polymerisation, by adding a molecule called "initiator". Through a particular extrusion process called "wet-spinning", the polyacrylonitrile fibres (PAN fibres) are extruded, in long filaments collected in coils (Table A45). The polyacrylonitrile fibres are subsequently woven into a cloth and carbonised at high temperature, forming the carbon fibre cloth (Table A46). A large amount of energy, both electrical and thermal, is required in the carbonisation process. The fibres are carbonised by keeping them in an inert environment at temperatures between 2000 and 3000 °C for fairly long times. It is possible to reduce the impact deriving from the production of carbon fibres using heat and electricity from renewable sources, however, to model an average European industrial process, natural gas has been considered for the supply of heat, and electricity taken from the grid using an average European electricity grid mix.

Once the carbon fibre mesh has been obtained, the GDL is then produced through a thermoforming with calendering process (Table A47).

The PTFE hydrophobic agent is applied to the GDL mesh by immersing the cloth in an aqueous solution of PTFE, followed by drying and sintering at temperatures between 350 and 400 °C. The MPL is then painted onto the GDL and heat treated.

Table A46. Carbon fibre cloth

Carbon fibre cloth				
Inputs	***Amount***	***Unit***	***Remarks***	***How it is calculated***
Natural gas, burned in industrial furnace low-NOx>100kW/ RER U	98.556	MJ	[190,324,325]	Thermal energy, takes into account the oxidation and stabilization of the fibres at 230 °C in air and subsequent carbonization at 1200 °C or more in an inert environment (nitrogen or argon), maximum temperature between 2000-3000 °C (long times at maximum temperature required, highly energy intensive process).
Polyacrylonitrile fibre (PAN fibre)	1	kg	[190,324,325]	
Electricity, medium voltage, production RER, at grid/RER U	262.08	MJ	[190,324,325]	
Output	***Amount***	***Unit***	***Remarks***	
Carbon fibre cloth	1	kg	Intermediate Product	

High grade graphite (for batteries, with high electrical conductivity) was considered for the production of the MPL. The final product thus obtained is the GDL.

Table A47. Thermoforming

Thermoforming				
Inputs	***Amount***	***Unit***	***Remarks***	***How it is calculated***
PTFE, Polytetrafluoroethylene	0.537	g	Amount from Gallo Stampino et al. (2011) [326] in [190]	Hydrophobic ink for GDL. 10%wt
Carbon cloth (fibre)	4.833	g	Amount from Gallo Stampino et al. (2011) [326] in [190]	90%wt
Graphite, battery grade, at plant/RER U	0.269	g	For MPL layer [189,190]	Added at 5%wt for MPL
Thermoforming, with calendering/RER U	5.638	g	Used to account for the application of PTFE to the carbon cloth and the necessary heat treatments. Includes the energy demands (1 kWh_{el}/kg, 0.81 MJ_{th} /kg & 0.058 kg_{steam} /kg) and other consumables [189]	The carbon fibre cloth is dipped in hydrophobic PTFE ink. Drying and sintering processes follow, at 400 °C. Finally, MPL is added with thermomechanical treatments.
Output	***Amount***	***Unit***	***Remarks***	
Gas Diffusion Layer (GDL)	1	p	Final Product	GDL mass= 5.638 g

MEA Assembly

Finally, the MEA, which represents the heart of a fuel cell, is assembled (Table A48). It includes the electrodes, made up of the set of GDLs and of the active layers on which the catalysts are deposited, and the electrolyte represented by the membrane. The MEA is then assembled by joining a catalysed reinforced membrane and two GDLs, in contact with the membrane on the MPL side. The pressing of the membrane with the GDL takes place at temperatures of around 130 °C and 80 bar pressure, in such a way as to guarantee the best possible contact. In the hot calendering process, acetic acid is also involved, which serves to preventively treat the cobalt present on the cathode, so that the weakly bound cobalt cannot leach from the catalyst layer during the fuel cell operation, poisoning the MEA. The final product obtained is a MEA about 1 mm thick.

Table A48. MEA assembly

MEA Assembly				
Inputs	***Amount***	***Unit***	***Remarks***	***How it is calculated***
Catalysed Reinforced Membrane	1	p	See production of catalysed reinforced membrane	Mass catalysed reinforced membrane = 1.06 g
Gas Diffusion Layer (GDL)	2	p	See production of gas diffusion layer	Mass of 2 GDL = 5.638 g *2= 11.276 g
Acetic acid, 98% in H2O, at plant/RER U	9.231	g	Weak acid for the pre-leaching of Co from the cathode catalyst [189]	From [189] (50 g acetic acid)/kW for the pre-leaching treatment of (0.035 g cobalt)/kW. Ratio g acid/g cobalt= 50/0.035=1428. Having in our case a cobalt content of (0.020 g cobalt)/kW, it is obtained: Mass of acetic acid/kW= 1428*0.020= 28.57 g acid/kW= 0.03 kg acid/kW Mass of acetic acid, total per one stack = 80 kW* 0.03 kg acid/kW =2.4 kg acid Amount of acid for one cell= 2.4 kg/260 cells = 0.009231 kg/cell = 9.231 g acid/cell
Thermoforming, with calendering/RER U	12.336	g	Used to represent the MEA laminating process. Includes the energy demands (0.1 kWh_{el}/kg, 0.4 MJ_{th}/kg & 0.085 kg_{steam} /kg) and other consumables. [189]	Processed material mass = 11.276 g + 1.06 g = 12.366 g
Output	***Amount***	***Unit***	***Remarks***	
MEA Assembly	1	p	Final Product	MEA weight = 12.336 g

Bipolar Plates

The bipolar plates distribute the reagents on the active areas of the cells via the flow-field channels engraved on them. Different design configurations can exist for the channels, which in general can be different between the anode and the cathode. The Toyota Mirai, for example, uses three-dimensional channels dug into the bipolar plates on the cathode side, with a particular geometry that makes it easier to remove the water produced on the cathode, avoiding flooding of the electrodes and improving cell performance.

Table A49. Titanium zinc plate

Titanium Zinc Plate				
Inputs	***Amount***	***Unit***	***Remarks***	***How it is calculated***
Aluminium, primary, at plant/RER U	0.00101	kg		
Brass, at plant/CH U	0.0396	kg		
Casting, brass/CH U	2.11	kg		
Copper, at regional storage/RER U	0.00127	kg		
Contour, brass/RER U	1	kg		
Zinc, primary, at regional storage/RER U	1.06	kg		
Electricity, medium voltage, production UCTE, at grid/UCTE U	0.435	kWh		
Aluminium casting, plant/RER/I U	1.01E-10	p		
Aluminium, production mix, at plant/RER U	0.000159	kg		
Output	***Amount***	***Unit***	***Remarks***	
Titanium Zinc Plate	1	kg	Final Product	Modified from ecoinvent [181]
Emissions in Air	***Amount***	***Unit***	***Remarks***	
Heat, waste	1.57	MJ		
Zinc	0.000318	kg		

For automotive applications it is particularly important that the bipolar plates are lightweight, have good electrical properties, and can be easily mass-produced from inexpensive materials. They can be made of non-porous graphite, specific metal alloys, or composite polymeric materials. Each of these has different advantages and disadvantages. For current technology, stainless steel is commonly used, covered with titanium oxide and graphite. However, the car manufacturers declare the use, in the most recent models, of bipolar plates in titanium, which will therefore be considered in this inventory. Pure titanium is not present in the ecoinvent version used; however, it was possible to consider a production process of a galvanized titanium plate, slightly modifying it to obtain the desired process (Table A49).

Bipolar plates are approximately 1 mm thick, however if the thickness of the plate also includes the channels, the plates cannot be considered as massive bodies. For this reason, the mass was calculated assuming half the density of the titanium, to take into account the voids created by the channels. The plates are produced by sheet metal stamping using a press. A conductive layer based on titanium oxide and graphite is then applied (Table A50).

Table A50. Bipolar plate

Bipolar Plate				
Inputs	***Amount***	***Unit***	***Remarks***	***How it is calculated***
Titanium Zinc Plate	83.6	g	From [189], using titanium instead of chromium steel Titanium is used in Toyota Mirai	Plate thickness = 1 mm= 0.1 cm Cell area = 380 cm^2 Bipolar plate volume = 38 cm^3 Titanium density = 4.4 g/cm^3 It is assumed a plate apparent density= 4.4/2= 2.2 g/cm^3 to take into account empty spaces where flow-field channels are engraved [37]. Titanium plate mass = 2.2 g/cm^3*38 cm^3 = 83.6 g
Titanium Dioxide, production mix, at plant/RER U	1.672	g	Coating material, 2012 scenario [189]	Coating, assumed as 2%wt
Graphite, at plant/RER U	1.672	g	Coating material in 2012 scenario. [189]	Coating, assumed as 2%wt
Selective coating, copper sheet, sputtering/DE U	0.076	m^2	Process for plate coating in 2012 scenario. Includes the energy demands (3.5 kWh of electricity/m^2 & 0.006 kg of fuel oil/m^2) and other consumables. [189]	Cell area*2= 380 cm^2*2=760 cm^2= 0.076 m^2 = Surface treated in the process = faces of the bipolar plate
Deep drawing, steel, 650 kN press, automode operation/RER U	83.6	g	Production process of the plates in 2012 scenario. Includes the energy demands (0.5 Wh of electricity/kg & 6.5 cm^3 compressed air/kg), infrastructure and other consumables. [189]	Drawing of base material for channel engraving (titanium only)
Output	***Amount***	***Unit***	***Remarks***	
Bipolar Plate	1	p	Final Product	Bipolar plate mass = 86.944 g

Gaskets

Table A51. Coolant gasket

Coolant Gasket				
Inputs	***Amount***	***Unit***	***Remarks***	***How it is calculated***
Synthetic rubber, at plant/RER U	15.6	g	Amount assuming 1 mm thickness. [190]	Gasket thickness = 1 mm Border width = from active area (250 cm^2) to cell area
Electricity, medium voltage, production RER, at grid/RER U	0.006	MJ	Based on Battelle (2013) [322] in [190]	Proportion from [190]
Output	***Amount***	***Unit***	***Remarks***	
Gasket	1	p	Final Product	Gasket mass = 15.6 g

The gaskets that seal the MEA to the bipolar plates can be made of various materials, for example glass fibre or synthetic rubber. In the case considered, they are produced starting from synthetic rubber (silicone roll) through a cutting process in a press, to obtain the desired shape (Table A51).

End Plates/Current Collector and Tie Rods

The end-plates are plates made of electrically conductive material, placed at the ends of the stack, which act both as current collectors and as collectors of the incoming and outgoing gases. Furthermore, together with the tie rods, they are the structural components that physically hold the cells together to form the stack. For the production of the current collectors, an aluminium alloy and a generic manufacturing process for aluminium products were considered. The final plate has a thickness of about 10 mm to also house the tie rods (Table A52). The tie rods are bars made of chromium steel, with a process that takes into account the working of the aforementioned metal alloy (Table A53).

Table A52. End plates and current collector

End Plates and Current Collector				
Inputs	***Amount***	***Unit***	***Remarks***	***How it is calculated***
Aluminium, production mix, cast alloy, at plant/RER U	1.026	kg	Collector & end plates [189]	End plate thickness = 10 mm [189] Cell area = 380 cm^2 End plate volume = 380 cm^3 Aluminium alloy density = 2.7 g/cm^3 End plate mass = 380 cm^3 *2.7 g/cm^3 = 1026 g
Aluminium product manufacturing, average metal working/RER U	1.026	kg	Accounts for the operation and infrastructure of average production processes. [189]	Generic metal working process. Processed aluminium mass = end plate mass
Output	***Amount***	***Unit***	***Remarks***	
End Plate/Current Collector	1	p	Final Product	End plate mass = 1.026 kg

Table A53. Tie rods

Tie Rods				
Inputs	***Amount***	***Unit***	***Remarks***	***How it is calculated***
Chromium steel 18/8, at plant/RER U	589	g	Tie rods [189]	Diameter = 10 mm [189] Area= 78 mm^2 ; Length = 1 m Volume=78.53 cm^3 Steel density = 7.5 g/cm^3 Mass of 1 tie-rod = 589 g 8 tie-rods are assumed [37]
Chromium steel product manufacturing, average metal working/RER U	589	g	Accounts for the operation and infrastructure of average production processes. [189]	Generic metal working process. Processed steel mass = mass of the tie-rod
Output	***Amount***	***Unit***	***Remarks***	
Tie-Rods	1	p	Final Product	Tie-rod mass = 589 g

Cell assembly

Table A54. Cell assembly

Cell Assembly				
Inputs	***Amount***	***Unit***	***Remarks***	***How it is calculated***
MEA	1	p		Mass of MEA = 12.336 g
Gasket	2	p	Gasket between MEA and bipolar plates	Mass of two gaskets =15.6 g*2 = 31.2 g
Bipolar Plate	1	p	The last bipolar plate that close the cell series, is accounted for here, to allow considering several cells in series while avoiding double-counting of bipolar plates in the cell process	Mass of bipolar plate = 86.944 g
Output	***Amount***	***Unit***	***Remarks***	
Cell	1	p	Final Product	Cell mass = 130.51 g

Once all the components necessary for the production of the stack have been obtained, it is possible to start assembling them together. In the cell assembly process, a single cell is produced from one MEA, two gaskets, and a single bipolar plate (to avoid double counting in the next step). The single cell has a weight very close to that found in the technical data sheet of the Toyota Mirai.

Stack assembly

Table A55. Stack assembly

Stack Assembly				
Inputs	***Amount***	***Unit***	***Remarks***	***How it is calculated***
Cell	260	p		130.51 g *260 cells = 33932.6 g = 33.9 kg
Gasket	2	p		15.6 g*2 gaskets = 31.2 g
Bipolar Plate	1	p		86.944 g
End Plate/Current Collector	2	p		1026 g*2 end plates =2052 g = 2.052 kg
Tie Rods	8	p		589 g*8 tie-rods = 4712 g = 4.7 kg
Output	***Amount***	***Unit***	***Remarks***	
Stack Assembly	1	p	Final Product	40814.744 g = 40.814 kg

Through the technical data sheet previously defined in the table (Table A38), 260 cells are assembled together to form a stack. The following were also added: the last bipolar plate, to close the last cell, two gaskets which join the outermost bipolar plates with the current collectors, the two current collectors/end-plates placed at the ends of the stack and the tie rods which hold all together. Once again, the obtained stack is very close in weight (40.8 kg) to the stack of the Toyota Mirai (40 kg). The final stack weight is essential to achieve the high-power densities (kW/kg) required by automotive applications.

Table A56. FC stack

FC Stack				
Inputs	***Amount***	***Unit***	***Remarks***	***How it is calculated***
Stack Assembly	1	p		Conversion from p to kW
Output	***Amount***	***Unit***	***Remarks***	
FC Stack	80	kW	Final Product	

Finally, through a process in SimaPro, the definition of the stack is "translated" using the rated power as a product flow, rather than the amount or the mass of the product. This definition will be useful later in the vehicle definition process.

Appendix B
Results of sensitivity analysis on vehicle technical parameters

This appendix provides additional figures for the results of the sensitivity analysis on the variation of key vehicle technical parameters provided in Section 3.3. GWP results for all vehicles and Hythane results for all the impact categories considered cand be found in Section 3.3.

FCEV

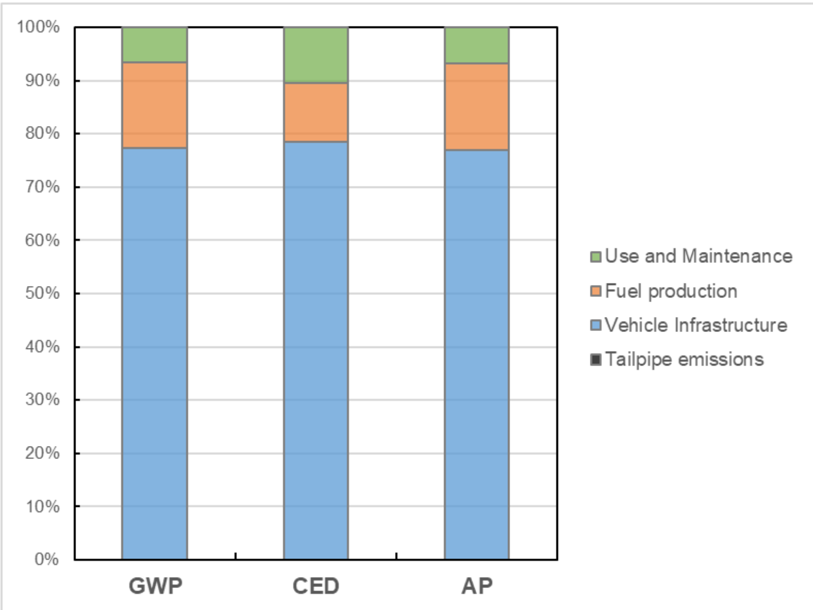

Figure 76. Impact breakdown of the FCEV (Baseline)

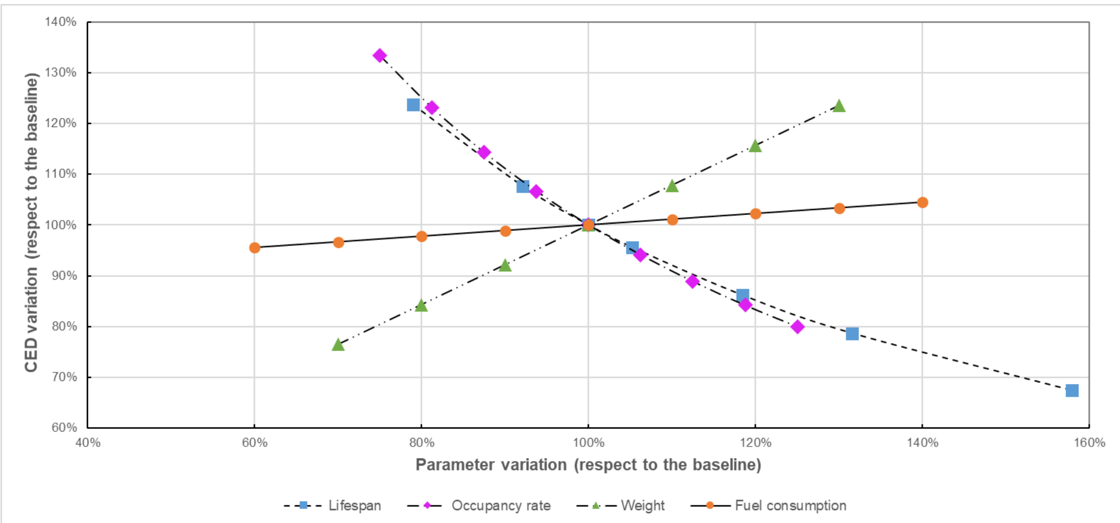

Figure 77. Influence of vehicle technical parameters on CED impact, FCEV

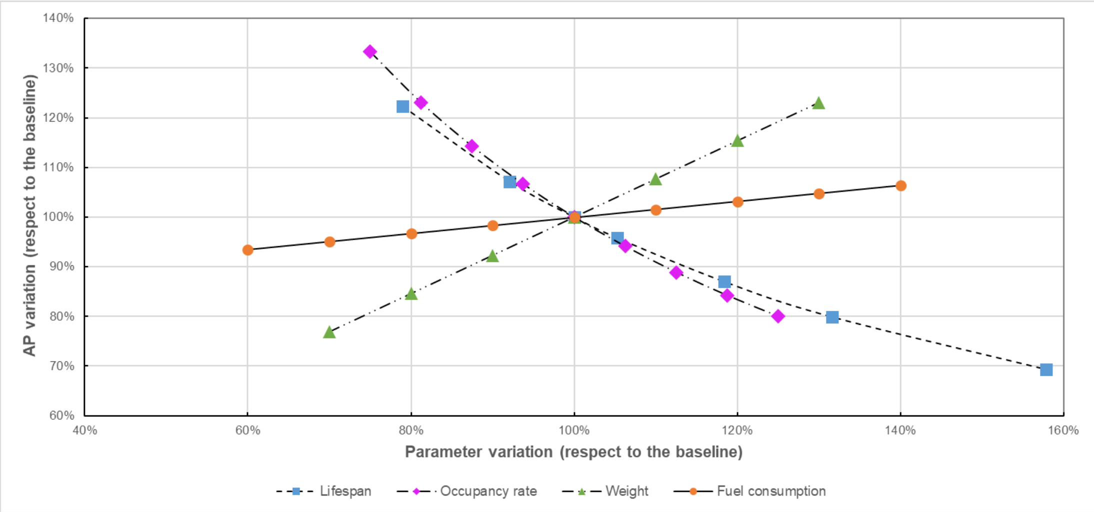

Figure 78. Influence of vehicle technical parameters on AP impact, FCEV

H2-ICE

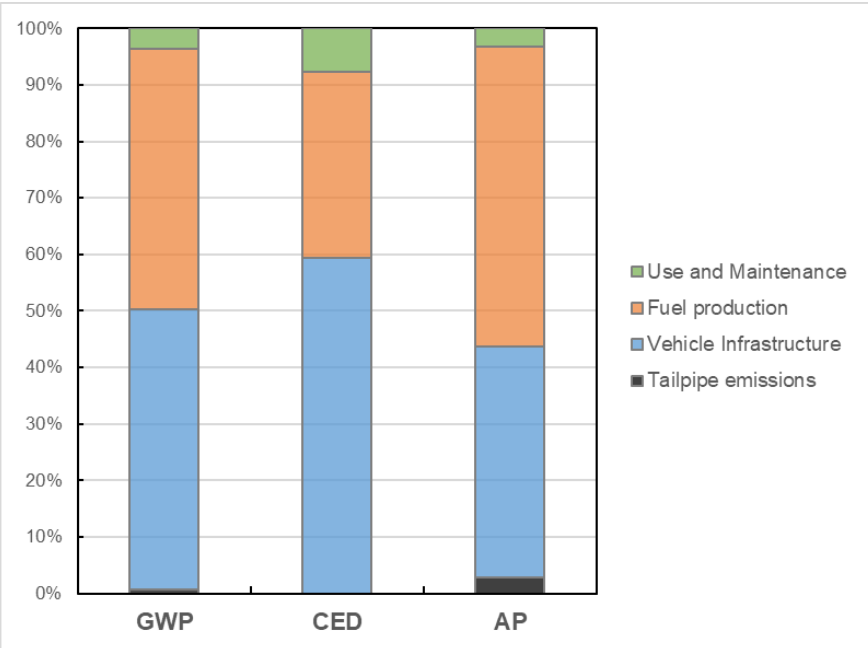

Figure 79. Impact breakdown of the H2-ICE vehicle (baseline)

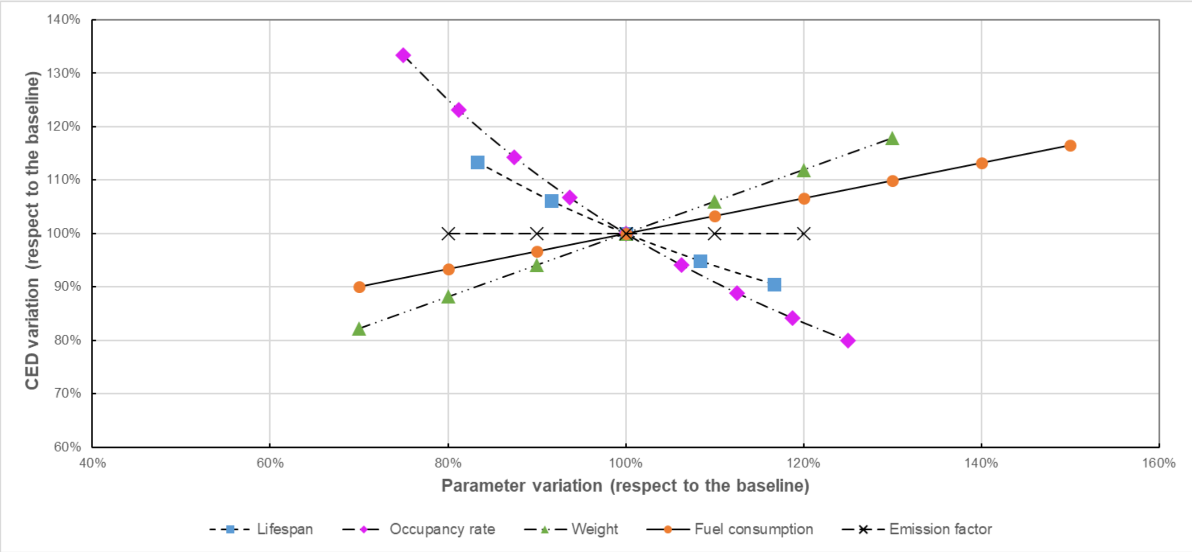

Figure 80. Influence of vehicle technical parameters on CED impact, H2-ICE

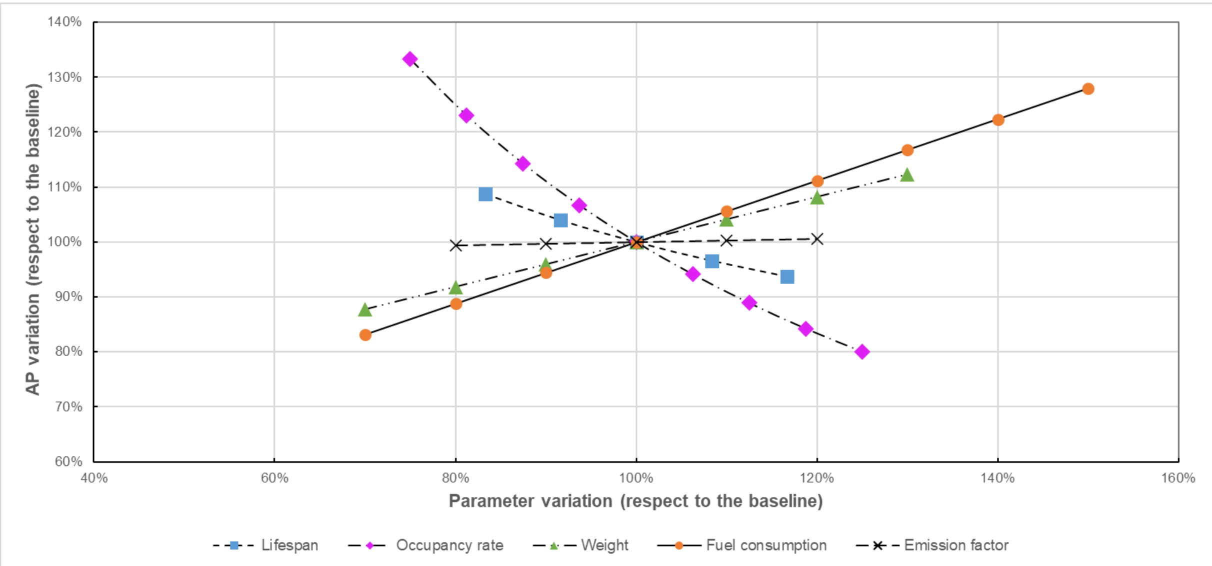

Figure 81. Influence of vehicle technical parameters on AP impact, H2-ICE

HEV H2-ICE

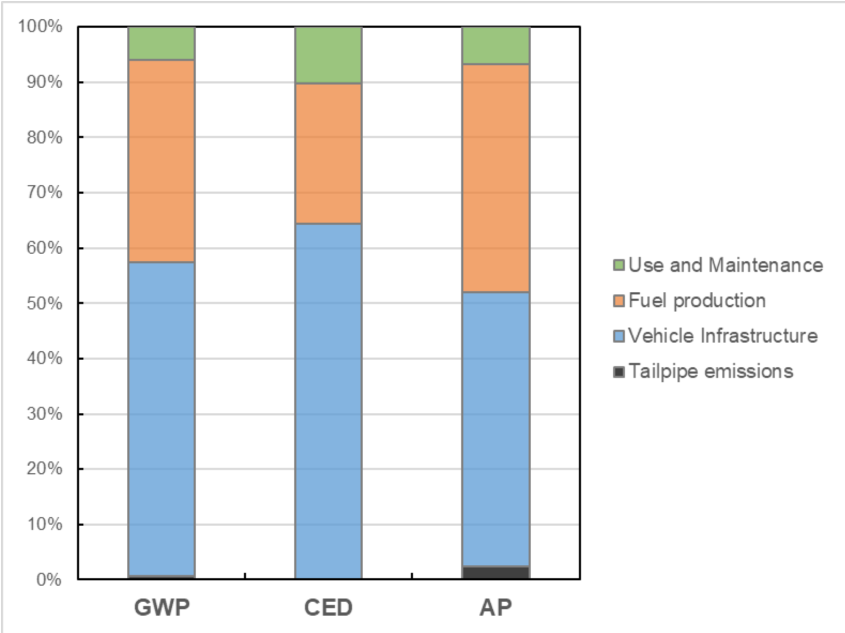

Figure 82. Impact breakdown of the HEV H2-ICE (baseline)

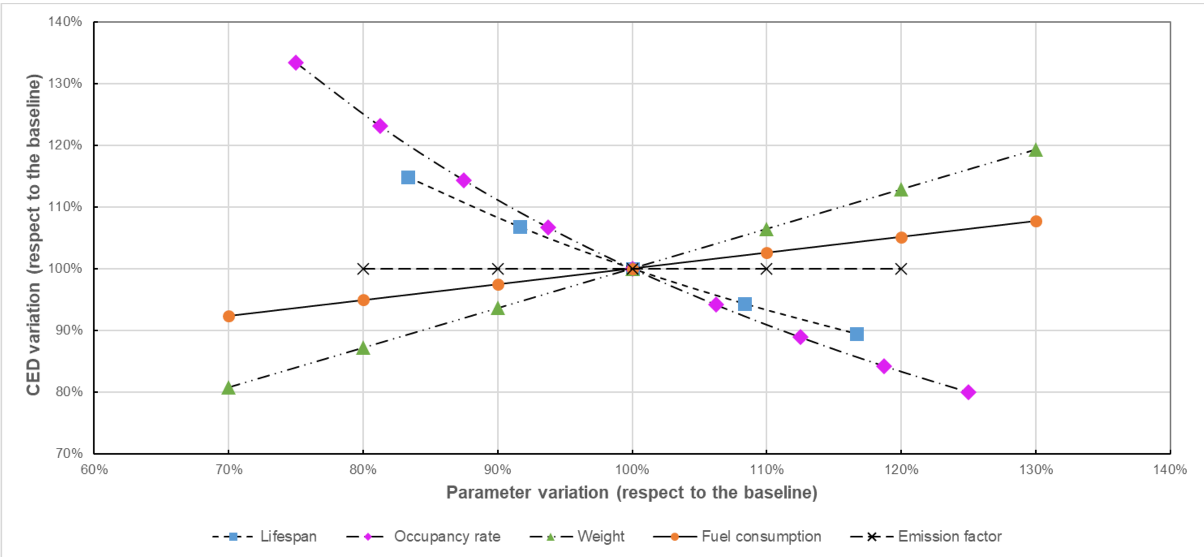

Figure 83. Influence of vehicle technical parameters on CED impact, HEV H2-ICE

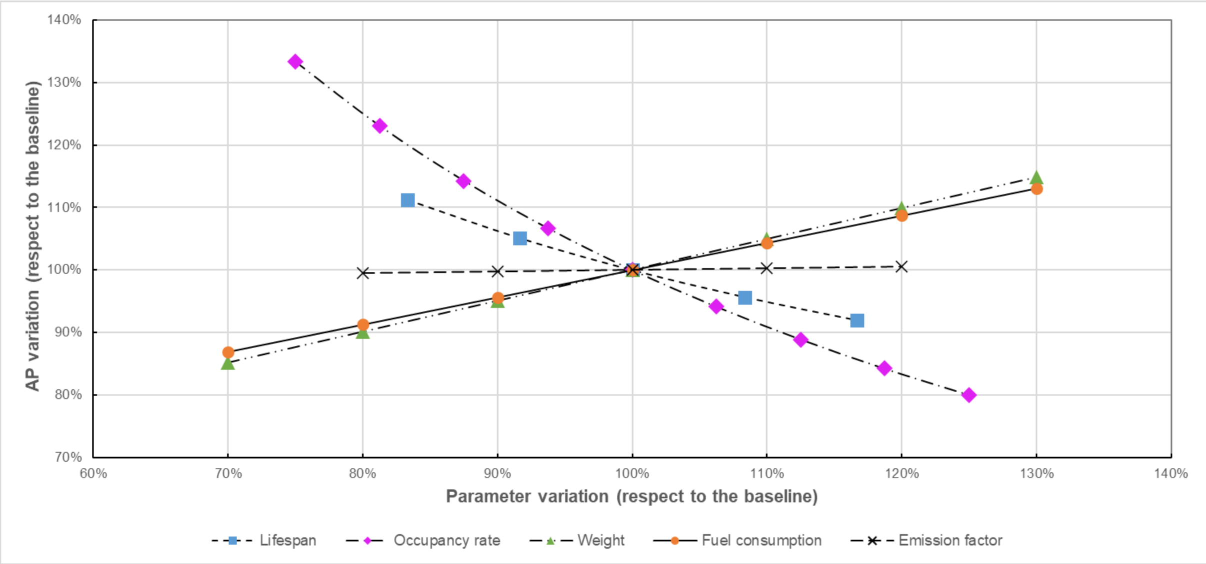

Figure 84. Influence of vehicle technical parameters on AP impact, HEV H2-ICE

Hythane

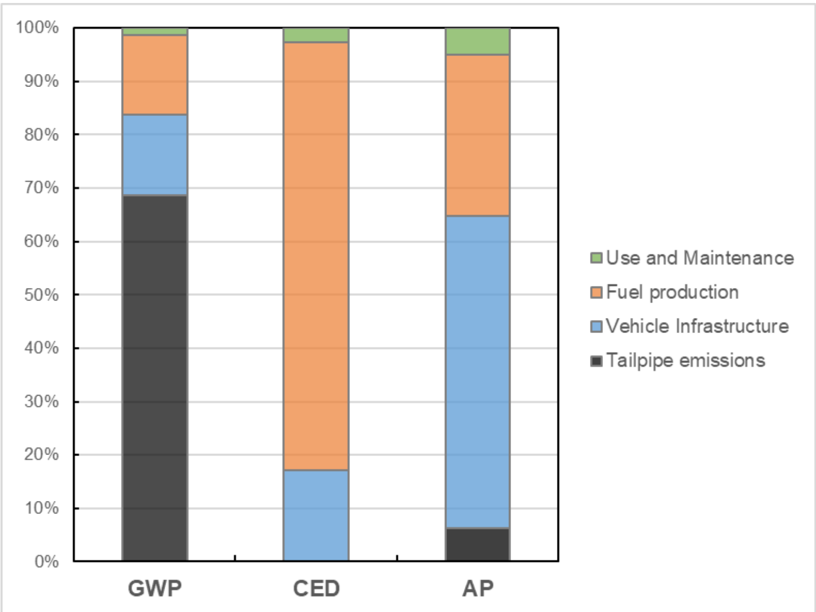

Figure 85. Impact breakdown of the Hyhtane vehicle (baseline)

H2-Gasoline

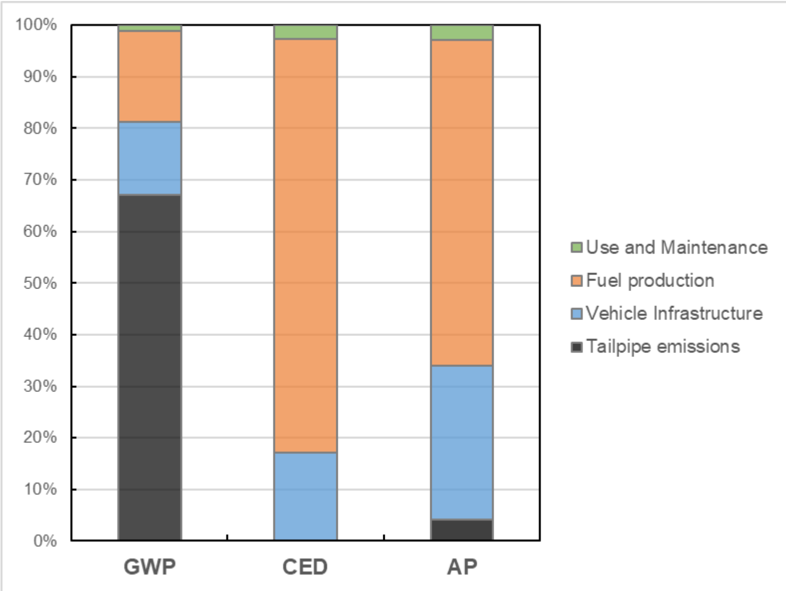

Figure 86. Impact breakdown of the H2-Gasoline vehicle (baseline)

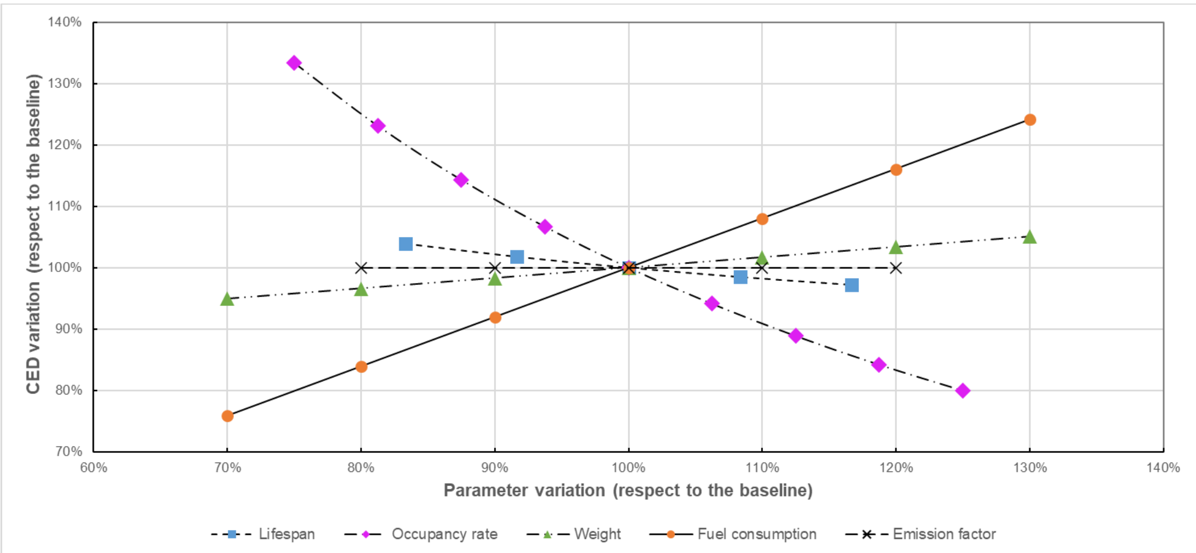

Figure 87. Influence of vehicle technical parameters on CED impact, H2-Gasoline vehicle

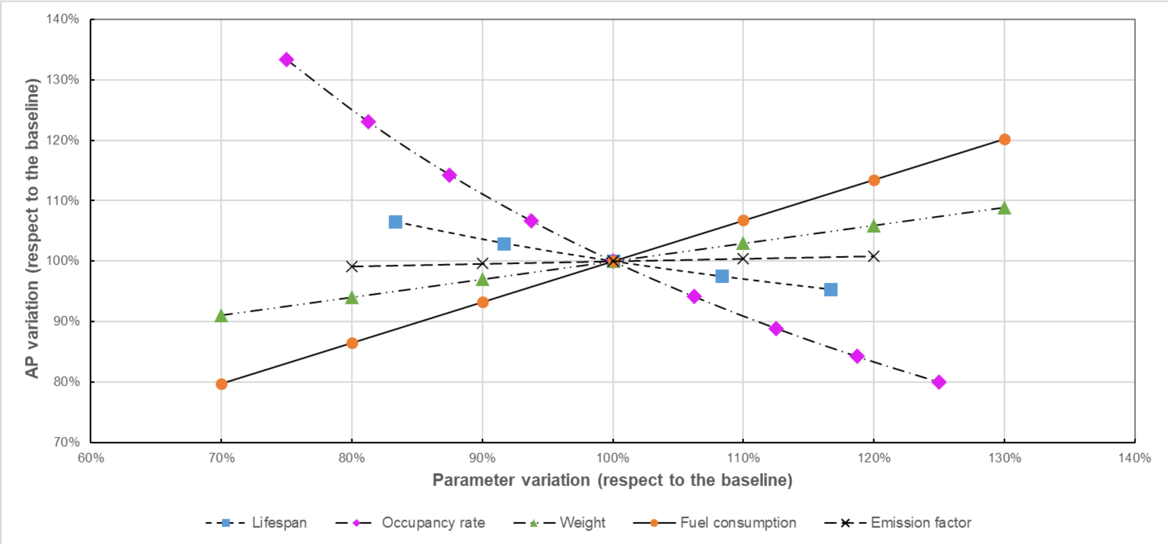

Figure 88. Influence of vehicle technical parameters on AP impact, H2-Gasoline vehicle